ASSESSING GROUNDWATER FLUX FROM UNDERLYING FRACTURED BEDROCK TO THE OVERBURDEN AQUIFER SYSTEM FREDERICTON, NEW BRUNSWICK, CANADA

NATALIE A. LIPPA

ASSESSING GROUNDWATER FLUX FROM UNDERLYING FRACTURED BEDROCK TO THE OVERBURDEN AQUIFER SYSTEM FREDERICTON, NEW BRUNSWICK, CANADA

By

Natalie A. Lippa

B.Sc.(Hons.), Memorial University of Newfoundland, 2000

A thesis submitted in partial fulfillment of the requirements for the degree of

Master of Science in the Department of Earth Sciences

This thesis is accepted

_____

Dean of Graduate Studies and Research

Memorial University of Newfoundland and Labrador

St. John's, Newfoundland and Labrador

June, 2010

ABSTRACT

Fredericton, the capital city of New Brunswick, Canada, draws its water from wells in a semi-confined river valley alluvial aquifer which produce approximately 25,000 m^3/day for a population of 50,535 (Statistics Canada, 2007). The water that is produced by the well field comes from either the Saint John River via riverbank induced infiltration, surface infiltration, the underlying fractured bedrock, or a combination of these sources. In the past, lower water supply demands from a smaller population in Fredericton were met from the aquifer system. As a result, the hydrogeology of the fractured sedimentary bedrock, in terms of contribution to the water supply was not addressed in depth. With the increased water supply demand from a growing population and the potential variation in recharge rates to affect groundwater quantity however, the need to understand and estimate the groundwater contribution from the bedrock aquifer has been recognized. A hydrogeological characterization, and 3D numerical model assessment of the Fredericton area, was completed to: 1) determine how the flux would vary under both natural flow and well field pumping conditions; and 2) determine how sensitivity to variations in recharge, would impact the quantity of the groundwater flux from the fractured bedrock to the overburden aquifer. The steady-state (natural flow) and transient (pumping) model simulations indicated the bedrock fluid flux in the well field area was approximately 1000 m^3/d and was not greatly affected by changes to recharge or pumping rates. With changes in precipitation or temperature, a possible result of climate change, the resulting hydraulic head and fluid flux in the overburden was more sensitive than that of the bedrock, which represented a more stable fluid flux because of the lower fractured rock mass permeability.

ACKNOWLEDGMENTS

I gratefully acknowledge the financial support provided by the Canadian Water Network (CWN), Memorial University of Newfoundland (MUN) and Fracflow Consultants Inc.

I thank my supervisor Dr. John Hanchar for his guidance through the final stages of this work. I also appreciate the invaluable assistance from Dr. John Gale (MUN) and Dr. Tom Al, Dr. Kerry MacQuarrie and Dr. Karl Butler of the University of New Brunswick.

To the students who worked with me in the field, during data analysis, modeling, and editing, including Matt Alexander, Larry Amskold, Mark Hodder, Norah Hyndman, Anne Jefford, Paul O'Neill, Barbara Petrunic, Eunjeong Seok and Jeff Whitter, I sincerely appreciate your time, effort and interest in this work.

I would also like to thank the technical staff at the University of New Brunswick, including Ken Noftell and Dan Wheaton, members of the City of New Brunswick Water Treatment Plant for providing well data and Pat Wall for granting access to the Odell Park site.

Special thanks go out to my parents, siblings and friends for listening and offering optimism and encouragement. And a very special thank you goes out to Paul Leonard, who has supported me with love, advice and patience throughout all these years.

TABLE OF CONTENTS

LIST OF TABLES

LIST OF FIGURES

LIST OF PLATES

NOMENCLATURE

Q_{tp}	=	total potential groundwater discharge
Q_o	=	baseflow at start of recession curve
t_l	=	time for baseflow to drop from Q_o to $0.1Q_o$
Q_t	=	potential baseflow remaining some time (t) after the start of the baseflow recession
t	=	time of interest
psi	=	pounds per square inch
RQD	=	rock quality designation
T	=	transmissivity (m^2/s)
Q	=	flowrate (m^3/s)
R_i	=	radius of well influence (m)
R_w	=	radius of well borehole (m)
H_w	=	hydraulic head of borehole during test interval (m)
H_i	=	initial hydraulic head of well (m)
K	=	hydraulic conductivity (m/s)
L	=	length of test interval (m)
Q	=	flow or discharge (m^3/s)
K	=	hydraulic conductivity (m/s)
A	=	cross sectional area (m^2)
$\frac{dh}{dl}$	=	change in hydraulic gradient (m/m = dimensionless) where dh is the change in head between two points dl is the change in length between two points
GMWL	=	the global meteoric water line
δ	=	$\frac{R_{samples} - R_{standard}}{R_{standard}}$ x 1000 reported in permillage ($^0/_{00}$)
TU	=	tritium units
C factor	=	run-off coefficient factor
FEFLOW	=	Finite Element FLOW
$\partial/\partial x$	=	discretization in x dimension
Kxx	=	hydraulic conductivity in the x-direction
$\partial h/\partial x$	=	change in hydraulic head in x dimension
$\partial/\partial y$	=	discretization in y dimension
Kyy	=	hydraulic conductivity in the y-direction
$\partial h/\partial y$	=	change in hydraulic head in y dimension
$\partial/\partial z$	=	discretization in z dimension
Kzz	=	hydraulic conductivity in the z-direction
$\partial h/\partial z$	=	change in hydraulic head in z dimension
W	=	source/sinks
Ss	=	specific storage
$\partial h/\partial t$	=	change in hydraulic head over time

ME	=	Mean error
MAE	=	Mean absolute error
RMS	=	Root mean square
n	=	number of samples
i	=	individual sample
$\sum$	=	sum of
hm	=	hydraulic head measured
hs	=	hydraulic head simulated

CHAPTER 1.0 INTRODUCTION

1.1 Statement of Problem

River valley alluvial aquifers are a significant source of potable water because of their potential to provide large volumes of water, through induced infiltration. In addition, even though the river water quality and quantity may vary seasonally, or in the long term, river valley alluvial aquifers act as a natural filter in a physical, chemical, and biological sense. This filtration ensures that any short or long term impacts from variations in the river water quality are reduced.

Fredericton, the capital city of New Brunswick, Canada, draws its water from wells in a river valley semi-confined alluvial aquifer (Fig. 1.1). The valley alluvial aquifer, adjacent to the Saint John River, is formed by a buried sand and gravel esker that runs from the northwest side to the southeast side of the city, intercepted by the river at both ends. The city wells produce approximately 25,000 m^3/day from this river valley alluvial aquifer system and supply a population of 50,535 inhabitants (Statistics Canada, 2007). The city has developed two well fields in this aquifer, approximately 1.5 km apart, which include Wilmot Park on the west end of the city and Queen's Square, on the east side of the city (Fig. 1.2). The water that is produced by these two well fields comes from either the Saint John River via riverbank induced infiltration, other surface water infiltration, possibly from the underlying fractured bedrock as a result of the drawdown cones generated by the well fields, or a combination of these sources.

Surface water bodies such as rivers, represent a different aqueous environment than groundwater in the adjacent aquifers in terms of pH, Eh, colour, turbidity, total

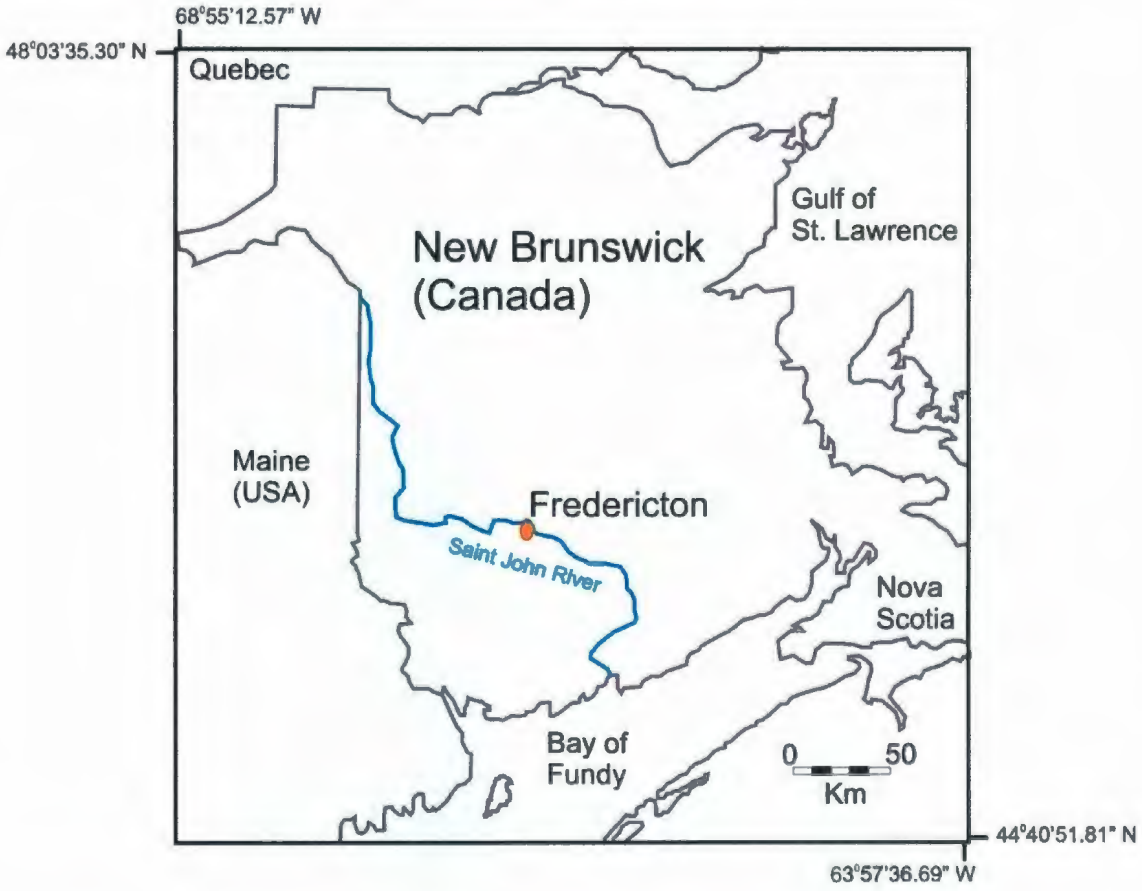

Figure 1.1. Location of Fredericton, New Brunswick, Canada.

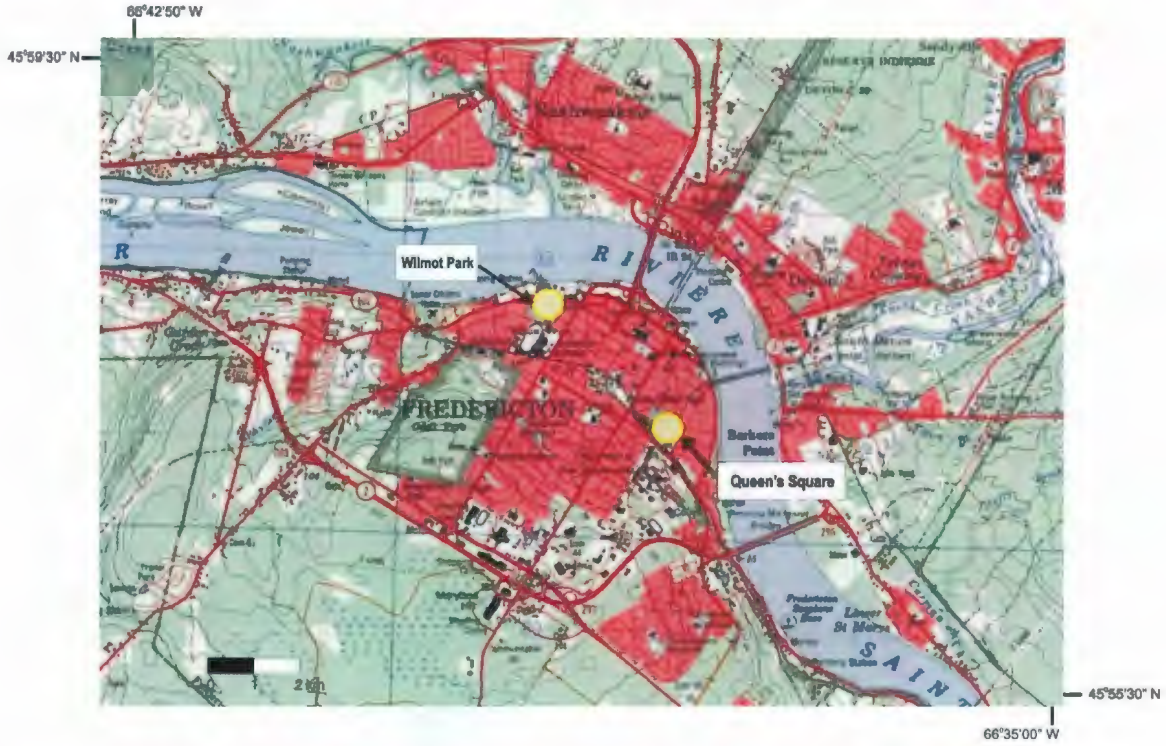

Figure 1.2. Well field locations of Wilmot Park and Queen's Square (Touratech-QV-Navigator, 2003).

dissolved solids (TDS) and total suspended solids (TSS). In moving from one aqueous environment to another, minerals can be precipitated or dissolved. For example, in the Fredericton aquifer, redox reactions occurring as the groundwater moves from oxygen rich to oxygen depleted environments prompts the dissolution of manganese and iron. At elevated levels, these oxides create water quality problems. Increased concentrations of manganese and iron were detected in the 1950s as the well fields were being developed.

The overburden aquifer in the Fredericton area is underlain by Carboniferous fractured porous sedimentary bedrock. This bedrock includes shale, siltstone, sandstone and conglomerate units. In general, groundwater moving through fractured sedimentary

bedrock aquifers has a longer residence time compared to the residence time of the groundwater in the river valley alluvial overburden aquifers. This is because bedrock aquifers tend to have lower permeability than overburden aquifers, and the groundwater at depth originates from a further distant location. Therefore, the bedrock aqueous geochemical signatures tend to be different from aqueous geochemical signatures in the overburden.

There is a natural regional groundwater flux towards the aquifer and the river itself, as part of the normal flow system hydrodynamics, since the recharge areas are at a much higher elevation of ~130 m above sea level (asl) than the aquifer (0 to ~ -40 m asl). In addition, the drawdown cones generated by the well fields impose strong local hydraulic gradients, which are superimposed on the natural flow system.

In the past, lower water supply demands from a smaller population in Fredericton were met from the overburden aquifer system. As a result, the hydrogeology of the fractured sedimentary bedrock in terms of a potential supply of water was not addressed in depth. However, with the increased water supply demand from a growing population and the future potential variation in precipitation and temperature to affect recharge rates and groundwater quantity, the need to understand and estimate the groundwater contribution from the bedrock aquifer has been recognized.

1.2 Objectives and Scope

In 2001, funding to Memorial University of Newfoundland and Labrador from the Canadian Water Network (CWN) enabled a detailed study of the role the bedrock aquifer

plays in contributing groundwater to the well fields, with an emphasis on the need to protect the water supply from anthropogenic impacts. Under the direction of Dr. Tom Al and Dr. Kerry MacQuarrie of the University of New Brunswick, a multidisciplinary research program was undertaken to investigate, "Coupling between a river and alluvial and fractured bedrock groundwater flow system," using the Fredericton aquifer as the study site.

One component of the overall research program, on which this thesis is based, is a field and 3D numerical model assessment of the groundwater flux from the fractured sedimentary bedrock to the river valley alluvial aquifer system. The 3D model is used:

(1) to determine how the groundwater flux varies under both natural flow and well field pumping conditions; and

(2) determine how sensitivity to variations in recharge, a potential result from climate change, impacts the quantity of the groundwater flux from the fractured bedrock to the overburden aquifer.

The overall approach taken in this thesis is presented in Figure 1.3. The thesis work is organized into the following components: 1) hydrogeological characterization; 2) 3D numerical model mesh development; 3) model calibration; and 4) model simulation.

Geological data, including stratigraphy and structure, are obtained from literature reviews, limited outcrop mapping, and by drilling three inclined boreholes into the fractured bedrock. These data are used to approximate the geometry of the main

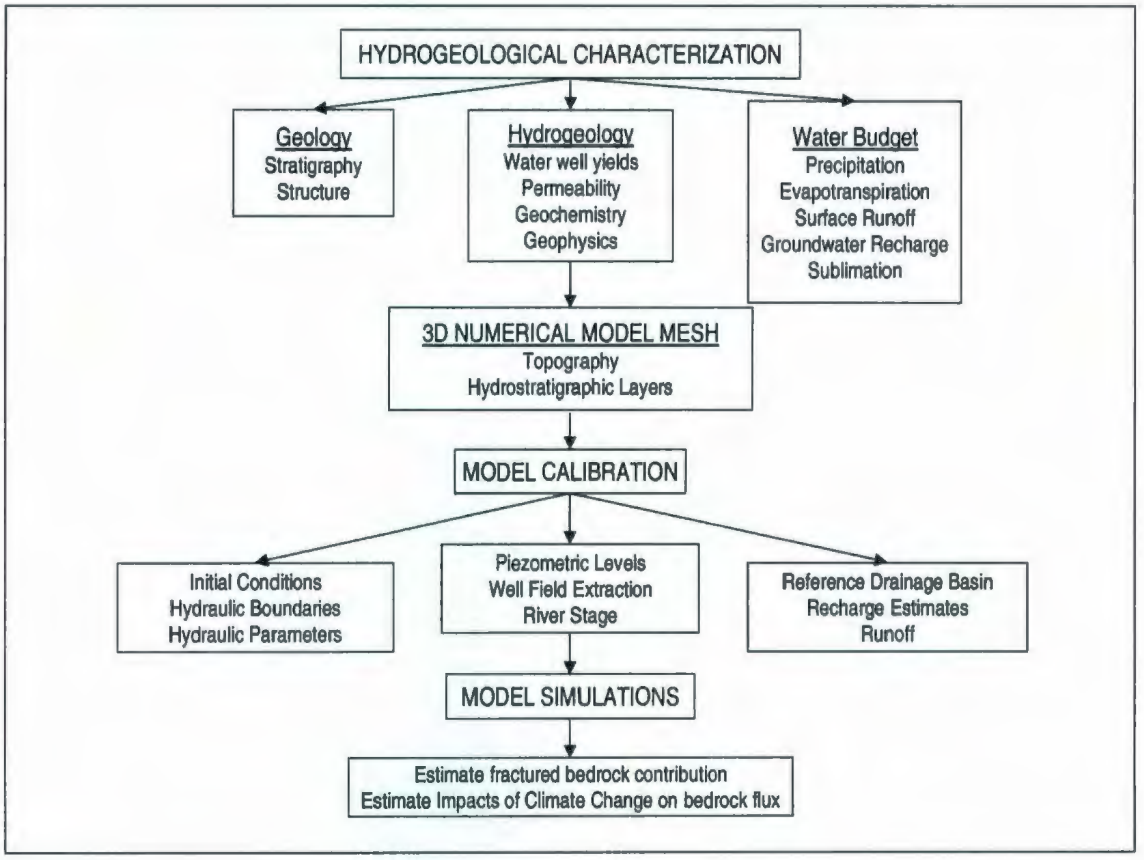

Figure 1.3. Flow chart of thesis activities.

geological units and the major structures in the model. Core from the three inclined boreholes give information on the fractures in the bedrock adjacent to the well field. Borehole packer tests are done to give estimates on fractured rock mass permeability and how it varies over and between each borehole.

Water samples are collected from the three inclined boreholes to characterize the local bedrock groundwater chemistry for comparison with historical bedrock groundwater chemistry. The Geological Survey of Canada logs each inclined borehole using a suite of geophysical tools. The data from the geophysical logs are used to

determine if there is variability in the geological and hydrogeological properties of the fractured bedrock.

Information needed to calculate the water budget is obtained from Environment Canada (2008), including daily precipitation and temperature dating back to 1953. Streamflow data (Water Survey of Canada, 2007) from a small drainage basin on the north side of the Saint John River is used to calculate groundwater recharge for model calibration.

The model area is chosen to include various hydraulic boundary conditions such as recharge zones, discharge zones and groundwater divides. A topographic database is imported into the 3D numerical model mesh, which gives the surface of the model area. The 3D distribution of the overburden materials and the fractured bedrock layers and structures are incorporated into the model mesh. Hydraulic parameters, as determined during the initial hydrogeological characterization, are assigned to each layer or zone. Data from the well field including drawdown and pumping rates are collected and used for the model calibration.

Model simulations are then run to: 1) determine how flux would vary under both natural flow and well field pumping conditions; and 2) determine how sensitivity to variations in recharge, as a possible result of climate change, impacts the quantity of the groundwater flux from the fractured bedrock into the overburden aquifer. It is anticipated that the results from the CWN multidisciplinary research program, including this study, will determine whether or not there exists a potential for long-or short-term water quantity issue depending on population increase and water use.

1.3 Previous Work

Historical Information on the Fredericton Well Field

Corbett (1993) presents the early history (1850 - 1993) of the well field's development including the infrastructure construction and the introduction of the water treatment system. In 1981, geochemical analyses show that the city's water supply is continuously exceeding the Canadian Drinking Water Quality Guidelines (Canadian Council of Ministers of the Environment [CCME], 1999) for manganese and iron concentrations. A water treatment plant using chlorine to reduce microorganisms and oxidize the manganese, sulphur dioxide to stabilize sulphur concentrations, and lime and soda ash during the pressure filtration process, is installed and successfully controls the manganese and iron levels (Corbett, 1993). In 2000, a Wellfield Protected Area Designation Order (New Brunswick Department of Environment, 2005) is developed in the Fredericton area. Additionally, research by the Geological Survey of Canada, the Bedford Institute of Oceanography, Queen's University, University of Calgary, and in particular, the Geology Department and the Civil Engineering Department of the University of New Brunswick, the city of Fredericton and engineering consultant groups, create a substantial database for the Fredericton Aquifer. Although approximately 937 boreholes are drilled in the Fredericton area, including the well field (Al et al., 2005), there is little to no data on the fractured bedrock underneath and adjacent to the aquifer.

Characterization of the Overburden Aquifer

ADI Ltd. (1982) describes the overburden aquifer, which consists of sand and gravel units, lacustrine silt and clay, and lodgement till (Fig. 1.4). The aquifer is formed by a glacial outwash sand and gravel unit and, based on historical borehole records, neither the overlying lacustrine silt and clay unit or the underlying till unit are continuous, providing 'window' opportunities for flowpaths and interaction between the surface river water and the fractured bedrock groundwater (ADI Ltd., 1982).

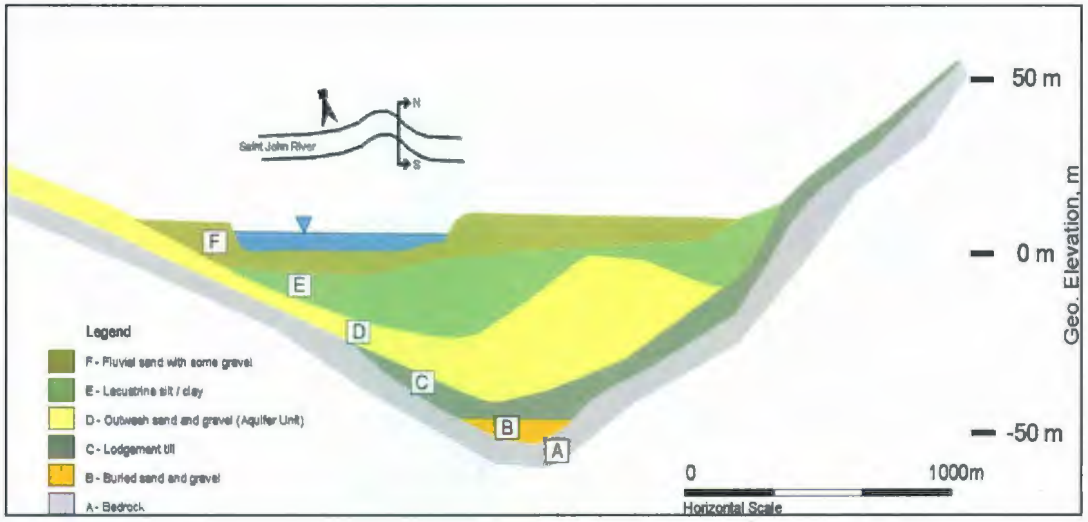

Figure 1.4. Overburden stratigraphy of the Saint John River valley in the Fredericton area (after Violette, 1990).

TerrAtlantic (2000) reviews the work of Hydrology Consultants Inc. (1981), McLean (1990), Violette (1990) and GEMTEC (1994), and presents a summary of the

hydrogeological characteristics of the aquifer, including results obtained from aquifer testing on the south east end of the aquifer.

Al et al. (2005) summarizes results obtained from the CWN multidisciplinary group investigation of the Fredericton aquifer, including results from Dawe (2005), Amskold (2005) and Nadeau (2003). Dawe (2005) studies the vertical velocity of the infiltrating surface water through the 'windows' in the aquitard unit and the stratigraphic controls influencing the flow paths. The vertical velocity of the infiltrating surface water through the 'windows' in the aquitard unit is in the range of 0.1 m/day to 5 m/day, based on the natural tracers, water temperature and radon (^{222}Rn), from nested monitoring wells sampled (Al et al., 2005). These vertical velocities suggest that the aquifer is vulnerable to surface contaminants.

Amskold (2005) investigates the geochemical variation that occurs along the infiltration pathway from the river to the aquifer, and determines that seasonal temperature variations within the groundwater affect the redox reactions occurring within the aquifer, which contribute to the increased concentration of manganese and iron.

Nadeau (2003) uses near-surface geophysical methods along the Saint John River and edge of the Wilmot Park well field to produce bathymetry-corrected apparent conductivity maps, seismic sections and resistivity depth sections. The interpreted sections show areas of the sand and gravel aquifer connected to the thin overlying surficial fluvial sand and subsequently the river (Nadeau, 2003). These sections, in addition to historical borehole records, confirm the presence of 'windows' and the direct hydraulic connection between the river and the aquifer unit (Al et al., 2005).

Bedrock Hydrogeology

Thomas (1991) notes that Fredericton, sitting within a river valley, is bounded on the north side by low hills (2 m asl up to 30 m asl) and on the south side by steep hills, (10 m asl up to 130 m asl) which slope towards the relatively flat flood plain (10 m asl) where the well fields and the downtown part of the city are located. The flood plain, which is underlain, in part, by the aquifer, starts from the edge of the riverbank and extends 1.5 km to the base of the slope. The upland areas are relatively flat terrain, which begin approximately 3 km on both the north and south side from the edge of the river. This topography favours the development of a groundwater flow system in which groundwater that recharges the bedrock in the upland areas will discharge at the low lying areas, either into the river, or the overburden aquifer. Artesian wells and springs are present along both slopes of the valley, which is evidence of groundwater flow towards the flood plain.

Francis (1981) reports on the characterization of a fractured sandstone aquifer on Prince Edward Island, which is part of the same Carboniferous bedrock system that underlies Fredericton. Borehole packer testing is used by Francis (1981) to estimate fractured rock mass permeability, and finds that fractures within the sandstone unit act as conduits for groundwater flow through the aquifer, but fractures in the siltstone and mudstone units become "smeared", producing a lower permeability layer. The borehole packer testing techniques and the calculations used by Francis were followed in this thesis work.

Loomer (2000) estimates the porosity of the bedrock in Fredericton (1.5 - 3.5 %) and carry out fracture trace analysis on selected outcrops. A dominant northeast trending fracture set and a northwest trending fracture set are identified in the sub-vertical to vertical fractures.

Bedrock Aqueous Geochemistry

Webb (1981), Thomas (1991), and Cunningham (2003) investigate the bedrock aqueous geochemistry in the Fredericton area. Webb (1981) analyzes samples of the bedrock groundwater for major ion concentrations. Webb considers that the resulting concentrations are possibly from weathering and/or the leaching of brackish water trapped in the fracture pore space and matrix of the sedimentary bedrock.

Thomas (1991) also samples local bedrock groundwater in an attempt to classify the groundwater and identify possible sources of recharge to the well fields. Geochemical analyses of the water samples collected from four bedrock groundwater wells do not show a consistent chemical signature.

Cunningham (2003) samples and analyzes local bedrock groundwater and groundwater from the production wells. Based on these geochemical analyses the bedrock groundwaters are classified as either Ca-Na-Cl-SO_4 or Na-Ca-Cl-SO_4 type. The production well water is classified as either a Ca-HCO_3 type, similar to the Saint John River chemistry, or a Na-HCO_3 type, possibly influenced by bedrock groundwater. Cunningham (2003) suggests that dissolution of the clays and altered feldspars in the bedrock potentially gives rise to higher Ca and Na concentrations, which might influence

the major ion groundwater geochemistry. Attempts to determine the contribution of bedrock water to the aquifer using the major ion data are inconclusive.

Aquifer Modelling

Violette (1990) completes a three-dimensional steady-state finite difference model of the Fredericton Aquifer to assess the impacts of increasing groundwater withdrawal from 25,000 m^3/day to 50,000 m^3/day. Violette (1990) concludes that this level of withdrawal would stress the aquifer.

The model constructed by Violette (1990) incorporated estimates of the hydrogeologic properties of the overburden materials, including the aquifer. Violette (1990) assumed that 66 % of the aquifer was supplied by the Saint John River through induced infiltration and 34% of the aquifer was supplied by precipitation infiltrating the surface to the aquifer through 'windows.' The groundwater contribution to the aquifer from the fractured bedrock was not considered. Since 1990, additional hydrogeologic data describing the overburden aquifer and underlying fractured bedrock have been collected. These data, along with more robust 3D flow and transport models, allow one to investigate the question whether there is a significant groundwater flux from the fractured bedrock to the overburden aquifer.

CHAPTER 2.0 GEOLOGICAL AND HYDROLOGICAL SETTING

The regional scale bedrock geology and tectonic divisions of New Brunswick have been compiled by the New Brunswick Department of Natural Resources and Energy (2000). A summary of the tectonic divisions is described below. The author refers the reader to the bedrock geology map of New Brunswick (New Brunswick Department of Natural Resources and Energy, 2000) for additional details regarding the regional geology.

The local scale bedrock and surficial geology and structure have been presented by authors including, but not limited to, Van de Poll (1973), Ball et. al (1981), McLeod and Johnson (1998), New Brunswick Department of Natural Resources and Energy (2000), Whitehead (2001) and Park and Whitehead (2003). A brief review of their work is presented below.

2.1 Regional Geology

New Brunswick is situated in the northeast trending Appalachian Mountain system (Whitehead, 2001) and lies in the tectonic divisions outlined in Figure 2.1 (New Brunswick Department of Natural Resources and Energy, 2000). The northwest region of New Brunswick (Fig 2.1) contains a series of belts from the Late Ordovician to Early Devonian. Moving southeast towards the Bay of Fundy, the Ordovician to Devonian Gander Zone and Dunnage Zone are present. Adjacent the Dunnage Zone is the Late Ordovician to Early Devonian Fredericton Belt that borders the Late Devonian to Permian Maritimes Basin. The Maritimes Basin unconformably overlies the central and

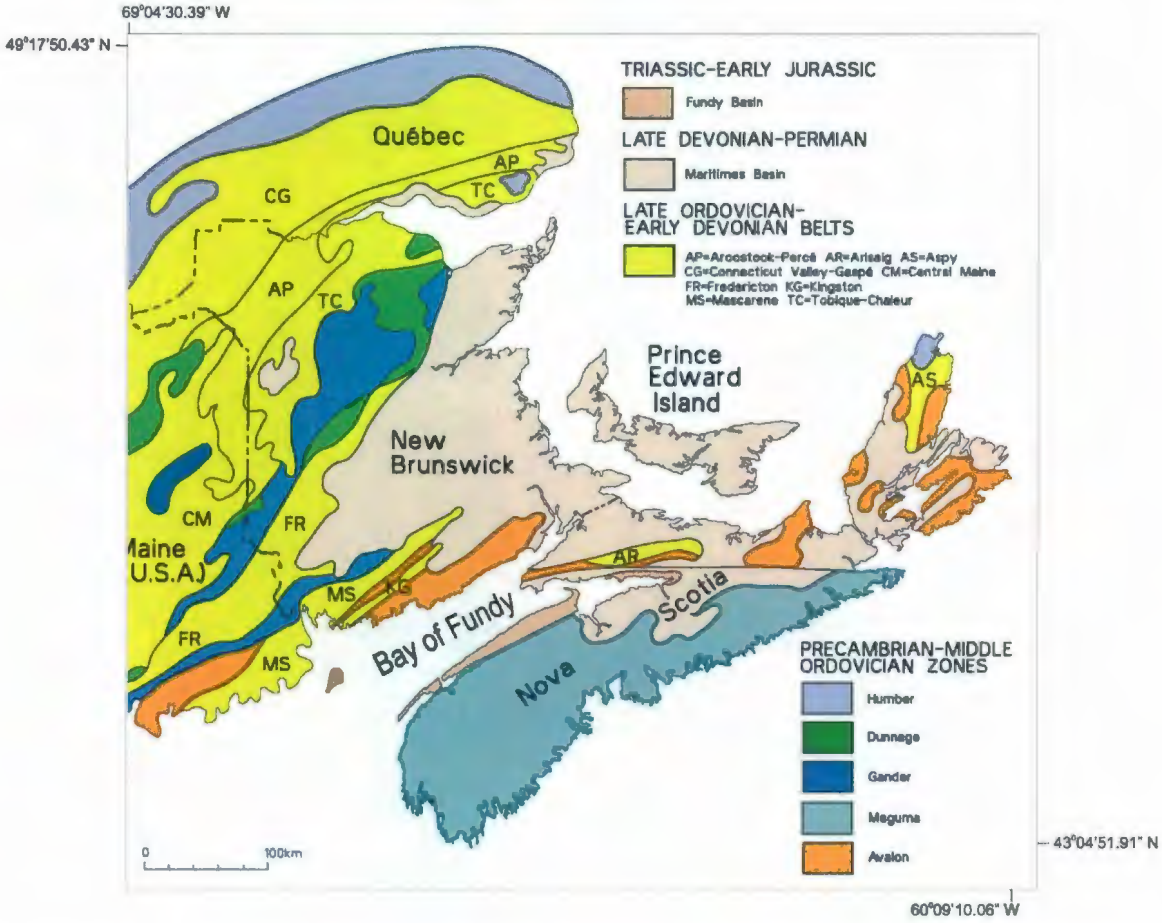

Figure 2.1. Tectonic Divisions of New Brunswick (New Brunswick Department of Natural Resources and Energy, 2000).

eastern portion of New Brunswick (Whitehead, 2001) and is the major stratigraphic unit of New Brunswick (Van de Poll, 1973). Continuing southeast, the Gander Zone adjoins the Late Ordovician to Early Devonian Mascarene Belt, which borders the Avalon Zone (New Brunswick Department of Natural Resources and Energy, 2000).

The upper bedrock geology of Fredericton and the surrounding area is part of the Maritimes Basin, comprised mainly of Carboniferous terrestrial sediments (New

Brunswick Department of Natural Resources and Energy, 2000) including red and grey conglomerate, sandstone, siltstone and shale (McLeod and Johnson, 1998).

2.2 Local Bedrock Geology, Structural Features and Surficial Geology

2.2.1 Local Geology

The bedrock geology of the Fredericton area (Fig. 2.2) consists of Carboniferous red and grey, very fine to coarse–grained, sandstone and conglomerates and minor red to grey clay, shale, and siltstone of the Pictou Group (~309 Ma) (Ball et. al, 1981) underlain by sedimentary units of the Cumberland Group (approximately ca. 321 – ca. 314 Ma). The Cumberland Group is underlain by Carboniferous sedimentary units and volcanic flows of the Mabou Group (approximately 330 Ma – 325 Ma) that unconformably overlie the basal unit of Silurian meta-wackes and interbedded shales and siltstones from the Kingsclear Group (428 Ma to 419 Ma) (Whitehead, 2001).

The Pictou Group is observed in Odell Park, Fredericton, NB in outcrop and is interpreted from the drilling of three inclined boreholes as part of this thesis work. Further discussion of this fieldwork is in Chapter 3. The drill core is described in the field as fractured, cemented grey sandstone containing thin coal laminae markers and minor pyrite grains, underlain by red siltstone and interbedded red sandstone. The Pictou Group unit extends to depths of over 1000 m and the beds dip 4 to 6 degrees northeast to near horizontal and strike northwest (Ball et. al, 1981). In the numerical model, discussed in Chapter 4, the Pictou Group bedrock is divided into ten layers, to represent the cyclic

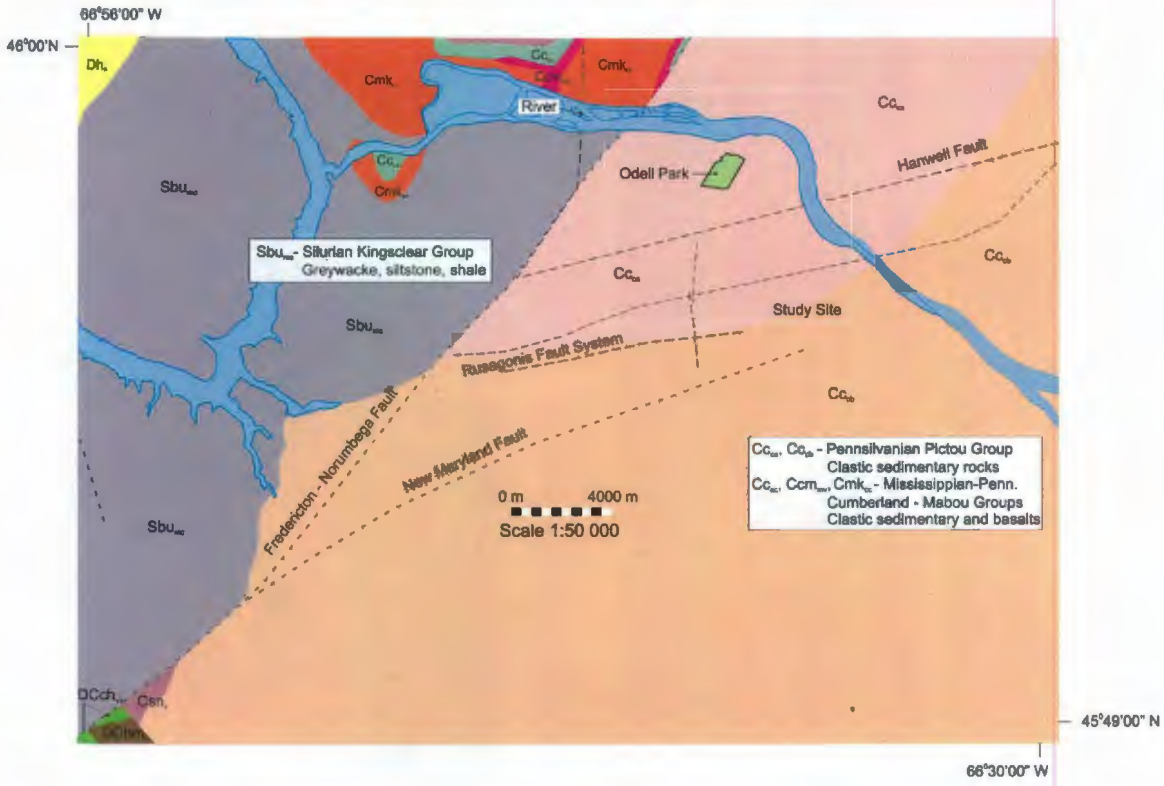

Figure 2.2. Geology of Fredericton Area (Modified from Whitehead (2001), Loomer (2001) and McLeod and Johnson (1998)).

siltstone and sandstone units (Van de Poll, 1973) and extended to depths – 500 m below sea level (bsl).

2.2.2 Structural Features

There are two structural geology trends in the Fredericton area. The first is a dominant northeast trend, and the second is a less obvious northwest trend. The west portion of the Carboniferous Pictou Group is faulted against the Silurian Kingsclear Group (Fig. 2.2) along the northeast trending Fredericton-Norumbega Fault (McLeod and Johnson, 1998). The fault acts as a geological boundary between the Carboniferous and

Silurian units and is a regionally significant fault zone (Park and Whitehead, 2003). This fault zone experienced strike-slip motion following the formation of the Kingsclear Group and dip-slip motion during and following the formation of the Mississippian and Pennsylvanian Carboniferous units, which include the Pictou Group (Park and Whitehead, 2003). It is understood this dip-slip motion propagates the northeast structural trend throughout the Pictou Group (Park and Whitehead, 2003).

The orientations of fractures mapped by Loomer (2001) and by the author in 2003 and 2004 mimic these dominant trends. The bedding planes dip approximately five degrees from the horizontal to the east and the sub-vertical to vertical fracture sets run predominantly in a northeast or northwest direction.

Parsons (1972) discusses methods to characterize the fracture geometry and the fracture flow behavior of the Pictou Group sandstone on Prince Edward Island. Parsons (1972) discusses two approaches, concerning scale, to interpret hydrogeological features of fractured rock. One, best applied to a small-scale problem, is the discontinuum approach, which uses known fracture geometries and flow behavior of discrete fractures. The second, more practical and best applied to large-scale problems, is the continuum approach, also referred to as an equivalent porous medium approach. This method states the fractured mass, geometry and flow behavior is hydraulically comparable to that of an intergranular porous body (Domenico and Schwartz, 1990). For this study, the continuum approach is used to represent the matrix and fractures in the model domain.

2.2.3 Surficial Geology

Violette (1990) describes the surficial geology of Fredericton consisting of unconsolidated sediments overlying the fractured bedrock in the river valley (Fig. 1.4). A basal sand and gravel unit (apparently discontinuous) is in direct contact with the bedrock surface. This sand and gravel unit is overlain by a discontinuous lodgement till, which in places, is also in direct contact with the bedrock (Fig. 1.4). The outwash sand and gravel unit, an esker-like body, forms the Fredericton Aquifer from which the city extracts its water supply. This aquifer overlies the lodgement till and in turn, is overlain by a lacustrine silt and clay unit (Fig. 1.4). The top layer of sediment is a fluvial sand and gravel unit (Violette, 1990) and is thought to be discontinuous under the riverbed and over the well field.

The overall structure of the aquifer (Fig. 2.3) is a linear body of sediments (e.g., eskers), running southeast below the city and following the general drainage direction of the river valley floor (TerrAtlantic, 2000). The esker body ranges up to 30 m thick and thins laterally outwards approximately 250 m to the northeast and southwest. The overlying lacustrine silty clay layer acts as a semi-confining layer and can range up to 40 m thick but is eroded completely in some areas (TerrAtlantic, 2000). These eroded areas connect the outwash unit below (the Fredericton Aquifer) to the sand and gravel unit above and consequently expose the aquifer to induced river infiltration or direct recharge from precipitation (TerrAtlantic, 2000). These eroded areas are commonly called "windows" (ADI Ltd., 1982). Of particular interest to this study are the windows through the till layer that allow direct contact between the aquifer and the underlying bedrock.

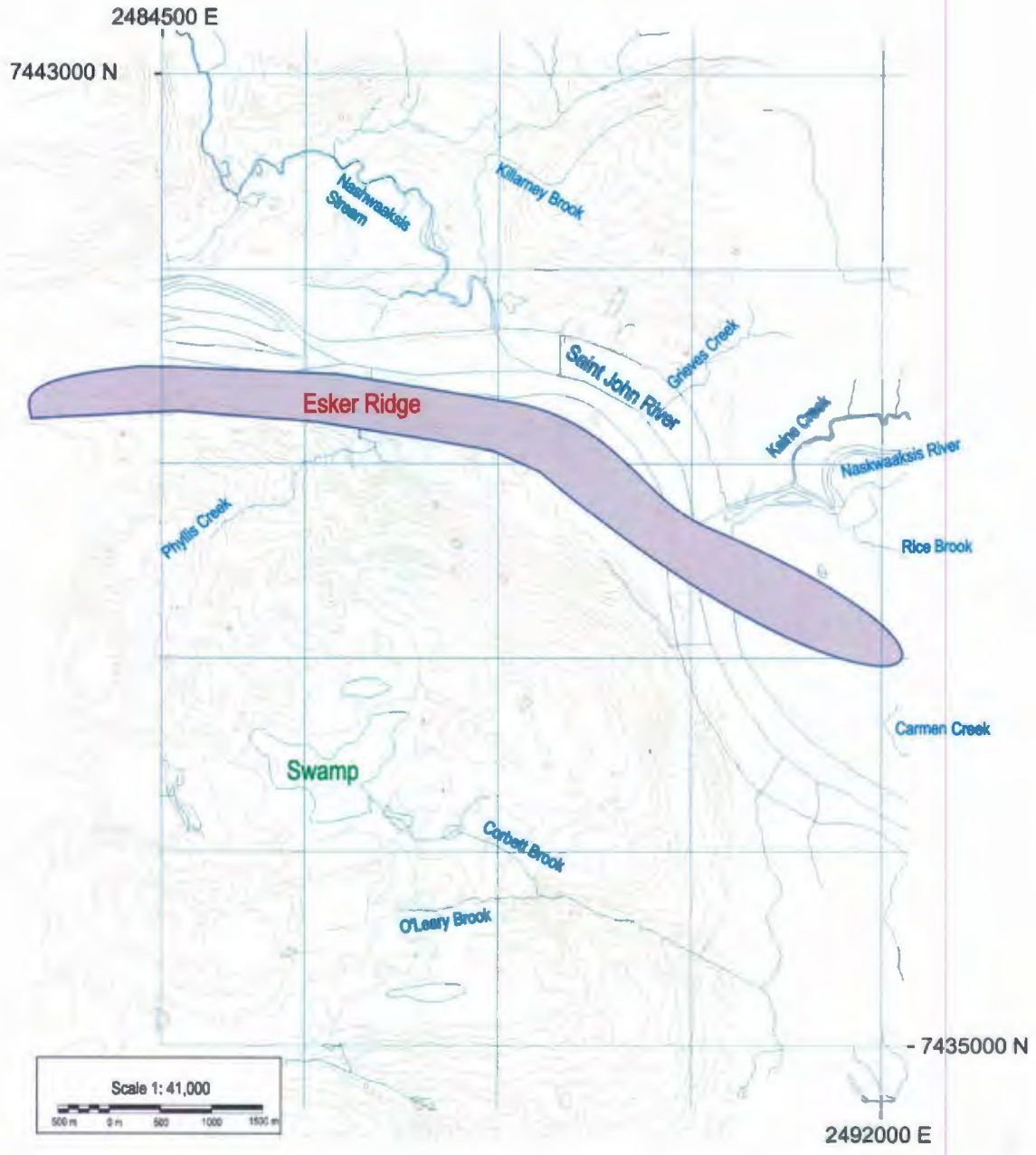

Figure 2.3. Hydrological surface features, including the esker location, in Fredericton. Modified from TerrAtlantic Engineering Ltd. (2000) and Touratech-QV-Navigator (2003).

2.3 Topography and Surface Water Hydrology

The surface elevation of the Fredericton river valley area ranges from 130 m asl to +/- 2.5 m asl along the Saint John River (Fig. 1.2). At Fredericton, the Saint John River is approximately 750 m wide and is bounded on both sides by low lying terrain, subject to flooding, as happened in the spring of 2008. The north and south downtown areas lie in this flood plain (< 15 m asl) that is approximately 1.0 km wide on the north side and 1.5 km wide on the south side. From the 15 m asl elevation, the slope of the terrain increases to elevations of 120 m asl on the north side of the river and to 130 m asl on the south side of the river. At these elevations, a relatively flat lying upland area exists and extends at least 10 km away from Fredericton in the southwest and northeast direction.

The surface water hydrology is directly influenced by the local and regional topography (Fig. 2.3). The upland area contains swamps, which reflect an elevated water table condition and forms recharge zones. Because these recharge zones extend back from the Fredericton area for 10's of km's, they are part of the local and regional scale hydrology. In the model domain, these upland areas are drained into the Saint John River by the Nashwaaksis River, the Nashwaaksis Stream, creeks (e.g., Phyllis, Grieves, Kaine, Carman) and brooks (e.g., Corbett, O'Leary, Rice, Killarney (Fig. 2.3).

This valley-upland terrain favours the development of a groundwater flow system in which the groundwater that recharges the bedrock in the upland areas will discharge at the low-lying areas, either into the river, or into the overburden aquifer. Flowing artesian wells completed in bedrock (e.g., two of the three inclined boreholes in Odell Park) and natural springs located on both sides of the river, along the approximately 25 m asl

topographic contour, indicate that the piezometric level in the aquifer at depth is above the ground surface. This supports the idea that the groundwater gradients created by the valley-upland terrain result in groundwater flow from the fractured bedrock, towards the aquifer and river (Thomas, 1991).

2.4 General Water Balance

2.4.1 Precipitation and Temperature

Meteorological data, including precipitation and temperature, are obtained from Environment Canada (2008) for the time period between 1953 and 2001. During this period, Fredericton's average temperatures in the year range between -15.4 ^{o}C and 25.6 ^{o}C. Box plots and normal curves of the maximum, minimum and mean temperatures for Fredericton are in Figure A.1 and Figure A.2, respectively, in Appendix A. Annual precipitation ranges from 690 mm/yr to 1521 mm/yr, with an average of 1101 mm/yr (Fig. 2.4). During the low precipitation cycles (years 1955-1971 and 1984-2001), annual precipitation ranges from 690 mm/yr to 1243 mm/yr with an average of 1036 mm/yr. Consecutive years of lower precipitation could impact the sustainability of the aquifer yield. During the high precipitation cycle (years 1972-1984), annual precipitation ranges from 1010 mm/yr to 1521 mm/yr with an average of 1241 mm/yr. There is a difference of approximately 200 mm/yr between the high and low precipitation cycles.

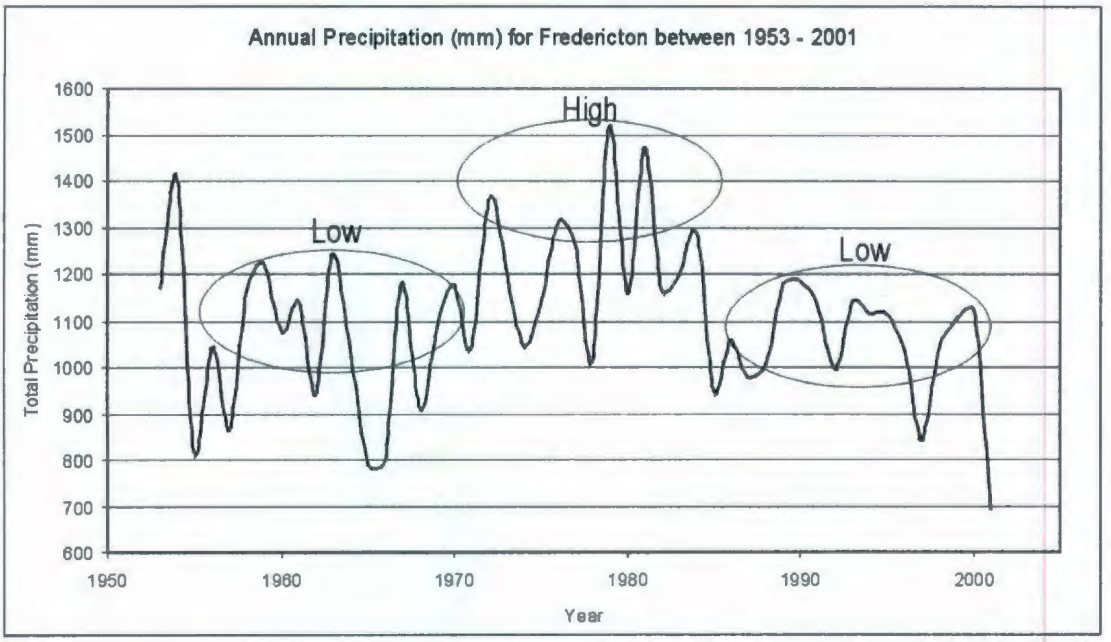

Figure 2.4. Annual precipitations showing high and low cycles.

The average annual snowfall for years 1953-2001 ranges from 139 cm/yr to 469 cm/yr, with an average of 276 cm/yr. The water equivalent of the snowfall component is an assumed 10:1 ratio (Environment Canada, 2008) so that the average annual snowfall of 276 cm represents 276 mm of rainfall. A box plot showing the monthly range of precipitation, rainfall and snowfall amount is in Appendix A, Figure A.3.

Mean monthly temperature and precipitation data are used in the Thornthwaite and Mather (1957) method to calculate the water balance. This method requires: 1) a record of mean monthly or daily air temperature; 2) a record of mean monthly or daily precipitation; 3) computational and conversion tables prepared for various values of water holding capacity; and 4) the water holding capacity of the depth of soil for which

the water balance was to be computed (75 mm) and 5) the latitude of Fredericton (45.9635°) in the northern hemisphere.

The water holding capacity of soil depends on the soil type, soil structure, vegetation type and age of the vegetation growing in the soil (Thornthwaite and Mather, 1957). For the Fredericton area it is assumed the surficial soil layer consists of fine, sandy loam (available water 150 mm/m) and the vegetation is shallow rooted plants (e.g., grass, root zone 0.50 m). The corresponding applicable soil moisture retention used for the calculations is 75 mm.

Calculations are completed for the heat index (I), potential evapotranspiration (PE), accumulated potential water loss, soil moisture storage, actual evapotranspiration (AE), moisture deficit and surplus, rain and snowmelt runoff and total moisture detention for years between 1953 and 2001. The data set is in Tables A.1A to A.1M and Table A.2, Appendix A.

2.4.2 Potential and Actual Evapotranspiration

Thornthwaite and Mather (1957) defines the potential evapotranspiration (PE) as the rate water loss will occur if there is a constant supply of water available for vegetation. The actual evapotranspiration (AE) is the rate water loss does occur in a particular setting. Evapotranspiration rates are calculated for years 1953 to 2001 using the Thornthwaite and Mather procedures and associated tables (1957). This method assumes that the potential and actual evapotranspiration is dependent on meteorological conditions, and does not take into account vegetation density or maturity (Fetter, 2001).

Despite the limitations imposed by these assumptions, the method is used and produces results similar to other methods. The data required for these analyses are obtained from Environment Canada (2008).

Previous hydrological studies for southern New Brunswick indicate a PE rate between 420 mm/yr (Michaud et. al., 2004) and 533 mm/yr (The National Atlas of Canada, 1974). Using the Thornthwaite and Mather procedures (1957) for Fredericton, the PE calculated is in the range from 524 mm/yr to 609 mm/yr. The AE calculated is in the range from 380 mm/yr to 578 mm/yr. Computing the rates for each season shows that >90% of the AE occurs between the months of April and September. A plot of PE and AE versus precipitation for 2001 (Fig. 2.5) indicates significant seasonal variation. As well, the PE, which occurs under climatic conditions if there is unlimited soil moisture, is higher than the AE, which occurs under the actual climatic and soil moisture conditions. For the purpose of this study, the AE is used in the conceptual model.

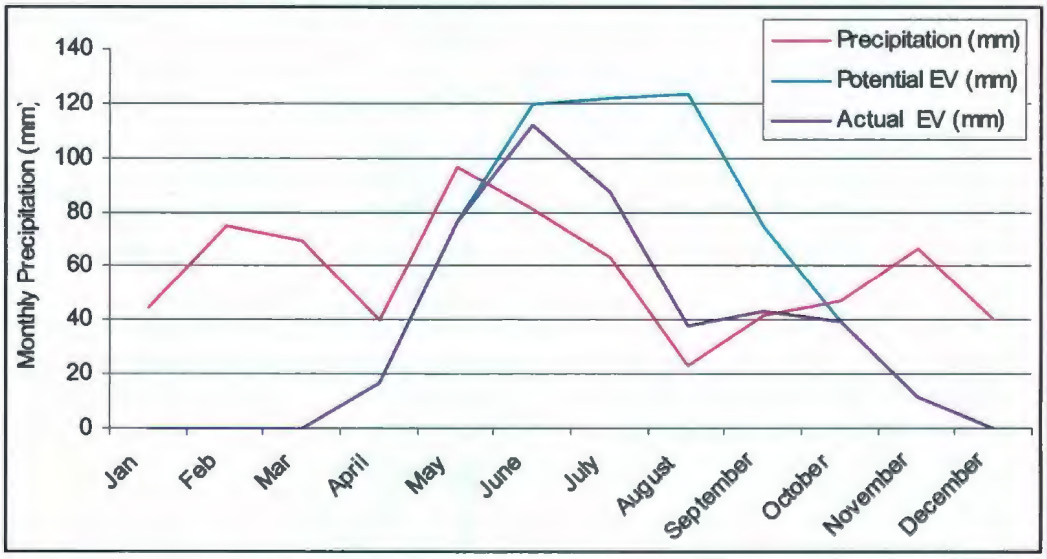

Figure 2.5. Potential and actual evapotranspiration rates for 2001.

2.4.3 Surface Runoff

Previous hydrological studies for southern New Brunswick report surface runoff rates between 532 mm/yr (Michaud et al., 2004) and 711 mm/yr per year (The National Atlas of Canada, 1974; Fig. A.4, Appendix A). Thornthwaite and Mather (1957) mention for large watersheds with surplus water available for runoff in any given month, approximately 50% of this water is retained on the watershed until the following month. The total runoff calculated for the years between 1953 and 2001 include the sum of the water surplus runoff and the snowmelt runoff. The total surface runoff is on average 495 mm/yr, representing 45% of the annual precipitation. Of this, 274 mm/yr is from the total snowmelt runoff. The minimum total surface runoff is 261 mm/yr with 138 mm/yr being snowmelt runoff. The maximum total surface runoff is 778 mm/yr with 465 mm/yr being snowmelt runoff. For the water balance and conceptual model, 495 mm/yr is used.

2.4.4 Groundwater Recharge

Previous studies indicate an annual groundwater recharge for southern New Brunswick as 148 mm/yr (Michaud et al., 2004) and for Fredericton as 100 mm/yr on the slope of the hill to 400 mm/yr (TerrAtlantic, 2000) in the relatively flat flood plain where the well fields and the downtown part of the city are located.

The Meyboom method, as described in Domenico and Schwartz (1990), was used to determine the total potential groundwater discharge and the groundwater recharge. The Meyboom method is a streamflow hydrograph analysis (Fig. 2.6) that estimates the

groundwater recharge availability using stream discharge. Using plots similar to Figure 2.6, Equation 2.1 and Equation 2.2 were used for the calculations.

$$Q_{tp} = Q_o \times t_1 / 2.3 \qquad \text{(Equation 2.1)}$$

where, Q_{tp} = total potential groundwater discharge
Q_o = baseflow at start of recession curve
t_1 = time for baseflow to drop from Q_o to $0.1Q_o$

and

$$Q_t = Q_{tp} / 10^{(t/t_1)} \qquad \text{(Equation 2.2)}$$

where, Q_t = potential baseflow remaining some time (t) after the start of the baseflow recession
t = time of interest

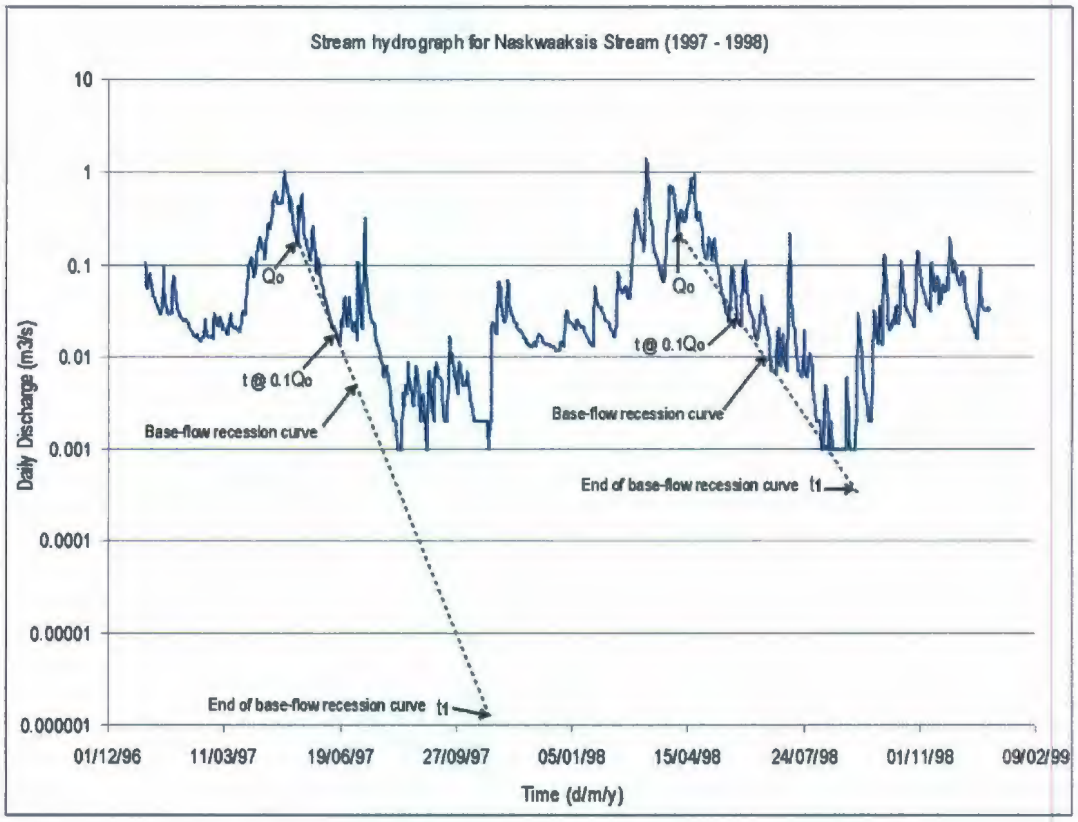

Figure 2.6. Streamflow hydrograph of the Nashwaaksis Stream 1997-1998.

The Meyboom calculations assume the catchment area has no regulated streamflow (e.g., a dam) and the contribution from snowmelt is not considered. The groundwater recharge is equal to the total potential baseflow remaining at the end of the first baseflow recession, subtracted from the total potential groundwater discharge for the beginning of the next year's recession (Fig. 2.6).

Daily stream discharge data from the middle branch of the Nashwaaksis Stream covering a drainage area of 5.7 km^2 are obtained from the Water Survey of Canada (2007) between 1978 and 1982 (high precipitation cycle) and 1997 to 2004 (low precipitation cycle). In the high precipitation cycle between the years 1978 and 1982, groundwater recharge is calculated to range from 35 to 95 mm/yr. In the low precipitation cycle between the years 1997 and 2004, the groundwater recharge is calculated to range from 36 mm/yr to 103 mm/yr. If we assume 10 to 15% of the annual precipitation is groundwater recharge (Davies, 1995) it is approximately 69 mm/yr to 228 mm/yr. Based on the range from 35 mm/yr to 228 mm/yr, a value of 110 mm/yr of groundwater recharge is used for the conceptual model. The streamflow hydrographs for each year are in Figure A.5 to Figure A.7 in Appendix A. An example calculation from the hydrograph analysis is in Appendix A. An additional stream discharge graph in the form of duration curves is attached in Appendix A in Figure A.8. Figure A.8 displays for approximately 80% of the time, flow exceeds 0.01 m^3/s along the Nashwaaksis Stream.

2.4.5 Sublimation

Sublimation is the evaporation of snow (solid ice to vapor) when temperatures are at or below 0°C and can occur from the surface and/or in blowing snow conditions (National Operational Hydrologic Remote Sensing Centre [NOHRSC], 2004). The process depends on the amount of direct sunlight available, groundcover features, latitude, elevation and climatic conditions (NOHRSC, 2004). Sublimation is considered for the water balance calculation for Fredericton because temperatures from December to March typically average below 0°C. Sublimation data are obtained from the NOHRSC Interactive Snow Information (NOHRSC, 2004) and range from ~0.5 mm/yr to ~9.0 mm/yr of water equivalent in the surrounding Fredericton area. This represents approximately 0.3% to 2 % of the total estimated water equivalent of snowfall. For the water balance and conceptual model, the high end of the range, 9 mm/yr, is used because this value was concentrated in the Fredericton area.

2.4.6 Water Balance Summary

A summary of the estimated general water balance for the Fredericton area is listed below, using Equation 2.4: Input = Output (Equation 2.4)

where,

Input =	Precipitation	=	1101 mm
Output =	Evapotranspiration	=	- 487 mm
	Surface Runoff	=	- 495 mm
	Groundwater Recharge	=	- 110 mm
	Sublimation	=	- 9 mm
			-1101 mm

This is an average estimate of the water balance, which will naturally change with variability in the precipitation and weather conditions occurring in any individual year. Compared to the total input precipitation, the output evapotranspiration represents 44.2%, surface runoff represents 45%, groundwater recharge represents 10% and sublimation represents 0.8%. There are consecutive years of lower and higher precipitation, which affect the remaining output fluxes and how much groundwater recharge becomes available to supply the overburden aquifer.

CHAPTER 3.0 SUBSURFACE FIELD INVESTIGATION

3.1 Drilling

The subsurface field investigation was initiated in August 2003 to evaluate the geological, hydrogeological, geochemical, and geophysical characteristics of the fractured bedrock units underlying Fredericton. A preliminary investigation by the author involved reviewing aerial photographs, topography, geology, and hydrology maps to select three inclined borehole drill locations (BH01, BH02, BH03). Odell Park (Fig. 3.1) was chosen as the drill site for a number of reasons: 1) approval by the City of Fredericton; 2) drill locations are clear of underground utilities; 3) accessibility; 4) elevation position between 10 and 30 m asl; 5) location between the discharge (Saint John River) and recharge (upland area) of the aquifer; and 6) anticipation of less overburden to reach bedrock.

The drilling company Boart Longyear used a 538 diesel drill rig with an NQ/NW triple tube core barrel to drill the inclined boreholes (Plate C.1 in Appendix C). Orientation, length, corrected depth, diameter and the amount of overburden encountered for the boreholes, BH01, BH02 and BH03 are listed in Table 3.1. The core was photographed and logged for geology, fracture frequency, fracture orientation, total core recovery and rock quality designation (RQD).

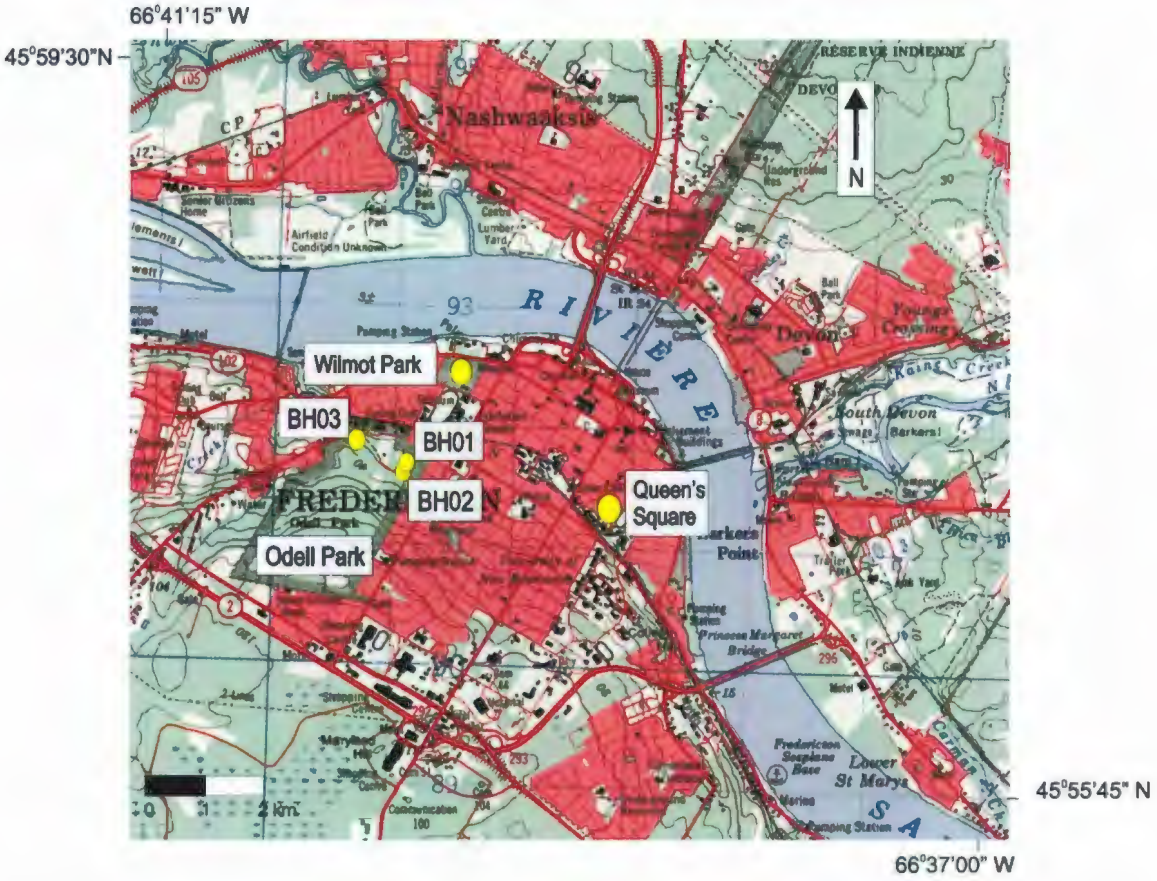

Figure 3.1. Location of Wilmot Park, Queen's Square and borehole BH01, BH02 and BH03 within Odell Park, Fredericton. Modified from Touratech-QV-Navigator (2003).

Table 3.1. Data on test boreholes.

Borehole	Easting/ Northing Zone 19 WGS 84	Orientation	Length	Vertical Depth	Diameter of BH	Overburden Vertical Depth	Total Recovery	RQD
No.	(m)		(m)	(m)	(mm)	(m)	%	%
BH01	681160 E / 5091849 N	200° SW / 51°	72	56	45 I.D / 76 O.D	16	98	74
BH02	681144 E / 5091845 N	250° SW / 51°	50	39	45 I.D / 76 O.D	14	99	75
BH03	680925 E / 5092116 N	S 030° E / 45°	58	41	45 I.D / 76 O.D	9	95	79

3.1.1 Core Logging

The geological features of each borehole were logged and photographed by the author. Geological descriptions are listed in Table 3.2 illustrated in Figure 3.2. The photographed logs are attached in Appendix B in Plate B.1, B.2, and B.3.

Table 3.2. Geologic descriptions of inclined boreholes BH01, BH02, and BH03.

Geologic description of BH01.		
Description	Start* (meters, m)	Stop* (meters, m)
Casing (overburden)	0	17.58
Bedrock – Grey, fine grained well-sorted sandstone. Minor coal and pyrite intermittent.	15.64	46.94
Bedrock – Greenish/grey grades to red siltstone w/ mudclasts.	46.94	48.00
Bedrock – Red, massive siltstone.	48.00	72.24 (end of hole)
* Lengths not corrected for borehole angle. Measurements represent length, not depth. Note: Borehole caved at 63 m length.		
Geologic description of BH02.		
Description	Start* (meters, m)	Stop* (meters, m)
Casing (overburden)	0	14.02
Bedrock – Grey, fine grained well-sorted sandstone. Minor coal.	13.56	25.30
Bedrock – Red siltstone (10 cm).	25.30	25.40
Bedrock – Grey, fine grained well-sorted sandstone.	25.40	44.50
Bedrock – Red, massive siltstone.	44.50	49.99 (end of hole)
*Lengths not corrected for borehole angle. Measurements represent length, not depth. Note: Borehole caved at 44 m length.		
Geologic description of BH03.		
Description	Start (meters, m)	Stop (meters, m)
Casing (overburden)	0	9.64
Bedrock – Grey, fine grained, well sorted sandstone.	8.23	35.97
Bedrock – Red, massive siltstone, minor silty red sandstone.	35.97	44.81
Bedrock – Red sandstone.	44.81	47.24
Bedrock – Red massive siltstone.	47.24	57.61 (end of hole)
* Lengths not corrected for borehole angle. Measurements represent length, not depth. Note: Borehole caved at 10 m length in 2003. Re-drilled in 2004.		

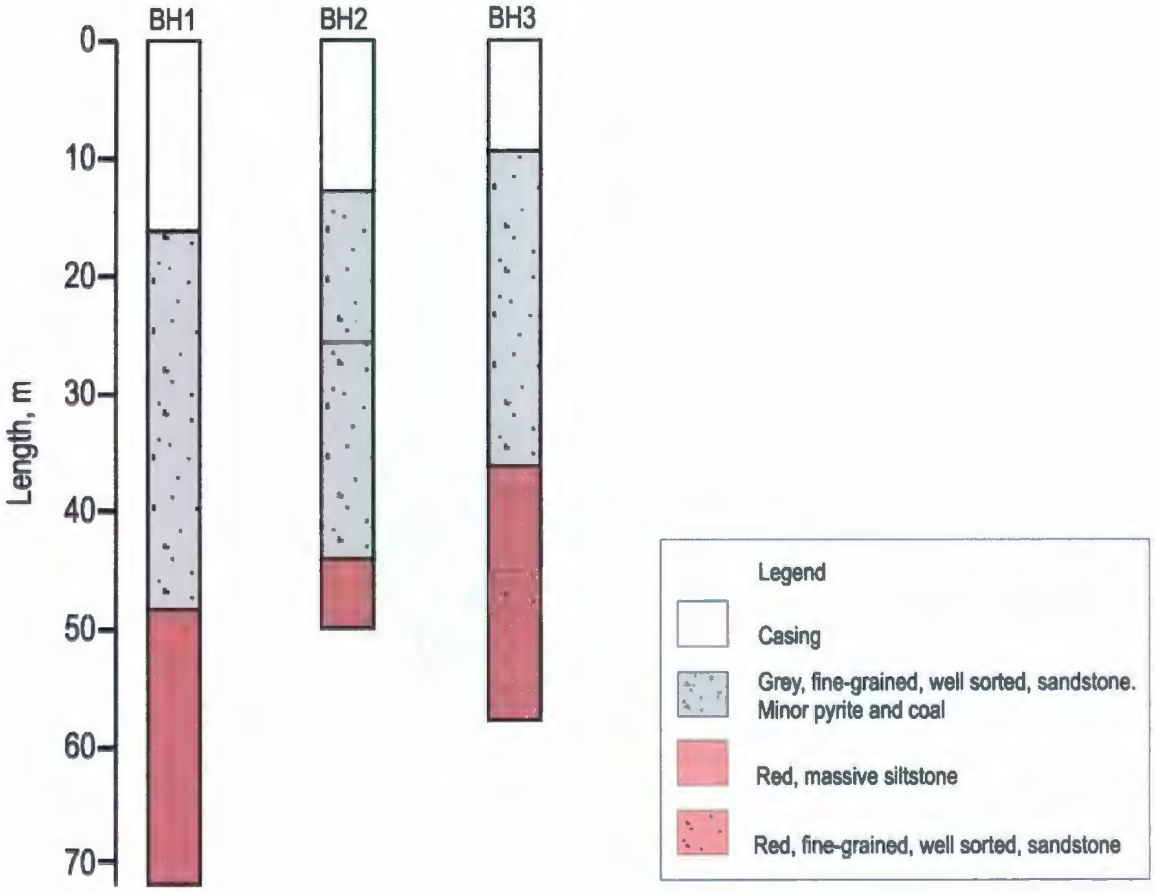

Figure 3.2. Inclined geological borehole logs.

3.1.1 Fracture Logging

A fractured rock system consists of a rock mass with primary porosity and permeability and a network of cracks, joints, fractures and/or shear zones that create, and can contribute to, the secondary porosity and permeability of the rock system (Anderson and Woessner, 1992). Depending on the aperture size (fracture opening), permeability (fracture connectivity) and porosity (pore spaces between grains), the fractures have the

potential to act as conduits for groundwater flow into the aquifer (Francis, 1981). The borehole locations in this study were chosen to obtain a representation of the fracture characteristics of the bedrock underlying Fredericton.

The orientations of the inclined boreholes were chosen to intersect the bedding planes and fracture sets, mapped in outcrop in Odell Park. The bedding planes dip approximately five degrees from the horizontal to the east and the sub-vertical to vertical fracture sets run predominantly in northeast or northwest directions. Results from the outcrop fracture mapping exercise in Odell Park are tabulated in Appendix B in Table B.1.

For the fracture logging exercise, each fracture intersecting the core is described as either occurring naturally, induced through drilling, or uncertain. It is noted whether the aperture is opened or closed, whether the fracture shape is planar, curved or irregular and the type of strata in which the fracture occurs. The colour, type of weathering if visible on the fracture plane and a roughness grade between 1 and 5 (i.e., how rough a fracture plane is with 1 being smooth and 5 being very rough) is recorded for each fracture. The hardness, a range also between 1 and 5 (i.e., with 1 being soft and 5 being hard), the apparent dip direction (beta) of the fracture, and angle of apparent dip (alpha) of the fracture are also documented.

Fracture descriptions are necessary for understanding how hydraulically conductive a fracture may be. A naturally open aperture will have higher hydraulic conductivity than a closed one. A planar and low roughness fracture will have higher hydraulic conductivity than an irregularly shaped and very rough fracture (Domenico and

Schwartz, 1990). A visibly weathered fracture surface indicates a hydraulically conductive zone. The colour of the weathering surface can be indicative of chemical reactions (e.g., brown or reddish surface can indicate iron oxidation reactions). Results of the detailed fracture logging for BH01 are listed in Table B.2 in Appendix B. The fracture analysis tools used in the field are shown in Figure B.1 in Appendix B. The fracture angle frequency for each inclined borehole is shown in Figure B.2 to Figure B.4 in Appendix B. The fracture frequency for each inclined borehole is shown in Figure B.5 to Figure B.7 in Appendix B.

3.1.2 Total Core Recovery and Rock Quality Designation (RQD)

Total core recovery is the sum of lengths of core, divided by the total length of core drilled. Referring to Table 3.1, the total recovery ranges from 95 to 99%, indicating an excellent core recovery rating for logging and analysis.

The rock quality designation (RQD) is defined as the cumulative length of core pieces longer than 10 cm, divided by the total length of the core drilled (Johnson and DeGraff, 1988). Core loss and/or the presence of <10 cm core results in a decreasing RQD rating which is assumed to be caused by fractures, shearing, faulting or weathering within the rock mass (Johnson and DeGraff, 1988). Rock quality designation is also affected by the orientation of the core to the fractures. Additionally, RQD percentages are inversely proportional to fracture frequency; an increase in fracture frequency would result in a decrease in RQD. Referring to Table 3.1, the RQD for each inclined borehole ranged from 74 to 79%, a fair to good rating of RQD.

3.2 Determining Transmissivity and Hydraulic Conductivity Through Borehole Packer Testing

3.2.1 Borehole Packer Test Method

A borehole double packer test involves sealing off portions of an open borehole with inflatable packers and monitoring downhole pressures and flowrates into, or naturally flowing out of, the cavity (Fig. 3.3). The data obtained from the test are used to calculate the transmissivity (Equation 3.1) and hydraulic conductivity (Equation 3.2) of the geological unit at that particular depth interval. The calculations are discussed further in Section 3.2.2.

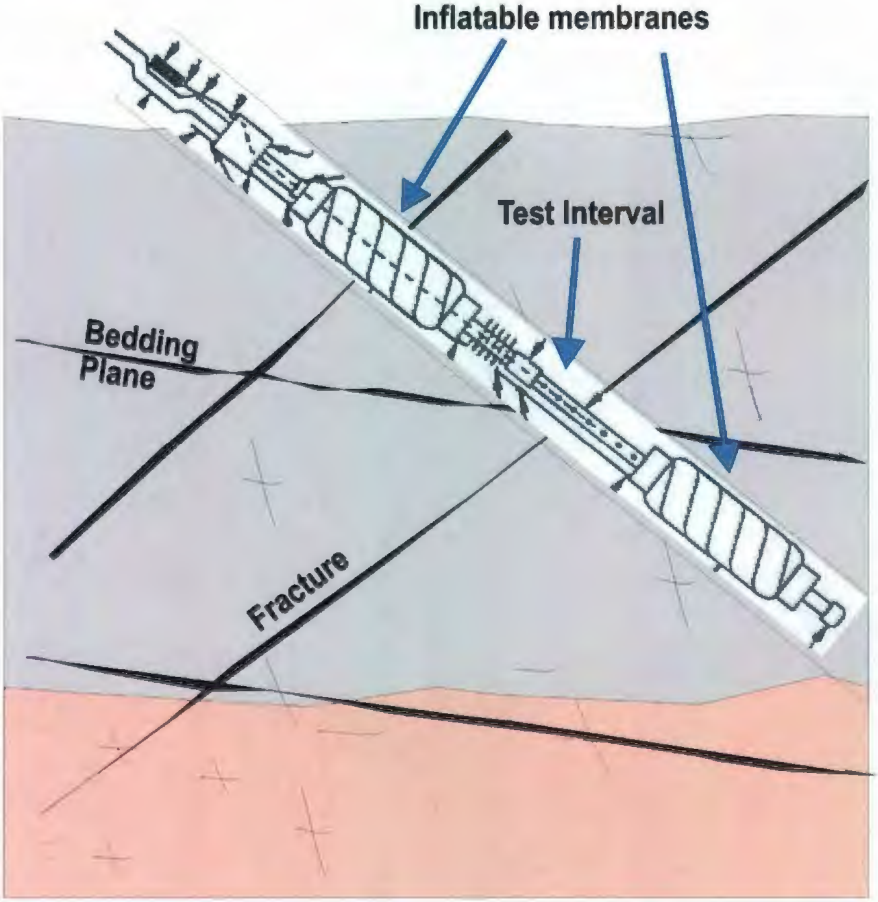

Figure 3.3. Schematic downhole dual-packer test assembly.

Borehole packer tests were completed on the inclined boreholes in 2003 and again in 2004 using a high flow, low flow, or through-the-bit method (Table 3.3). The high flow configuration was used initially, to identify the flow rates along the length of the borehole. The water meter dial in this configuration was able to register a change of 0.04 litres (L). Where test intervals showed no flow zones or volumes registering less than 0.04 L in the high flow test, the low flow configuration was used. Using the low flow configuration, the tank meter was able to register a change of 0.008 L. The through-the-bit method was used only on BH03 because of time constraints and unsuitable ground conditions. By using the high flow, the low flow and the through-the-bit configuration at some of the same depth intervals, a comparison of test results can be completed. Photographs of each configuration are shown in Appendix C in Plate C.2 and Plate C.3.

Table 3.3. Number of packer tests completed on the three boreholes in Odell Park.

Well	No. Packer Tests (September 2003)	No. Packer Tests (September 2003)	No. Packer Tests (August 2004)
BH01	26 (high flow set-up)	18 (low flow set-up)	19 (high flow set-up)
BH02	18 (high flow set-up)	6 (low flow set-up)	16 (high flow set-up)
BH03	8 (through-the-bit set-up)	None (hole caved)	32 (high flow set-up)

Prior to testing, the double packer system was checked on the surface for potential air or water leaks. The double packer system was then lowered down to a specific discrete depth interval using a winch and cable pulley system. The discrete depth interval is the space between the two packers after inflation. In 2003 the discrete depth interval was 1.73 m and the entire length of the borehole was packer tested. In 2004, the discrete

depth interval was 0.90 m and each borehole was tested at specific intervals to fill any gaps in the record and to supplement the previous year's data.

Once the packers were at the test depth, the packer membranes were inflated with nitrogen gas to pressures between 300-375 psi through a 3/16" tube. During inflation, care was taken not to over inflate and damage the packer membranes. After inflation, a few minutes are allotted for steady-state conditions to be reached. A record of the initial surface and downhole pressure gauge readings and the visible surface flow conditions (flow or no flow, from or around the casing) were noted prior to the start of the water injection.

The water injection source for the borehole packer test was supplied by the Odell Park facilities and held in a 750 L storage tank for the high flow tests and a 4-inch polyvinylchorethane (PVC) tank for the low flow tests. For the high flow tests, a Grundfos® submersible pump was placed in the storage tank and used to pump water through the flow system into the borehole. For the low flow tests, a pump was not required as the hydraulic head from the PVC tank to the borehole was large enough to register pressures on the gauges to carry out the test. The through-the-bit borehole packer test used the pump system supplied with the drill rig.

The electrical source required for the pump was supplied by the Odell Park facilities for BH01 and BH02, inside the old enclosed horse-riding ring. For BH03, the drillers used their own generator, and an additional generator supplied by the University of New Brunswick engineering facilities was used for the high flow BH03 configuration.

At the start of the borehole packer test, the water supply level in the storage tank was checked to be full, prior to starting the pump, to prevent the pump from burning out. With the pump on, water was injected through the flow system and the flowrate adjusted to the low end (Step 1) of the test flowrates. The flowrate, surface, and downhole pressures were recorded until a steady-state flowrate was reached over a period of time, usually between five and ten minutes. At this point, increasing the flow to the discrete depth interval increased the pressure settings and Step 2 was initiated and the procedure repeated. The final step, Step 3 was the highest pressure setting for that depth interval and the procedure was repeated. After completion of the 3 step tests, the packers were deflated for 15 minutes prior to being lowered to the next discrete depth interval.

The data collected from each borehole packer test are included in Tables C.1 to C.6 in Appendix C. These data are used to calculate the transmissivity and hydraulic conductivity of the geological unit at that particular depth interval. The calculations are discussed further in Section 3.2.2.

3.2.2 Transmissivity and Hydraulic Conductivity Calculations

By definition, transmissivity is the rate of flow through a specified unit thickness under a hydraulic gradient (Fetter, 2001). Hydraulic conductivity is the rate at which water can move through a permeable medium (Fetter, 2001). Both transmissivity (Equation 3.1) and hydraulic conductivity (Equation 3.2) are calculated for each packer test interval to identify the locations of the transmissive fracture planes.

The Theim (1906) Equation is used to calculate transmissivity (T):

$$T = \frac{Q \times (\ln Ri - \ln Rw)}{(2\pi \times (Hw - Hi))} \qquad \text{(Equation 3.1)}$$

where,

T	= transmissivity (m^2/sec)
Q	= flowrate (m^3/sec)
Ri	= radius of well influence (m)
Rw	= radius of well borehole (m)
Hw	= hydraulic head of borehole during test (m)
Hi	= initial hydraulic head of well

The Theim (1906) Equation that determined transmissivity (T) was then used to calculate the hydraulic conductivity (K):

$$K = T / L \qquad \text{(Equation 3.2)}$$

where,

K	= hydraulic conductivity (m/sec)
T	= transmissivity (m^2/sec)
L	= length of test interval (m)

Francis (1981) discusses the assumptions used with these equations. These include: 1) the groundwater system experiences steady-state radial flow; 2) the fractures present in the system are continuous with constant aperture opening; 3) the fractures are horizontal and intersect a vertical borehole; 4) the entrance head losses from the flow system may be negligible; and 5) based on the measured flowrates, Darcy's Law (Equation 3.3) is considered valid. The above parameters required for the calculations are determined from the packer test observations except for the radius of influence (Ri) around the borehole. This is initially selected to be 10 m because of the expected low hydraulic conductivity of the fractures. Calculations are completed for Ri of 1 m, 5m, 10 m and 20 m but the resulting difference between 1 m and 20 m is less than an order of magnitude.

Darcy's Law $$Q = -KA\left[\frac{dh}{dl}\right]$$ (Equation 3.3)

where,
- Q = discharge (m^3/s)
- K = proportionality constant hydraulic conductivity (m/s)
- A = cross sectional area (m^2)
- $\frac{dh}{dl}$ = hydraulic gradient (m/m) = dimensionless; dh is the change in head between two points; dl is the change in length between two points

Summaries of the hydraulic conductivity and transmissivity calculations are in Table 3.4 and Table 3.5, respectively. A graphical display of the resulting hydraulic conductivity values for each of the inclined boreholes is shown in Figure 3.4. Areas considered potential fracture flow zones were those with a resulting hydraulic conductivity value greater than 5×10^{-6} m/s.

Table 3.4. Hydraulic conductivity summary from the borehole packer tests.

	BH01		BH02		BH03	
	2003	2004	2003	2004	2003	2004
Sandstone unit (m/s)	3.1×10^{-5}	1.8×10^{-5}	7.3×10^{-6}	4.2×10^{-5}	6.6×10^{-6}	1.8×10^{-6}
Siltstone unit (m/s)	1.4×10^{-7}	1.3×10^{-6}	n/a	n/a	2.9×10^{-6}	2.9×10^{-6}
Borehole Maximum (m/s)	4.3×10^{-4}	1.6×10^{-4}	5.2×10^{-5}	2.9×10^{-4}	2.0×10^{-5}	1.3×10^{-5}
Borehole Minimum (m/s)	1.6×10^{-8}	4.3×10^{-7}	2.3×10^{-8}	3.1×10^{-7}	5.2×10^{-7}	8.9×10^{-7}
Borehole Average (m/s)	2.1×10^{-5}	1.0×10^{-5}	7.3×10^{-6}	4.2×10^{-5}	5.0×10^{-6}	2.2×10^{-6}
% > 5×10^{-6}	12%	16%	28%	73%	33%	7%

Table 3.5. Transmissivity summary from the borehole packer tests.						
	BH01		BH02		BH03	
	2003	2004	2003	2004	2003	2004
Sandst. unit (ave) (m^2/s)	2.6×10^{-5}	1.6×10^{-5}	6.6×10^{-6}	2.1×10^{-5}	7.3×10^{-6}	2.2×10^{-6}
Siltstone unit (ave) (m^2/s)	9.8×10^{-8}	1.1×10^{-6}	n/a	n/a	2.2×10^{-6}	2.6×10^{-6}
Borehole Maximum (m^2/s)	3.9×10^{-4}	1.5×10^{-4}	4.7×10^{-5}	8.2×10^{-5}	1.8×10^{-5}	1.2×10^{-5}
Borehole Minimum (m^2/s)	1.4×10^{-8}	3.9×10^{-7}	2.1×10^{-8}	2.8×10^{-7}	4.7×10^{-7}	8.1×10^{-7}
Borehole Average (m^2/s)	1.9×10^{-5}	1.5×10^{-6}	6.6×10^{-6}	2.1×10^{-5}	4.5×10^{-8}	2.0×10^{-6}

Referring to BH01 data in Figure 3.4, there are peaks in hydraulic conductivity at the 17 m to 19 m length[1], 40 m and 62 m lengths. Referring to BH02 data in Figure 3.4, there are peaks in hydraulic conductivity between the 14.5 m and 18.5 m length, 27 m to 29 m length and 37 m to 39 m length. Referring to BH03, there are hydraulic conductivity value peaks at the 10.5 m, 36 m and 47 m to 50 m length. These areas are considered fracture flow zones.

Problems encountered during the borehole packer tests included "caved" sections in all three boreholes in which the packer string was caught on the low side of the inclined borehole, likely after encountering an open fracture zone. BH01 caved at 63 m length, blocking the borehole and preventing access below 63 m length. BH02 caved at 44 m length, preventing access below 44 m length, which includes the siltstone unit. BH03 caved at the end of the casing (10 m length) in 2003 after borehole packer testing was completed, blocking the borehole and preventing access. The borehole was cleared in 2004 and caved at 55 m length, preventing access below this depth.

[1] Borehole data are collected with reference to length along the inclined borehole rather than actual vertical depth. Length is reported throughout.

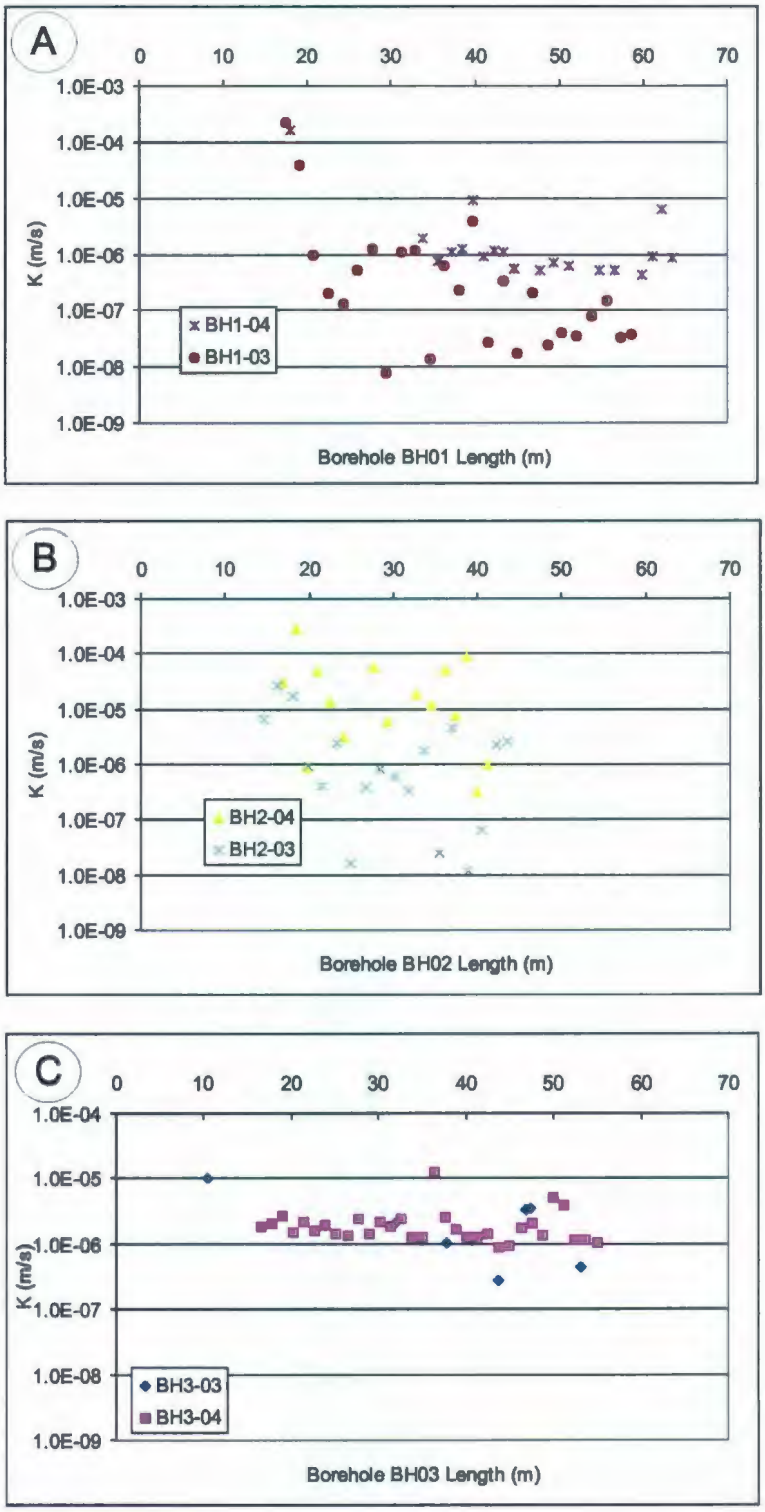

Figure 3.4. Hydraulic conductivity of: A) BH01; B) BH02; and C) BH03. Higher K > 5.0 x 10^{-6} m/s indicates potential fracture flow zones.

Of interest to this study, is why a relatively competent borehole would collapse at these locations. The collapsed zone in BH01 is within the red siltstone unit at approximately 63 m length. Transmissivity at 62.3 m length is close to a full order of magnitude higher than the 63.5 m length value (Table 3.6) indicating a potential fracture flow zone. The collapsed zone in BH02 occurs at the geological boundary between the grey sandstone and red siltstone units at approximately 44 m length. Transmissivity at 42.3 m length and 43.7 m length are almost an order of magnitude higher than the results 2 m above, indicating again a potential fracture flow zone.

Table 3.6 Caved (weak) zones of boreholes and respective transmissivities.

BH01		BH02		BH03	
Length (m)	T (m^2/s)	Length (m)	T (m^2/s)	Length (m)	T (m^2/s)
				10.5	1.8 E-05
62.3	5.7 E-06	42.3	3.8 E-06	53.7	1.1 E-06
63.5	7.7 E-07	43.7	4.6 E-06	55.0	9.5 E-07

It is also interesting to note that two of the three boreholes (BH01 and BH02) are artesian. The location of BH03 is down-gradient from these boreholes, with similar geological properties, so it was expected BH03 would also have artesian flow. Instead, BH03 collapsed just below the casing in 2003, close to the geological boundary between the overburden and the bedrock, but within the grey sandstone unit and at a zone of higher transmissivity (Table 3.6). It is believed that this zone has high enough transmissivity to accept the flow from below into the higher transmissive zone, so that flow does not reach the surface but instead flows up and outwards on the transmissive

fracture plane at the 10.5 m length. Therefore, it appears that these collapsed zones likely represent increased transmissive fracture zones and/or structurally weaker zones.

3.2.3 Temperature Logging

A thermistor cable, made in house, was attached to the borehole packer test configuration to record the temperature of the fluid in the borehole at each packer test length interval, prior to water injection. A thermistor is a stable thermal-sensitive resistor that registers readings in kilo-ohms, which are then converted, using a calibration curve, into °C temperature. The thermistor calibration was done in the laboratory prior to use and these results, which are used for the conversion in this study, are in Table C.9 and Figure C.2, Appendix C. This type of measurement is used because changes in temperature within a borehole are possible indicators of transmissive fracture zones. The temperature profile for each inclined borehole is shown in Figure 3.5.

The temperatures for BH01, BH02 and BH03 were between 4 °C and 9 °C, 4 °C and 8.3 °C and 4.2 °C and 10.4 °C, respectively. Referring to the BH01 temperature profile, temperature spikes occur at the 17.5 m, 18 m, 19 m, 40 m and 63.5 m length. All of these temperature spikes coincide with the hydraulic conductivity peaks from BH01, shown in Figure 3.4. Referring to the BH02 temperature profile, there are temperature spikes at the 14.5 m, 16.3 m, 17 m, 18 m, 20 m, 38.7 m and the 43.7 m length. Again, hydraulic conductivity peaks coincide with the temperature spikes for BH02, shown in Figure 3.4. Referring to the BH03 temperature profile, there are temperature spikes at the 10.5 m, 23.9 m, 27.6 m, 47.5 m and the 50 m length. Coinciding peaks between hydraulic

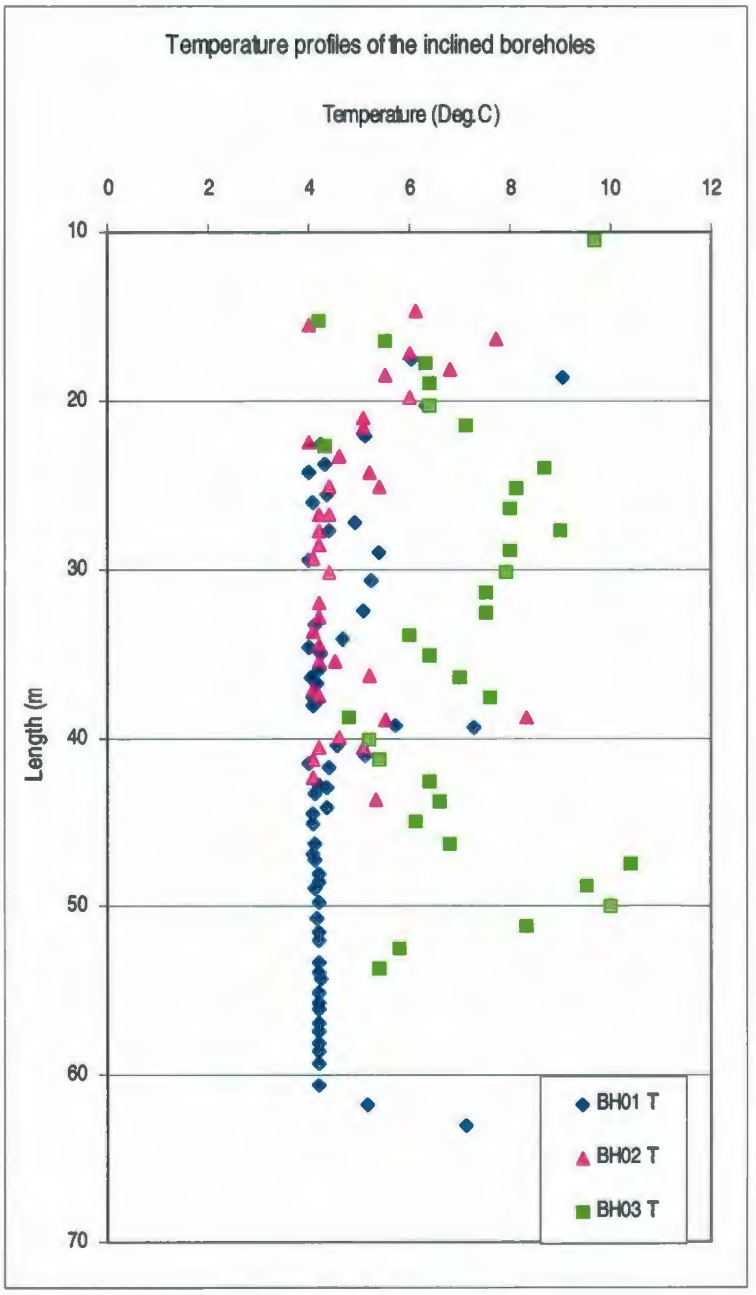

Figure 3.5. Temperature profiles of the inclined boreholes

conductivity and temperature are observed at the 10.5 m, 47.5 m and the 50 m length for BH03. These results indicate that temperature profiling may in some cases, be a good

indicator of fracture flow zones. Temperature data are also collected during the geophysical logging of the inclined boreholes, discussed in Section 3.4.

3.2.4 Bedrock Well 98-2 Slug Test

In the summer of 2004, well 98-2, located in Wilmot Park, was re-drilled to install a piezometer (i.e., small diameter monitoring well) in the bedrock unit. Nested (e.g., two wells within one well, completed at different depths) adjacent to this piezometer is aquifer well 98-2, a piezometer installed in the aquifer unit. At present, this is the only nested well with one piezometer in the bedrock and one piezometer in the aquifer, used to monitor the hydraulic connection between the underlying bedrock and the overlying aquifer. Water level measurements indicate the bedrock well hydraulic head is approximately 0.5 m elevation above the aquifer well hydraulic head.

In August 2004, the bedrock well 98-2 was slug tested. Piezometers are commonly tested with the slug or bail-down test to determine the hydraulic conductivity of the formation in the immediate vicinity of the well screen (Fetter, 2001). A known volume of water or material (e.g., sand-filled PVC tube) is quickly added (slug) or removed (bail-down) from the monitoring well and the rate at which the water level falls or rises to 80% of recovery is measured using a water-level measuring device such as a water tape-meter or levelogger® and barologger® combination. These data were analysed using WHI AquiferTest Version 3.0 program, using the Bower and Rice method. The resulting hydraulic conductivity of the bedrock 98-2 well is 3.56×10^{-5} m/s. For comparison, the hydraulic conductivity of the upper sandstone unit in the three

inclined boreholes is between 1.8×10^{-6} m/s and 4.2×10^{-5} m/s. A graph of the data obtained from the slug test of bedrock well 98-2 and the graphical analysis result of the slug test are located in Figure C.3 and Figure C.4 in Appendix C.

3.3 General Geochemistry and Isotope Analysis

In the summer of 2004, discrete interval groundwater samples from the inclined boreholes in Odell Park and bedrock well 98-2 were collected to determine the geochemical signature of the groundwater. Samples were analysed for major ions, trace elements and isotopes of oxygen ($\delta^{18}O$), deuterium ($\delta^{2}H$) and tritium (^{3}H). Sample length locations were chosen depending on geology, fracture data and hydraulic conductivity results from the previous year. Table 3.7 outlines the details of each groundwater sample location.

Table 3.7 Groundwater sample location details.

Sample No.	Depth	Date Sampled	Geology	Fracture Frequency	Hydraulic Conductivity
	(m)	2004		(#/m)	(m/s)
BH1 – 21	21	August 4	Grey fine-grained well-sorted sandstone. Minor coal and pyrite intermittent.	7	1.8×10^{-6}
BH1 – 40	40	August 5	Grey fine-grained well-sorted sandstone. Minor coal and pyrite intermittent.	3	8.3×10^{-6}
BH1 – 63	63	August 6	Red massive siltstone	1	8.5×10^{-7}
BH2 – 17	17	July 29	Grey fine-grained well-sorted sandstone. Minor coal.	3	4.1×10^{-5}
BH2 – 38	38	July 31	Grey fine-grained well-sorted sandstone.	5	4.6×10^{-5}
BH2 – 43	43	July 31	Grey fine-grained well-sorted sandstone.	1	5.1×10^{-6}

Table 3.7 continued. Groundwater sample location details.					
BH3 – 27	27	August 12	Grey fine-grained, well-sorted sandstone.	1	1.9×10^{-6}
BH3- 31	31	August 12	Grey fine-grained, well-sorted sandstone.	2	2.9×10^{-6}
BH3 – 50	50	August 11	Red massive siltstone.	1	3.9×10^{-6}
Bedrock 98-2	61	August 17	Grey fine-grained, well-sorted sandstone.	n/a	3.6×10^{-5}
Notes: Depth = inclined length along borehole except for 98-2 which represents vertical depth.					

3.3.1 Sampling Methodology

Prior to borehole packer testing, groundwater samples from the inclined holes were collected. The borehole packers were used to obtain three discrete interval samples per borehole. A water sampling tube was connected from the surface to the discrete interval between the two inflatable packers. The sampling interval of 0.9 m was assembled with stainless steel fittings. The packer assembly was lowered to the desired interval, the packers slowly inflated and water samples were collected after three interval volumes (12.2 L) were removed by natural artesian conditions for BH01 (0.013 L/min to 0.049 L/min) and BH02 (0.045 L/min to 0.125 L/min) and by a peristaltic pump for BH03 at a constant rate between 0.145 L/min and 0.189 L/min. Bedrock well 98-2 was sampled using a low-flow purging groundwater sampling procedure (Puls and Barcelona, 1996).

In all sampling episodes, field parameters including pH, temperature, Eh, conductivity, alkalinity and dissolved oxygen were measured prior to collecting samples for major ions, trace metals and isotopes oxygen ($\delta^{18}O$), deuterium ($\delta^{2}H$) and tritium (^{3}H). The major ion analyses were done at the University of New Brunswick and the trace

element analyses were done at Memorial University of Newfoundland. The $\delta^{18}O$ and $\delta^{2}H$ were analysed at Queen's University and ^{3}H was analysed at the University of Waterloo. A detailed sampling protocol and analytical results are in Appendix D. The results of the field parameter monitoring are in Table D.1 to Table D.2D in Appendix D.

3.3.2 Major Ion and Trace Element Analysis

The field parameters and geochemical analyses indicate possible controls on the bedrock groundwater geochemical signature. AquaChem (WHI, 2005), a program for the graphical analysis of aqueous geochemical data sets, is used to categorize the water types of the borehole bedrock groundwater samples (Table 3.8, Fig. 3.6). There were four different geochemical signatures from the borehole samples in Odell Park, and a fifth geochemical signature from the bedrock well 98-2.

Table 3.8. Water type summary for BH01, BH02, BH03 and bedrock 98-2.

Sample Number	Water Type
BH01-21, BH01-40	Ca - Na - HCO_3 - Cl
BH01-63	Na - HCO_3
BH02-17, BH02-38, BH03-27 BH03-31 BH03-50	Ca - Na - HCO_3
BH02-43	Na - Ca - HCO_3
98-2	Na - Ca - HCO_3 - Cl

The most common water type is calcium-sodium-bicarbonate (Ca-Na-HCO_3), observed at the BH02 17 m and 38 m intervals and at each of the sampling intervals for BH03. Referring to BH01, the chemistry varies between calcium-sodium-bicarbonate-chlorine (Ca-Na-HCO_3-Cl) water type at the 21 m and 40 m interval to a Na-HCO_3 water

type at the 63 m interval. The BH02 43 m interval sample is a Na-Ca-HCO_3 water type. Bedrock well 98-2 differs from the Odell Park wells and is a Na-Ca-HCO_3-Cl water type.

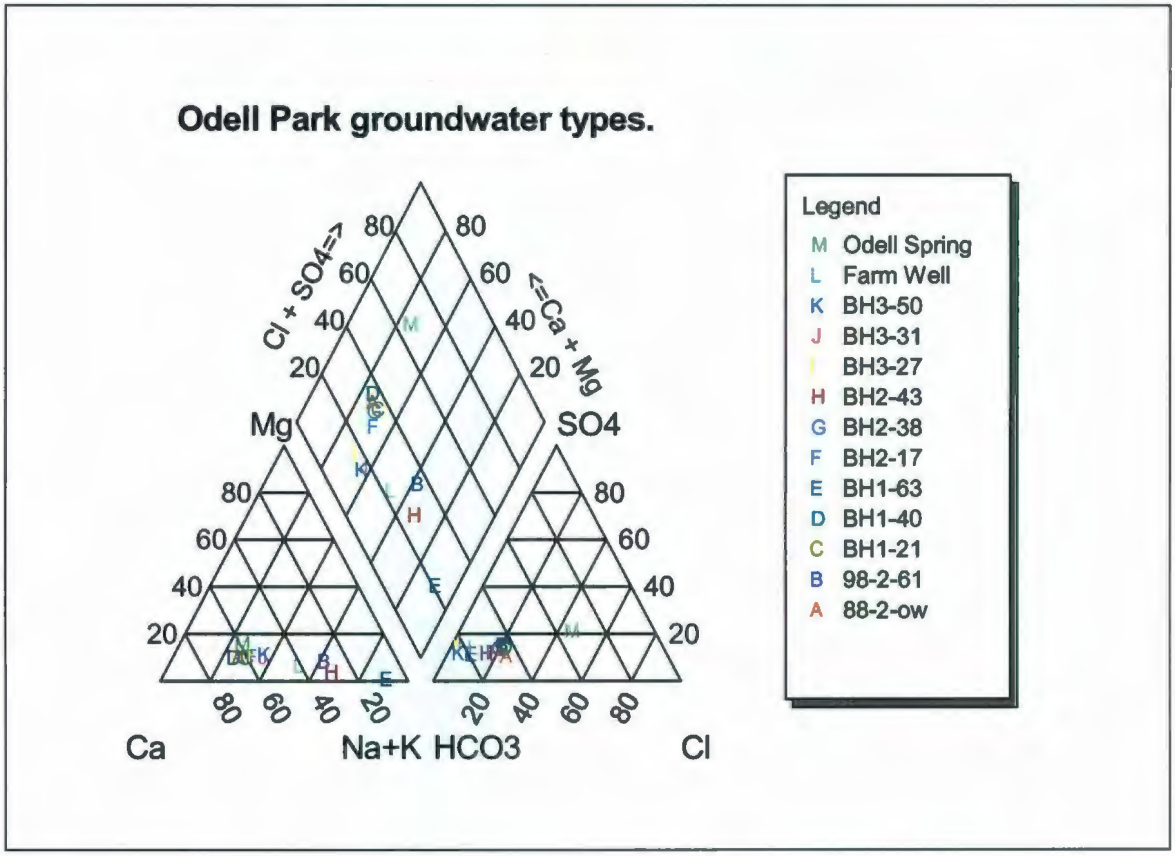

Figure 3.6. Piper plot of groundwater from Odell Park and St. Anne's Point.

The presence of Na and HCO_3 in every sample is a potential signature of groundwater from within deeper sedimentary terrain (Thomas, 1991). The higher concentrations of Ca and Na are possibly from the dissolution of feldspars within the Pictou Group (Cunningham, 2003). Table 3.9 lists selected bedrock groundwater analyses obtained from the inclined holes and vertical wells (Thomas, 1991) within Odell Park, bedrock well 98-2 and a natural spring within Odell Park (Thomas, 1991). Though the wells are in close proximity, the geochemical signatures are distinctly different.

Table 3.9 Selected bedrock well water field parameters and chemical data.

Sample Number	pH	Conductivity[1]	Alkalinity[2]	Ca	Mg	Na	K	Cl	SO4	Fe	Mn	DO
		uS/cm	mg/L	mg/L	mg/L	mg/L	mg/L	mg/L	mg/L	mg/L	mg/L	mg/L
BH01-21	8.2	17.8	116.4	35.3	3.6	19.8	1.1	22.9	19.3	0.03	**0.09**	1.39
BH01-40	7.4	16.0	132.7	43.0	3.9	17.5	1.1	26.2	24.0	0.01	**0.07**	0.51
BH01-63	9.1	17.9	166.0	5.6	0.3	69.5	0.6	12.1	18.8	0.01	0.01	0.40
BH02-17	8.1	17.5	111.8	29.9	3.3	18.4	1.2	16.8	15.2	0.00	**0.06**	1.46
BH02-38	7.8	17.1	138.9	37.7	3.7	19.3	1.1	22.8	22.6	0.00	**0.09**	0.34
BH02-43	8.2	16.2	125.4	15.8	1.2	40.3	0.9	15.3	15.8	0.00	0.04	0.55
BH03-27	7.5	16.1	141.5	31.6	3.7	20.1	1.0	3.4	19.7	0.08	**0.33**	0.25
BH03-31	7.7	16.0	136.4	28.3	3.3	21.8	0.9	2.2	20.4	0.04	**0.27**	0.25
BH03-50	8.6	15.8	163.5	30.8	4.0	23.8	1.1	5.0	18.0	**1.09**	**0.27**	0.27
98-2	7.8	18.6	100.9	14.7	2.5	34.0	1.7	18.5	18.7	**0.50**	**0.08**	1.90
88-2-OW[3]	7.9	299.0	105.0	38.0	3.8	17.8	0.8	23.0	13.5	**0.35**	0.05	0.03
Farm Well (Odell)[3]	8.0	242.0	99.3	20.0	2.0	29.8	0.7	7.4	14.5	0.19	0.03	0.11
Odell Spring[3]	6.4	85.0	15.1	8.7	1.4	3.9	0.3	11.6	7.4	0.02	0.01	8.32

1. All units in mg/L except for conductivity in uS/cm and pH.

2. Alkalinity expressed as HCO_3.

3. Previously sampled bedrock wells by Thomas (1991).

Value: Shaded and bold value exceeded Canadian Drinking Water Quality Guidelines (CCME, 1999)

Manganese (Mn) exceeds the Canadian Drinking Water Quality Guidelines (CCME, 1999) of 0.05 mg/L in every borehole sampled in 2004 with values ranging between 0.06 mg/L and 0.33 mg/L. Iron (Fe) exceeds the Canadian Drinking Water Quality Guidelines (CCME, 1999) of 0.3 mg/L in BH03 with a value of 1.09 mg/L at the deepest sampling interval of 63 m and at bedrock well 98-2 with a value of 0.5 mg/L. Elevated concentrations of dissolved Mn and Fe, first detected in the 1950's, continues to be a concern for the City of Fredericton. According to Thomas et al. (1994), in the Fredericton Aquifer, the dissolution of Mn and Fe oxides is a result of increasing dissolved organic carbon entering the aquifer.

3.3.3 Isotope Analysis

The study of stable isotopes in groundwater from fractured bedrock can be useful to determine groundwater trajectories, groundwater velocities, residence time, and thermal history of recharge (Davis, 1969). In the summer of 2004, samples from BH01, BH02, BH03 and 98-2 were extracted for the analysis of isotopes of oxygen ($\delta^{18}O$), deuterium ($\delta^{2}H$), and tritium (^{3}H), the radioactive isotope of H.

Analysis of $\delta^{18}O$ and $\delta^{2}H$ is useful in determining the origin and climatic conditions of the water prior to recharge (Domenico and Schwartz, 1990). The results of the $\delta^{18}O$ and $\delta^{2}H$ isotope analysis are reported as positive or negative deviations of isotope ratios away from a standard, in this case, the Standard Mean Ocean Water (SMOW) standard (Domenico and Schwartz, 1990). As discussed by Craig (1961), approximately 400 water samples from rivers, rain, lakes and snow are analysed for $\delta^{18}O$ and $\delta^{2}H$, relative to SMOW, and show a linear relationship for most samples. The linear equation fitted to these data is the equation for the global meteoric water line (GMWL) (Craig, 1961).

$$GMWL = \delta^{2}H = 8\delta^{18}O + 10 \qquad \text{(Equation 3.4)}$$

where,

$$\delta = \frac{R_{samples} - R_{standard}}{R_{standard}} \times 1000$$

and δ is reported in permillage ($^{0}/_{00}$), is the deviation from the standard expressed in ($^{0}/_{00}$) notation

Samples that fall on the GMWL, are assumed to have originated from the atmosphere (Domenico and Schwartz, 1990). Samples that deviate from the GMWL have been subjected to isotopic fractionation processes such as evaporation from open

surfaces, condensation, high temperature exchange with rock or minerals, carbon dioxide exchange, and hydrogen sulphide exchange (Domenico and Schwartz, 1990).

Outlined in Clark and Fritz (1997), a Canadian meteoric water line (CMWL) is determined using: $CMWL = \delta^2H = 7.75\delta^{18}O + 9.83$ (Equation 3.5), and a local meteoric water line (LMWL) based on averages between observation stations in Ottawa, Ontario and Truro, Nova Scotia is determined using:

$$LMWL = \delta^2H = 7.5\delta^{18}O + 6 \quad \text{(Equation 3.6).}$$

The groundwater sample analysis results for $\delta^{18}O$ and δ^2H, relative to the CMWL and LMWL are plotted in Figure 3.7[2]. The $\delta^{18}O$ values range between $-11.5^0/_{00}$ to $-10.3^0/_{00}$ and the δ^2H range between $-81^0/_{00}$ to $-72^0/_{00}$. In general, isotopic signatures of groundwater are considered to be a reflection of the precipitation in the recharge zone (Praamsma et al., 2009). In this case, the sample results fall within the range of meteoric water origin for both $\delta^{18}O$ and δ^2H (Clark and Fritz, 1997) and all sample results fall below the CMWL.

Three groundwater samples, BH01-40, BH03-31 and BH03-50 fall on the LMWL, a potential result of groundwater originating from the atmosphere without significant influence from isotopic fractionation processes and indicating a possible vertical fracture connection directly to the surface. Bedrock well 98-2 lies below the LMWL and is the most depleted in $\delta^{18}O$ and δ^2H of all samples, a result of river dilution or possible contamination from the aquifer prior to the installation of the piezometer

[2] Precision of analysis not available from Queen's Isotope Laboratory at time of submission. Unable to determine if data scatter is within analytical precision.

(Al, Pers. comm., 2010). The remaining samples also deviate below the LMWL including samples BH01-21, BH01-63, BH02-17, BH02-38, BH02-43, and BH03-27, explained by possible greater evaporative enrichment than the other samples (Clark and Fritz, 1997).

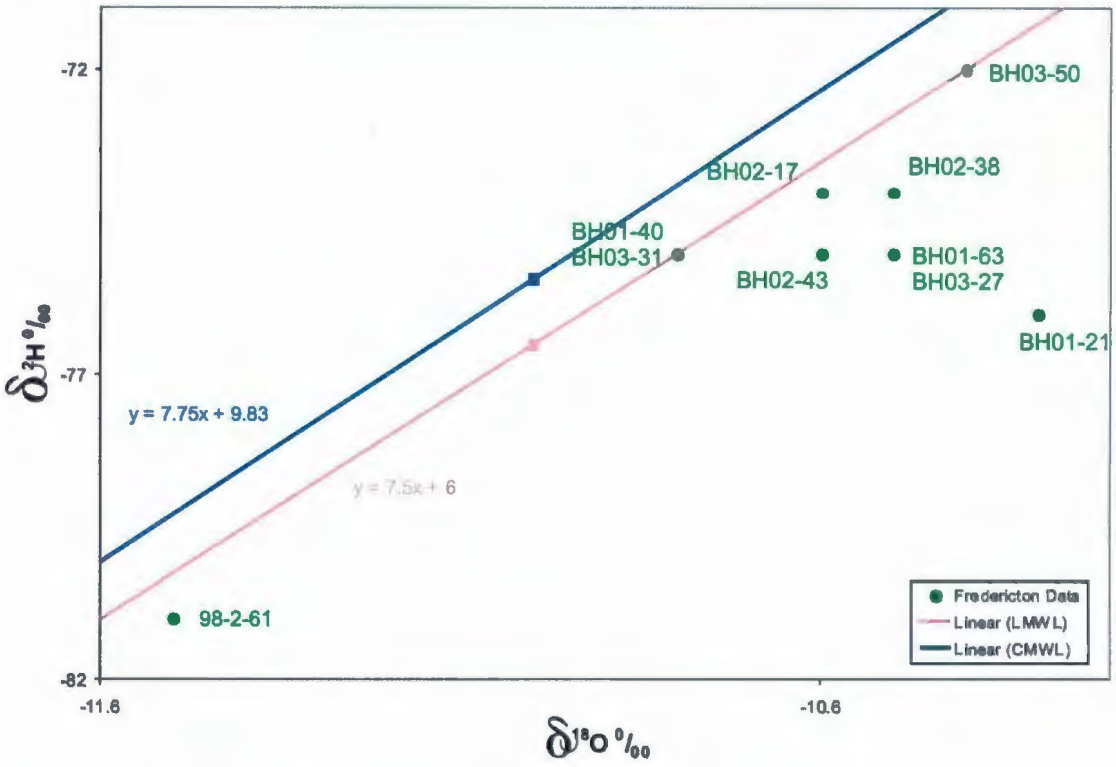

Figure 3.7. Bedrock groundwater distributions along LMWL and CMWL.

For $\delta^{18}O$ and $\delta^{2}H$ comparison, Newbury (unpublished data, 2004) took river, lake, and bedrock groundwater samples in the Fredericton area and analysed for $\delta^{18}O$ and $\delta^{2}H$. These results are in Figure 3.8 (Susan Newbury, unpublished data, 2004). Referring to Figure 3.8, the $\delta^{18}O$ values from the bedrock samples range between $-11.2^{0}/_{00}$ and $-8.75^{0}/_{00}$ and the $\delta^{2}H$ range between $-75.6^{0}/_{00}$ and $-67.5^{0}/_{00}$, which are comparable to the bedrock groundwater samples analysed for this thesis work. The samples collected from the production wells cover the greatest $\delta^{18}O$ and $\delta^{2}H$ range of values with $\delta^{18}O$ between

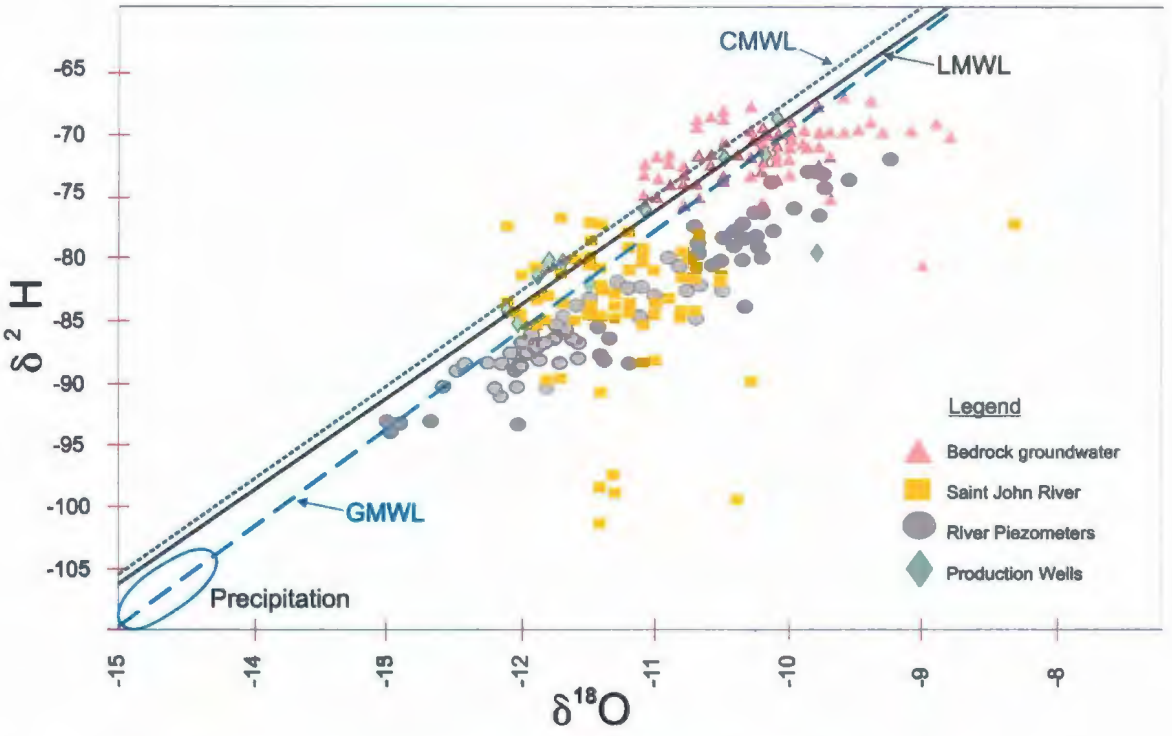

Figure 3.8. Water isotope comparison for samples collected by Newbury (modified from unpublished data, 2004).

$-13.0^0/_{00}$ and $-9.25^0/_{00}$ and δ^2H between $-94^0/_{00}$ and $-72.5^0/_{00}$. The river samples analysed are between the production well and bedrock groundwater samples, with values for $\delta^{18}O$ between $-12.1^0/_{00}$ and $-10.5^0/_{00}$ and δ^2H between $-90^0/_{00}$ and $-77.5^0/_{00}$. These results are tabulated in Table 3.10. The difference in isotopic compositions between the bedrock groundwater and the river water allow us to determine where waters in the production wells originate. Referring to the production well analysis, it would appear that a number of the production wells are influenced directly by the bedrock groundwater, others by the river, and some in combination of these sources, a result of groundwater-surface interaction.

It is interesting to note, a number of the sample results from Newbury (Unpublished data, 2004) lie above both the CMWL and LMWL. A possible explanation is δ^2H excess in the meteoric waters, a result of low humidity in the vapours influencing the amount of δ^2H in the precipitation (Clark and Fritz, 1997). A second possible explanation is the hydration of primary silicate minerals because of a low-temperature water-rock interaction (Clark and Fritz, 1997). The result is waters enriched in δ^2H and depleted in $\delta^{18}O$, plotting above the CMWL and LMWL (Clark and Fritz, 1997).

The stable isotopic signatures of the water from the bedrock groundwater, Saint John River and production wells show that groundwater-surface water interaction is present in the Fredericton area. This supports evidence from the 3D modeling, described in Chapter 4 and Chapter 5, that both the groundwater and surface water of the hydrogeological system is sensitive to changes in recharge because of this interaction.

Table 3.10 Isotope analysis results from bedrock wells.

Water Sample Location	$\delta^{+18}O$ Range (‰)	$\delta^{+2}H$ Range (‰)
Bedrock	– 11.5‰ to – 10.3‰	– 81‰ to – 72‰
Bedrock[1]	– 11.2‰ to – 8.75‰	– 75.6‰ to – 67.5‰
Production Wells[1]	– 13.0‰ to – 9.25‰	– 94‰ to – 72.5‰
River[1]	– 12.1‰ to – 10.5‰	– 90‰ to – 77.5‰

[1] Samples collected and analyzed by Susan Newbury (unpublished data, 2004).

Analysis of ^3H is commonly used to determine if the age of the groundwater post- or pre-dates1952, the approximate peak year of thermonuclear testing which released ^3H into the atmosphere (Domenico and Schwartz, 1990). Between November, 1952 and 1963, thermonuclear testing released ^3H, increasing concentrations to 100's of tritium units (TU) in precipitation from natural background conditions of 5 (Domenico and

Schwartz, 1990). Tritium concentrations have been in decline since 1963 but remain above the natural background conditions.

Odell Park well BH01 and bedrock well 98-2 were analysed for ^{3}H and contain approximately 2 TU and 6 TU respectively. Using the assumption that pre-1952 TU levels are 5 TU, with a ^{3}H half-life of 12.35 years, in approximately 2014, values will be at 0.16 TU. Since both results are greater than 2 TU, we can assume the groundwater is younger than 1952. If present day ^{3}H concentration is in the 2 to 6 TU range, the groundwater residence time must be on the order of 10 years or less. Without information on the historical ^{3}H loading for the Fredericton area, or present day ^{3}H concentration in the precipitation, we assume that the presence of ^{3}H in the groundwater is an indication that since 1952, the atmosphere has recharged some portion of the groundwater. The higher value for 98-2-61-01 could also be possible from contamination from the aquifer prior to the installation of the piezometer. Results of the ^{3}H analyses are in Table 3.11.

Table 3.11 Tritium analysis results from BH01 and bedrock well 98-2.

Sample	Tritium Units (TU)	Comments
98 - 2 - 61 – 01	6.2 +/- 0.7	1TU = 3.149 Picocuries/L
BH01 - 63 – 01	2.0 +/- 0.6	1 TU= 0.11815 Becquerels/L

3.4 Geophysical Investigation

The Geological Survey of Canada (GSC) logged each inclined borehole using a suite of geophysical tools in September 2003. These data are used to complement the existing information on the geology and fracture flow characteristics obtained following

the drilling program. The geophysical logging methods done are listed in Table 3.12 and an analysis of the BH01 log is detailed below.

Table 3.12 Geophysical methods used in Odell Park.

Borehole	BH01	BH02	BH03
Natural Gamma	✓	✓	✓
Conductivity	✓	✓	✓
Magnetic Susceptibility	✓	✓	✓
Temperature	✓	✓	✓
Single Point Resistivity	✓	✓	
Self-Potential	✓	✓	
Tube wave/Fracture	✓		

Natural gamma log spectroscopy is used to measure the intensity of gamma radiation emitted by natural radioactive elements such as uranium, thorium, and potassium, and is often used in hydrogeological studies for stratigraphic correlation, and understanding aquifer permeability and fracturing conditions (United States Environmental Protection Agency, 2004). In most instances, higher natural gamma readings are associated with clay and shale units, while lower readings are associated with sand, sandstone, or limestone for example. Using BH01 as an example for the analysis of the geophysical logs, the stratigraphic correlation between the geologic log and the natural gamma log can be seen in Figure 3.9.

Referring to the geologic log of BH01 (Fig. 3.9), below the casing at 17.6 m to 46.9 m, bedrock consists of grey fine-grained, well-sorted, sandstone with inclusions of thin coal laminae markers and minor pyrite grains. At 46.9 m the colour changes to

greenish grey grading into red siltstone with mud clasts and then into red massive siltstone to the end of the hole at 72.2 m. Referring to the natural gamma log, this change

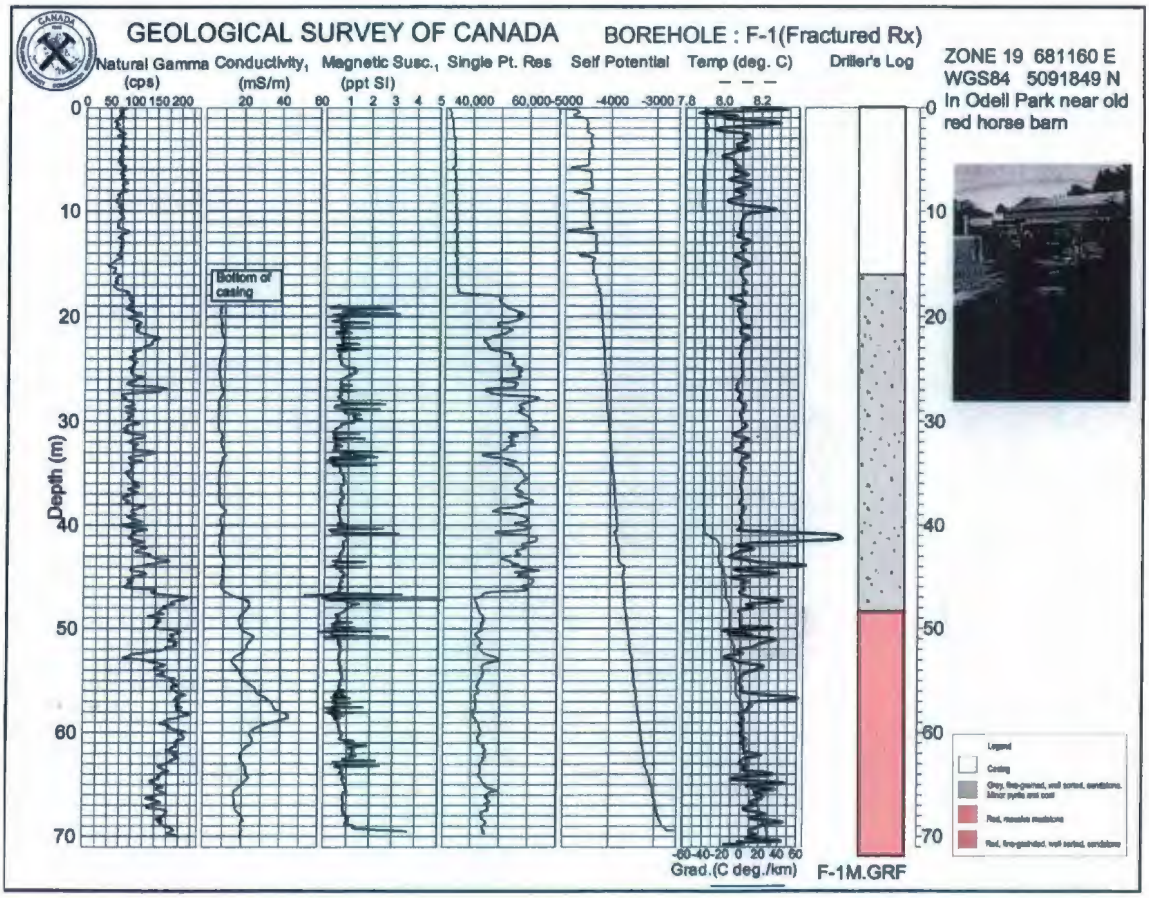

Figure 3.9. Geophysical log of BH01 provided by J. A. Hunter of the GSC, Ottawa, Canada (Unpublished data, 2003).

in geology, as expected, is visible at the 48 m depth with an increase from approximately 100 counts per second (cps) to approximately 175 cps.

The conductivity measurement is influenced by the composition and porosity of the rock and fluids encountered along the borehole (United States Environmental

Protection Agency, 2004). Referring to the conductivity log (Fig. 3.9), at 48 m there is an increase from approximately 10 microsiemens (mS)/m to 20 mS/m, corresponding to the lithologic change from sandstone into siltstone. At the 58.5 m depth, there is an increase to 45 mS/m and decreasing again to 20 mS/cm. The photo log of this borehole at this depth (Plate B1. Appendix B) shows a less competent section of core possibly from an increase of clay material within the siltstone grading back to a competent section of siltstone. It is typical to see higher conductivity readings associated with clay and shale formations and lower readings associated with sand, sandstone or limestone.

A temperature change along a borehole profile indicates groundwater flow or anomalies within the groundwater flow from fractures (United States Environmental Protection Agency, 2004). From the BH01 survey by the GSC (Unpublished data, 2003), the temperature log shows an average 8.1 °C from the surface casing until the 41 m interval where it increases approximately 0.5 °C. Additional temperature increases follow to the end of the borehole at 44 m, 47 m, 50 m, 51 m, 54 m, 57 m indicating potential fracture flow locations. The thermistor measurements for BH01 taken during the packer test events show there is an abrupt temperature increase from 4.1°C to 7.2 °C at the 38 m interval. Differing thermistors and differing thermistor calibration may account for the differences in temperatures, but both profiles have temperature increases at the 41 m interval, a potential indication of transmissive fractures.

Single point resistivity measures the resistance of materials between two probes, where one electrode is located within the borehole and the second electrode is positioned on ground surface (Fetter, 2001). The geophysical logs from the GSC of BH01, BH02

and BH03 (Unpublished data, 2003) indicate changes in lithology and potential fracture locations and can be compared with the core and fracture logs obtained during the drilling program. The higher resistance readings are associated with sand, gravel and sandstone and the lower resistance readings are associated with clay and shale. Other causes for a lower resistance include increasing salinity or increasing borehole size due to a fracture zone. Referring to the BH01 log (Fig. 3.9), the single point resistivity values below the surface casing are an average 55,000 Ohms until approximately 47 m where this is an obvious drop in readings to 45,000 Ohms, correlating to the change in lithology from sandstone to siltstone, as noted in the geologic and natural gamma logs.

Magnetic susceptibility measures the magnetite concentration of sediments within a borehole. Increasing values of magnetic susceptibility are possible indicators of iron rich sediments and weathered zones (United States Environmental Protection Agency, 2004). A weathered zone in particular could create an environment favourable for groundwater flow. Referring to BH01 (Fig. 3.9), there are increased spikes along the borehole at locations 20 m, 29 m, 34 m, 40 m, 47 m, 51 m, 58 m and 63 m signifying potential weathered zones and subsequently, potential fracture flow zones as a result of this weathering. Zones including the 20 m, 40 m and 63 m locations, correlate to the higher hydraulic conductivity calculation results obtained from the packer tests.

The tube wave radiation survey indicates fracture zones that are open to fluid flow at the time of the survey (Fig. 3.10). Interpretation of the downhole seismic record of BH01 (labeled F-01) by J. A. Hunter of the GSC in Ottawa, Canada (Unpublished data, 2003) is as follows:

"Shown is a filtered (50-400-800-1200 Hz) downhole seismic section acquired using a buffalo gun source at surface and a hydrophone streamer (with 0.5 m hydrophone spacing) in fractured rock borehole F-01 at Odell Park, Fredericton. The interpreted positions of cracks open to fluid flow are indicated with arrows on the depth axis. These are based on the radiation patterns of tube waves emanating from the P-wave first arrival. The interpretation must take into account interference associated with overlapping wave-trains emanating from some closely spaced fractures."

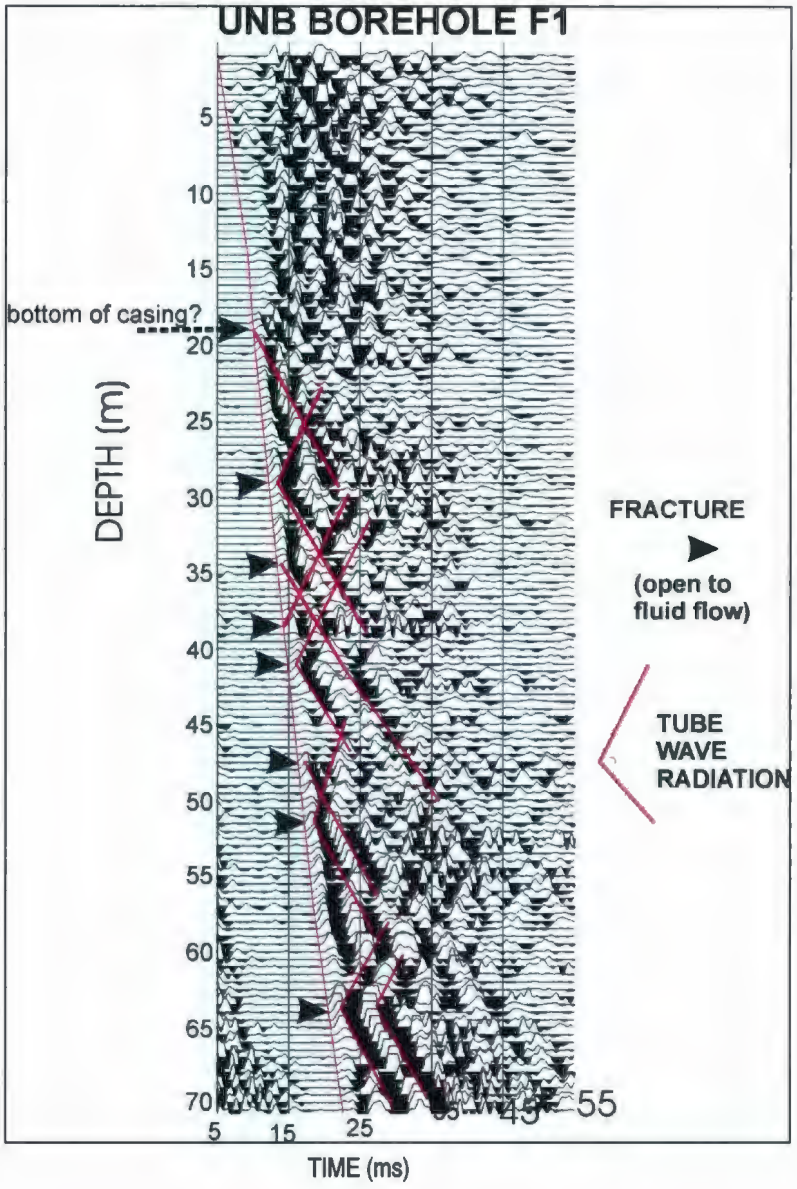

Figure 3.10. Downhole seismic survey of BH01 using tube wave radiation. Provided by J. A. Hunter of the GSC, Ottawa, Canada (Unpublished data, 2003).

Based on the tube-wave radiation survey, fracture flow is indicated by arrows at the 29 m, 34.5 m, 38.5 m, 41 m, 47.5 m, 51 m and 64 m intervals. These strongly correlate to the magnetic susceptibility log. As expected, they also correlate to the hydraulic conductivity calculation results from the packer test data.

3.3 Summary of the subsurface field investigation

The field tools and data collection obtained during this portion of the thesis work, are used to understand the flow system and assist in developing the conceptual and numerical model, discussed in Chapter 4. It is evident from the core logging, packer test results, and geophysical logs that transmissive fractures are present in the bedrock underlying Fredericton. Hydraulic conductivity of the bedrock in Odell Park ranges between 1.6×10^{-8} m/s and 4.3×10^{-4} m/s and these data are used as material properties for the numerical model. The geophysical logs obtained from the GSC are used as a complementary data set to those obtained during the core logging and packer test analyses. The geochemical signature of the bedrock groundwater samples is not one dominant water type, but each sample contains Na and HCO_3, a potential signature of groundwater originating in deeper sedimentary terrain (Thomas, 1991). In individual boreholes BH01 and BH02, there are different geochemical signatures at different intervals. This is an indication of differences in bedrock geology, groundwater pathway origins, and/or residence time of fracture flow at different depths in the bedrock. The stable isotopic signatures of the water from the bedrock groundwater, Saint John River and production wells show that groundwater-surface water interaction is present in the

Fredericton area. This supports evidence from the 3D modeling, described in Chapter 4 and Chapter 5, that both the groundwater and surface water of the hydrogeological system is sensitive to changes in recharge because of this interaction.

CHAPTER 4.0 CONCEPTUAL MODEL AND NUMERICAL SIMULATION OF THE HYDROGEOLOGICAL FLOW SYSTEM

4.1 Conceptual Model

Developing a conceptual model is the first and most important step in the modeling process (National Research Council, 2001). The conceptual model is a representation of the essential features, processes, and events which control the fluid flow at a specific field site (National Research Council, 2001). It incorporates the hydrogeological components that are used in the numerical model and allows one to organize the field and desk-top data including the hydrostratigraphic properties and the water budget information (Anderson and Woessner, 1992). The conceptual model for this study is detailed in Figure 4.1 and outlines various features of the model domain.

4.1.1 Hydrogeological Properties

A total of sixteen layers are used for the conceptual and subsequent numerical model. The hydrogeological properties for each layer, including unit thickness, transmissivity and hydraulic conductivity estimates are listed in Table 4.1. The actual hydraulic conductivity values used in the numerical model are listed in Table 4.2. Figures F.1 to F.7 in Appendix F display the hydraulic conductivity values used in the model for the overburden layers. The transmissivity and hydraulic conductivity values for the overburden material are obtained from Violette (1990), McGuigan (1995), TerrAtlantic (2000) and Dawe (2005). The transmissivity and hydraulic conductivity values for the

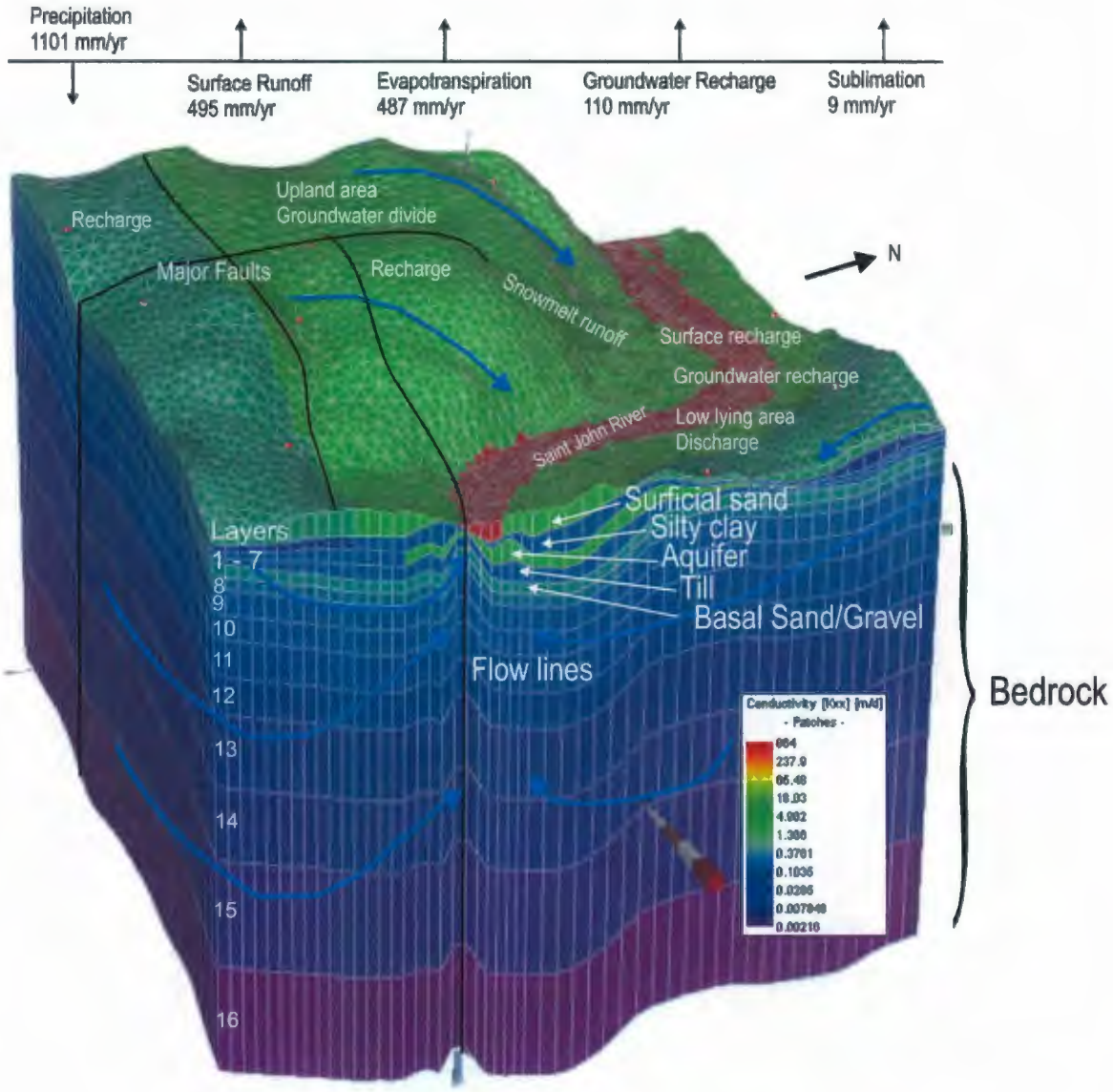

Figure 4.1. Conceptual model of Fredericton, New Brunswick. Shown: 1) water budget information; 2) hydrostratigraphic layers and properties; 3) estimated groundwater flowlines; 4) estimated recharge and discharge locations; and 5) estimated fault line locations.

underlying bedrock are obtained from the packer test results. The associated element numbers with each layer and corresponding hydraulic conductivity used in the numerical model are listed in Table F.1 of Appendix F.

Table 4.1 Hydrogeological parameters used for the conceptual model.			
Parameter	Thickness	Transmissivity	Kx = Ky*
	(m)	(m2/s)	(m/s) Estimates
Fluvial sand with gravel [1, 2]	0 - 5	$5.0 \times 10^{-5} - 5 \times 10^{-3}$	$8.1 \times 10^{-5} - 5.3 \times 10^{-4}$
Lacustrine silt and clay [3]	0 - 30	$8.7 \times 10^{-7} - 3 \times 10^{-5}$	$2.9 \times 10^{-8} - 1.0 \times 10^{-6}$
Outwash sand (aquifer) [1, 2, 4]	0 - 25	$9.5 \times 10^{-3} - 1.2 \times 10^{-2}$	$8.1 \times 10^{-5} - 1.2 \times 10^{-3}$
Outwash gravel (aquifer) [1, 2, 4]	0 - 5	$9.5 \times 10^{-3} - 1.2 \times 10^{-2}$	$8.1 \times 10^{-5} - 1.2 \times 10^{-3}$
Lodgement till [1]	0 - 10	$1.0 \times 10^{-7} - 1.0 \times 10^{-5}$	$1.0 \times 10^{-6} - 1.0 \times 10^{-6}$
Sand and gravel [1]	0 - 5	$5.0 \times 10^{-5} - 5.0 \times 10^{-3}$	$1.0 \times 10^{-5} - 1.0 \times 10^{-3}$
Sandstone bedrock [5]	5 - 10	$1.6 \times 10^{-6} - 3.8 \times 10^{-5}$	$1.0 \times 10^{-6} - 1.0 \times 10^{-5}$
Mudstone bedrock [5]	10	$1.3 \times 10^{-7} - 2.7 \times 10^{-6}$	$1.0 \times 10^{-6} - 1.0 \times 10^{-5}$
Bedrock [5]	20	$1.3 \times 10^{-7} - 2.7 \times 10^{-6}$	$1.0 \times 10^{-6} - 1.0 \times 10^{-5}$
Bedrock [5]	20	$1.3 \times 10^{-7} - 2.7 \times 10^{-6}$	$1.0 \times 10^{-7} - 1.0 \times 10^{-6}$
Bedrock [5]	30	$1.3 \times 10^{-7} - 2.7 \times 10^{-6}$	$1.0 \times 10^{-7} - 1.0 \times 10^{-6}$
Bedrock [5]	30	$1.3 \times 10^{-7} - 2.7 \times 10^{-6}$	$1.0 \times 10^{-7} - 1.0 \times 10^{-6}$
Bedrock [5]	60	$1.3 \times 10^{-7} - 2.7 \times 10^{-6}$	$1.0 \times 10^{-7} - 1.0 \times 10^{-6}$
Bedrock [5]	60	$1.3 \times 10^{-7} - 2.7 \times 10^{-6}$	$1.0 \times 10^{-8} - 1 \times 10^{-7}$
Bedrock [5]	90	$1.3 \times 10^{-7} - 2.7 \times 10^{-6}$	$1.0 \times 10^{-8} - 1 \times 10^{-7}$
Bedrock [5]	90	$1.3 \times 10^{-7} - 2.7 \times 10^{-6}$	$1.0 \times 10^{-8} - 1 \times 10^{-7}$
Additional Information			
Bedding Planes [5]	Dipping 5^{O} NE/Strike NW		
Fracture Sets [5]	NE/SW and NW/SE both vertical to sub-vertical		
Fracture Equivalent Porous Medium	Same as rock mass hydraulic conductivity determined above.		
Aquifer Porosity [6]	30% - 35%		
Bedrock Porosity [5]	1.5% – 3%		
Aquifer Storativity [4]	3×10^{-3} to 5×10^{-2}		
Sand, Gravel Storativity	1×10^{-5} to 1×10^{-1}		
Clay/Silt Storativity	1×10^{-5} to 1×10^{-4}		
Till Storativity	1×10^{-5} to 1×10^{-4}		
Bedrock Storativity	1×10^{-4}		
Topographic contours (m asl)	+/- 2 – 130		

* Note that Kz = 1 / 10Kx. The Fracture Equivalent Porous Medium approach was used in the model, though it is recognized that in some areas of vertical fracture flow, the Kz would be greater than the Kx.

[1] Violette (1990), [2] Dawe (2005), [3] McGuigan (1995), [4] TerrAtlantic (2000), [5] Loomer (2001), [6] Davis (1969)

Table 4.2 Hydraulic conductivities used for the numerical model.

Layer No.	Area Description	Kx = Ky (m/s)
1	NE corner, south end	1.0×10^{-5}
	Outer edge of river, south slope	1.0×10^{-4}
	River	1.0×10^{-2}
2	NE corner, mid to south end	1.0×10^{-6}
	River region, south slope	1.0×10^{-5}
	Windows	3.0×10^{-2}
3	NE corner, mid to south end	1.0×10^{-7}
	River region, south slope	1.0×10^{-6}
	Windows	3.0×10^{-2}
4	NE corner, mid to south end	1.0×10^{-6}
	NE corner, NW corner	1.0×10^{-5}
	River region, esker excluded	8.0×10^{-5}
	Esker area	3.0×10^{-2}
5	Entire layer except for windows	1.0×10^{-6}
	Windows	5.0×10^{-6}
6	Entire layer except for esker	1.0×10^{-6}
	Esker area	1.0×10^{-3}
7	Entire sandstone layer	5.0×10^{-6}
8	Entire mudstone layer	2.5×10^{-6}
9	Entire bedrock layer	1.0×10^{-6}
10	Entire bedrock layer	7.5×10^{-7}
11	Entire bedrock layer	5.0×10^{-7}
12	Entire bedrock layer	2.5×10^{-7}
13	Entire bedrock layer	1.0×10^{-7}
14	Entire bedrock layer	7.5×10^{-8}
15	Entire bedrock layer	5.0×10^{-8}
16	Entire bedrock layer	2.5×10^{-8}

As mentioned in earlier chapters, the lacustrine silt and clay layer overlying the aquifer is not present in some areas, connecting the aquifer layer below to the sand and gravel layer above. Additionally, there are eroded areas in the till layer underlying the aquifer, connecting the aquifer to the bedrock and/or basal sand and gravel layer. These eroded areas are commonly referred to as "windows" (ADI Ltd., 1982). The window locations, which form a hydraulic connection between the Saint John River and the aquifer, and the underlying fractured bedrock and/or basal sand and gravel unit and the aquifer, are constrained to the general area of the esker (Al and MacQuarrie, Pers. comm., 2008). Window locations in the silty clay layer that hydraulically connect the Saint John River to the aquifer, are reported by Nadeau (2003). Window locations in the till layer connecting the aquifer to either the basal sand and gravel unit and/or the underlying bedrock are chosen based on the borehole database records (Jeff Whitter, unpublished data, 2005) and through a random sampling of the numerical elements in the esker area, described in detail in Section 4.3.3.

The fractures observed in outcrop in Odell Park and in the inclined boreholes, are used to interpret the structural orientation, frequency and spacing of the fractures, fracture characteristics and flow behaviour. Major faults in the model area are interpreted from structural geology maps (McLeod and Johnson, 1998). Fracture orientations are dominantly in the northeast direction and less so in the northwest direction. Both sets of fractures measured in outcrop are plunging near vertical. The fracture mapping on drill core from the boreholes illustrates that fractures exist in the bedrock mass, decrease with depth and fracture spacing slightly increases with depth (Fig B.5 – B.7). Evidence of

weathering along the fracture surface indicates potential zones of fluid flow. The packer test results demonstrate that certain zones of the borehole have hydraulic conductivities orders of magnitude greater than that of other zones.

It is understood by the author that infiltration into the fractures will occur in the upland (recharge) areas and along the slope of the hills towards the Saint John River where the overburden layers are either less thick or not present. Because of the hydraulic head gradient, fracture flow will facilitate discharge further down the slope of the hills towards the Saint John River and into the window locations where the aquifer is in direct contact with the basal sand and gravel unit or the fractured bedrock.

An equivalent porous medium (continuum) model approach, described in Chapter 2, is used to represent the bedrock-mass matrix and the fractures in the model domain. Ten bedrock layers in the numerical model are chosen by the author to represent the bedrock extending to a depth of -500 m below seal level (bsl). Hydraulic conductivity values from the packer test results are applied to the ten individual bedrock layers, with the hydraulic conductivity values incrementally decreasing with depth and the layer thickness incrementally increasing with depth. This was done to facilitate a smooth transition of decreasing the hydraulic conductivity with depth.

4.1.2 Hydrological Data

Hydrological influx components (i.e., water entering hydrologic system) considered in the conceptual model to impact recharge to the groundwater system are: 1)

precipitation, snowmelt and total runoff amounts, influenced by topography and ground surface features; and 2) direct recharge from the Saint John River into the aquifer.

Hydrological outflux components (i.e., water exiting hydrologic system) considered in the conceptual model to impact recharge to the groundwater system are: 1) evapotranspiration; 2) Saint John River discharge; 3) small stream baseflow; 4) sublimation during the winter months; and 5) the pumping wells for the city's water supply.

Groundwater recharge is estimated between 30 mm/yr and 400 mm/yr over zones of the model domain. The 65 km^2 model area is divided into four zones and each assigned a run-off coefficient factor (*C* factor) depending on land use (Fetter, 2001). These zones included the river (8 km^2, 0 *C* factor), pavement (12 km^2, 0.7 *C* factor), buildings (12 km^2, 0.5 *C* factor) and vegetation cover (38 km^2, 0.1 *C* factor). During the numerical model calibration, discussed in Section 4.4, recharge for each zone is adjusted until calibration is reached. Table 4.3 and Table 4.4 outline the meteorological and hydrological data used in the conceptual model.

Table 4.3 Meteorological Data (1953 -2000) used for the conceptual model.

	Minimum	Maximum	Average
Precipitation[1] (mm/yr)	690	1521	1101
Lower ppt. years 1955 - 1971, 1984 – 2000 (mm/yr)	690	1243	1036
Higher ppt. years 1972 – 1983 (mm/yr)	1010	1521	1241
Precipitation monthly partitions 1953 – 2000			
Jan + Feb + Mar + Dec (mm)	221	587	382
April + May (mm)	58	335	172
June + July (mm)	88	307	171
August + September (mm)	65	325	177
October + November (mm)	75	323	198

Table 4.3 continued. Meteorological Data (1953 -2000) used for the conceptual model.			
	Minimum	Maximum	Average
Evapotranspiration[2] (mm/yr)	380	578	487
Evapotranspiration monthly partitions 1953 –2000			
Jan + Feb + Mar + Dec (mm)	0	6	0
April + May (mm)	52	122	95
June + July (mm)	215	258	235
August + September (mm)	161	204	183
October + November (mm)	25	59	42
Temperature[1] (°C)	-15.4	25.6	5.4
Relative Humidity[1] (%)	67	78	72
[1] Environment Canada (2008)			
[2] Calculation method outlined by Thornthwaite and Mather (1957)			

Table 4.4 Hydrological data used for conceptual model.			
	Minimum	Maximum	Average
Snowmelt runoff [1] (mm/yr)	138	465	274
Total runoff [1] (mm/yr)	261	778	495
Recharge from surface infiltration [2] (mm/yr)	100	400	-
Recharge to SJR area, 8 km^2 (mm/yr)	100	400	
Recharge to vegetative area, 38 km^2 (mm/yr)	90	360	
Recharge to building area, 12 km^2 (mm/yr)	50	200	
Recharge to pavement area, 12 km^2 (mm/yr)	30	120	
Recharge from groundwater [3] (mm/yr)	49	165	160
Vertical linear velocity of SJR to aquifer [4] (m/day)	0.1	5	-
[1] Thornthwaite and Mather calculations, [2] TerrAtlantic (2000), [3] Davies (1995), [4] Dawe (2005)			

4.2 3D Numerical Groundwater Modeling Objectives and Overview

The purpose of developing a 3D numerical groundwater model for the Fredericton area is: 1) determine how flux from the fractured bedrock varies under both natural flow and well field pumping conditions; and 2) determine how variations in recharge, as a result of climate change, will impact the quantity of the groundwater flux from the fractured bedrock to the overburden aquifer.

Finite element models can represent complex hydrogeologic geometries, such as those found in the Fredericton Aquifer and adjacent area. This is possible because finite element modeling allows for discrete elements to vary in size and shape in contrast to the rectangular less flexible grid system represented in finite difference models. As well, finite element modeling allows for variations in the flexible discretization (i.e., process of subdividing an element domain into a finite number of elements) of the mesh, grid refinement in specified areas and natural boundaries are represented in the boundary conditions, and the mesh design permits simulation of the phreatic surface formed by the water table (WHI, 2006).

The numerical 3D modeling program Finite Element FLOW (FEFLOW) version 5.306 modeling package (WASY GmbH, 2007) can simulate groundwater flow, heat transfer and dissolved species mass transport, all of which are governed by similar mathematical equations. This software is used to simulate the hydrogeologic flow system of the Fredericton area. The physical properties and site geometry are represented in FEFLOW using mathematical expressions (WHI, 2006), which are governed by the equation for a deformable porous media (Equation 4.1). This groundwater flow equation has been derived using a unit volume approach and the conservation of mass, outlined in Bear and Verruijt (1987).

$$\underbrace{\frac{\partial}{\partial x}\left(K_{xx}\frac{\partial h}{\partial x}\right)+\frac{\partial}{\partial y}\left(K_{yy}\frac{\partial h}{\partial y}\right)+\frac{\partial}{\partial z}\left(K_{zz}\frac{\partial h}{\partial z}\right)}_{\text{Groundwater flux in / out}}+\underbrace{W}_{\text{Source/ Sinks}}=\underbrace{S_s\frac{\partial h}{\partial t}}_{\text{Change in storage}} \qquad \text{(Equation 4.1)}$$

where,

$\partial/\partial x$ = discretization in x dimension
Kxx = hydraulic conductivity in the x-direction
$\partial h/\partial x$ = change in hydraulic head in x dimension

$\partial/\partial y$ = discretization in y dimension
Kyy = hydraulic conductivity in the y-direction
$\partial h/\partial y$ = change in hydraulic head in y dimension

$\partial/\partial z$ = discretization in z dimension
Kzz = hydraulic conductivity in the z-direction
$\partial h/\partial z$ = change in hydraulic head in z dimension

W = source/sinks
Ss = specific storage
$\partial h/\partial t$ = change in hydraulic head over time

The 3D numerical model is constructed in a series of steps. The model area includes hydraulic boundary conditions such as recharge zones, discharge zones, and groundwater divides. A topographic database is imported into the 3D numerical model mesh, which gives the surface of the model area. The 3D distribution of the overburden materials and the fractured bedrock layers are incorporated into the model. The model mesh is discretized and refined in the areas of the river, the aquifer, the pumping wells, and observation wells. Hydrogeologic parameters are assigned to each layer or zone. Data from the well field including drawdown and pumping rates are collected and used for the model calibration, model verification and for the transient simulations. The steps and assigned parameters used in building the model are discussed in the following sections, based on the steps outlined by Anderson and Woessner (1992).

4.3 Model Mesh

4.3.1 Topography

A digital terrain map, consisting of 10,953 x, y and z coordinates to represent the topography for the top layer of the model, is imported using the regionalization kriging method available in FEFLOW. The total area of the model domain is 65 km^2 and the northing and easting coordinates of the corners of the model are:

E 2484531, N 7441963	E 2491997, N 7441963
E 2484531, N 7433507	E 2491997, N 7433507

4.3.2 Hydrostratigraphic Layers and Mesh Generation

Hydrostratigraphic layers (i.e., the stratigraphic layers containing hydrogeologic properties) are imported into the model using a borehole database coordinate file compiled by Jeff Whitter (Unpublished data, 2005). This file has the x, y, and z coordinates of the hydrostratigraphic units for 937 boreholes. The northing and easting locations of the majority of the boreholes in this file are concentrated in the downtown core and the general location of the esker. An additional file consisting of 287 x, y and z coordinate locations for the hydrostratigraphic units is created with reference to the topography map, the hydrologic map, and the inclined borehole geologic information to cover the north and south end of the model domain. These data are tabulated in Table F.2 in Appendix F. Note that the basal sand and gravel unit is not included in this dataset and is added later to the model by dividing the entire upper sandstone bedrock unit in half and adding zones of various hydraulic conductivities values. Further discussion of including

and excluding this basal sand and gravel unit in the numerical model is described in Section 4.3.4.

A total of sixteen layers are used for the model (Fig. 4.1). Starting at the surface and moving downwards; the sand and gravel layer, the silty clay layer (divided into two layers), the aquifer layer, the till layer, the basal sand and gravel layer and the fractured bedrock layer divided into ten layers. The thickness of the ten additional bedrock layers, chosen by the author, are in sequence, 5 m, 10 m, 20 m, 20 m, 30 m, 30 m, 60 m, 60 m, 90 m and 90 m thick, respectively. The vertical extent of the model ranges from approximately -500 m bsl to +132 m asl and the total volume of the model domain is 28 km^3. A graphic display of the model elevation is presented in Appendix F, Figure F.8.

Three superelements (i.e., biggest area units of the model to vary mesh density later, if desired) covering the esker location, the north end, and the south end of the model are created. An add-in line segment is used to represent the Saint John River. These sections are discretized to create the finite element mesh, as seen in Figure 4.2. The mesh has 45968 nodes, 83696 elements, and sixteen layers. The Tmesh (Delaunay) generator, a triangle mesh generator option in FEFLOW that allows local variation of mesh density (WASY GmbH, 2007), is applied according to areas, subscribing 3000 nodes initially. Refinement is done in the esker location to the window locations, the pumping well locations (e.g., PW01, PW02, PW03, PW05, PW06, PW07 and PW08), and selected observations points (Fig. 4.2 and Fig. 4.3). The finite element mesh is checked for obtuse angles and whether the triangles meet the Delaunay criterion, which is if the circumcircle of the finite element includes a node not belonging to the finite

element (WASY GmbH, 2007). Approximately 4% of the triangles are between 90^0 and 120^0 and all of the mesh meet the Delaunay criterion. If the mesh has to be adjusted to meet the Delaunay criterion, the edges of the triangles are flipped or moved accordingly.

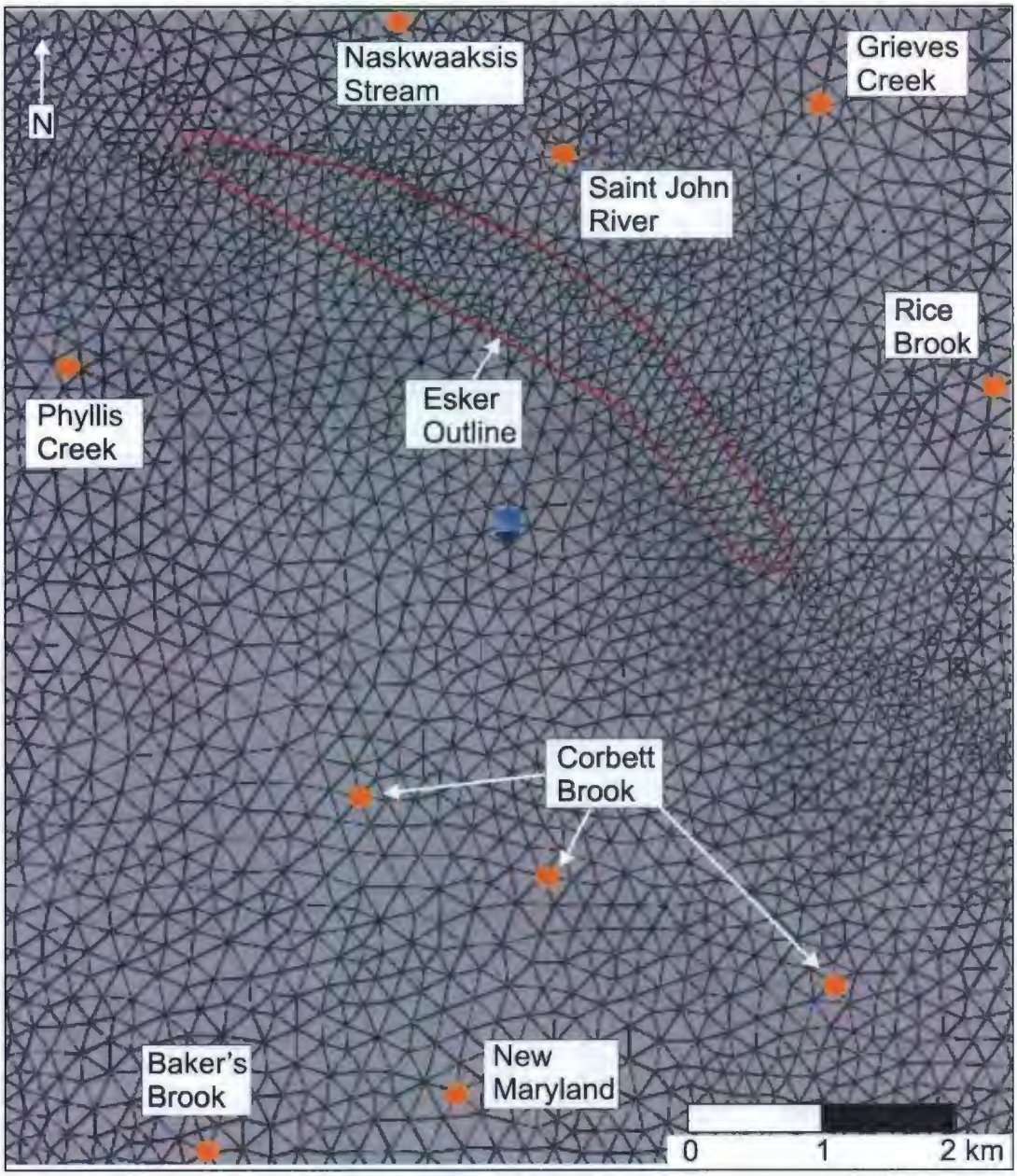

Figure 4.2. Mesh design and surface observation points.

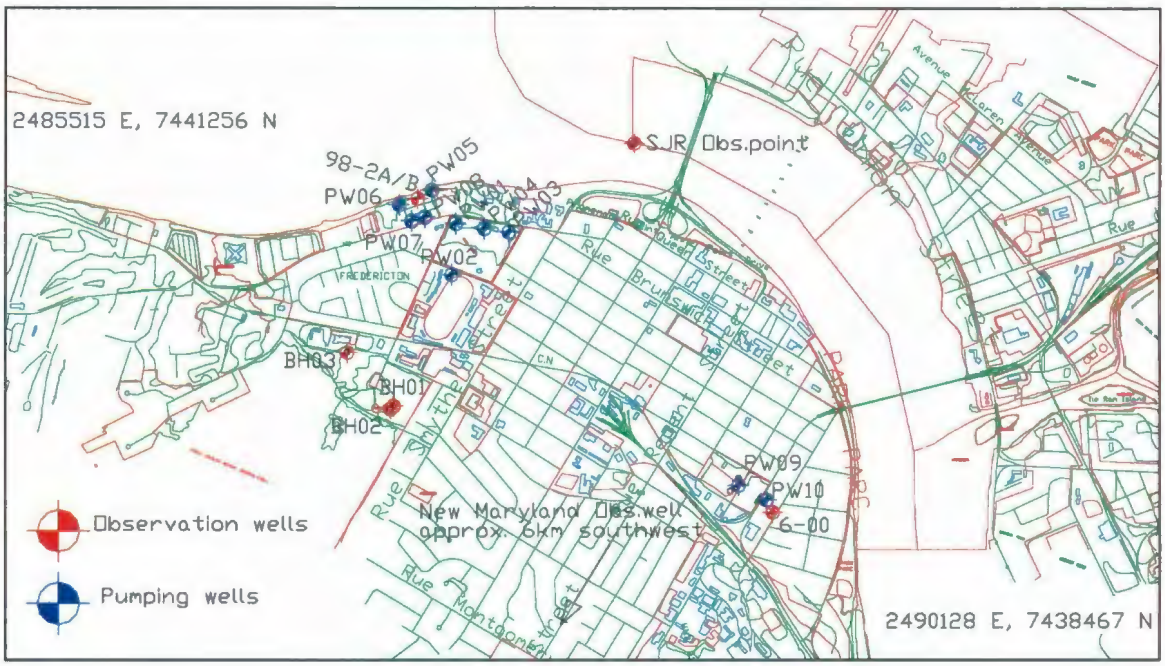

Figure 4.3. Pumping well and observation well locations.

4.3.3 Window Locations in the Till Layer

The till (Layer 5) is considered to have window locations hydraulically connecting the aquifer and the basal sand and gravel unit and/or the underlying fractured bedrock. These window locations are added to the numerical model in two ways: 1) based on the borehole database records compiled by Jeff Whitter (Unpublished data, 2005); and 2) by random sampling of the element numbers in layer five located in the esker area. This is done to investigate how these windows can affect the flux coming from the basal sand and gravel unit and/or the fractured bedrock up into the aquifer.

Referring to the borehole database (Jeff Whitter, unpublished data, 2005), borehole locations in the esker where the sand and gravel (aquifer) unit is underlain directly by bedrock (no till layer reported) are considered to have a window (Fig. 4.4).

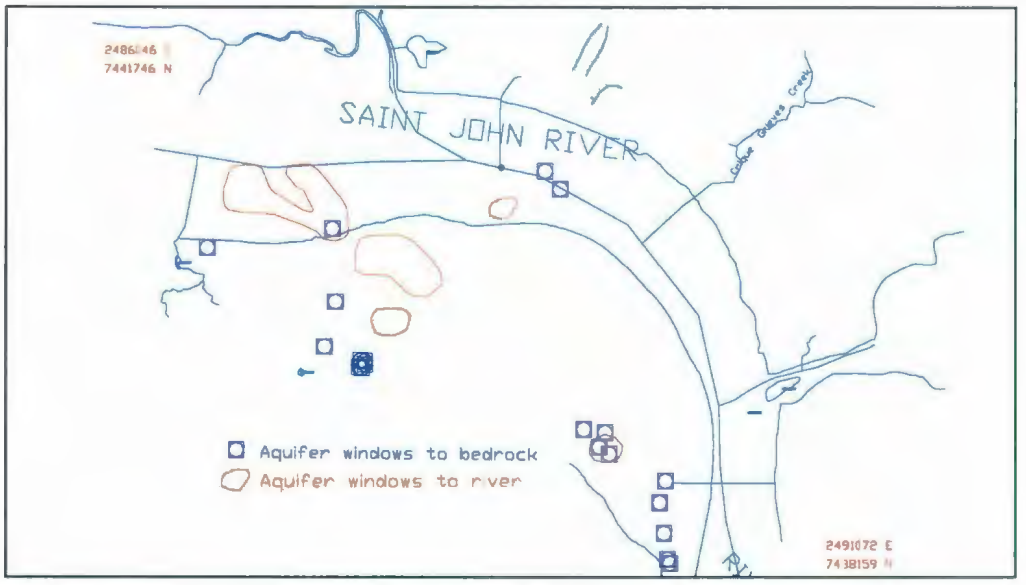

Figure 4.4. Window locations above and below the aquifer.

Of the 938 borehole records in the borehole database, approximately 740 boreholes are drilled in the esker location. Of these 740 boreholes, 91 boreholes are drilled to bedrock. Of these 91 boreholes, 18 boreholes (20%) have a window into the till layer, hydraulically connecting the aquifer and the underlying bedrock and/or basal sand and gravel unit. A total of 21 elements, out of the 518 elements that make up the esker in layer five, are used to represent the 18 boreholes and subsequently the window locations (Fig. 4.5 and Table F.3 in Appendix F). The corresponding element number, representing the window location, is assigned a higher hydraulic conductivity value than that assigned

to the surrounding till layer. This method of applying the window locations based on the borehole database reporting no till layer is considered to be a conservative estimate as it represents 4.1% of the total 518 elements in the esker area.

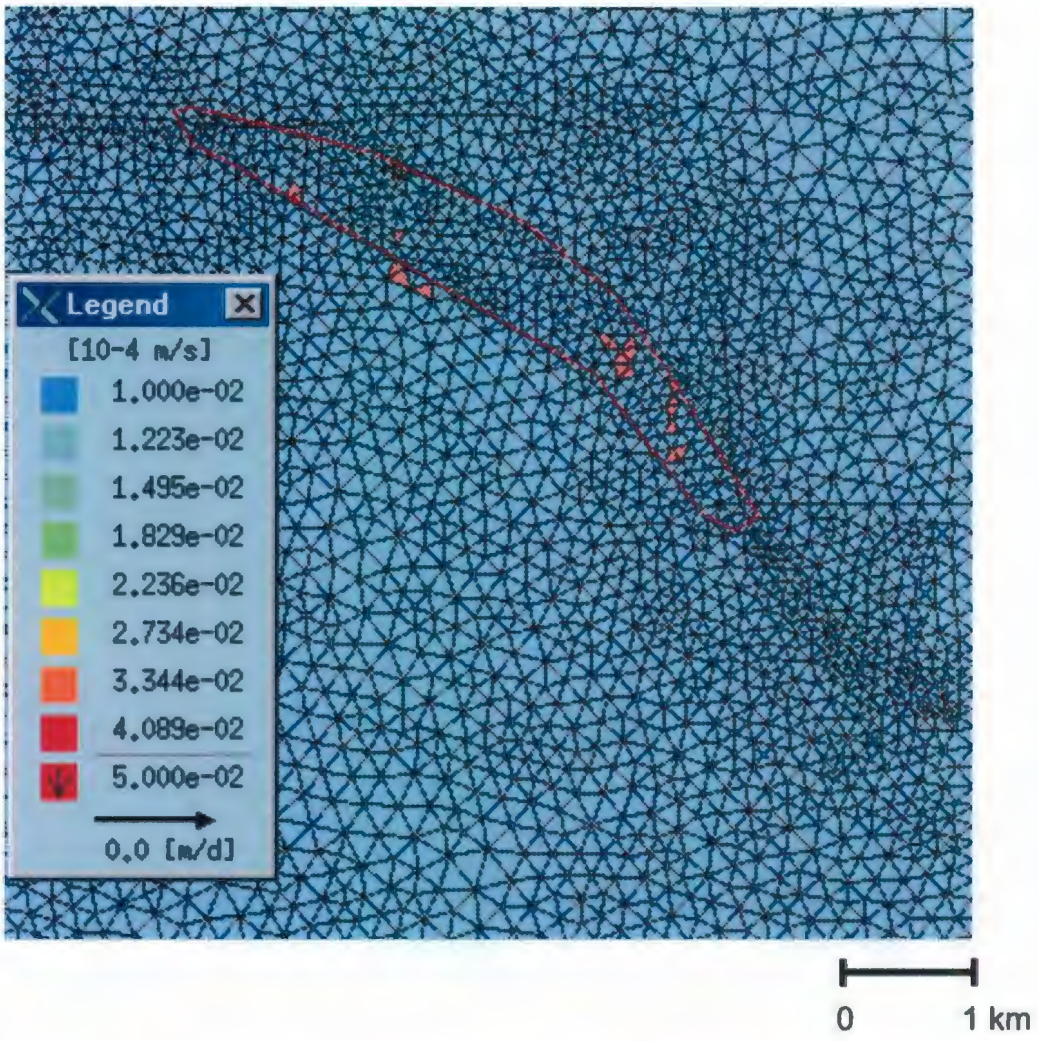

Figure 4.5. Window locations (pink elements) in the till layer using the borehole database records. Esker location outlined in red.

The second method used to handle the windows in the till layer is completed by random sampling a total of 20% of the 518 element numbers in the area of the esker. The

resulting 104 elements, which are not duplicated nor replicated by the original 21 elements, are assigned a higher hydraulic conductivity value than that assigned to the surrounding till layer. These elements are shown in Figure 4.6 and listed in Table F.4 in Appendix F. This is considered to be a realistic representation of the esker area coverage with window locations in the till layer. The results of the steady-state model simulations using the randomly assigned windows in the till layer and the windows in the till layer using the borehole database records are presented in Section 4.5 of this study.

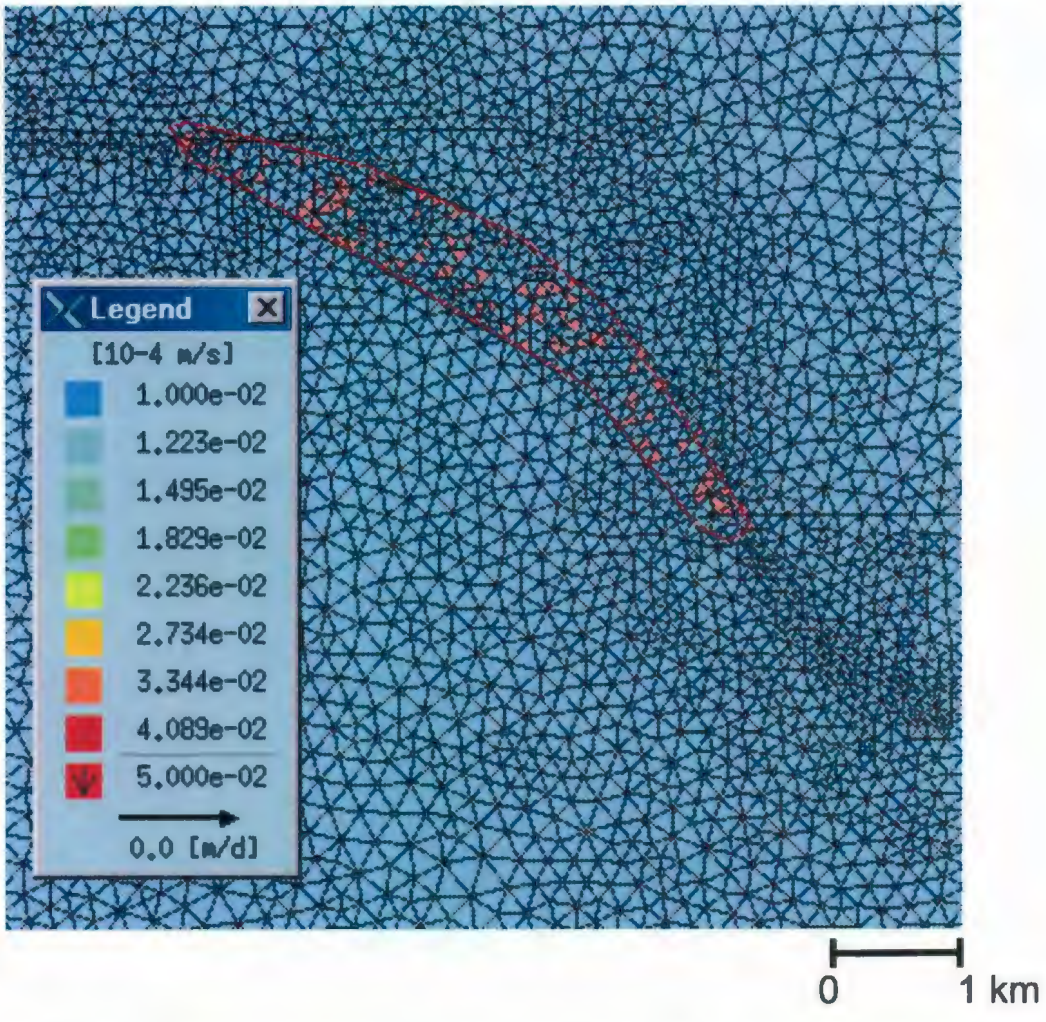

Figure 4.6. Window locations (pink elements) in the till layer using the randomly assigned data.

4.3.4 Excluding and Including the Basal Sand and Gravel Layer in the Model

A numerical model is created to include the basal sand and gravel layer. If the basal sand and gravel layer is included, a layer 5 m thick is created below the till layer by dividing the 10 m thick upper sandstone bedrock layer in half, making a total of sixteen layers. The remaining nine bedrock layers are unchanged. The hydraulic conductivity values assigned to this additional layer are 1×10^{-3} m/s to represent the basal sand and gravel, constrained to the esker area, and 1×10^{-6} m/s for the remainder of the layer to represent the lower permeable material at this depth and area, presented in Figure F.7. With the basal sand and gravel layer included in the model, the resulting increase in hydraulic conductivity would allow for groundwater flux across and upwards towards the till window locations connecting to the aquifer layer above, shown in Figure 4.7. It is expected a greater flux from the basal sand and gravel layer through the till layer in the area of the esker would be present, than if the layer is excluded from the model.

By not including the basal sand and gravel layer, the 10 m thick upper sandstone bedrock layer is in direct contact with the till layer, hydraulically connecting the aquifer and the bedrock in areas of the till windows. Because of the low hydraulic conductivity of this layer (5×10^{-6} m/s) it is expected that flux from the bedrock through the till windows into the aquifer would be upwards and less than that of the basal sand and gravel layer. A schematic is presented in Figure 4.7. The results of the steady-state and transient model simulations using the combination of excluding and including the basal sand and gravel layer are presented in Section 4.5 of this study.

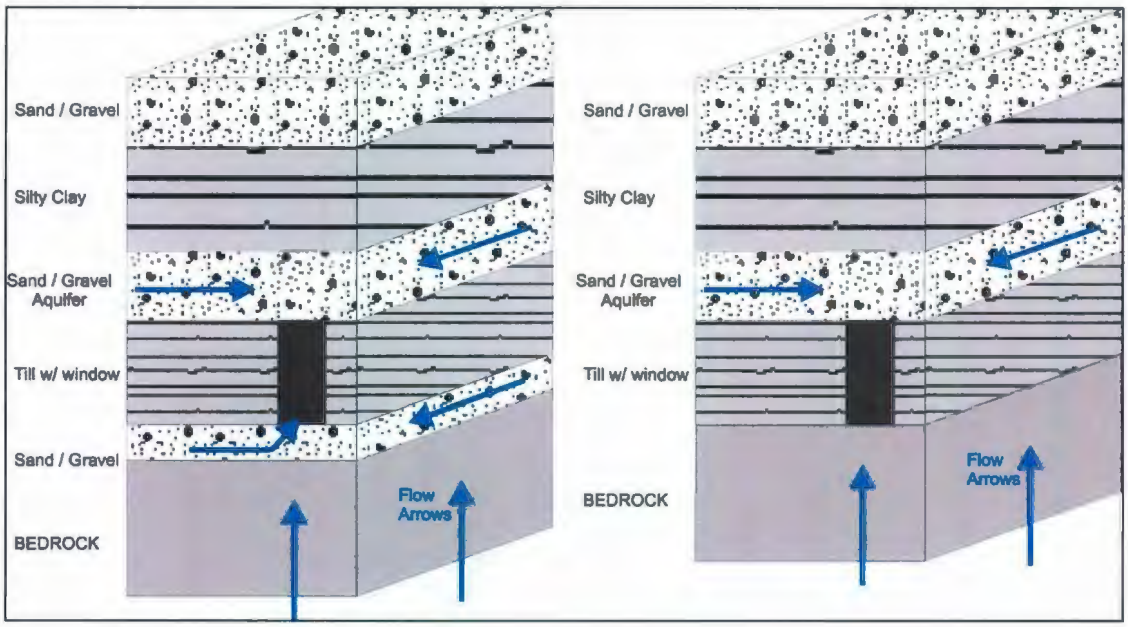

Figure 4.7. Schematic block diagram showing difference in flow when including and excluding the basal sand and gravel unit in the area of the esker.

4.4 Model Calibration

4.4.1 Boundary Conditions

Assigning boundary conditions to a model domain is a critical step in the model construction, with potential for large error if not applied properly (Anderson and Woessner, 1992). Boundary conditions are categorized as either physical or hydraulic.

Physical boundary conditions are those of an impermeable nature or where no-flow is assumed to exist (Anderson and Woessner, 1992). Examples of this type of boundary condition are impermeable fault zones, impermeable bedrock, low permeability deposits, a difference of two orders of magnitude or greater in hydraulic conductivity, or large bodies of surface water (Anderson and Woessner, 1992).

Hydraulic boundary conditions are those that are influenced by the hydrologic conditions of the model domain. In FEFLOW, there are four types considered to be hydraulic boundary conditions, which are listed in FEFLOW as the 1st type Dirichlet conditions, 2nd type Neumann conditions, 3rd type Cauchy conditions and 4th type pumping well boundary.

The 1st type (Dirichlet) describes a hydraulic head boundary for either fixed or time-varying hydraulic heads on nodal points (WASY GmbH, 2007). Examples of this 1st type are constant head surface water bodies such as large streams, rivers, lakes and reservoirs, which should have a strong hydraulic connection to the aquifer in question (ASCE, 1996). The Saint John River, including the width and length in the model area, is assigned a 1st type boundary condition to the top slice for the steady-state and transient model with a constant head of 3.3 m. A second constant head boundary is applied to the outer edge of the top slice of the model domain using a hydraulic head estimated to be 2 m below the surface elevation, with the exception of the river. Where the river intersects the border of the model domain, a constant hydraulic head of 3.3 m is applied. This constant head boundary is applied to the top slice outer border, as opposed to a no-flow boundary condition, because it is considered that the outlying regional hydrology and hydrogeology can influence the behaviour of the flow system in the model area.

The option of using time-varying 1st type hydraulic heads is applied to the well fields pumping well nodal points during the model verification, a transient case where field data is collected between April 1 and May 20, 2005. Discussion of the model verification using this time-varying 1st type hydraulic head is outlined in Section 4.4.6.

The 2nd type (Neumann) boundary condition describes a specified flux across a boundary and is applied to nodes or slices in FEFLOW. Examples of this 2nd type are a specified flux to a surface water body, recharge, springflow, baseflow, and seepage to and from fractured bedrock to the overlying system (Anderson and Woessner, 1992). In FEFLOW, it is possible to enter specified flux using the option "in or out flow to the top or bottom layer." It is determined a groundwater recharge value between 30 mm/yr and 400 mm/yr occurs in the model area, with varying percentages of the recharge applied to different areas of the model (Table 4.4) to reach calibration. These recharge zones, depending on the surface cover of building coverage, pavement coverage, river location or vegetation coverage, are regularly adjusted during the calibration of the model. A figure of the actual recharge applied to the surface model domain is presented in Appendix F in Figure F.9.

A special case 2nd type boundary condition is where the flux is equal to zero. This is used to represent no-flow boundaries such as a topographic high, which acts as a groundwater divide, or an impermeable rock or sediment layer. The 2nd type no-flux boundary condition is applied to the bottom slice of the model because the low hydraulic conductivity ($K_x = 2.5 \times 10^{-8}$ m/s) and depth (~-500 m bsl) will likely have little hydraulic influence to the upper layers of the model.

The 3rd type (Cauchy) is a transfer head-dependent flow boundary, such as a leaky hydraulic connection between a river and an aquifer, separated by a mostly impermeable (colmation) layer. This 3rd type boundary condition is not used in this model.

The 4th type (pumping well) boundary condition is used for the model verification and transient model simulations by applying pumping rates to the well field pumping wells that are screened in the aquifer. For this study, pumping wells PW01, PW02, PW03, PW05, PW06, PW07, and PW08 are used for the model verification exercise, described in detail in Section 4.4.6. Additional pumping wells, PW09 and PW10, installed and brought on-line in 2003 in the Queen's Square area, are included in the transient model simulations. Further discussion of the initial conditions and the 4th type boundary condition are described for the transient model simulation in Section 4.4.2.

4.4.2 Initial Hydraulic Head Conditions

Initial hydraulic head conditions are the hydraulic head distribution data at time = 0 s. Initial conditions are necessary for a transient model simulation and in this study, are also applied to the steady-state model to aid in calibration. The initial hydraulic head data are applied to the top layer of the model. The set of initial conditions for the steady-state model does not have hydraulic head data from wells in the aquifer. These wells in the aquifer are influenced by constant pumping of the well field and cannot be considered at steady-state conditions.

The hydraulic head data used for the steady-state and initial hydraulic head data transient model simulations are collected at various locations in the model domain over a specific time period referred to as a "snapshot." The snapshot is taken between April 1, 2005 starting at 16:45 and ending on May 20, 2005 at 14:45 and these data are presented in Table 4.5.

The observation locations for both steady-state and transient simulations include a point in the Saint John River close to the Wilmot Park well field. These real-time data for the snapshot for the Saint John River are obtained from the Water Survey of Canada (2005) and are graphed in Figure F.10 in Appendix F. Snapshot data are also collected

Table 4.5 Initial hydraulic head data used for model calibration and verification.

Hydraulic heads (m)	Northing (m)	Easting (m)	April 1, 2005 16:45	May 20, 2005 14:40
Saint John River – spatially variable (m)			3.36 – 3.22	3.36 – 3.22
Saint John River (m)	2488657	7440910	3.3	3.3
98-2 bedrock well (m)	2487552	7440628	1.4	2.0
98-2 aquifer well (m)	2487552	7440628	0.9	1.5
BH03 well (m)	2487232	7439898	7.5	7.2
New Maryland well (south Fredericton) (m)	2487812	7433914	97.8	97.5
6-00 well (m)	2489336	7439069	2.3	3.6
Phyllis Creek (m)	2485040	7439238	85.0	n/a
Grieves Creek (m)	2490576	7441293	22.0	n/a
Rice Brook (m)	2491860	7439147	13.0	n/a
Corbett Brook – 3 locations (m)	2490570 2488512 2487141	7434674 7435528 7436128	107.4, 79.7, 44.5	n/a
Baker Brook (m)	2486092	7433536	115.5	n/a
Naskwaaksis Stream (m)	2487446	7441955	4.8	n/a

from inclined well BH03 and these data are presented in Figure F.11. As well, a monitoring well in New Maryland and surface water points from the Nashwaaksis Stream, Phyllis Creek, Grieves Creek, Baker Brook, Corbett Brook, and Rice Brook are also used for the snapshot. The Government of New Brunswick provides data for the monitoring well in New Maryland (Hydrologic Services Water Sciences Section, 2006) that are graphed in Figure F.12 in Appendix F.

The surface water points are taken from a topographic map by estimating the surface water elevation to be equivalent to the topographic elevation. Additional snapshot points for the initial conditions for the transient simulations are from the 98-2 bedrock

well, 98-2 aquifer well, and bedrock well 6-00. Wells 98-2-bedrock, 98-2-aquifer, 6-00, and BH03 are installed with Leveloggers ® to measure real-time hydraulic head data during the snapshot period and are graphed in Figure F.11 in Appendix F. There are gaps in the hydraulic head data for wells 6-00, 98-2-bedrock, and 98-2-aquifer where the water level exceeds the available logger range because of a large rain event on April 28, 2005, during the snapshot period. The precipitation record during the snapshot period is presented in Figure F.13 in Appendix F.

Well field information supplied by the City of Fredericton Water and Sewer Division (Laurie Corbett and Rick Larlee, Pers. comm., 2008), including hydraulic head and pumping rates, for wells PW01, PW02, PW03, PW05, PW06, PW07, and PW08 during the snapshot period are outlined in Table F.5 and Table F.6 in Appendix F. The pumping well elevations, transducer depth, and transducer elevations used for this study to convert the hydraulic heads are located in Table F.7 in Appendix F. Pumping well water levels and pumping rates during the snapshot period are displayed, in Figures F.14 and F.15, respectively, in Appendix F.

4.4.3 Fluid-flux Analysis using Fences

Fluid-flux analysis is completed in FEFLOW to determine the fluid-flux from the fractured bedrock and/or basal sand and gravel layer to the overburden aquifer under the natural conditions, pumping conditions and with variations to recharge rates. "Fences" are created in FEFLOW for the fluid-flux analysis for areas of interest in the model domain. To create these fences (i.e., polygons drawn on the top layer and extend down

through each layer), a total of 17 polygons are added to the model, dividing up the Saint John River, downtown core, well field, aquifer, base of the hill and the window locations in the silty clay and the till layers. These polygons represent the fences and the locations are presented in Figure 4.8 in 2D plan and in Figure 4.9 in 3D view.

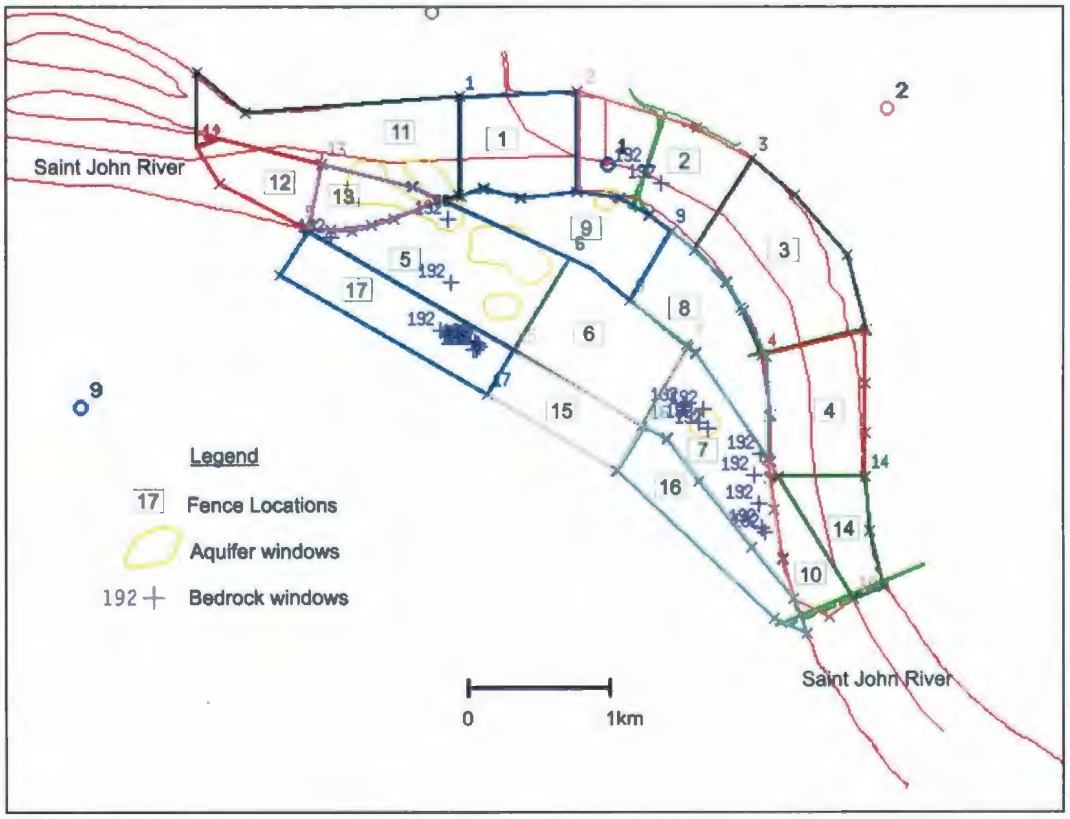

Figure 4.8. 2D view of fence locations 1 – 17 in the model domain.

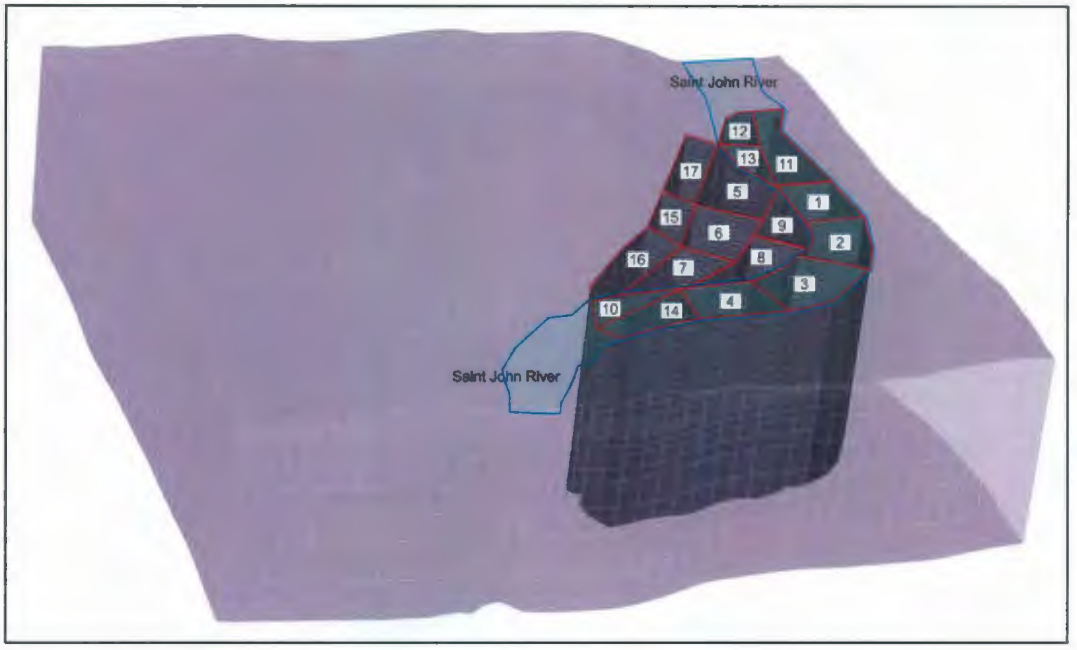

Figure 4.9. 3D view of fence locations 1 – 17 in the model domain.

Following the model simulation for both steady-state and transient conditions, the fluid-flux analyser is applied to each fence and each top six or seven slices, as a normal flux through each individual slice, to obtain the total integral fluid-flux, reported as m^3/d. The fluid-flux from the top six or seven slices, depending whether the basal sand and gravel layer is excluded or included, are analysed. The author chose not to include the fluid-flux data from the remaining nine bedrock slices since the fluid-flux is consistently upwards and decreases to near zero fluid-flux on the bottom slice.

The total integral fluid-flux is a result of the upward fluid-flux minus the downward fluid-flux normal to the surface of the slice in question. A positive total integral fluid-flux represents net upward fluid-flux in the positive z-direction. A negative total integral fluid-flux represents net downward fluid-flux in the negative z-direction.

This method of fluid-flux analysis is used to obtain the fluid-flux from the fractured bedrock and/or basal sand and gravel layer and the remaining overburden layers.

4.4.4 Calibration of Model

Using the model with the randomly assigned window locations in the till layer, excluding the basal sand and gravel layer as the example, the model is calibrated in FEFLOW for steady-state using the trial-and-error method and following calibration steps outlined in Anderson and Woessner (1992). The calibration procedure involves adjusting parameter values (Tables 4.1 to Table 4.4) until the field-measured hydraulic heads and calculated hydraulic heads are in the low acceptable residual error tolerance and convergence is met. The error tolerance and convergence criteria data used for the steady-state model are listed in Table 4.6.

Table 4.6 Error and convergence criteria set in FEFLOW for steady-state model.

Initial Time	0 day
Time to switch to CN-scheme	2000 time steps
Error Tolerance	Default: 0.001%
Applied to:	Default: Euclidian L2 Integral (RMS) Norm
Maximum number of iterations per time step	24
Adaptive Mesh Error	0.001%
A posteriori error estimator	Onate-Bugeda
Upwinding to stabilize numerical results	Default: No upwind. Galerkin FEM

To check the simulation results, the field-measured hydraulic heads are plotted against the calculated hydraulic head results (Fig. 4.10) and tabulated in Table 4.7. If the slope of the line is close to 1.0 and the y-intercept is close to 0, then the model results are acceptable for quantitative criteria calculations including the mean error (ME), mean

absolute error (MAE) and the root mean square (RMS) error. The ME is the mean difference between measured heads (hm) and simulated head (hs) and calculated using Equation 4.2. The MAE is the mean of the absolute value of the differences in measured and simulated heads and calculated using Equation 4.3. The RMS error is the average of the squared differences in measured and simulated heads and calculated using Equation 4.4. This RMS error should be less than 5% (WHI, 2006).

$$ME = \frac{1}{n}\sum_{i=1}^{n}(h_m - h_s)_i$$

Equation 4.2

$$MAE = \frac{1}{n}\sum_{i=1}^{n}\left|(h_m - h_s)_i\right|$$

Equation 4.3

$$RMS = \frac{1}{n}\sum_{i=1}^{n}\left[(h_m - h_s)_i^2\right]^{0.5}$$

Equation 4.4

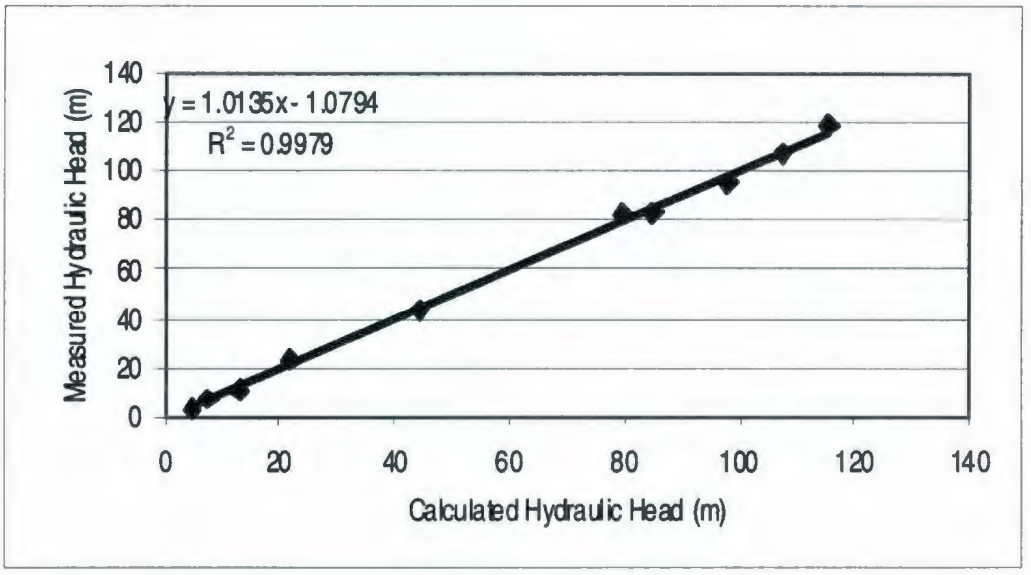

Figure 4.10. Steady-state calibration results.

Table 4.7 Results of the calibrated steady-state model and associated errors using the randomly assigned windows in the till layer, excluding the basal sand and gravel layer.

			Hydraulic Head		
	Measured in field (m)	Calculated (m)	Ho - Hc (m)	Ho - Hc Absolute (m)	Square Difference
Grieves Brook	22.00	23.23	-1.23	1.23	1.52
Rice Brook	13.00	10.66	2.34	2.34	5.46
New Maryland Well	97.80	95.07	2.73	2.73	7.45
Nashwaaksis Stream	4.80	3.06	1.74	1.74	3.04
Corbett Brook	44.50	43.31	1.19	1.19	1.41
Corbett Brook	79.70	82.55	-2.85	2.85	8.12
Corbett Brook	107.40	107.44	-0.04	0.04	0.00
Phyllis Creek	85.00	82.71	2.29	2.29	5.24
Baker Brook	115.50	118.58	-3.08	3.08	9.50
BH03	7.50	7.58	-0.08	0.08	0.01
			0.3	1.76	2.04
ME = Mean Error			ME	MAE	RMS
MAE = Mean Absolute Error					
RMS = Root Mean Square					

It is also considered that if the ratio of RMS error to the total head loss in the model domain is small, the error among the hydraulic heads is a small portion of the general model response (Anderson and Woessner, 1992) and the model calibration is considered acceptable. In this example, the ratio between the root mean square (RMS) error of 2.04 m and the calculated total head loss of 115.52 m (maximum hydraulic head minus minimum hydraulic head) is 0.02, acceptable for the calibration of the model.

A second method of checking the model calibration, numerical instabilities, and associated residual error, is to assess the water balance by comparing the simulated inflows with the simulated outflows (Anderson and Woessner, 1992). Error in the water balance should be less than 1% and is calculated by the difference between the total outflow and inflow divided by either the inflow or outflow (Anderson and Woessner, 1992). In FEFLOW, the budget analyser tool is used to assess the water balance as it computes the quantity of fluid mass entering or leaving the simulated region (WASY GmbH, 2007). The steady-state calibration results in Table 4.8 indicate a 0% error in the water balance using the randomly assigned window locations in the till layer.

The steady-state model using the randomly assigned window locations in the till layer and excluding the basal sand and gravel layer is used for the sensitivity analysis and model verification exercise described in Section 4.4.5 and 4.4.6 respectively.

Table 4.8 Results of steady state calibration fluid flux mass balance comparing the randomly assigned and borehole database window locations in the till layer, basal sand and gravel layer excluded.

	RANDOMLY ASSIGNED		BOREHOLE DATABASE ASSIGNED	
FLUX_TYPE	FLUX_IN(+)	FLUX_OUT(-)	FLUX_IN(+)	FLUX_OUT(-)
UNIT	Q [m3/d]	Q [m3/d]	Q [m3/d]	Q [m3/d]
BC123_FLUXES	1.5721E+04	-2.9034E+04	1.5718E+04	-2.9030E+04
WELL_FLUXES	0.00E+00	0.00E+00	0.00E+00	0.00E+00
AREAL_FLUXES	1.33E+04	0.00E+00	1.33E+04	0.00E+00
IMBALANCE	1.21E-04	0.00E+00	1.06E-03	0.00E+00
% Error	0%		0%	

4.4.5 Sensitivity Analysis

Sensitivity analysis of the model calibration is done to measure the uncertainty in the model, if small changes in the input data create large changes in the computed results and if the model is defensible (WHI, 2006; Anderson and Woessner, 1992). Sensitivity analysis for this study is done by making systematic changes of hydraulic conductivity and recharge values and comparing the resulting hydraulic heads to the previously calibrated steady-state hydraulic heads (Anderson and Woessner, 1992). Hydraulic conductivity and recharge are the chosen parameters for the sensitivity analysis because these two parameters should have the greatest effect on the flux from the bedrock to the aquifer, as governed by Darcy's Law (Equation 3.3).

In the sensitivity analysis, hydraulic conductivity and recharge values are changed independently by 50%, a percentage chosen by the author. The resulting percentage change in the hydraulic head values are compared with the calibrated steady-state model simulation results. The second stage of the sensitivity analysis is to change simultaneously the hydraulic conductivity and the recharge values by 50%, a percentage

chosen by the author. The resulting percentage change in the hydraulic head values are compared with the calibrated steady-state model simulation results.

A third stage in the sensitivity analysis is to increase the z-direction hydraulic conductivity (Kz) by one order of magnitude greater than the Kx and Ky. Although the equivalent porous medium approach is used for the model, it is recognized vertical fractures can create Kz greater than Kx and Ky. This is tested in the sensitivity analysis.

The sensitivity analysis clearly demonstrates that some regions of the model domain are not affected by the changing parameters, regardless of how great a change. In particular, observation points at the Rice Brook and the Nashwaaksis Stream have little change in hydraulic head to the 50% parameter value change. This can be explained by the close proximity of these points to the constant head boundary conditions. The calculated hydraulic heads and the RMS error results are listed in Table 4.9. The additional results are tabulated in Appendix F in Table F.8 to Table F.14.

Table 4.9 Results of sensitivity analysis using the randomly assigned window locations in the till layer, excluding the basal sand and gravel layer. Hydraulic head changes for recharge and hydraulic conductivity (K) displayed.

			Recharge 50%		K values 50%	
		Calibrated	Increase	Decrease	Decrease	Increase
	Measured	Calculated	Calculated	Calculated	Calculated	Calculated
	in field (m)	(m)	(m)	(m)	(m)	(m)
Grieves Brook	22.0	23.2	25.58	20.88	27.93	21.67
Rice Brook	13.0	10.6	10.95	10.37	11.24	10.47
New Maryland Well	97.8	96.7	104.18	85.96	113.29	89.00
Nashwaaksis Stream	4.8	3.1	3.07	3.05	3.08	3.05
Corbett Brook	44.5	45.8	48.35	38.27	53.39	39.95
Corbett Brook	79.7	85.1	97.71	67.39	112.87	72.44
Corbett Brook	107.4	112.5	124.88	90.01	142.31	95.82
Phyllis Creek	85.0	79.2	87.08	78.34	91.45	79.80
Baker Brook	115.5	120.1	124.44	112.72	130.30	114.67
BH03	7.5	7.4	8.69	6.48	9.80	6.85
RMS Error	-	2.0	6.8	10.3	15.1	7.5

The remaining observation points, not located on or close to a constant head boundary condition, are affected by the parameter changes. Figure 4.11 shows the effect hydraulic conductivity and recharge values have on the absolute value of mean residual hydraulic head. In Figure 4.11, the positive (+) 50% and negative (-) 50% change in recharge value produce near opposite results on either side of the +% and –% change from the calibrated value scale. Figure 4.12 shows the change in hydraulic heads when increasing or decreasing the recharge rates. Referring again to Figure 4.11, the + 50% and -50% change in hydraulic conductivity values produce slightly different extents of opposite percentage change in the values of the residual versus the percent change from the calibrated value. Figure 4.13 shows the change in hydraulic head when increasing or decreasing the hydraulic conductivity.

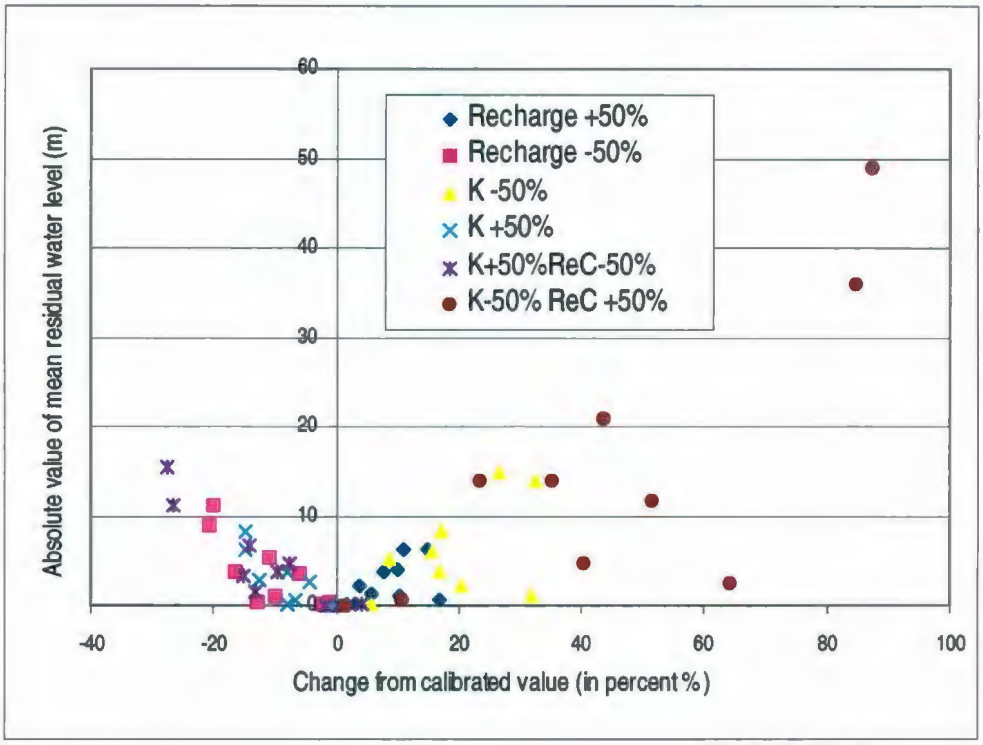

Figure 4.11. Results of the sensitivity analysis comparing the change in hydraulic head from the calibrated values and the absolute value of mean residual hydraulic head.

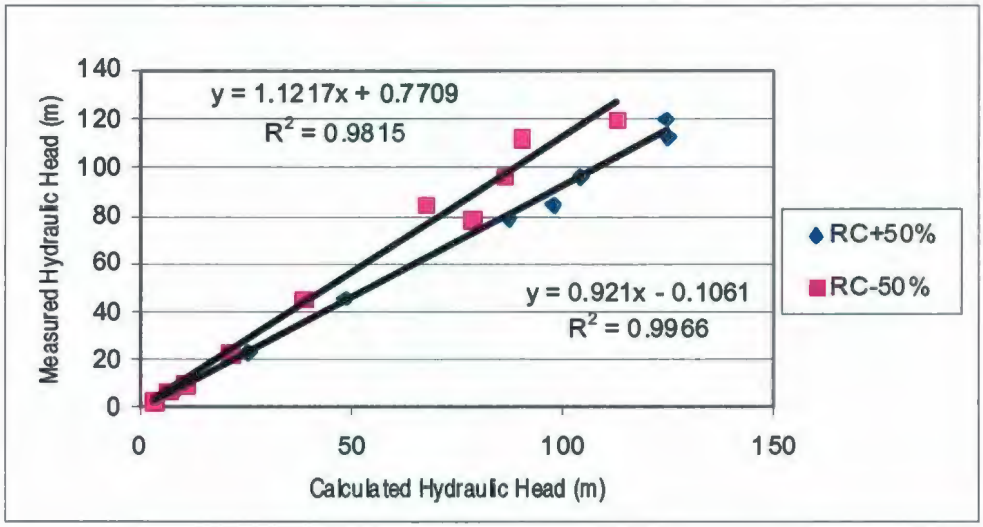

Figure 4.12. Sensitivity analysis of recharge on the steady-state model using the randomly assigned windows in the till layer, excluding the basal sand and gravel layer.

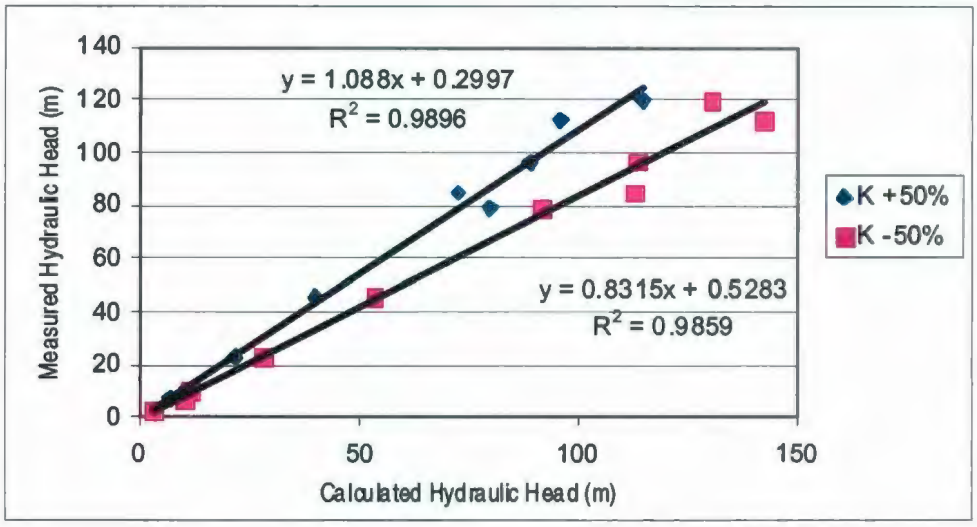

Figure 4.13. Sensitivity analysis of hydraulic conductivity on the steady-state model using the randomly assigned windows in the till layer, excluding the basal sand and gravel layer.

The second step of the sensitivity analysis is to change both the recharge and the hydraulic conductivity values simultaneously and see how the hydraulic heads will change. When the recharge is decreased by 50% and the hydraulic conductivity is increased by 50%, the results lay mostly in the negative percent change from the calibrated value scale, as viewed in Figure 4.11. The hydraulic head results of this analysis are listed in Table 4.10. When the recharge is increased by 50% and the hydraulic conductivity is decreased by 50%, the results lay mostly in the positive percent change from the calibrated value scale, as viewed in Figure 4.11. The results between the measured and calculated hydraulic heads of this analysis are listed in Table 4.10 and displayed in Figure 4.14. The maximum change from the calibrated value scale and the absolute value of mean residual hydraulic head occurs when the hydraulic conductivity is

decreased simultaneously with an increase in recharge. The second greatest change occurs when the hydraulic conductivity is decreased on its own.

The third step of the sensitivity analysis involves increasing the Kz one order of magnitude greater than the Kx and Ky. The hydraulic head results and RMS error are presented in Table 4.10 and Table F.14. All hydraulic heads increased with the exception of the observation points at Nashwaaksis Stream and Grieves Brook.

Table 4.10 Results of sensitivity analysis using the randomly assigned window locations in the till layer, excluding the basal sand and gravel layer. Hydraulic head changes for simultaneous adjustments to recharge and hydraulic conductivity (K) and z-direction K changes displayed.

Location	Measured in field (m)	Calibrated Calculated (m)	K 50% increase ReCh 50% decrease (m)	K 50% decrease ReCh 50% increase (m)	Z - direction K 2^{0} increase (m)
Grieves Brook	22.0	23.2	20.15	32.61	23.11
Rice Brook	13.0	10.6	10.46	11.78	11.80
New Maryland Well	97.8	96.7	83.07	138.64	107.92
Nashwaaksis Stream	4.8	3.1	3.07	3.10	2.99
Corbett Brook	44.5	45.8	38.86	69.34	46.92
Corbett Brook	79.7	85.1	62.61	157.23	94.39
Corbett Brook	107.4	112.5	81.44	210.60	123.44
Phyllis Creek	85.0	79.2	71.40	106.97	86.97
Baker Brook	115.5	120.1	110.83	148.09	126.85
BH03	7.5	7.4	7.74	12.20	8.18
RMS Error	-	2.0	13.64	43.36	6.65

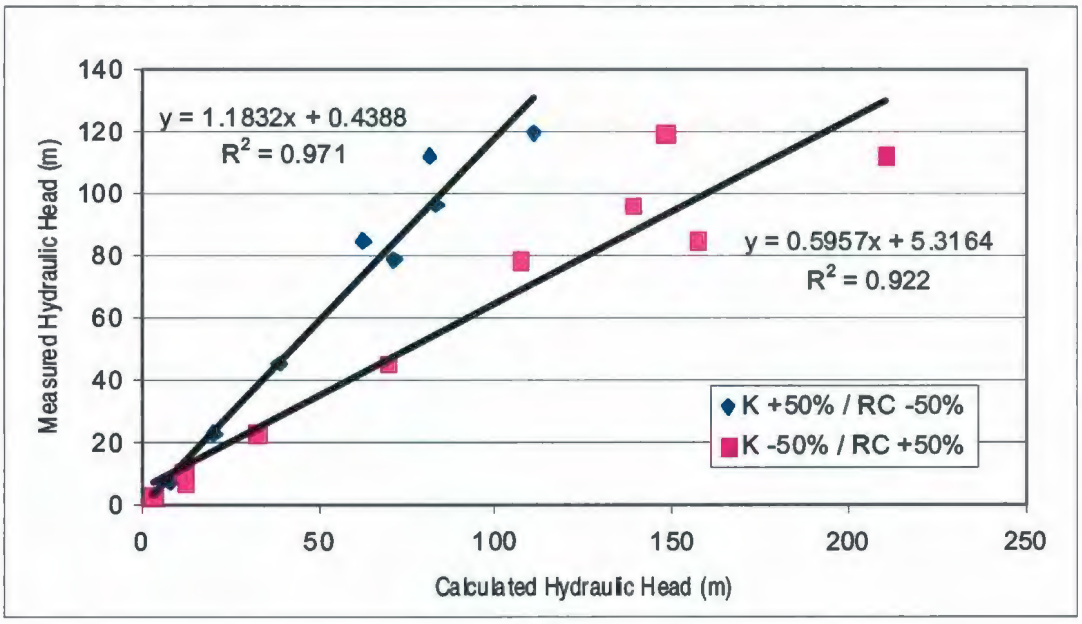

Figure 4.14. Sensitivity analysis of recharge (RC) and hydraulic conductivity (K) on the steady-state model using the randomly assigned windows in the till layer, excluding the basal sand and gravel layer.

4.4.6 Model Verification

Model verification is completed following the sensitivity analysis by comparing the numerical solution to a valid data source independent from the calibration data to test the model for accuracy and predictability (WHI, 2006; Anderson and Woessner, 1992). For this study, a transient simulation using pumping rates and hydraulic head data from the well field during the snapshot period between April 1, 2005 and May 20, 2005 is completed for the model verification exercise.

The data are input to FEFLOW using the time-varying functions editor, which allows the user to add hydraulic head data for the 1st type Dirichlet (i.e., hydraulic head data for specific nodes that vary with time) and the 4th type pumping well data (i.e.,

pumping rates for specific wells that vary with time) as hydraulic boundary conditions. The time-varying hydraulic head (1st type) data added to the model includes snapshot data for bedrock wells BH03, 98-2-BR and 6-00 (Layer 6), aquifer well 98-2-A (Layer 4), pumping wells PW01, PW02, PW03, PW05, PW06, PW07, PW08 (Layer 4) and the Saint John River (e.g., Slice 1). The time-varying pumping rates (4th type) at pumping wells PW01, PW02, PW03, PW05, PW06, PW07, and PW08 are added to the respective well locations in Layer 4, as it is assumed the well screens are positioned in the aquifer layer only. To indicate that well screens do not advance into the till layer, a 4th type boundary condition pumping rate of 0 m^3/d is applied in Layer 5 to the nodes directly beneath the pumping wells in Layer 4. The total number of days for the model verification simulation is 49.7 days, which represents the total time of the snapshot period between April 1, 2005 at 16:45 and May 20, 2005 at 14:45.

The initial simulated hydraulic head results on April 1, 2005 and the final calculated hydraulic head results on May 20, 2005 are compared with the existing field data (Fig. 4.15). The temporal and control data set used for the model verification is listed in Table F.15. Calculations are completed for the ME, MAE, and RMS error, and results are listed in Tables 4.11 for Day 1 (April 1, 2005) and Table 4.12 for Day 49.7 (May 20, 2005). Results of the model verification fluid-flux mass balance and associated error are listed in Table 4.13.

The results from the model verification exercise establish that the model is able to produce hydraulic head data below the acceptable RMS error using data independent

from the calibrated steady-state model. This example increases the overall confidence in the model construction.

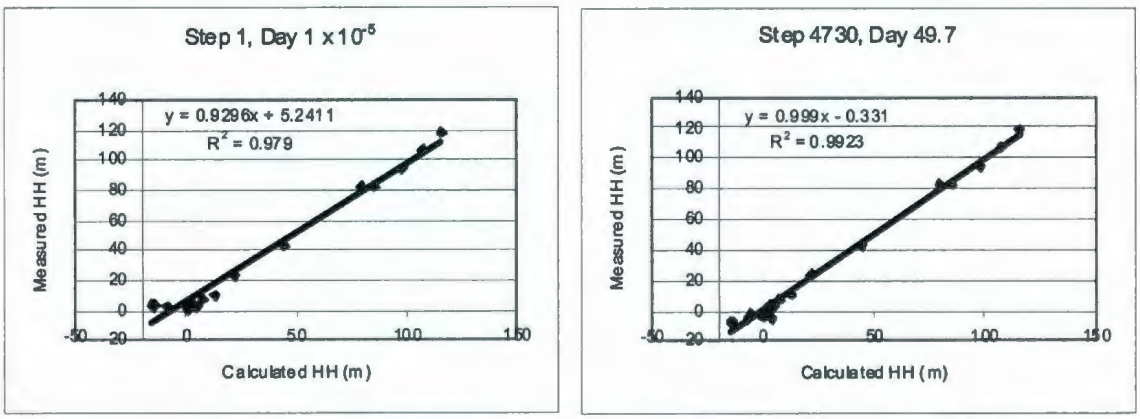

Figure 4.15. Results of the model verification simulation for days 1 x 10^{-5} and 49.7.

Table 4.11 Results of the model verification at Step 1, Day 0.00001.							
					Hydraulic Head		
	Northing	Easting	Measured	Calculated	Ho - Hc	Ho - Hc	Square
	(m)	(m)	in field (m)	(m)	(m)	Absolute (m)	Difference
Grieves B	2490576	7441293	22.00	23.22	-1.22	1.22	1.50
Rice B	2491860	7439147	13.00	10.64	2.36	2.36	5.56
NM	2487812	7433914	97.80	95.05	2.75	2.75	7.55
Nashw S	2487446	7441955	4.80	3.06	1.74	1.74	3.04
Corbett B	2490570	7434674	44.50	43.30	1.20	1.20	1.44
Corbett B	2488512	7435528	79.70	82.47	-2.77	2.77	7.66
Corbett B	2487141	7436128	107.40	107.35	0.05	0.05	0.00
PC	2485040	7439238	85.00	82.68	2.32	2.32	5.40
Baker B	2486092	7433536	115.50	118.58	-3.08	3.08	9.46
BH03	2487232	7439898	7.50	7.50	0.00	0.00	0.00
98-a	2487541	7440656	0.90	0.91	-0.01	0.01	0.00
98-b	2487527	7440598	1.40	1.38	0.02	0.02	0.00
6-00	2489288	7439203	2.30	3.75	-1.45	1.45	2.09
PW01	2487754	7440557	-0.37	3.27	-3.64	3.64	13.25
PW08	2487619	7440519	-14.56	2.43	-16.99	16.99	288.62
PW02	2487775	7440259	-8.39	2.77	-11.16	11.16	124.60
PW07	2487531	7440459	-14.27	3.24	-17.51	17.51	306.56
PW06	2487437	7440596	-0.27	3.10	-3.37	3.37	11.38
PW03	2488072	7440466	-15.27	3.33	-18.60	18.60	346.10
PW05	2487595	7440631	0.04	3.28	-3.24	3.24	10.52
					-3.63	4.67	2.16
ME = Mean Error					ME	MAE	RMS
MAE = Mean Absolute Error							
RMS = Root Mean Square							

Table 4.12 Results of the model verification at Step 4730, Day 49.7.

					Hydraulic Head		
DAY 49.7	Northing (m)	Easting (m)	Measured in field (m)	Calculated (m)	Ho - Hc (m)	Ho - Hc Absolute (m)	Square Difference
Grieves B	2490576	7441293	22.00	23.22	-1.22	1.22	1.48
Rice B	2491860	7439147	13.00	10.52	2.48	2.48	6.15
NM	2487812	7433914	97.80	95.05	2.75	2.75	7.55
Nashw S	2487446	7441955	4.80	3.05	1.75	1.75	3.05
Corbett B	2490570	7434674	44.50	43.30	1.20	1.20	1.44
Corbett B	2488512	7435528	79.70	82.47	-2.77	2.77	7.66
Corbett B	2487141	7436128	107.40	107.35	0.05	0.05	0.00
PC	2485040	7439238	85.00	82.68	2.32	2.32	5.40
Baker B	2486092	7433536	115.50	118.58	-3.08	3.08	9.46
BH03	2487232	7439898	7.20	7.17	0.03	0.03	0.00
98-a	2487541	7440656	1.5	1.54	-0.04	0.04	0.00
98-b	2487527	7440598	2	2.02	-0.02	0.02	0.00
6-00	2489288	7439203	3.6	0.17	3.43	3.43	11.76
PW01	2487754	7440557	0.15	-4.46	4.61	4.61	21.21
PW08	2487619	7440519	-14.04	-7.93	-6.11	6.11	37.34
PW02	2487775	7440259	-6.34	-5.02	-1.32	1.32	1.73
PW07	2487531	7440459	-13.89	-6.64	-7.25	7.25	52.50
PW06	2487437	7440596	-5.68	-2.64	-3.04	3.04	9.26
PW03	2488072	7440466	1.22	-2.88	4.10	4.10	16.84
PW05	2487595	7440631	4.26	-5.37	9.63	9.63	92.76
					0.38	2.86	1.69
ME = Mean Error					ME	MAE	RMS
MAE = Mean Absolute Error							
RMS = Root Mean Square							

Table 4.13 Results of the model verification exercise fluid flux mass balance and associated error.

FLUX_TYPE:	Fluid flux mass balance	
BALANCE_TYPE:	Total	
CURRENT_TIME:	49.700001 [d]	
FLUX_TYPE	Flux In (+)	Flux Out (-)
UNIT	Q [m3/d]	Q [m3/d]
BC123_FLUXES	2987359	-2988983
WELL_FLUXES	0	-18244
AREAL_FLUXES	13312	0
IMBALANCE	0	-6556
% Error	0.20%	

4.5 Discussion of Model Results

4.5.1 Steady-state model using randomly assigned windows in the till layer, excluding the basal sand and gravel layer

The steady-state model results of hydraulic head and error using the randomly assigned windows in the till layer with the basal sand and gravel layer excluded, are presented in Section 4.4.4 for the discussion of the model calibration. Figure 4.8 shows the comparison between the calculated hydraulic head and the field-measured hydraulic head of the model simulation. Table 4.7 shows the results of the model simulation associated error and Table 4.8 for the water balance results and error calculation.

The results of the fluid-flux analysis for this steady-state model are tabulated in Table 4.14. The following discussion references Figure 4.8 and Table 4.14 throughout. Starting from the top layer of sand and gravel and moving downward through the model layers, upward fluid-flux occurs entirely throughout Fences 1-4, 10-14 and 16. The upward fluid-flux in the overburden layers ranges between 12 m^3/d and 1824 m^3/d. It is expected that the Fences 1-4 and 10-14, lying in the river area, will have upward fluid-flux, as that represents a natural discharge location in the model. Fence 16 lies at the base of the south slope without till or clay windows present, representing an additional discharge zone in the model since all fluid-flux in that area is upwards.

Downward fluid-flux occurs in the overburden for Fences 5-9, 15 and 17 at a rate between 12 m^3/d and 717 m^3/d. Fences 5-9 encompass the downtown core and the esker that has the clay windows connecting the aquifer to the overlying sand and gravel layer.

Fences 15 and 17 are in or adjacent the locations of the till windows connecting the aquifer and the bedrock. As well, the downward fluid-flux occurring in the top four layers of Fence 17 is because a higher recharge value is assigned in this area of Odell Park, a vegetative and grassy area.

Table 4.14 Vertical fluid influx and outflux between slices for the steady-state randomly assigned windows in the till layer model, basal sand and gravel layer excluded.

		FENCE																
		1	2	3	4	5	6	7	8	9	10	11	12	13	14	15	16	17
LAYER	SLICE	m^3/d	m^3/d	m^3/d	m^3/d	m^3/d	m^3/d	m^3/d	m^3/d	m^3/d	m^3/d	m^3/d	m^3/d	m^3/d	m^3/d	m^3/d	m^3/d	m^3/d
sand/gravel	1	299	556	505	325	170	-194	-400	-23	-20	317	865	85	1404	481	19	206	-717
Clay	2	260	648	1083	461	572	-209	-266	39	84	399	878	138	1538	531	111	489	-494
Clay	3	191	336	490	343	464	-79	75	28	144	418	801	134	1292	463	-46	100	-285
aquifer	4	131	310	402	256	-151	99	-96	50	117	177	457	135	844	339	12	448	-519
till	5	59	219	264	194	1824	27	433	-12	63	156	152	112	288	161	517	903	656
bedrock	6	26	131	156	56	342	168	244	-0.2	13	28	65	91	38	23	188	268	343
	Fluid flux in negative/downward direction.																	

The bedrock layer including all the fences has fluid-flux between –0.2 m^3/d and 343 m^3/d. It is expected that groundwater fluid-flux from the fractured bedrock in Fences 15, 16 and 17, between 188 m^3/d and 343 m^3/d, will be greater because of their position at the base of the hill, in close proximity to the natural windows in the till layer, and where overburden is not as thick as towards the river. Upward fluid-flux between 168 m^3/d and 342 m^3/d from the bedrock is present in Fences 5, 6, and 7, which encompass the esker on land and where natural windows in the till layer are present.

4.5.2 Steady-state model using borehole database assigned windows in the till layer, excluding the basal sand and gravel layer

The mass balance and percent error results of this model simulation are presented in Table 4.8. The fluid-flux analyses results for this steady-state model are tabulated in Table 4.15. The hydraulic head and associated errors using the model with the borehole database assigned windows are presented in Table F.16. The RMS error is 2.04, the same as that of the model using the randomly assigned windows in the till layer. A comparison on the steady-state observed and calculated hydraulic heads of the two till window placement scenarios is presented in Figure 4.16.

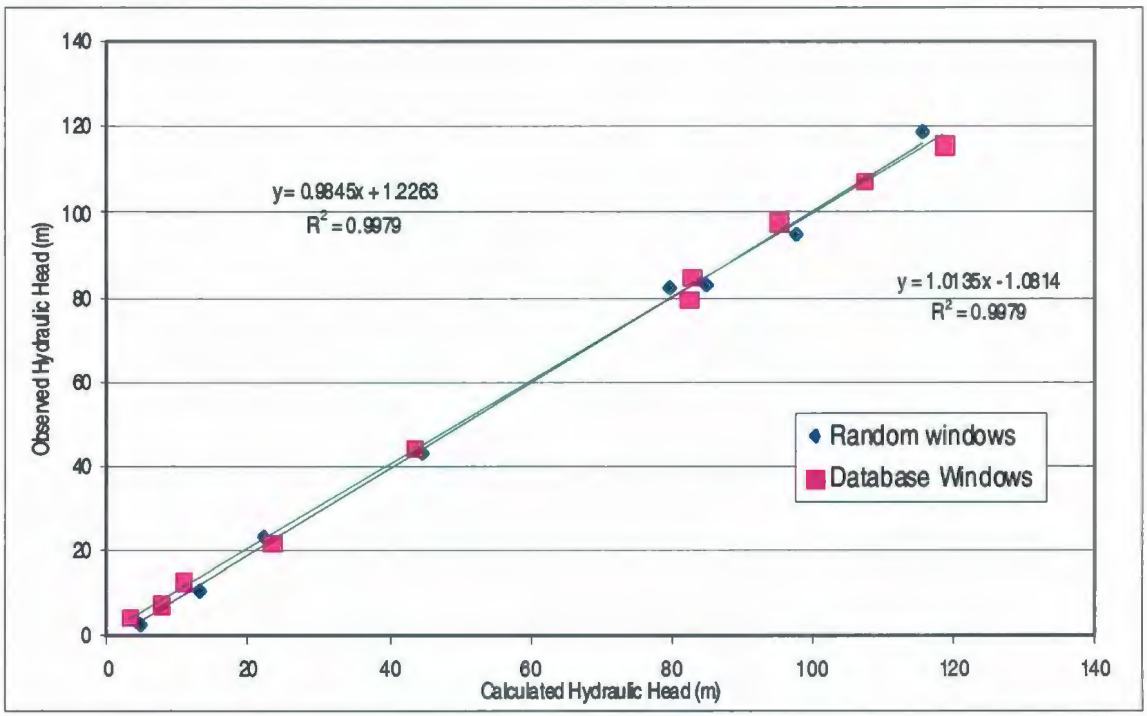

Figure 4.16. Steady-state hydraulic head results for both till window placement scenarios, basal sand and gravel layer excluded, show little difference between the two.

Table 4.15 Vertical fluid influx and outflux between slices for the steady-state database assigned windows in the till layer model, basal sand and gravel layer excluded.

		FENCE																
		1	2	3	4	5	6	7	8	9	10	11	12	13	14	15	16	17
LAYER	SLICE	m³/d	m³/d	m³/d	m³/d	m³/d	m³/d	m³/d	m³/d	m³/d	m³/d	m³/d	m³/d	m³/d	m³/d	m³/d	m³/d	m³/d
sand/gravel	1	315	536	430	254	319	-197	-485	-34	-77	167	1249	39	2210	308	27	232	-715
clay	2	268	637	991	383	926	-213	-394	-1	-56	219	1080	92	2319	353	119	466	-504
clay	3	195	326	418	269	752	-78	-42	-5	47	227	1133	92	1966	288	-45	54	-289
aquifer	4	136	303	346	228	-555	780	-319	7	21	86	604	74	1277	221	42	466	-553
till	5	53	211	243	144	3114	-693	423	8	87	39	185	82	414	108	557	962	657
bedrock	6	25	127	149	54	321	172	245	9	11	30	67	79	40	25	203	273	371
	Fluid flux in negative/downward direction.																	

Starting from the top layer of sand and gravel and moving downward through the model layers, upward fluid-flux occurs entirely throughout Fences 1-4, 10-14 and 16. The upward fluid-flux in the overburden is between 7 m^3/d and 3114 m^3/d. Again, the fences lying in the river area, Fences 1-4 and 10-14, represent a natural discharge location in the model and thus have upward fluid-flux throughout the slices, in steady-state. Fence 16 lies at the base of the south slope without till or clay windows present, representing an additional discharge zone in the model since all fluid-flux in this area is upwards.

Downward fluid-flux occurs in layers of the overburden for Fences 5-9, 15 and 17 at a rate between 1 m^3/d and 715 m^3/d. Again, Fences 5-9 encompass the downtown core and the esker. Fences 15 and 17 are in or adjacent the locations of the till windows connecting the aquifer and the bedrock, and Fence 17 is assigned a higher recharge value.

The bedrock layer, including all the fences, has upward fluid-flux between 9 m^3/d and 371 m^3/d. Again, the groundwater fluid-flux from the fractured bedrock in Fences 15, 16 and 17, between 203 m^3/d and 371 m^3/d, will be greater because of their position at the base of the hill, in close proximity to the natural windows in the till layer and where

overburden is not as thick as towards the river. As with the model using the randomly assigned windows, the upward fluid-flux from the bedrock layer for Fences 5, 6, and 7 is similar, between 172 m^3/d and 321 m^3/d, which is the location of the esker in the downtown area where natural windows in the till layer are present.

4.5.3 Steady-state model using randomly assigned windows in the till layer, including the basal sand and gravel layer

The hydraulic head results from the model simulation using the randomly assigned windows in the till layer, including the basal sand and gravel layer, are presented in Table F.17 in Appendix F. The hydraulic heads are approximately the same, whether the basal sand and gravel layer is included or excluded.

The results of the fluid-flux analysis are tabulated in Table F.18 and show differences in fluid-flux compared with the steady-state models that exclude the basal sand and gravel layer. Upward fluid-flux occurs entirely through all slices in Fences 1-4, 10-14 and 16, fences directly covering the river area, a natural discharge location in the model. For the overburden materials, all fences included, the upward fluid-flux occurs at a rate between 1 m^3/d and 1711 m^3/d.

Upward fluid-flux from the basal sand and gravel layer in the location of the esker (e.g., Fences 5, 6, 7, 10, 12, and 13 all in Slice 6) occurs at a rate between 31m^3/d and 668 m^3/d. Fences 15, 16 and 17 with higher recharge assigned to the area, have upward fluid-flux from this same Slice 6 at a rate between 123 m^3/d and 265 m^3/d.

For the bedrock materials, all fences included, fluid-flux is upwards and occurs at a rate between 0.2 m^3/d and 299 m^3/d. The greatest fluid-flux occurs in Fences 5-7 and 15-17 (Slice 7) and occurs at a rate between 173 m^3/d and 299 m^3/d.

Downward fluid-flux occurs solely in the overburden layers in Fences 5-9, 15 and 17 at a rate between 5 m^3/d and 724 m^3/d. These fences lie on or adjacent to the locations of the clay windows connecting the aquifer to the overlying river and/or the top sand and gravel layer. Fences 15 and 17 are adjacent to or on the locations of the till windows connecting the aquifer and the basal sand and gravel layer.

4.5.4 Steady-state model using borehole database windows in the till layer, including the basal sand and gravel layer

A fourth model scenario is run using the borehole database windows in the till layer, including the basal sand and gravel layer. The hydraulic head result of this steady-state model simulation is presented in Table F.17 in Appendix F. The hydraulic heads are approximately the same whether the basal sand and gravel layer is included or excluded.

The results of the fluid-flux analysis are tabulated in Table F.19 in Appendix F, and show differences in fluid-flux compared with the steady-state models that exclude the basal sand and gravel layer. As with the model using the randomly assigned windows in the till layer and including the basal sand and gravel layer, upward fluid-flux occurs entirely through all slices in Fences 1-4, 10-14 and 16, fences directly covering the river area. For the overburden materials, all fences included, the upward fluid-flux occurs at a rate between 11 m^3/d and 3032 m^3/d.

Upward fluid-flux from the basal sand and gravel layer in the location of the esker (e.g., Fences 5, 6, 7, 10, 12 and 13 all in Slice 6) occurs at a rate between 56 m^3/d and 502 m^3/d. Fences 15, 16 and 17 that lie at the base of the hill with higher recharge assigned to the area, have upward fluid-flux from this same Slice 6 at a rate between 179 m^3/d and 322 m^3/d.

For the bedrock materials, all fences included, fluid-flux is upwards and occurs at a rate between and 11 m^3/d and 299 m^3/d. The greatest fluid-flux from the sandstone bedrock layer is in Fences 5-7 and 15-17 (Slice 7) and occurs at a rate between 188 m^3/d and 299 m^3/d.

Downward fluid-flux occurs solely in the overburden layers in fences 5-9, 15 and 17 at a rate between 2 m^3/d and 727 m^3/d. These fences lie on or adjacent to the locations of the clay windows connecting the aquifer to the overlying river and/or the top sand and gravel layer. Fences 15 and 17 are adjacent to or on the locations of the till windows connecting the aquifer and the basal sand and gravel layer.

4.5.5 Discussion of Steady-State Results

A summary of the fluid-flux results from the steady-state model simulations is presented in Table 4.16. The upward fluid-flux from the upper sandstone bedrock layer to the till layer, including all fences for both till window scenarios but excluding the basal sand and gravel layer, ranges between 9 m^3/d and 371 m^3/d and in the area constrained to the esker, ranges between 28 m^3/d and 342 m^3/d. Including the basal sand and gravel layer for both till window scenarios, the upward fluid-flux from the sandstone bedrock

layer into the basal sand and gravel layer ranges between 0.2 m^3/d and 299 m^3/d. In the area constrained to the esker, the fluid-flux ranges between 9 m^3/d and 291 m^3/d.

Table 4.16 Fluid flux results of excluding and including the sand and gravel layer for two till window scenarios in steady-state.

	Random Windows			Database Windows		
	Upward Fluid Flux into Till Layer			Upward Fluid Flux into Till Layer		
	Bedrock	Bedrock	S+G	Bedrock	Bedrock	S+G
	S+G excluded	S+G included		S+G excluded	S+G included	
	m^3/d	m^3/d	m^3/d	m^3/d	m^3/d	m^3/d
All Fences Flux Range	13 - 343	0.2 - 299	10 - 668	9 - 371	11 - 299	13 – 502
Flux Range for Fences in Esker (5 – 7,10,12,13)	28 - 342	9 - 291	31 - 668	30 - 321	15 - 288	56 - 502
Total Flux for Esker (Fences 5 - 7,10,12,13)	911	852	1147	887	874	1158
Total Flux for on-land downtown area (Fences 5 - 9, 15 – 17)	1566	1412	1463	1605	1485	1661

The upward fluid-flux from the basal sand and gravel layer for both till window scenarios including all fences, ranges between 10 m^3/d and 668 m^3/d. In the area constrained to the esker, the fluid-flux ranges between 56 m^3/d and 502 m^3/d for the borehole database assigned till windows and between 31 m^3/d and 668 m^3/d for the randomly assigned window locations in the till.

The fluid-flux analysis indicates the maximum upward fluid-flux from the basal sand and gravel layer occurs in the esker area at a rate 668 m^3/d when using the randomly assigned windows compared with 502 m^3/d, when using the borehole database assigned windows. The fluid-flux analysis of the bedrock indicates the maximum upward fluid-flux occurs at the south slope base at 371 m^3/d when the borehole database till windows, excluding the basal sand and gravel layer, is used. When the basal sand and gravel layer is included, the upward fluid-flux from the bedrock drops to a maximum rate 299 m^3/d in

the south slope base area and to 291 m^3/d in the esker area when using the randomly assigned windows in the till layer.

For each model simulation, the fluid-flux varies depending which model is used. These changes though are not great enough to affect changes in the steady-state hydraulic heads, which remain similar for each model simulation.

4.5.6 Transient Model Simulations

The transient model simulations are run using the hydraulic head solution generated by the steady-state models. In addition to the observation points used for the steady-state simulation, bedrock wells 98-2-BR and 6-00 and aquifer well 98-2-A are used to analyse the transient simulation hydraulic head results. These wells cannot be used during the steady-state simulations because they are under the influence of constant pumping conditions of the well field.

The transient model is run using the models with the randomly assigned till windows and the borehole database windows in the till layer, as described in Section 4.3.3. In general, the resulting hydraulic heads and fluid-flux are very similar; as such, only the transient simulation results using the randomly assigned till windows are presented. The exception is when the basal sand and gravel layer is included. The simulations exclude and include the basal sand and gravel layer for: 1) well field pumping conditions from current usage of approximately 26,000 m^3/d and doubling the usage to 52,000 m^3/d; and 2) determining how variations in recharge from a 50% increase and 50% decrease impact the quantity of the groundwater fluid-flux from the fractured

bedrock and/or the basal sand and gravel layer, to the overburden aquifer while the well field is pumping 26,000 m^3/d.

4.5.6.1 Well Field Pumping 26,000 m^3/d for 365 days and 5 year period - Randomly assigned till windows, basal sand and gravel layer excluded

A constant pumping rate of 2889 m^3/d is applied to each of the production wells PW01, PW02, PW03, PW05, PW06, PW07, PW08, PW09, and PW10. Two transient simulations are run, one for 365 days and another for 5 years. The resulting hydraulic head data are presented in Table F.20 in Appendix F, and the head differences between the 365 day period and the 5 year period range from 0 m to 0.11 m. A mass balance and associated error is tabulated in Table F.21 in Appendix F. The associated errors for the 365 day and 5 year simulations are 1.4% and 0.5% respectively.

Fluid-flux analysis on each of the 17 fences is completed for the 365 day period (Table F.22 in Appendix F) and the 5 year period (Table F.23 in Appendix F). For the 365 day period (Table F.22) and the 5 year period (Table F.23), there is a downward fluid-flux in 14 of the 17 fences in 65% of the overburden fence slices. The downward fluid-flux for the 365 day period is between 17 m^3/d and 11,147 m^3/d and for the 5 year period between 29 m^3/d and 11,189 m^3/d. The upward fluid-flux in the overburden materials ranges between 8 m^3/d and 1038 m^3/d for the 365 day period and between 4 m^3/d and 1027 m^3/d for the 5 year period.

For comparison, the steady-state simulation has downward fluid-flux in 7 of the 17 fences in 18% of the overburden materials at a rate between 0.2 m^3/d and 717 m^3/d. The increase in downward fluid-flux in the areas of the pumping wells during the

transient simulation illustrate the flow direction is reversed from the steady-state simulation to travel toward the pumping wells rather than discharge upwards towards the river.

As in the steady-state model, there is upward fluid-flux from the bedrock layer. In the transient simulation this fluid-flux is in the range between 18 m^3/d and 356 m^3/d for the 365 day period and between 16 m^3/d and 342 m^3/d for the 5 year period. For comparison with the steady-state simulation, there is an upward fluid-flux in the bedrock layer in the range between 13 m^3/d and 343 m^3/d. Therefore, the difference between the steady-state and transient simulation fluid-flux from the bedrock layer, using the randomly assigned till window locations and excluding the basal sand and gravel layer, is minimal.

4.5.6.2 Well Field Pumping 52, 000 m^3/d for 365 day and 5 year period - Randomly assigned till windows, basal sand and gravel layer excluded

A constant pumping rate of 5778 m^3/d is applied to each of the production wells PW01, PW02, PW03, PW05, PW06, PW07, PW08, PW09, and PW10. Transient simulations are run for a 365 day and a 5 year period. The resulting hydraulic head data are presented in Table F.20 in Appendix F, and the head differences between the 365 day period and the 5 year period range from 0 m to 0.22 m. The mass balance and associated error are tabulated in Table F.24 in Appendix F. The associated errors for the 365 day and 5 year simulations are 1.8% and 0.7% respectively.

Fluid-flux analysis on each of the 17 fences is presented for only the 5 year period (Table F.25 in Appendix F) since results from the 365 day period are similar. Referring to

Table F.25 in Appendix F, there is downward fluid-flux in the 17 fences for 69% of the overburden fence slices. The downward fluid-flux is between 5 m^3/d and 17,464 m^3/d. The upward fluid-flux in the overburden materials ranges between 6 m^3/d and 2027 m^3/d. As expected, the maximum results of fluid-flux are approximately double that from the 26,000 m^3/d pumping rate.

The upward fluid-flux from the bedrock layer pumping 52,000 m^3/d is in the range between 4 m^3/d and 363 m^3/d. For comparison with the 26,000 m^3/d pumping scenario, the upward fluid-flux is between 16 m^3/d and 342 m^3/d. Therefore, the difference between the transient simulations fluid-flux from the bedrock layer, using the randomly assigned till window locations and excluding the basal sand and gravel layer, while pumping either 26,000 m^3/d or 52,000 m^3/d, is minimal.

4.5.6.3 Recharge Increased 50% and Pumping 26,000 m^3/day – Randomly assigned till windows, basal sand and gravel layer excluded

A 50% increase in recharge from the calibrated steady-state values is applied to the top slice while pumping 2889 m^3/d from each production well PW01, PW02, PW03, PW05, PW06, PW07, PW08, PW09, and PW10, totalling 26,000 m^3/d. One simulation is run for 365 days. The resulting hydraulic head data are presented in Table F.26 in Appendix F. There is not a significant change in hydraulic head when using the calibrated transient simulation recharge rate and the 50% increase in recharge rates. A mass balance and associated error are tabulated in Table F.27 in Appendix F. The associated error for the 50% increase in recharge while pumping 26,000 m^3/d is 5%.

Fluid-flux analysis on each of the 17 fences is completed for the 365 day period and is presented in Table F.28 in Appendix F. There is downward fluid-flux in 14 of 17 fences, 64% of the overburden fence slices, between 10 m^3/d and 10,948 m^3/d. The rate of upward fluid-flux in the overburden materials ranges between 14 m^3/d and 1062 m^3/d.

The upward fluid-flux for the bedrock layer is in the range between 18 m^3/d and 387 m^3/d compared to 18 m^3/d and 356 m^3/d for the 26,000 m^3/d calibrated recharge simulation. Therefore, a 50% increase in recharge has no great affect on the upward fluid-flux from the bedrock.

4.5.6.4 Recharge Decreased 50% and Pumping 26,000 m^3 / day – Randomly assigned till windows, basal sand and gravel layer excluded

A 50% decrease in recharge from the calibrated steady-state values is applied to the top slice while pumping 2889 m^3/d from production wells PW01, PW02, PW03, PW05, PW06, PW07, PW08, PW09, and PW10 for a total of 26,000 m^3/d. One simulation is run for 365 days. The resulting hydraulic head data are presented in Table F.26 in Appendix F. There is not a significant change in hydraulic head between the calibrated transient simulation recharge rate, the 50% increase and the 50% decrease in recharge rates. A mass balance and associated error are tabulated in Table F.29 in Appendix F. The associated error for the 50% increase in recharge while pumping 26,000 m^3/d is 7%.

Fluid-flux analysis on each of the 17 fences is completed for the 365 day period and is presented in Table F.30 in Appendix F. There is a downward fluid-flux in 14 of 17 fences and in 65% of the overburden fence slices at a rate between 20 m^3/d and 11,346

m^3/d. The rate of upward fluid-flux in the overburden materials ranges between 26 m^3/d and 1041 m^3/d.

The upward fluid-flux from the bedrock layer for this simulation is between 18 m^3/d and 339 m^3/d compared to 18 m^3/d and 356 m^3/d for the 26,000 m^3/d calibrated recharge simulation. Therefore, a 50% decrease in recharge has no great affect on the upward fluid-flux from the bedrock.

4.5.6.5 Well Field Pumping 26,000 m^3/d for 365 day period - Randomly assigned till windows, basal sand and gravel layer included

A constant pumping rate of 2889 m^3/d is applied to each of the production wells PW01, PW02, PW03, PW05, PW06, PW07, PW08, PW09, and PW10. A transient simulation is run for 365 days. The resulting hydraulic head data are presented in Table F.26 in Appendix F. A mass balance and associated error is tabulated in Table F.31 in Appendix F. The associated error is 0.7%.

Fluid-flux analysis on each of the 17 fences is completed for the 365 day period (Table F.32 in Appendix F). There is a downward fluid-flux in 14 of the 17 fences in 67% of the overburden fence slices. The downward fluid-flux is between 8 m^3/d and 11,162 m^3/d. The upward fluid-flux in the overburden materials ranges between 4 m^3/d and 1212 m^3/d.

As with previous model simulations, there is an upward fluid-flux from the bedrock layer. For this case, it is in the range between 18 m^3/d and 360 m^3/d. For comparison with the similar case excluding the basal sand and gravel layer, the fluid-flux is between 18 m^3/d and 356 m^3/d. Therefore, including the basal sand and gravel layer

does not greatly affect the bedrock fluid-flux. Except in this case, there is additional fluid-flux from the basal sand and gravel layer upwards to the till in the esker area, Fences 5-9, between 54 m^3/d and 608 m^3/d than when the sand and gravel layer is excluded.

4.5.6.6 Well Field Pumping 26,000 m^3/d for 365 day period - Database till windows, basal sand and gravel layer included

A constant pumping rate of 2889 m^3/d is applied to each of the production wells PW01, PW02, PW03, PW05, PW06, PW07, PW08, PW09 and PW10. A transient simulation is run for 365 days. The resulting hydraulic head data are presented in Table F.26 in Appendix F. A mass balance and associated error is tabulated in Table F.31. The associated error is 0.7%.

Fluid-flux analysis on each of the 17 fences is completed for the 365 day period (Table F.33 in Appendix F). There is a downward fluid-flux in 14 of the 17 fences in 67% of the overburden fence slices. The downward fluid-flux is between 6 m^3/d and 11,145 m^3/d. The upward fluid-flux in the overburden materials ranges between 8 m^3/d and 1177 m^3/d.

As with previous model simulations, there is an upward fluid-flux from the bedrock layer. For this case, it is between 18 m^3/d and 357 m^3/d. For comparison with the similar case excluding the basal sand and gravel layer, the fluid-flux range is between 18 m^3/d and 371 m^3/d, presented in Table F.34 in Appendix F. Except in this case, again, there is additional fluid-flux from the basal sand and gravel layer upwards to the till in the

esker area, Fences 5-9, between 54 m^3/d and 568 m^3/d, than when the sand and gravel layer is excluded.

4.5.7 Discussion of Transient Model Simulations

A summary of the fluid-flux results from the transient model simulations is presented in Table 4.17. The upward fluid-flux from the bedrock layer to the till layer using the randomly assigned windows in the till, excluding the basal sand and gravel layer, pumping 26,000 m^3/d for 365 d, ranges between 18 m^3/d and 356 m^3/d. Considering the same scenario but using the database assigned windows in the till, the fluid-flux ranges between 18 m^3/d and 371 m^3/d. When the basal sand and gravel layer is included, considering the same pumping scenario, the fluid-flux from the bedrock ranges between 18 m^3/d and 360 m^3/d using the randomly assigned till windows and between 18 m^3/d and 357 m^3/d when using the database assigned till windows.

It is evident that in comparison to the steady-state model and the transient pumping model, the fluid-flux from the bedrock does not vary much for either till window scenario or whether the basal sand and gravel layer is included or excluded. The lower hydraulic conductivity of this unit does not allow for increases in fluid-flux, regardless of pumping and/or recharge scenarios.

Table 4.17 Transient simulation fluid flux results of excluding and including the sand and gravel layer for two till window scenarios, pumping 26,000 m^3/d, 365 d.

	Random Windows			Database Windows		
	Upward Fluid Flux into Till Layer			Upward Fluid Flux into Till Layer		
	Bedrock S+G excluded	Bedrock S+G included	S+G	Bedrock S+G excluded	Bedrock S+G included	S+G
	m^3/d	m^3/d	m^3/d	m^3/d	m^3/d	m^3/d
All Fences	18 – 356	18 – 360	-67 – 608	18 – 371	18 – 357	-59 – 568
Fences in Esker	32 – 356	24 – 360	-67 – 608	35 – 371	24 – 357	-59 – 568
Total Flux for Esker (Fences 5 – 7, 10,12,13)	1124	1149	1522	1077	1144	1499
Total Flux for on-land downtown area Fences 5 - 9, 15 - 17	1922	1860	2245	1911	1873	2251

The upward bedrock fluid-flux to the till layer in the downtown area, which includes Fences 5-9 and 15-17, excluding the basal sand and gravel layer while pumping 26,000 m^3/d for 365 days, refer again to Table 4.35. The totals are 1922 m^3/d using the randomly assigned windows in the till and 1911 m^3/d for the borehole database assigned windows. Including the basal sand and gravel layer, the fluid-flux from the bedrock is decreased to 1860 m^3/d using the randomly assigned windows in the till and 1873 m^3/d for the borehole database assigned windows.

As expected, with the inclusion of the higher conductive basal sand and gravel layer, the fluid-flux from this layer to the till when pumping 26,000 m^3/d for 365 days is greater than that of the bedrock upward fluid-flux. The fluid-flux including all fences for this layer is between -67 m^3/d and 608 m^3/d using the randomly assigned windows in the till and between -59 m^3/d and 568 m^3/d for the borehole database assigned windows. Considering the downtown area (Fences 5-9, 15-17) the fluid-flux totals from the basal sand and gravel layer are 2245 m^3/d using the randomly assigned windows in the till and 2251 m^3/d for the borehole database assigned windows. Therefore, the presence of the

basal sand and gravel layer allows for increased fluid-flux to the till layer and through the windows to the overlying aquifer.

From the transient simulation fluid-flux results, the bedrock fluid-flux range of 18 m^3/d to 371 m^3/d is not greatly affected by changes in recharge or pumping rates. With changes in precipitation or temperature, a possible result of climate change, this would not greatly affect the groundwater fluid-flux from the bedrock upwards into the overburden. The following chapter runs through a few examples of the potential impacts on the hydrologic system in Fredericton from the theoretical effects of climate change.

CHAPTER 5.0 HYDROLOGIC IMPACTS FROM CLIMATE CHANGE

The potential impacts on the hydrologic system in Fredericton, New Brunswick from the effects of climate change are investigated in this chapter. It is understood by the author that climate change can affect both the short-term and long-term hydrology of the area because of changes in precipitation and temperature.

Should there be a short-term increase in precipitation, the effect it will have on the Fredericton area is reviewed. As occurred in May, 2008, a short-term rapid seasonal high precipitation event, coupled with increased spring temperatures and the snowmelt runoff, caused the banks of the Saint John River to spill over and flood many parts of the downtown Fredericton area and communities along the Saint John River. The maximum height of the river stage at Fredericton during this flood event was 8.6 m asl. With a marked increase in spring temperatures after a winter with high precipitation rates and snow pack accumulation, a fast occurring spring runoff can lead to a low baseflow remaining for the rest of the year, decreasing the amount of groundwater recharge available to the aquifer.

The possibility of wider ranging temperature variations can also create problems for the Fredericton Aquifer. As determined by Amskold (2005), the variation in seasonal groundwater temperatures affects the redox reactions occurring within the aquifer. The temperature variation contributes to an increased concentration of manganese and iron in the groundwater, a concern for the City of Fredericton's drinking water supply. Should surface temperatures reach extremes, it is possible it can increase the groundwater

temperature variations and the dissolved manganese and iron issue can become more pronounced.

If there is a long-term period of drought, the effects of this can also be detrimental to the Fredericton Aquifer. The recharge to the Fredericton area can be reduced to very low amounts, reducing the snow pack accumulation, which can in-turn, reduce the amount of freshwater available for spring runoff. Eventually, the reservoir behind the Mactaquac Dam, located 18 km upstream from Fredericton, would slowly deplete. Evidently, the Saint John River stage would be reduced, reducing the volume of fresh water and available recharge for the aquifer.

Two scenarios are run in the steady-state model to investigate the effects of a high and low Saint John River stage and are discussed below in Section 5.1. One scenario uses an increased Saint John River stage elevation of 8.0 m asl and two different recharge rates to reflect a high precipitation trend. The second scenario uses a decreased Saint John River stage of 1.0 m asl and two different recharge rates to reflect a long-term drought trend.

5.1 Two Scenarios of Potential Hydrologic Impacts from Climate Change

1. Severe increase in precipitation results in high river stage of 8.0 m asl.

Two simulations are run in steady-state using two different recharge rates and an 8.0 m asl constant head boundary condition for the Saint John River stage. The resulting hydraulic head data for the observation points are presented in Table 5.1. The mass balance results are presented in Table 5.2.

Table 5.1 Hydraulic head results of various climate change scenarios.

		Simulation Calculated Hydraulic Heads (m)				
	Field	Calibrated	Calibrated	50% Increase	Calibrated	0 m/d
	Measured	Recharge	Recharge	Recharge	Recharge	Recharge
River Stage	**3.3 m**	**3.3 m**	**8 m**	**8 m**	**1 m**	**1 m**
Grieves Brook	22.00	23.22	25.77	28.12	21.99	17.29
Rice Brook	13.00	10.64	12.20	12.49	9.91	9.33
New Maryland Well	97.80	95.05	95.47	104.58	94.88	76.66
Nashwaaksis Stream	4.80	3.06	3.61	3.63	2.78	2.76
Corbett Brook	44.50	43.30	44.44	49.48	42.76	32.68
Corbett Brook	79.70	82.47	84.30	99.46	81.69	51.37
Corbett Brook	107.40	107.35	108.76	126.20	106.80	71.93
Phyllis Creek	85.00	82.68	83.72	88.09	82.22	73.48
Baker Brook	115.50	118.58	118.68	124.54	118.53	106.81
BH03	7.50	7.39	12.17	13.28	5.34	3.12

Table 5.2 Mass balance results using 8 m river stage.

FLUX_TYPE:	Fluid flux mass balance			
BALANCE_TYPE:	Total			
CURRENT_TIME:	0.001000 [d]			
	Calibrated Recharge		50% Increase in Recharge	
FLUX_TYPE	FLUX_IN(+)	FLUX_OUT(-)	FLUX_IN(+)	FLUX_OUT(-)
UNIT	Q [m3/d]	Q [m3/d]	Q [m3/d]	Q [m3/d]
BC123_FLUXES	19378.15	-32690.56	18877.27	-38845.90
WELL_FLUXES	0.00	0.00	0.00	0.00
AREAL_FLUXES	13312.42	0.00	19968.62	0.00
IMBALANCE	0.00	0.00	0.00	0.00
ERROR %	0%		0%	

The first simulation uses the calibrated steady-state recharge rates but changes the constant head boundary condition river stage from 3.3 m asl to 8.0 m asl. This increases the average hydraulic head across the observation points by 2.0 m. The % error for the difference in mass balance is 0%.

The second simulation uses a 50% increase in recharge rates and a constant head boundary condition river stage of 8.0 m asl. This increases the average hydraulic head across the observation points by 7.5 m. The % error for the difference in mass balance is 0%.

This example indicates that with an increase in precipitation, the amount of recharge available to the hydrologic system is increased and the hydraulic head is increased substantially, thereby increasing the amount of fresh water available to the aquifer from the river and the upland recharge areas. There can be however, a damaging effect with flooding of the Saint John River and low-lying areas around Fredericton and communities along the Saint John River.

2. *Severe reduction in precipitation results in low river stage of 1.0 m asl.*

Two simulations are run in steady-state using two different recharge rates and a 1.0 m constant head boundary condition for the Saint John River stage. The resulting hydraulic head data for the observation points are presented in Table 5.1. The mass balance results are presented in Table 5.3.

The first simulation uses the calibrated steady-state recharge rates but changes the constant head boundary condition river stage from 3.3 m asl to 1.0 m asl. This decreases the average hydraulic head across the observation points by –0.9 m. The % error for the difference in mass balance is 0%.

Table 5.3 Mass balance results using 1 m river stage.				
FLUX_TYPE:	Fluid flux mass balance			
BALANCE_TYPE:	Total			
CURRENT_TIME:	0.001000 [d]			
	Calibrated Recharge		0 m/d Recharge	
FLUX_TYPE	FLUX_IN(+)	FLUX_OUT(-)	FLUX_IN(+)	FLUX_OUT(-)
UNIT	Q [m3/d]	Q [m3/d]	Q [m3/d]	Q [m3/d]
BC123_FLUXES	24520.45	-37832.87	27986.74	-27986.74
WELL_FLUXES	0.00	0.00	0.00	0.00
AREAL_FLUXES	13312.42	0.00	0.00	0.00
IMBALANCE	3.4×10^{-4}	0.00	0.00	-5.0×10^{-5}
ERROR %	0%		0%	

The second simulation, to represent drought conditions, removes all recharge from the hydrologic system by using 0 m/d recharge rate and a constant head boundary condition river stage of 1.0 m asl. This decreases the average hydraulic head across the observation points by –11.9 m. The % error for the difference in mass balance is 0%.

This example indicates that with a long-term period of drought, where little to no recharge is occurring in the hydrologic system, the hydraulic head will drop substantially, thereby reducing the amount of fresh water available to the aquifer from the river and the upland recharge areas.

CHAPTER 6.0 CONCLUSIONS AND RECOMMMENDATIONS

6.1 Conclusions

The intent of this thesis was to use field data and a 3D numerical model to assess the groundwater flux from the fractured sedimentary bedrock to the river valley alluvial aquifer system in Fredericton, New Brunswick. The need to understand and estimate the groundwater contribution from the bedrock aquifer was recognized because of the potential increased water supply demand from a growing population and the potential variation in recharge rates to affect groundwater quantity.

A hydrogeological characterization of the Fredericton area was undertaken to create a conceptual model as a base for the 3D finite element numerical model mesh development, model calibration and model simulations. The hydrogeological information collected included bedrock and surficial geology and structure, fractured rock mass permeability of the bedrock through borehole packer testing, local bedrock groundwater chemistry, geophysical properties of the fractured bedrock and a water budget summary. The stable isotopic signatures of the water from the bedrock groundwater, Saint John River and production wells show groundwater-surface water interaction is present. This supports evidence from the 3D modeling that both the groundwater and surface water of the hydrogeological system would be sensitive to changes in recharge.

The 3D finite element numerical model was constructed and calibrated, followed by running model simulations to: 1) determine how groundwater flux from the fractured bedrock to the overburden aquifer would vary under both natural flow and well field

pumping conditions; and 2) determine how variations in recharge, a potential result of climate change, would impact the hydrological system in the Fredericton area.

The steady-state (natural flow) and transient (pumping) model simulations indicated in the esker portion of the model domain, using calibrated recharge rates, the total upward flux from the bedrock layer to the overlying till and/or basal sand and gravel layer was:

(1) Using the randomly assigned windows in the till layer:

Steady-state, basal sand and gravel layer excluded = 911 m^3/d
Steady-state, basal sand and gravel layer included = 852 m^3/d

Transient, pumping 26,000 m^3/d for 365 day;
Basal sand and gravel layer excluded = 1124 m^3/d
Basal sand and gravel included = 1149 m^3/d; and

(2) Using the database assigned windows in the till layer:

Steady-state, basal sand and gravel layer excluded = 887 m^3/d
Steady-state, basal sand and gravel layer included = 874 m^3/d

Transient, pumping 26,000 m^3/d for 365 day;
Basal sand and gravel layer excluded = 1077 m^3/d
Basal sand and gravel included = 1144 m^3/d

The results of these model simulations indicate the groundwater fluid-flux from the bedrock upwards into the overburden is slightly higher when using the randomly assigned windows in the till layer than the database assigned windows in the till layer. This is expected since the database assigned windows represent 4% of the elements covering the esker area while the random windows represent 20% of the elements allowing an increase in fluid-flux through the additional windows.

The transient model results show that fluid flux from the bedrock in the esker area is approximately 1000 m^3/d, which represents 4% of the 26,000 m^3/d being pumped from the aquifer. The model simulations also indicate that groundwater fluid-flux from the fractured bedrock to the overburden does not vary a great deal whether running steady-state (natural) or transient (pumping) simulations. This is likely associated with the lower fractured rock mass permeability, which does not allow for great changes in flux, regardless of natural or pumping scenarios.

Considering the variations in recharge, a potential result of changing temperatures and precipitation because of climate change, the hydrological impact on the Fredericton area was investigated using the steady-state numerical model.

When the amount of recharge available to the hydrologic system is dramatically increased in the model, the resulting hydraulic head and the amount of fresh water available to the aquifer from the river and the upland recharge areas also increases. This scenario represents the Saint John River banks spilling over and flooding low-lying areas around Fredericton and communities along the Saint John River.

When the amount of recharge available to the hydrologic system is dramatically decreased in the model, the resulting hydraulic head drops substantially and the amount of fresh water available to the aquifer from the river and the upland recharge areas is reduced.

This signifies with changes in precipitation or temperature, a possible result of climate change, the resulting hydraulic head and fluid-flux in the overburden is more

sensitive than that of the bedrock, which represents a more stable fluid-flux because of the lower fractured rock-mass permeability.

6.2 Recommendations

Based on the results of this thesis, recommendations can be made for future field and modeling studies of the Fredericton Aquifer:

(1) Additional seasonal surface water, river and bedrock groundwater sampling and analyses for stable isotopes is recommended to clarify the signature, origin and the groundwater velocities of the bedrock groundwater.

(2) Additional numerical model transient simulations using updated pumping well information and actual long-term pumping test data should be done. Running long-term transient simulations greatly increases the run-time of the model, and would be beneficial in determining long-term effects of changing precipitation and temperatures, a potential result of climate change.

REFERENCES

ADI Ltd. 1982. City of Fredericton upgrading water system. Project File 83-147; Volume 1 – Water supply, Fredericton, New Brunswick, Canada.

Al, T.A., MacQuarrie, K.T.B., Butler, K.E., Nadeau, J-C., Dawe, M.R. and Amskold, L. 2005. River – connected aquifers: Geophysics, stratigraphy, hydrogeology and geochemistry. In *Water Encyclopedia: Ground Water*. J.H. Lehr and J. Keeley (eds), John Wiley & Sons Publishing, pp. 677-688.

Amskold, L. 2005. Variation of redox zonation along an infiltration pathway in a river-recharged aquifer, Fredericton, New Brunswick. M.Sc.Thesis 7507, University of New Brunswick, Fredericton, N.B., 137 p.

ASCE (American Society of Civil Engineers Committee on Groundwater). 1996. *Quality of Groundwater*. ASCE Manuals and Report on Engineering Practice No. 85, 200 p.

Anderson, M. P., Woessner, W.W. 1992. *Applied Groundwater Modeling: Simulation of Flow and Advective Transport*. San Diego, California: Academic Press. 381 p.

Ball, F.D., Sullivan, R.M., and Peach, A.R. 1981. Carboniferous drilling project. Report of investigation 18; Mineral Resources, Dept. of Natural Resources, Fredericton, N.B.

Canadian Council of Ministers of the Environment (CCME). 1999. Canadian water quality guidelines for the protection of aquatic life. In: Canadian Environmental Quality Guidelines, 1999, Winnipeg.

Clark, I. and Fritz, P. 1997. *Environmental Isotopes in Hydrogeology*. New York: Lewis Publishers, 328 p.

Corbett, L. 1993. *History of Fredericton's Water Supply*. City of Fredericton, Fredericton, New Brunswick.

Craig, H. 1961. Isotopic Variations in Meteoric Waters. *Science* 133, 3465: 1702-1703.

Cunningham, C.A. 2003. Geochemistry of groundwater from bedrock underlying the Fredericton Aquifer. New Brunswick, Canada: University of New Brunswick. Hons. Geol no. 86, 74 p.

Davies, J.J.A. 1995. A hydrogeological investigation of bedrock features using magnetic and electromagnetic methods in New Maryland, New Brunswick, Canada. M.Sc. Thesis no. 5578, University of New Brunswick, Fredericton, N.B., 277 p.

Davis, S.N. 1969. Porosity and permeability of natural materials. De Wiest, R. J. M. (ed). In *Flow Through Porous Media*: New York, Academic Press, p. 54-89.

Dawe, M.R. and MacQuarrie, K.T.B. 2005. Assessing water travel times during riverbank filtration. Thomson, N. R. (ed). *Bringing Groundwater Quality Research to the Watershed Scale* 297: p. 97-102.

Dingman, S.L. 1994. *Physical Hydrology*. University of New Hampshire: New York, Macmillan Publishing Company, 575 p.

Domenico, P.A. and Schwarz, F.W. 1990. *Physical and Chemical Hydrogeology*. New York: John Wiley & Sons, Inc., 506 p.

Environment Canada. 2008. *National Climate Archive*. Fredericton monthly meteorological data for years 1953 – 2001. Available at: http://www.climate.weatheroffice.ec.gc.ca/climateData/monthlydata_e.html?timeframe=2&Prov=XX&StationID=6157&Year=1953&Month=11&Day=1 (November 18, 2008).

Fetter, C.W. 2001. *Applied Hydrogeology*. Upper Saddle River: New Jersey, Prentice-Hall, Inc., 691 p.

Francis, R.M. 1981. Hydrogeological properties of a fractured porous aquifer, Winter River basin, Prince Edward Island. M.Sc. Thesis, University of Waterloo, Waterloo, Ontario.

Hydrologic Services Water Sciences Section. 2006. New Brunswick Water Quantity Information. *Sciences and Reporting Branch - New Brunswick Department of Environment.* Available at: http://www.gnb.ca/0009/0371/0007/0001-e.asp (February 14, 2008).

Johnson R. B. and DeGraff J. V. 1988. *Principles of Engineering Geology*. New York, John Wiley & Sons, Inc., 497 p.

Loomer, D. 2001. Investigations into some hydrogeologic parameters of fractured sandstone bedrock at Fredericton, New Brunswick. Honours Thesis, University of New Brunswick, Fredericton, N.B., 81 p.

McLeod, M.J. and Johnson, S.C. 1998. Bedrock geological compilation of the Fredericton area (NTS 21 G/15). York and Sunbury counties, New Brunswick. New Brunswick Department of Natural Resources and Energy. Minerals and Energy Division. Plate 98-33.

Michaud, Y., Rivard, C., Lefebvre, R., Rivera, A. and Pupek, D.A. 2004. Preliminary assessment of groundwater resources in southeastern New Brunswick in the context of climate change. Climate change impacts and adaptation: Water resources and fisheries in New Brunswick. 2004 Mar 15 – 16, Moncton, N.B. Fisheries and Oceans Canada.

McGuigan, B. 2005. Evaluation of the hydraulic conductivity of the clay/silt aquitard overlying the Fredericton aquifer. Senior Report, Department of Civil Engineering, University of New Brunswick. Fredericton, N.B., 125 p.

Nadeau, J-C., Butler, K.E., and Parrott, R. 2003. Application of riverine geophysics for delineating recharge to a river valley aquifer, Fredericton, N.B. Proceedings of 16th Symposium on Application of Geophysics to Engineering and Environmental Problems (SAGEEP 2003), 12 p.

National Operational Hydrologic Remote Sensing Center. 2004. *Snow Data Assimilation System (SNODAS) data products at NSIDC.* Boulder, CO: National Snow and Ice Data Center. Digital media. Available at: http://www.nohrsc.noaa.gov/nsa/ (November 20, 2008).

National Research Council. 2001. *Conceptual Models of Flow and Transport in the Fractured Vadose Zone.* Washington, D.C. National Academy Press, 374 p.

New Brunswick Department of Environment. 2005. Protecting sources of municipal drinking water. An overview of New Brunswick's Wellfield Protection Program. Available at: www.gnb.ca/0009/0371/0001/index.html (February 24, 2010).

New Brunswick Department of Natural Resources and Energy. 2000. Bedrock Geology of New Brunswick, Mineral and Energy Division Map NR-1 (2000 Edition) Scale 1:500,000.

Park, A. and Whitehead, J. 2003. Structural transect through Silurian turbidites of the Fredericton Belt southwest of Fredericton, New Brunswick: the role of the Fredericton Fault in late Iapatus convergence. *Atlantic Geology*, Vol. 39, pp. 227 – 237.

Parsons, M.L. 1972. Determination of hydrogeological properties of fissured rock, *International Geological Congress 24th Session Section II Hydrogeology*, Montreal, pp. 89 – 99.

Praamsma, T., Novakowski, K., Kyser, K., and Hall, K. 2009. Using stable isotopes and hydraulic head data to investigate groundwater recharge and discharge in a fractured rock aquifer. *Journal of Hydrology,* 366(1-4), March 2009, pp. 35-45.

Puls, R.W. and Barcelona, M.J. 1996. Low-flow (minimal drawdown) ground-water sampling procedures. U.S. Environmental Protection Agency, Office of Research and Development, Office of Solid Waste and Emergency Response, Washington, DC. 12 p.

Statistics Canada. 2007. *2006 Community Profiles*. Fredericton, New Brunswick, 2006 Census. Statistics Canada Catalogue no. 92-591-XWE. Ottawa, Canada. Available at: http://www12.statcan.ca/english/census06/data/profiles/community/Index.cfm?Lang=E (March 19, 2008).

TerrAtlantic Engineering Ltd. 2000. Development and Protection of the Groundwater Resource, Fredericton, NB. Status Report - 2000. File 201.01.

The National Atlas of Canada. 1974. *Average annual runoff*, 4th Ed. Engineering Division, Inland Water Directorate, Department of Fisheries and the Environment. Available at: http://atlas.nrcan.gc.ca/site/english/maps/archives/hydrological_atlas_1974/water_quantity_general/24_Annual_Runoff_1974 (November 16, 2008).

Thiem, G. 1906. *Hydrologische methoden*. Leipzig: Gebhardt, 56 p.

Thomas, N.E., Kan, K.T., Bray, D.I. and MacQuarrie, K.T.B. 1994. Temporal changes in manganese concentrations in water from the Fredericton aquifer, New Brunswick. *Ground Water*, 32(4), pp. 650-656.

Thomas, N.E. 1991. Geochemistry of groundwater in the Wilmot Park Well Field, Fredericton, N.B. M.Sc.E. Thesis 4781, Dept. of Civil Engineering, University of New Brunswick, Fredericton, New Brunswick. 198 p.

Thornthwaite, C.W. and Mather, J.R. 1957. The Water Balance – Instructions and tables for computing potential evapotranspiration and the water balance. Drexel Institute of Technology, Laboratory of Climatology. *Climatology*, Volume X, Number 3.

Touratech-QV-Navigator. 2003. Map of Fredericton Area 21-G-15, Edition 5.

United States Environmental Protection Agency. 2004. *Site Characterization Technologies for DNAPL Investigations*. Office of Solid Waste and Emergency Response (5102G), EPA 542-R-04-017, September, 2004. Available at: http://www.epa.gov/tio/download/char/542r04017.pdf (November 21, 2008).

Van de Poll, H.W. 1973. Stratigraphy, sediment dispersal and facies analysis of the Pennsylvanian Pictou Group in New Brunswick. *Maritime Sediments*, Vol. 9, No. 3, December 1973, pp. 72–77.

Violette, G.G. 1990. The application of a computer model to assess the potential effects of groundwater withdrawals from the Fredericton aquifer, Fredericton, New Brunsiwck. M.Sc.E Thesis, Dept. of Civil Engineering, Univ. of New Brunswick, Fredericton, N.B., 204 p.

WASY GmbH. 2007. FEFLOW; Interactive Graphics-based Finite Element Simulation System for Subsurface Flow and Transport Processes. Version 5.306 3D + 2D.

Webb, T.C. 1981. Origin of brackish formational groundwaters in the Pennsylvanian of New Brunswick. Fredericton, Mineral Development Branch Department of Natural Resources New Brunswick: 21.

Whitehead, J. 2001. The geology of the Fredericton-Mactaquac Dam area. *In:* Pickerill, R.K. and Lentz, D.L. (eds), *Geology of New Brunswick, New England Intercollegiate Geological Conference, Guidebook,* 83, pp. A1-1 - A1-12.

WHI. 2005. AquaChem; Water quality data analysis, plotting, reporting and modeling program.

WHI. 2006. FEFLOW V.5.1 model course notes April, 2006. Waterloo Hydrologic Inc. Schlumberger. Waterloo, Ontario.

Water Survey of Canada. 2005. *National Water Quantity Survey Program.* Environment Canada. Archived Hydrometric Data Saint John River At Fredericton (01AK003) Available at: http://www.wsc.ec.gc.ca/hydat/H2O/index_e.cfm?cname=WEBfrmDailyReport_e.cfm (February 14, 2008).

Water Survey of Canada. 2007. *National Water Quantity Survey Program.* Environment Canada. Archived Hydrometric Data Middle Branch Nashwaaksis Stream At Sandwith's Farm (01AK006). Available at: http://www.wsc.ec.gc.ca/hydat/H2O/index_e.cfm?cname=WEBfrmDailyReport_e.cfm&RequestTimeout=300 (February 14, 2008).

APPENDIX A WATER BALANCE DATA

A.1 Box Plots used to visualize the variation in temperature and precipitation for the Fredericton area.

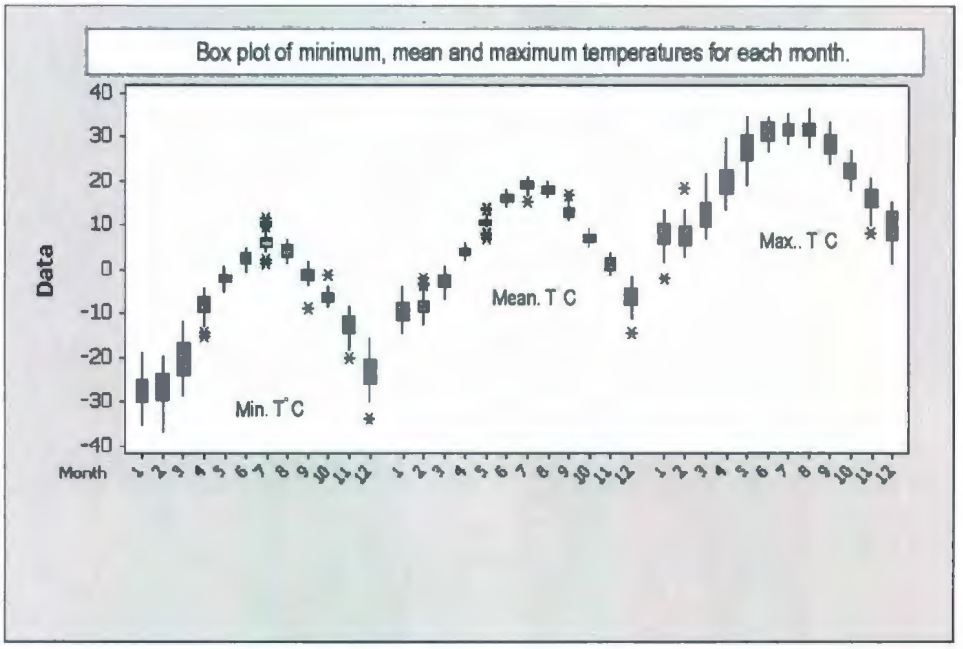

Figure A.1. Box plot of minimum, mean and maximum temperatures observed monthly for years 1971 – 2000.

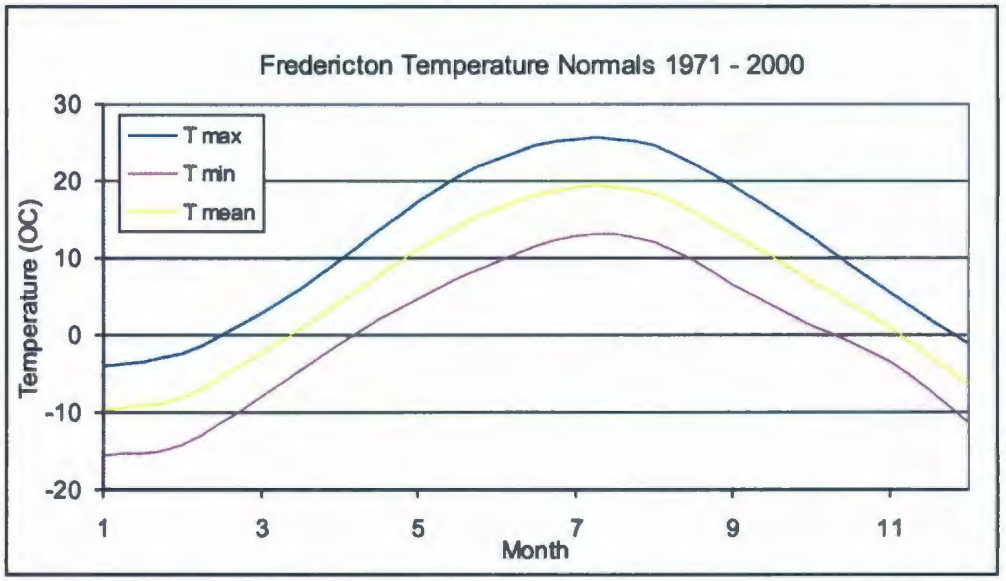

Figure A.2. Normal curve graph of monthly minimum, mean and maximum temperatures for years 1971 – 2000.

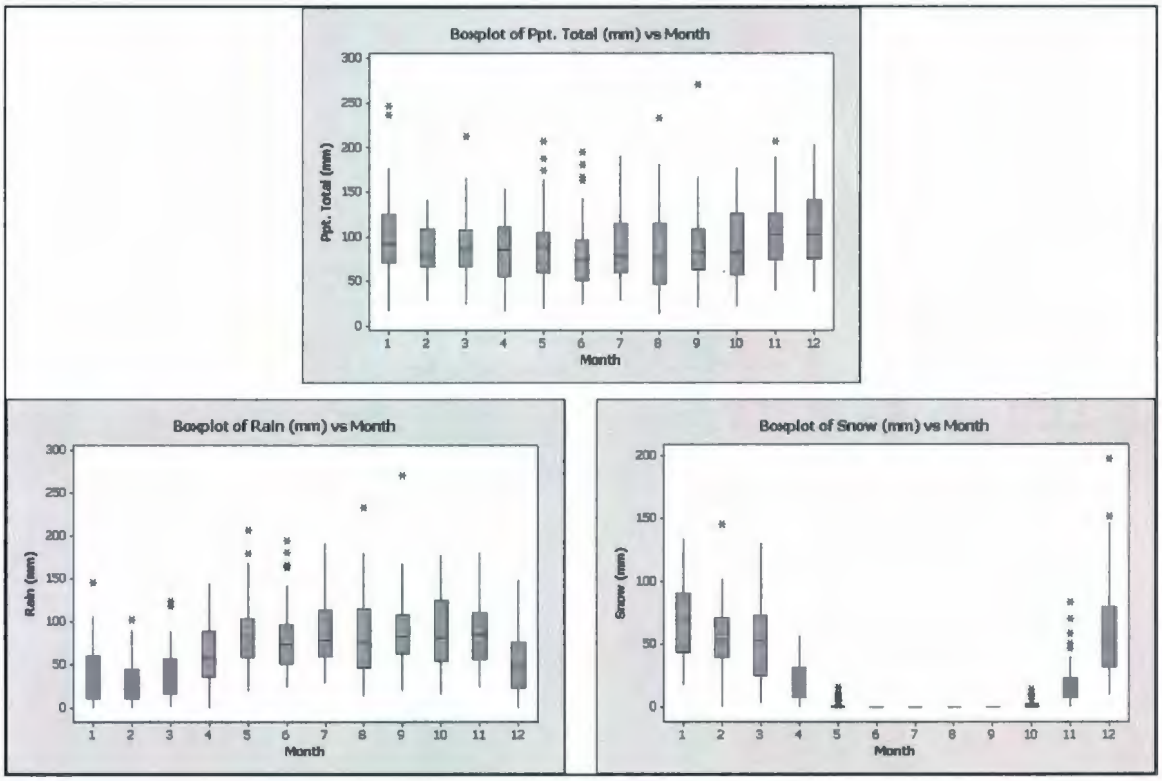

Figure A.3. Boxplots of total precipitation, rainfall and snowfall for years 1971 - 2001 showing the range of variability between monthly periods.

A.2 Thornthwaite and Mather (1957) method results to determine various parameters to calculate potential evapotranspiration and the water balance.

Table A.1 – A.X Legend

i = Heat index for monthly temperatures

I = Heat index for total year

Unadj-PE = Unadjusted potential evapotranspiration

Adj PE = Adjusted potential evapotranspiration

P = Precipitation

P – PE = Precipitation minus potential evapotranspiration

Acc Pot WL = Accumulated potential water loss

ST = Storage

Change in ST = Change in storage

AE = Actual evapotranspiration

D = Moisture Deficit

S = Moisture surplus

RO = Water Runoff

SMRO = Snowmelt runoff

Tot RO = Total runoff

DT = Total moisture detention

Table A.1A Results of the PE and water balance calculations (Thornthwaite and Mather).

	Line 1		Line 2	Line 3		Line 4	Line 5	Line 6	Line 7	Line 8	Line 9	Line 10	Line 11	Line 12	Line 13	Line 14	Line 15	Line 16
	Mean			Un-Adj	Corr.	Adj-			Acc Pot		Change						Tot	
Date	Temp			PE	45 deg.	PE	P	P- PE	WL	ST	in ST	AE	D	S	RO	SMRO	RO	DT
M / Y	(°C)	(i)	(I)	(mm)	Lat. N	(mm)	(mm)	(mm)	(mm)	(mm)	(mm)	(mm)	(mm)	(mm)	(mm)	(mm)	(mm)	(mm)
Jan-53	-5.8	0.0		0.0	24.0	0.0	105.9	105.9		321.1	0.0	0.0	0.0	0.0	12.4	0.0	12.4	333.5
Feb-53	-5.4	0.0		0.0	24.3	0.0	96.0	96.0		417.1	0.0	0.0	0.0	0.0	6.2	0.0	6.2	423.3
Mar-53	-1.3	0.0		0.0	30.6	0.0	105.4	105.4		522.5	0.0	0.0	0.0	0.0	3.1	0.0	3.1	525.6
Apr-53	6.0	1.3		1.0	33.9	33.9	97.3	63.4		75.0	0.0	33.9	0.0	63.4	31.7	14.2	45.9	237.6
May-53	11.3	3.4		1.9	38.4	73.0	81.8	8.8		75.0	0.0	73.0	0.0	8.8	20.3	63.9	84.2	159.2
Jun-53	16.1	5.9		2.7	38.7	104.5	51.3	-53.2	-53.2	36.0	-39.0	90.3	14.2	0.0	10.1	32.0	42.1	78.1
Jul-53	19.3	7.7		3.2	39.3	125.8	161.3	35.5		71.5	35.5	125.8	0.0	0.0	5.1	16.0	21.0	92.6
Aug-53	17.5	6.7		3.0	36.3	108.9	60.5	-48.4	-48.4	38.0	-33.5	94.0	14.9	0.0	2.5	8.0	10.5	48.5
Sep-53	14.8	5.2		2.5	31.2	78.0	94.7	16.7		54.7	16.7	78.0	0.0	0.0	1.3	4.0	5.3	60.0
Oct-53	8.0	2.0		1.3	28.2	36.7	86.6	49.9		75.0	0.0	36.7	0.0	49.9	25.6	2.0	27.6	102.6
Nov-53	4.0	0.7		0.6	23.7	14.2	88.1	73.9		75.0	0.0	14.2	0.0	73.9	49.7	1.0	50.7	125.7
Dec-53	-2.1	0.0	32.9	0.0	22.5	0.0	140.2	140.2		215.2	0.0	0.0	0.0	0.0	24.9	0.0	24.9	241.1
Jan-54	-10.7	0.0		0.0	24.0	0.0	135.4	135.4		340.2	0.0	0.0	0.0	0.0	18.5	0.0	18.5	358.7
Feb-54	-3.8	0.0		0.0	24.3	0.0	118.9	118.9		459.1	0.0	0.0	0.0	0.0	9.2	0.0	9.2	468.3
Mar-54	-2.2	0.0		0.0	30.6	0.0	84.8	84.8		543.9	0.0	0.0	0.0	0.0	4.6	0.0	4.6	548.5
Apr-54	3.9	0.7		0.7	33.9	23.7	123.2	99.5		75.0	0.0	23.7	0.0	99.5	49.7	30.4	80.1	402.9
May-54	10.1	2.9		1.7	38.4	65.3	97.0	31.7		75.0	0.0	65.3	0.0	31.7	40.7	136.8	177.5	252.5
Jun-54	15.9	5.8		2.8	38.7	108.4	163.6	55.2		75.0	0.0	108.4	0.0	55.2	48.0	68.4	116.4	191.4
Jul-54	17.8	6.8		3.0	39.3	117.9	81.3	-36.6	-36.6	45.0	-30.0	111.3	6.6	0.0	24.0	34.2	58.2	103.2
Aug-54	16.7	6.2		2.9	36.3	105.3	113.5	8.2		53.2	8.2	105.3	0.0	0.0	12.0	17.1	29.1	82.3
Sep-54	12.8	4.2		2.2	31.2	68.6	101.6	33.0		75.0	21.8	68.6	0.0	21.8	16.9	8.6	25.4	100.4
Oct-54	6.9	2.4		1.5	28.2	42.3	170.4	128.1		75.0	0.0	42.3	0.0	128.1	72.5	4.3	76.8	151.8
Nov-54	2.2	0.3		0.4	23.7	9.5	84.6	75.1		75.0	0.0	9.5	0.0	75.1	73.8	2.1	75.9	150.9
Dec-54	-4.5	0.0	29.2	0.0	22.5	0.0	129.8	129.8		204.8	0.0	0.0	0.0	0.0	36.9	0.0	36.9	243.8
Jan-55	-8.7	0.0		0.0	24.0	0.0	92.2	92.2		183.1	0.0	0.0	0.0	0.0	0.1	0.0	0.1	183.1
Feb-55	-7.2	0.0		0.0	24.3	0.0	121.4	121.4		304.5	0.0	0.0	0.0	0.0	0.0	0.0	0.0	304.5
Mar-55	-4.0	0.0		0.0	30.6	0.0	91.9	91.9		396.4	0.0	0.0	0.0	0.0	0.0	0.0	0.0	396.4
Apr-55	4.4	0.8		0.7	33.9	23.7	54.9	31.2		75.0	0.0	23.7	0.0	31.2	15.6	27.9	43.5	341.7
May-55	11.2	3.4		1.9	38.4	73.0	83.6	10.6		75.0	0.0	73.0	0.0	10.6	13.1	125.6	138.7	213.7
Jun-55	15.5	5.6		2.6	38.7	100.6	56.6	-44.0	-44.0	40.0	-35.0	91.6	9.0	0.0	6.6	62.8	69.3	109.3
Jul-55	20.5	8.5		3.5	39.3	137.6	58.9	-78.7	-122.7	14.0	-26.0	84.9	52.7	0.0	3.3	31.4	34.7	48.7
Aug-55	19.0	7.6		3.2	36.3	116.2	94.5	-21.7	-144.3	10.0	-4.0	98.5	17.7	0.0	1.6	15.7	17.3	27.3
Sep-55	12.6	4.1		2.1	31.2	65.5	47.0	-18.5	-162.9	8.0	-2.0	49.0	16.5	0.0	0.8	7.8	8.7	16.7
Oct-55	7.8	2.0		1.3	28.2	36.7	29.5	-7.2	-170.0	7.0	-1.0	30.5	6.2	0.0	0.4	3.9	4.3	11.3
Nov-55	1.3	0.1		0.2	23.7	4.7	45.7	41.0		48.0	41.0	4.7	0.0	0.0	0.2	2.0	2.2	50.1
Dec-55	-9.5	0.0	31.9	0.0	22.5	0.0	42.9	42.9		90.9	42.9	0.0	0.0	0.0	0.1	0.0	0.1	92.9
Jan-56	-3.5	0.0		0.0	24.0	0.0	177.8	177.8		344.2	0.0	0.0	0.0	0.0	5.7	0.0	5.7	349.9
Feb-56	-8.0	0.0		0.0	24.3	0.0	66.8	66.8		411.0	0.0	0.0	0.0	0.0	2.8	0.0	2.8	413.8
Mar-56	-5.9	0.0		0.0	30.6	0.0	96.5	96.5		507.5	0.0	0.0	0.0	0.0	1.4	0.0	1.4	508.9
Apr-56	3.7	0.6		0.7	33.9	23.7	86.4	62.7		75.0	0.0	23.7	0.0	62.7	31.3	30.2	61.5	379.6
May-56	7.9	2.0		1.5	38.4	57.6	98.6	41.0		75.0	0.0	57.6	0.0	41.0	36.2	135.9	172.1	247.1
Jun-56	16.1	5.9		2.8	38.7	108.4	73.9	-34.5	-34.5	46.0	-29.0	102.9	5.5	0.0	18.1	68.0	86.0	132.0
Jul-56	17.6	6.7		3.0	39.3	117.9	56.6	-61.3	-95.8	20.0	-26.0	82.6	35.3	0.0	9.0	34.0	43.0	63.0
Aug-56	16.8	6.3		2.9	36.3	105.3	96.0	-9.3	-105.0	18.0	-2.0	98.0	7.3	0.0	4.5	17.0	21.5	39.5
Sep-56	12.0	3.8		2.2	31.2	68.6	74.2	5.6		23.6	5.6	68.6	0.0	0.0	2.3	8.5	10.8	34.3
Oct-56	7.7	1.9		1.4	28.2	39.5	46.7	7.2		30.8	7.2	39.5	0.0	0.0	1.1	4.2	5.4	36.2
Nov-56	1.7	0.2		0.4	23.7	9.5	78.0	68.5		75.0	44.2	9.5	0.0	44.2	22.7	2.1	24.8	99.8
Dec-56	-6.2	0.0	27.4	0.0	22.5	0.0	91.4	91.4		166.4	0.0	0.0	0.0	0.0	11.3	0.0	11.3	179.9

Table A.1B Results of the PE and water balance calculations (Thornthwaite and Mather).

	Line 1		Line 2	Line 3		Line 4	Line 5	Line 6	Line 7	Line 8	Line 9	Line 10	Line 11	Line 12	Line 13	Line 14	Line 15	Line 16
	Mean			Un-Adj	Corr.	Adj-			Acc Pot		Change						Tot	
Date	Temp			PE	45 deg.	PE	P	P- PE	WL	ST	in ST	AE	D	S	RO	SMRO	RO	DT
M / Y	(°C)	(i)	(I)	(mm)	Lat. N	(mm)	(mm)	(mm)	(mm)	(mm)	(mm)	(mm)	(mm)	(mm)	(mm)	(mm)	(mm)	(mm)
Jan-57	-14.1	0.0		0.0	24.0	0.0	86.1	86.1		311.0	0.0	0.0	0.0	0.0	9.1	0.0	9.1	320.1
Feb-57	-6.5	0.0		0.0	24.3	0.0	74.4	74.4		385.4	0.0	0.0	0.0	0.0	4.6	0.0	4.6	390.0
Mar-57	-0.9	0.0		0.0	30.6	0.0	42.9	42.9		428.3	0.0	0.0	0.0	0.0	2.3	0.0	2.3	430.6
Apr-57	4.5	0.9		0.7	33.9	23.7	93.2	69.5		75.0	0.0	23.7	0.0	69.5	1.0	20.5	21.5	330.3
May-57	11.4	3.5		1.9	38.4	73.0	51.6	-21.4	-21.4	56.0	-19.0	70.6	2.4	0.0	34.7	92.3	127.0	114.5
Jun-57	16.7	6.2		2.8	38.7	108.4	53.1	-55.3	-76.6	26.0	-30.0	83.1	25.3	0.0	17.4	46.1	63.5	89.5
Jul-57	18.2	7.1		3.1	39.3	121.8	48.3	-73.5	-150.2	10.0	-16.0	64.3	57.5	0.0	8.7	23.1	31.7	41.7
Aug-57	17.1	6.4		2.9	36.3	105.3	50.3	-55.0	-205.1	4.0	-6.0	56.3	49.0	0.0	4.3	11.5	15.9	19.9
Sep-57	14.4	5.0		2.4	31.2	74.9	50.8	-24.1	-229.2	3.0	-1.0	51.8	23.1	0.0	2.2	5.8	7.9	10.9
Oct-57	8.9	2.4		1.5	28.2	42.3	26.9	-15.4	-244.6	3.0	0.0	26.9	15.4	0.0	1.1	2.9	4.0	7.0
Nov-57	3.3	0.5		0.5	23.7	11.9	137.7	125.9		75.0	72.0	11.9	0.0	72.0	36.5	1.4	38.0	113.0
Dec-57	-1.6	0.0	31.9	0.0	22.5	0.0	149.9	149.9		224.9	0.0	0.0	0.0	0.0	18.3	0.0	18.3	244.6
Jan-58	-4.5	0.0		0.0	24.0	0.0	150.6	150.6		290.6	0.0	0.0	0.0	0.0	13.6	0.0	13.6	304.2
Feb-58	-8.3	0.0		0.0	24.3	0.0	94.0	94.0		384.6	0.0	0.0	0.0	0.0	6.8	0.0	6.8	391.4
Mar-58	1.1	0.1		0.2	30.6	6.1	66.8	60.7		75.0	0.0	6.1	0.0	60.7	30.3	28.2	58.5	366.0
Apr-58	5.9	1.3		1.1	33.9	37.3	85.9	48.6		75.0	0.0	37.3	0.0	48.6	39.5	126.9	166.4	241.4
May-58	10.3	3.0		1.8	38.4	69.1	89.2	20.1		75.0	0.0	69.1	0.0	20.1	29.8	63.5	93.2	168.2
Jun-58	14.0	4.8		2.4	38.7	92.9	86.4	-6.5	-6.5	68.0	-7.0	93.4	-0.5	0.0	14.9	31.7	46.6	114.6
Jul-58	18.6	7.3		3.2	39.3	125.8	149.9	24.1		92.1	24.1	125.8	0.0	24.1	19.5	15.9	35.4	127.5
Aug-58	18.3	7.1		3.1	36.3	112.5	101.1	-11.4	-11.4	64.0	-28.1	129.2	-16.7	0.0	9.8	7.9	17.7	81.7
Sep-58	13.2	4.4		2.3	31.2	71.8	58.7	-13.1	-24.5	53.0	-11.0	69.7	2.1	0.0	4.9	4.0	8.8	61.8
Oct-58	6.7	1.6		1.2	28.2	33.8	116.8	83.0		75.0	22.0	33.8	0.0	22.0	13.4	2.0	15.4	90.4
Nov-58	1.3	0.1		0.2	23.7	4.7	100.3	95.6		75.0	0.0	4.7	0.0	95.6	54.5	1.0	55.5	130.5
Dec-58	-11.4	0.0	29.6	0.0	22.5	0.0	65.0	65.0		140.0	0.0	0.0	0.0	0.0	27.2	0.0	27.2	168.2
Jan-59	-8.7	0.0		0.0	24.0	0.0	99.6	99.6		284.8	0.0	0.0	0.0	0.0	24.3	0.0	24.3	309.1
Feb-59	-10.3	0.0		0.0	24.3	0.0	66.8	66.8		351.6	0.0	0.0	0.0	0.0	12.2	0.0	12.2	363.8
Mar-59	-3.0	0.0		0.0	30.6	0.0	82.3	82.3		433.9	0.0	0.0	0.0	0.0	6.1	0.0	6.1	440.0
Apr-59	5.0	1.0		0.8	33.9	27.1	53.3	26.2		75.0	0.0	27.1	0.0	26.2	13.1	19.6	32.7	270.6
May-59	13.0	4.3		2.1	38.4	80.6	36.3	-44.3	-44.3	40.0	-35.0	71.3	9.3	0.0	6.5	88.2	94.7	134.7
Jun-59	14.2	4.9		2.3	38.7	89.0	143.3	54.3		94.3	54.3	89.0	0.0	54.3	30.4	44.1	74.5	168.8
Jul-59	21.6	9.2		3.6	39.3	141.5	112.5	-29.0	-29.0	50.0	-44.3	156.8	-15.3	0.0	15.2	22.1	37.3	87.3
Aug-59	18.7	7.4		3.1	36.3	112.5	110.0	-2.5	-31.5	48.0	-2.0	112.0	0.5	0.0	7.6	11.0	18.6	66.6
Sep-59	14.9	5.2		2.5	31.2	78.0	87.1	9.1		57.1	9.1	78.0	0.0	0.0	3.8	5.5	9.3	66.4
Oct-59	7.9	2.0		1.3	28.2	36.7	131.8	95.1		75.0	17.9	36.7	0.0	17.9	10.9	2.8	13.6	88.6
Nov-59	1.9	0.2		0.3	23.7	7.1	191.0	183.9		75.0	0.0	7.1	0.0	183.9	97.4	1.4	98.7	173.7
Dec-59	-4.3	0.0	34.1	0.0	22.5	0.0	110.2	110.2		185.2	0.0	0.0	0.0	0.0	48.7	0.0	48.7	235.3
Jan-60	-8.9	0.0		0.0	24.0	0.0	138.2	138.2		312.5	0.0	0.0	0.0	0.0	1.5	0.0	1.5	314.0
Feb-60	-3.0	0.0		0.0	24.3	0.0	122.9	122.9		435.4	0.0	0.0	0.0	0.0	0.7	0.0	0.7	436.1
Mar-60	-3.1	0.0		0.0	30.6	0.0	51.6	51.6		487.0	0.0	0.0	0.0	0.0	0.4	0.0	0.4	487.4
Apr-60	4.2	0.8		0.6	33.9	20.3	58.7	38.4		75.0	0.0	20.3	0.0	38.4	19.2	26.3	45.5	331.2
May-60	14.2	4.9		2.3	38.4	88.3	133.4	45.1		75.0	0.0	88.3	0.0	45.1	32.1	118.4	150.5	225.5
Jun-60	17.4	6.6		2.9	38.7	112.2	74.9	-37.3	-37.3	45.0	-30.0	104.9	7.3	0.0	16.1	59.2	75.2	120.2
Jul-60	19.0	7.6		3.2	39.3	125.8	100.8	-25.0	-62.3	32.0	-13.0	113.8	12.0	0.0	8.0	29.6	37.6	69.6
Aug-60	19.5	7.9		3.3	36.3	119.8	14.5	-105.3	-167.6	7.0	-25.0	39.5	80.3	0.0	4.0	14.8	18.8	25.6
Sep-60	14.1	4.8		2.3	31.2	71.8	60.2	-11.6	-179.1	6.0	-1.0	61.2	10.6	0.0	2.0	7.4	9.4	15.4
Oct-60	6.6	1.5		1.0	28.2	28.2	86.6	58.4		64.4	58.4	28.2	0.0	0.0	1.0	3.7	4.7	69.1
Nov-60	2.9	0.4		0.5	23.7	11.9	135.6	123.8		75.0	10.6	11.9	0.0	10.6	5.8	1.8	7.7	82.7
Dec-60	-6.1	0.0	34.4	0.0	22.5	0.0	99.3	99.3		174.3	0.0	0.0	0.0	0.0	2.9	0.0	2.9	179.1

Table A.1C Results of the PE and water balance calculations (Thornthwaite and Mather).

	Line 1		Line 2	Line 3		Line 4	Line 5	Line 6	Line 7	Line 8	Line 9	Line 10	Line 11	Line 12	Line 13	Line 14	Line 15	Line 16
	Mean			Un-Adj	Corr.	Adj-			Acc Pot		Change						Tot	
Date	Temp			PE	45 deg.	PE	P	P- PE	WL	ST	in ST	AE	D	S	RO	SMRO	RO	DT
M / Y	(°C)	(i)	(I)	(mm)	Lat. N	(mm)	(mm)	(mm)	(mm)	(mm)	(mm)	(mm)	(mm)	(mm)	(mm)	(mm)	(mm)	(mm)
Jan-61	-13.3	0.0		0.0	24.0	0.0	83.6	83.6		271.1	0.0	0.0	0.0	0.0	13.1	0.0	13.1	284.2
Feb-61	-9.2	0.0		0.0	24.3	0.0	77.0	77.0		348.1	0.0	0.0	0.0	0.0	6.5	0.0	6.5	354.6
Mar-61	-4.1	0.0		0.0	30.6	0.0	76.2	76.2		424.3	0.0	0.0	0.0	0.0	3.3	0.0	3.3	427.6
Apr-61	2.6	0.4		0.4	33.9	13.6	94.7	81.1		75.0	0.0	13.6	0.0	81.1	40.6	33.3	73.9	416.5
May-61	10.5	3.1		1.8	38.4	69.1	164.8	95.7		75.0	0.0	69.1	0.0	95.7	68.1	149.9	218.0	293.0
Jun-61	16.7	6.2		2.8	38.7	108.4	82.8	-25.6	-25.6	52.0	-23.0	105.8	2.6	0.0	34.1	74.9	109.0	161.0
Jul-61	18.8	7.4		3.2	39.3	125.8	60.5	-65.3	-90.8	21.0	-31.0	91.5	34.3	0.0	17.0	37.5	54.5	75.5
Aug-61	18.8	7.4		3.2	36.3	116.2	77.2	-39.0	-129.8	12.0	-9.0	86.2	30.0	0.0	8.5	18.7	27.2	39.2
Sep-61	16.5	6.1		2.8	31.2	87.4	76.2	-11.2	-140.9	11.0	-1.0	77.2	10.2	0.0	4.3	9.4	13.6	24.6
Oct-61	9.3	2.6		1.5	28.2	42.3	154.4	112.1		75.0	64.0	42.3	0.0	64.0	34.1	4.7	38.8	113.8
Nov-61	3.3	0.5		0.5	23.7	11.9	82.3	70.5		75.0	0.0	11.9	0.0	70.5	52.3	2.3	54.6	129.6
Dec-61	-3.5	0.0	33.7	0.0	22.5	0.0	112.5	112.5		187.5	0.0	0.0	0.0	0.0	26.1	0.0	26.1	216.0
Jan-62	-9.3	0.0		0.0	24.0	0.0	63.8	63.8		247.5	0.0	0.0	0.0	0.0	15.1	0.0	15.1	262.6
Feb-62	-12.1	0.0		0.0	24.3	0.0	69.3	69.3		316.8	0.0	0.0	0.0	0.0	7.5	0.0	7.5	324.3
Mar-62	0.5	0.0		0.1	30.6	3.1	27.4	24.3		75.0	0.0	3.1	0.0	24.3	12.2	26.7	38.9	335.0
Apr-62	3.8	0.7		0.7	33.9	23.7	96.0	72.3		75.0	0.0	23.7	0.0	72.3	42.2	120.2	162.4	237.4
May-62	10.4	3.0		1.9	38.4	73.0	29.2	-43.8	-43.8	40.0	-35.0	64.2	8.8	0.0	21.1	60.1	81.2	121.2
Jun-62	16.3	6.0		2.8	38.7	108.4	52.6	-55.8	-99.5	19.0	-21.0	73.8	34.8	0.0	10.6	30.0	40.6	59.6
Jul-62	15.7	5.7		2.8	39.3	110.0	117.9	7.9		26.9	7.9	110.0	0.0	0.0	5.3	15.0	20.3	47.2
Aug-62	17.6	6.7		3.0	36.3	108.9	100.8	-8.1	-8.1	67.0	40.1	140.9	-32.0	0.0	2.6	7.5	10.1	77.1
Sep-62	12.3	3.9		2.2	31.2	68.6	94.5	25.9		75.0	8.0	68.6	0.0	8.0	5.3	3.8	9.1	84.1
Oct-62	7.5	1.9		1.4	28.2	39.5	81.0	41.5		75.0	0.0	39.5	0.0	41.5	23.4	1.9	25.3	100.3
Nov-62	1.0	0.1		0.2	23.7	4.7	101.9	97.2		75.0	0.0	4.7	0.0	97.2	60.3	0.9	61.2	136.2
Dec-62	-6.8	0.0	27.9	0.0	22.5	0.0	108.7	108.7		183.7	0.0	0.0	0.0	0.0	30.1	0.0	30.1	214.8
Jan-63	-7.3	0.0		0.0	24.0	0.0	111.5	111.5		253.8	0.0	0.0	0.0	0.0	26.0	0.0	26.0	279.8
Feb-63	-11.9	0.0		0.0	24.3	0.0	112.3	112.3		366.1	0.0	0.0	0.0	0.0	13.0	0.0	13.0	379.1
Mar-63	-4.5	0.0		0.0	30.6	0.0	86.4	86.4		452.5	0.0	0.0	0.0	0.0	6.5	0.0	6.5	459.0
Apr-63	3.3	0.5		0.5	33.9	17.0	68.3	51.4		75.0	0.0	17.0	0.0	51.4	25.7	32.9	58.6	403.3
May-63	10.9	3.3		1.8	38.4	69.1	70.1	1.0		75.0	0.0	69.1	0.0	1.0	13.3	148.1	161.4	236.4
Jun-63	16.6	6.2		2.8	38.7	108.4	46.5	-61.9	-61.9	32.0	-43.0	89.5	18.9	0.0	6.7	74.0	80.7	112.7
Jul-63	20.5	8.5		3.5	39.3	137.6	118.9	-18.7	-80.5	24.0	-8.0	126.9	10.7	0.0	3.3	37.0	40.3	64.3
Aug-63	16.6	6.2		2.8	36.3	101.6	137.4	35.8		59.8	35.8	101.6	0.0	0.0	1.7	18.5	20.2	79.9
Sep-63	11.2	3.4		1.9	31.2	59.3	125.0	65.7		75.0	15.2	59.3	0.0	15.2	8.5	9.3	17.7	92.7
Oct-63	9.7	2.7		1.6	28.2	45.1	118.9	73.8		75.0	0.0	45.1	0.0	73.8	41.1	4.6	45.7	120.7
Nov-63	3.6	0.6		0.6	23.7	14.2	180.8	166.6		75.0	0.0	14.2	0.0	166.6	103.8	2.3	106.2	181.2
Dec-63	-11.1	0.0	31.3	0.0	22.5	0.0	67.3	67.3		142.3	0.0	0.0	0.0	0.0	51.9	0.0	51.9	196.5
Jan-64	-7.5	0.0		0.0	24.0	0.0	55.6	55.6		370.8	0.0	0.0	0.0	0.0	9.4	0.0	9.4	380.1
Feb-64	-7.3	0.0		0.0	24.3	0.0	98.0	98.0		468.8	0.0	0.0	0.0	0.0	4.7	0.0	4.7	473.4
Mar-64	-2.8	0.0		0.0	30.6	0.0	91.2	91.2		560.0	0.0	0.0	0.0	0.0	2.3	0.0	2.3	562.3
Apr-64	3.7	0.6		0.7	33.9	23.7	101.1	77.4		75.0	0.0	23.7	0.0	77.4	38.7	36.4	75.1	443.6
May-64	11.3	3.4		2.0	38.4	76.8	50.0	-26.8	-26.8	51.0	-24.0	74.0	2.8	0.0	19.3	163.8	183.1	234.1
Jun-64	15.6	5.6		2.7	38.7	104.5	56.1	-48.4	-75.2	27.0	-24.0	80.1	24.4	0.0	9.7	81.9	91.6	118.6
Jul-64	19.3	7.7		3.3	39.3	129.7	56.9	-72.8	-148.0	10.0	-17.0	73.9	55.8	0.0	4.8	41.0	45.8	55.8
Aug-64	16.3	6.0		2.8	36.3	101.6	114.3	12.7		22.7	12.7	101.6	0.0	0.0	2.4	20.5	22.9	45.6
Sep-64	11.5	3.5		2.1	31.2	65.5	77.2	11.7		34.3	11.7	65.5	0.0	0.0	1.2	10.2	11.4	45.8
Oct-64	7.2	1.7		1.4	28.2	39.5	66.3	26.8		61.2	26.8	39.5	0.0	0.0	0.6	5.1	5.7	66.9
Nov-64	-0.2	0.0		0.0	23.7	0.0	74.2	74.2		135.4	74.2	0.0	0.0	74.2	37.4	0.0	37.4	177.9
Dec-64	-6.6	0.0	28.7	0.0	22.5	0.0	179.8	179.8		315.2	0.0	0.0	0.0	0.0	18.7	0.0	18.7	339.0

Table A.1D Results of the PE and water balance calculations (Thornthwaite and Mather).

	Line 1		Line 2	Line 3		Line 4	Line 5	Line 6	Line 7	Line 8	Line 9	Line 10	Line 11	Line 12	Line 13	Line 14	Line 15	Line 16
	Mean			Un-Adj	Corr.	Adj-			Acc Pot		Change						Tot	
Date	Temp			PE	45 deg.	PE	P	P- PE	WL	ST	in ST	AE	D	S	RO	SMRO	RO	DT
M / Y	(°C)	(i)	(I)	(mm)	Lat. N	(mm)	(mm)	(mm)	(mm)	(mm)	(mm)	(mm)	(mm)	(mm)	(mm)	(mm)	(mm)	(mm)
Jan-65	-11.5	0.0		0.0	24.0	0.0	62.0	62.0		341.4	0.0	0.0	0.0	0.0	1.7	0.0	1.7	343.1
Feb-65	-9.4	0.0		0.0	24.3	0.0	69.1	69.1		410.5	0.0	0.0	0.0	0.0	0.9	0.0	0.9	411.4
Mar-65	-2.3	0.0		0.0	30.6	0.0	23.6	23.6		434.1	0.0	0.0	0.0	0.0	0.4	0.0	0.4	434.5
Apr-65	3.1	0.5		0.5	33.9	17.0	55.6	38.7		75.0	0.0	17.0	0.0	38.7	19.3	23.5	42.8	306.3
May-65	10.2	2.9		1.8	38.4	69.1	67.3	-1.8	-1.8	73.0	-2.0	69.3	-0.2	0.0	9.7	105.8	115.4	188.4
Jun-65	16.8	6.3		2.9	38.7	112.2	42.9	-69.3	-71.2	28.0	-45.0	87.9	24.3	0.0	4.8	52.9	57.7	85.7
Jul-65	18.1	7.0		3.1	39.3	121.8	45.2	-76.6	-147.8	10.0	-18.0	63.2	58.6	0.0	2.4	26.4	28.9	38.9
Aug-65	18.0	7.0		3.1	36.3	112.5	116.3	3.8		13.8	3.8	112.5	0.0	0.0	1.2	13.2	14.4	28.2
Sep-65	13.1	4.3		2.3	31.2	71.8	39.4	-32.4	-32.4	48.0	34.2	73.6	-1.9	0.0	0.6	6.6	7.2	55.2
Oct-65	6.2	1.4		1.1	28.2	31.0	64.3	33.3		75.0	27.0	31.0	0.0	27.0	13.8	3.3	17.1	92.1
Nov-65	-1.2	0.0		0.0	23.7	0.0	137.9	137.9		212.9	0.0	0.0	0.0	0.0	6.9	0.0	6.9	223.1
Dec-65	-7.0	0.0	29.3	0.0	22.5	0.0	66.5	66.5		279.4	0.0	0.0	0.0	0.0	3.5	0.0	3.5	286.2
Jan-66	-6.2	0.0		0.0	24.0	0.0	72.4	72.4		224.9	0.0	0.0	0.0	0.0	12.4	0.0	12.4	237.3
Feb-66	-7.6	0.0		0.0	24.3	0.0	76.7	76.7		301.6	0.0	0.0	0.0	0.0	6.2	0.0	6.2	307.8
Mar-66	0.2	0.0		0.0	30.6	0.0	66.8	66.8		75.0	0.0	0.0	0.0	66.8	33.4	22.9	56.3	320.7
Apr-66	3.7	0.6		0.6	33.9	20.3	15.7	-4.6	-4.6	70.0	-5.0	20.7	-0.4	0.0	16.7	103.1	119.8	189.8
May-66	10.2	2.9		1.8	38.4	69.1	57.7	-11.4	-16.1	59.0	-11.0	68.7	0.4	0.0	8.4	51.5	59.9	118.9
Jun-66	16.5	6.1		2.8	38.7	108.4	51.8	-56.6	-72.6	27.0	-32.0	83.8	24.6	0.0	4.2	25.6	29.9	56.9
Jul-66	18.4	7.2		3.2	39.3	125.8	72.9	-52.9	-125.5	13.0	-14.0	86.9	38.9	0.0	2.1	12.9	15.0	28.0
Aug-66	18.5	7.3		3.2	36.3	116.2	36.8	-79.4	-204.8	4.0	-9.0	45.8	70.4	0.0	1.0	6.4	7.5	11.5
Sep-66	11.8	3.7		2.0	31.2	62.4	100.8	38.4		42.4	38.4	62.4	0.0	0.0	0.5	3.2	3.7	46.1
Oct-66	7.3	1.8		1.3	28.2	36.7	70.6	33.9		75.0	32.6	36.7	0.0	32.6	16.6	1.6	18.2	93.2
Nov-66	3.4	0.6		0.6	23.7	14.2	97.0	82.8		75.0	0.0	14.2	0.0	82.8	49.7	0.8	50.5	125.5
Dec-66	-4.3	0.0	30.1	0.0	22.5	0.0	77.5	77.5		152.5	0.0	0.0	0.0	0.0	24.8	0.0	24.8	178.1
Jan-67	-7.7	0.0		0.0	24.0	0.0	78.7	78.7		356.9	0.0	0.0	0.0	0.0	16.4	0.0	16.4	373.3
Feb-67	-12.5	0.0		0.0	24.3	0.0	123.7	123.7		480.6	0.0	0.0	0.0	0.0	8.2	0.0	8.2	488.8
Mar-67	-7.0	0.0		0.0	30.6	0.0	46.5	46.5		527.1	0.0	0.0	0.0	0.0	4.1	0.0	4.1	531.2
Apr-67	2.0	0.3		0.3	33.9	10.2	22.9	12.7		75.0	0.0	10.2	0.0	12.7	6.4	46.8	53.2	506.7
May-67	7.1	1.7		1.1	38.4	42.2	162.6	120.4		75.0	0.0	42.2	0.0	120.4	63.4	210.6	274.0	349.0
Jun-67	17.3	6.6		2.9	38.7	112.2	100.8	-11.4	-11.4	64.0	-11.0	111.8	0.4	0.0	31.7	105.3	137.0	201.0
Jul-67	21.0	8.8		3.6	39.3	141.5	68.3	-73.2	-84.6	23.0	-41.0	109.3	32.2	0.0	15.8	52.7	68.5	91.5
Aug-67	19.4	7.8		3.3	36.3	119.8	46.7	-73.1	-157.7	9.0	-14.0	60.7	59.1	0.0	7.9	26.3	34.2	43.2
Sep-67	13.4	4.5		2.3	31.2	71.8	168.1	96.3		75.0	66.0	71.8	0.0	66.0	37.0	13.2	50.1	125.1
Oct-67	8.0	2.0		1.3	28.2	36.7	48.0	11.3		75.0	0.0	36.7	0.0	11.3	24.2	6.6	30.7	105.7
Nov-67	0.9	0.1		0.2	23.7	4.7	111.8	107.1		75.0	0.0	4.7	0.0	107.1	65.6	3.3	68.9	143.9
Dec-67	-7.0	0.0	31.6	0.0	22.5	0.0	203.2	203.2		278.2	0.0	0.0	0.0	0.0	32.8	0.0	32.8	314.3
Jan-68	-12.0	0.0		0.0	24.0	0.0	76.2	76.2		426.5	0.0	0.0	0.0	0.0	0.0	0.0	0.0	426.5
Feb-68	-10.8	0.0		0.0	24.3	0.0	33.8	33.8		460.3	0.0	0.0	0.0	0.0	0.0	0.0	0.0	460.3
Mar-68	-2.1	0.0		0.0	30.6	0.0	107.2	107.2		567.5	0.0	0.0	0.0	0.0	0.0	0.0	0.0	567.5
Apr-68	5.3	1.1		0.9	33.9	30.5	51.1	20.6		75.0	0.0	30.5	0.0	20.6	10.3	24.4	34.7	304.9
May-68	9.7	2.7		1.7	38.4	65.3	42.7	-22.6	-22.6	54.0	-21.0	63.7	1.6	0.0	5.1	109.8	114.9	168.9
Jun-68	14.7	5.1		2.5	38.7	96.8	86.1	-10.7	-33.2	47.0	-7.0	93.1	3.7	0.0	2.6	54.9	57.5	104.5
Jul-68	20.3	8.3		3.5	39.3	137.6	28.7	-108.9	-142.1	11.0	-36.0	64.7	72.9	0.0	1.3	27.5	28.7	39.7
Aug-68	16.6	6.2		2.8	36.3	101.6	58.7	-42.9	-185.0	6.0	-5.0	63.7	37.9	0.0	0.6	13.7	14.4	20.4
Sep-68	14.7	5.1		2.5	31.2	78.0	30.5	-47.5	-232.5	3.0	-3.0	33.5	44.5	0.0	0.3	6.9	7.2	10.2
Oct-68	9.6	2.7		1.6	28.2	45.1	115.8	70.7		73.7	70.7	45.1	0.0	0.0	0.2	3.4	3.6	77.3
Nov-68	-0.9	0.0		0.0	23.7	0.0	165.6	165.6		239.3	165.6	0.0	0.0	0.0	0.1	0.0	0.1	242.8
Dec-68	-5.4	0.0	31.2	0.0	22.5	0.0	111.0	111.0		350.3	0.0	0.0	0.0	0.0	0.0	0.0	0.0	353.8

Table A.1E Results of the PE and water balance calculations (Thornthwaite and Mather).

	Line 1		Line 2	Line 3		Line 4	Line 5	Line 6	Line 7	Line 8	Line 9	Line 10	Line 11	Line 12	Line 13	Line 14	Line 15	Line 16
	Mean			Un-Adj	Corr.	Adj-			Acc Pot		Change						Tot	
Date	Temp			PE	45 deg.	PE	P	P- PE	WL	ST	in ST	AE	D	S	RO	SMRO	RO	DT
M / Y	(°C)	(i)	(I)	(mm)	Lat. N	(mm)	(mm)	(mm)	(mm)	(mm)	(mm)	(mm)	(mm)	(mm)	(mm)	(mm)	(mm)	(mm)
Jan-69	-7.6	0.0		0.0	24.0	0.0	81.5	81.5		321.3	0.0	0.0	0.0	0.0	16.9	0.0	16.9	338.2
Feb-69	-5.8	0.0		0.0	24.3	0.0	49.0	49.0		370.3	0.0	0.0	0.0	0.0	8.5	0.0	8.5	378.8
Mar-69	-2.2	0.0		0.0	30.6	0.0	45.5	45.5		415.8	0.0	0.0	0.0	0.0	4.2	0.0	4.2	420.0
Apr-69	3.2	0.5		0.6	33.9	20.3	75.2	54.9		75.0	0.0	20.3	0.0	54.9	27.4	25.4	52.8	335.3
May-69	10.0	2.9		1.7	38.4	65.3	68.8	3.5		75.0	0.0	65.3	0.0	3.5	15.5	114.3	129.8	204.8
Jun-69	17.4	6.6		3.0	38.7	116.1	66.3	-49.8	-49.8	38.0	-37.0	103.3	12.8	0.0	7.7	57.2	64.9	102.9
Jul-69	17.9	6.9		3.1	39.3	121.8	151.1	29.3		67.3	29.3	121.8	0.0	0.0	3.9	28.6	32.4	99.7
Aug-69	19.1	7.6		3.2	36.3	116.2	71.9	-44.3	-44.3	40.0	-27.3	99.2	17.0	0.0	1.9	14.3	16.2	56.2
Sep-69	13.5	4.5		2.3	31.2	71.8	130.3	58.5		75.0	35.0	71.8	0.0	35.0	18.5	7.1	25.6	100.6
Oct-69	8.6	1.5		1.1	28.2	31.0	61.5	30.5		75.0	0.0	31.0	0.0	30.5	24.5	3.6	28.0	103.0
Nov-69	2.3	0.3		0.4	23.7	9.5	120.4	110.9		75.0	0.0	9.5	0.0	110.9	67.7	1.8	69.5	144.5
Dec-69	-3.7	0.0	30.8	0.0	22.5	0.0	164.8	164.8		239.8	0.0	0.0	0.0	0.0	33.8	0.0	33.8	275.4
Jan-70	-12.7	0.0		0.0	24.0	0.0	15.7	15.7		256.8	0.0	0.0	0.0	0.0	12.7	0.0	12.7	269.5
Feb-70	-7.8	0.0		0.0	24.3	0.0	134.9	134.9		391.7	0.0	0.0	0.0	0.0	6.4	0.0	6.4	398.1
Mar-70	-1.6	0.0		0.0	30.6	0.0	65.3	65.3		457.0	0.0	0.0	0.0	0.0	3.2	0.0	3.2	460.2
Apr-70	4.2	0.8		0.7	33.9	23.7	90.9	67.2		75.0	0.0	23.7	0.0	67.2	33.6	34.3	67.9	420.5
May-70	10.7	3.2		1.8	38.4	69.1	92.5	23.4		75.0	0.0	69.1	0.0	23.4	28.5	154.4	182.8	257.8
Jun-70	16.0	5.8		2.7	38.7	104.5	95.3	-9.2	-9.2	66.0	-9.0	104.3	0.2	0.0	14.2	77.2	91.4	157.4
Jul-70	20.5	8.5		3.5	39.3	137.6	93.5	-44.1	-53.2	36.0	-30.0	123.5	14.1	0.0	7.1	38.6	45.7	81.7
Aug-70	18.8	7.4		3.2	36.3	116.2	167.4	51.2		75.0	39.0	116.2	0.0	39.0	23.1	19.3	42.4	117.4
Sep-70	12.4	3.9		2.1	31.2	65.5	86.9	21.4		75.0	0.0	65.5	0.0	21.4	22.2	9.6	31.9	106.9
Oct-70	8.6	2.3		1.4	28.2	39.5	104.9	65.4		75.0	0.0	39.5	0.0	65.4	43.8	4.8	48.6	123.6
Nov-70	1.9	0.2		0.3	23.7	7.1	65.0	57.9		75.0	0.0	7.1	0.0	57.9	50.9	2.4	53.3	128.3
Dec-70	-10.6	0.0	32.0	0.0	22.5	0.0	166.1	166.1		241.1	0.0	0.0	0.0	0.0	25.4	0.0	25.4	268.9
Jan-71	-12.6	0.0		0.0	24.0	0.0	52.8	52.8		192.3	0.0	0.0	0.0	0.0	2.5	0.0	2.5	194.8
Feb-71	-8.6	0.0		0.0	24.3	0.0	135.6	135.6		327.9	0.0	0.0	0.0	0.0	1.2	0.0	1.2	329.1
Mar-71	-2.3	0.0		0.0	30.6	0.0	123.2	123.2		451.1	0.0	0.0	0.0	0.0	0.6	0.0	0.6	451.7
Apr-71	4.0	0.7		0.6	33.9	20.3	84.3	64.0		75.0	0.0	20.3	0.0	64.0	32.0	34.8	66.8	420.8
May-71	11.6	3.6		1.9	38.4	73.0	97.0	24.0		75.0	0.0	73.0	0.0	24.0	28.0	156.6	184.6	259.6
Jun-71	15.8	5.7		2.7	38.7	104.5	88.6	-15.9	-15.9	59.0	-16.0	104.6	-0.1	0.0	14.0	76.3	92.3	151.3
Jul-71	19.2	7.7		3.2	39.3	125.8	76.7	-49.1	-65.0	31.0	-28.0	104.7	21.1	0.0	7.0	39.2	46.2	77.2
Aug-71	18.4	7.2		3.1	36.3	112.5	69.9	-42.6	-107.6	17.0	-14.0	83.9	28.6	0.0	3.5	19.6	23.1	40.1
Sep-71	14.5	5.0		2.4	31.2	74.9	73.9	-1.0	-108.6	17.0	0.0	73.9	1.0	0.0	1.8	9.8	11.5	28.5
Oct-71	9.1	2.5		1.5	28.2	42.3	81.5	39.2		56.2	39.2	42.3	0.0	0.0	0.9	4.9	5.8	62.0
Nov-71	0.2	0.0		0.0	23.7	0.0	93.5	93.5		75.0	18.8	0.0	0.0	18.8	9.8	2.4	12.3	87.3
Dec-71	-8.2	0.0	32.4	0.0	22.5	0.0	64.5	64.5		139.5	0.0	0.0	0.0	0.0	4.9	0.0	4.9	146.9
Jan-72	-9.4	0.0		0.0	24.0	0.0	73.9	73.9		475.3	0.0	0.0	0.0	0.0	1.0	0.0	1.0	476.3
Feb-72	-10.4	0.0		0.0	24.3	0.0	92.7	92.7		568.0	0.0	0.0	0.0	0.0	0.5	0.0	0.5	568.5
Mar-72	-6.0	0.0		0.0	30.6	0.0	212.3	212.3		780.3	0.0	0.0	0.0	0.0	0.3	0.0	0.3	780.6
Apr-72	2.3	0.3		0.4	33.9	13.6	45.5	31.9		75.0	0.0	13.6	0.0	31.9	16.0	46.9	62.9	513.3
May-72	11.5	3.5		2.0	38.4	76.8	89.7	12.9		75.0	0.0	76.8	0.0	12.9	14.4	211.1	225.5	300.5
Jun-72	16.2	5.9		2.8	38.7	108.4	123.4	15.0		75.0	0.0	108.4	0.0	15.0	14.7	105.5	120.3	195.3
Jul-72	18.9	7.5		3.2	39.3	125.8	68.3	-57.5	-57.5	34.0	-41.0	109.3	16.5	0.0	7.4	52.8	60.1	94.1
Aug-72	17.9	6.9		3.1	36.3	112.5	95.3	-17.2	-74.7	27.0	-7.0	102.3	10.2	0.0	3.7	26.4	30.1	57.1
Sep-72	13.8	4.7		2.4	31.2	74.9	108.5	33.6		60.6	33.6	74.9	0.0	0.0	1.8	13.2	15.0	75.7
Oct-72	5.3	1.1		0.9	28.2	25.4	128.3	102.9		75.0	14.4	25.4	0.0	14.4	8.1	8.6	14.7	89.7
Nov-72	-0.5	0.0		0.0	23.7	0.0	122.4	122.4		197.4	0.0	0.0	0.0	0.0	4.1	0.0	4.1	208.1
Dec-72	-9.7	0.0	29.9	0.0	22.5	0.0	204.0	204.0		401.4	0.0	0.0	0.0	0.0	2.0	0.0	2.0	410.0

Table A.1F Results of the PE and water balance calculations (Thornthwaite and Mather).

	Line 1		Line 2	Line 3		Line 4	Line 5	Line 6	Line 7	Line 8	Line 9	Line 10	Line 11	Line 12	Line 13	Line 14	Line 15	Line 16
	Mean			Un-Adj	Corr.	Adj-			Acc Pot		Change						Tot	
Date	Temp			PE	45 deg.	PE	P	P- PE	WL	ST	in ST	AE	D	S	RO	SMRO	RO	DT
M / Y	(°C)	(i)	(I)	(mm)	Lat. N	(mm)	(mm)	(mm)	(mm)	(mm)	(mm)	(mm)	(mm)	(mm)	(mm)	(mm)	(mm)	(mm)
Jan-73	-8.9	0.0		0.0	24.0	0.0	110.7	110.7		445.9	0.0	0.0	0.0	0.0	12.7	0.0	12.7	458.5
Feb-73	-8.3	0.0		0.0	24.3	0.0	97.5	97.5		543.4	0.0	0.0	0.0	0.0	6.3	0.0	6.3	549.7
Mar-73	0.1	0.0		0.0	30.6	0.0	83.8	83.8		75.0	0.0	0.0	0.0	83.8	41.9	23.0	64.9	330.2
Apr-73	5.2	1.1		0.9	33.9	30.5	131.3	100.8		75.0	0.0	30.5	0.0	100.8	71.3	103.5	174.8	249.8
May-73	10.2	2.9		1.7	38.4	65.3	97.0	31.7		75.0	0.0	65.3	0.0	31.7	51.5	51.8	103.3	178.3
Jun-73	17.7	6.8		3.0	38.7	116.1	89.7	-26.4	-26.4	52.0	-23.0	112.7	3.4	0.0	25.8	25.9	51.6	103.6
Jul-73	21.3	9.0		3.6	39.3	141.5	66.5	-75.0	-101.4	19.0	-33.0	99.5	42.0	0.0	12.9	12.9	25.8	44.8
Aug-73	19.5	7.9		3.3	36.3	119.8	140.5	20.7		39.7	20.7	119.8	0.0	0.0	6.4	6.5	12.9	52.6
Sep-73	12.5	4.0		2.1	31.2	65.5	83.6	18.1		57.8	18.1	65.5	0.0	0.0	3.2	3.2	6.5	64.2
Oct-73	7.4	1.8		1.2	28.2	33.8	43.7	9.9		67.7	9.9	33.8	0.0	0.0	1.6	1.6	3.2	70.9
Nov-73	-0.1	0.0		0.0	23.7	0.0	99.6	99.6		167.3	99.6	0.0	0.0	99.6	50.6	0.0	50.6	219.5
Dec-73	-1.4	0.0	33.4	0.0	22.5	0.0	167.9	167.9		335.2	0.0	0.0	0.0	0.0	25.3	0.0	25.3	362.1
Jan-74	-9.6	0.0		0.0	24.0	0.0	81.0	81.0		236.0	0.0	0.0	0.0	0.0	17.4	0.0	17.4	253.4
Feb-74	-8.1	0.0		0.0	24.3	0.0	70.9	70.9		306.9	0.0	0.0	0.0	0.0	8.7	0.0	8.7	315.6
Mar-74	-2.9	0.0		0.0	30.6	0.0	82.0	82.0		388.9	0.0	0.0	0.0	0.0	4.3	0.0	4.3	393.2
Apr-74	3.9	0.7		0.7	33.9	23.7	134.1	110.4		75.0	0.0	23.7	0.0	110.4	55.2	27.0	82.2	377.5
May-74	8.2	2.1		1.4	38.4	53.8	78.0	24.2		75.0	0.0	53.8	0.0	24.2	39.7	121.5	161.2	236.2
Jun-74	17.1	6.4		2.9	38.7	112.2	67.1	-45.1	-45.1	40.0	-35.0	102.1	10.1	0.0	19.9	60.8	80.6	120.6
Jul-74	18.5	7.3		3.2	39.3	125.8	106.4	-19.4	-64.5	31.0	-9.0	115.4	10.4	0.0	9.9	30.4	40.3	71.3
Aug-74	19.3	7.7		3.3	36.3	119.8	31.2	-88.6	-153.1	9.0	-22.0	53.2	66.6	0.0	5.0	15.2	20.2	29.2
Sep-74	12.7	4.1		2.2	31.2	68.6	145.3	76.7		75.0	66.0	68.6	0.0	66.0	35.5	7.6	43.1	118.1
Oct-74	4.9	1.0		0.9	28.2	25.4	67.3	41.9		75.0	0.0	25.4	0.0	41.9	38.7	3.8	42.5	117.5
Nov-74	0.7	0.1		0.1	23.7	2.4	102.6	100.2		75.0	0.0	2.4	0.0	100.2	69.5	1.9	71.4	146.4
Dec-74	-4.8	0.0	29.4	0.0	22.5	0.0	80.0	80.0		155.0	0.0	0.0	0.0	0.0	34.7	0.0	34.7	191.6
Jan-75	-9.0	0.0		0.0	24.0	0.0	101.6	101.6		315.5	0.0	0.0	0.0	0.0	22.5	0.0	22.5	338.0
Feb-75	-9.9	0.0		0.0	24.3	0.0	42.2	42.2		357.7	0.0	0.0	0.0	0.0	11.2	0.0	11.2	368.9
Mar-75	-3.9	0.0		0.0	30.6	0.0	105.7	105.7		463.4	0.0	0.0	0.0	0.0	5.6	0.0	5.6	469.0
Apr-75	2.5	0.4		0.4	33.9	13.6	81.5	67.9		75.0	0.0	13.6	0.0	67.9	34.0	37.9	71.9	455.7
May-75	11.5	3.5		1.9	38.4	73.0	78.2	5.2		75.0	0.0	73.0	0.0	5.2	19.6	170.6	190.2	265.2
Jun-75	16.7	6.2		2.8	38.7	108.4	84.8	-23.6	-23.6	53.0	-22.0	106.8	1.6	0.0	9.8	85.3	95.1	148.1
Jul-75	20.9	8.7		3.6	39.3	141.5	85.9	-55.6	-79.1	25.0	-28.0	113.9	27.6	0.0	4.9	42.6	47.5	72.5
Aug-75	18.2	7.1		3.1	36.3	112.5	35.1	-77.4	-156.6	9.0	-16.0	51.1	61.4	0.0	2.5	21.3	23.8	32.8
Sep-75	13.2	4.4		2.2	31.2	68.6	113.5	44.9		53.9	44.9	68.6	0.0	0.0	1.2	10.7	11.9	65.7
Oct-75	6.7	1.6		1.1	28.2	31.0	82.6	51.6		75.0	21.1	31.0	0.0	21.1	11.2	5.3	18.5	91.5
Nov-75	2.6	0.4		0.4	23.7	9.5	178.1	168.6		75.0	0.0	9.5	0.0	168.6	89.9	2.7	92.6	167.6
Dec-75	-8.5	0.0	32.2	0.0	22.5	0.0	138.9	138.9		213.9	0.0	0.0	0.0	0.0	45.0	0.0	45.0	261.5
Jan-76	-12.3	0.0		0.0	24.0	0.0	143.8	143.8		448.9	0.0	0.0	0.0	0.0	2.9	0.0	2.9	451.8
Feb-76	-7.3	0.0		0.0	24.3	0.0	142.5	142.5		591.4	0.0	0.0	0.0	0.0	1.4	0.0	1.4	592.8
Mar-76	-2.8	0.0		0.0	30.6	0.0	96.5	96.5		687.9	0.0	0.0	0.0	0.0	0.7	0.0	0.7	688.6
Apr-76	4.6	0.9		0.8	33.9	27.1	75.9	48.8		75.0	0.0	27.1	0.0	48.8	24.4	36.0	60.4	424.1
May-76	10.9	3.3		1.9	38.4	73.0	103.4	30.4		75.0	0.0	73.0	0.0	30.4	27.4	182.0	189.4	264.4
Jun-76	17.8	6.8		3.0	38.7	116.1	115.8	-0.3	-0.3	75.0	0.0	115.8	0.3	0.0	13.7	81.0	94.7	169.7
Jul-76	18.3	7.1		3.1	39.3	121.8	122.2	0.4		75.0	0.0	121.8	0.0	0.4	7.0	40.5	47.5	122.5
Aug-76	18.4	7.2		3.2	36.3	116.2	67.3	-48.9	-48.9	38.0	-37.0	104.3	11.9	0.0	3.5	20.3	23.8	61.8
Sep-76	12.8	4.2		2.2	31.2	68.6	53.8	-14.8	-63.7	31.0	-7.0	60.8	7.8	0.0	1.8	10.1	11.9	42.9
Oct-76	6.2	1.4		1.1	28.2	31.0	160.8	129.8		75.0	44.0	31.0	0.0	44.0	22.9	5.1	27.9	102.9
Nov-76	-0.8	0.0		0.0	23.7	0.0	65.3	65.3		140.3	0.0	0.0	0.0	0.0	11.4	0.0	11.4	156.8
Dec-76	-9.5	0.0	30.8	0.0	22.5	0.0	164.8	164.8		305.1	0.0	0.0	0.0	0.0	5.7	0.0	5.7	315.9

Table A.1G Results of the PE and water balance calculations (Thornthwaite and Mather).

	Line 1		Line 2	Line 3		Line 4	Line 5	Line 6	Line 7	Line 8	Line 9	Line 10	Line 11	Line 12	Line 13	Line 14	Line 15	Line 16
	Mean			Un-Adj	Corr.	Adj-			Acc Pot		Change						Tot	
Date	Temp			PE	45 deg.	PE	P	P- PE	WL	ST	in ST	AE	D	S	RO	SMRO	RO	DT
M / Y	(°C)	(i)	(I)	(mm)	Lat. N	(mm)	(mm)	(mm)	(mm)	(mm)	(mm)	(mm)	(mm)	(mm)	(mm)	(mm)	(mm)	(mm)
Jan-77	-12.1	0.0		0.0	24.0	0.0	92.2	92.2		325.4	0.0	0.0	0.0	0.0	7.6	0.0	7.6	333.0
Feb-77	-8.6	0.0		0.0	24.3	0.0	84.2	84.2		409.6	0.0	0.0	0.0	0.0	3.8	0.0	3.8	413.4
Mar-77	0.5	0.0		0.1	30.6	3.1	115.9	112.8		75.0	0.0	3.1	0.0	112.8	56.4	33.0	89.4	432.2
Apr-77	3.5	0.6		0.6	33.9	20.3	54.4	34.1		75.0	0.0	20.3	0.0	34.1	45.2	148.5	193.7	268.7
May-77	11.4	3.5		2.0	38.4	76.8	59.4	-17.4	-17.4	58.0	-17.0	76.4	0.4	0.0	22.6	74.3	96.9	154.9
Jun-77	14.5	5.0		2.5	38.7	96.8	195.3	98.6		75.0	17.0	96.8	0.0	17.0	19.8	37.1	56.9	131.9
Jul-77	19.0	7.6		3.2	39.3	125.8	57.3	-68.5	-68.5	29.0	-46.0	103.3	22.5	0.0	9.9	18.6	28.5	57.5
Aug-77	18.5	7.3		3.2	36.3	116.2	90.7	-25.5	-93.9	20.0	-9.0	99.7	16.5	0.0	5.0	9.3	14.2	34.2
Sep-77	12.0	3.8		2.1	31.2	65.5	110.7	45.2		65.2	45.2	65.5	0.0	0.0	2.5	4.6	7.1	72.3
Oct-77	7.6	1.9		1.3	28.2	36.7	178.5	141.8		75.0	9.8	38.7	0.0	9.8	6.1	2.3	8.5	83.5
Nov-77	2.2	0.3		0.4	23.7	9.5	64.3	54.8		75.0	0.0	9.5	0.0	54.8	30.5	1.2	31.6	106.6
Dec-77	-6.1	0.0	29.8	0.0	22.5	0.0	158.2	158.2		233.2	0.0	0.0	0.0	0.0	15.2	0.0	15.2	249.6
Jan-78	-10.0	0.0		0.0	24.0	0.0	247.3	247.3		439.9	0.0	0.0	0.0	0.0	3.1	0.0	3.1	443.0
Feb-78	-9.0	0.0		0.0	24.3	0.0	36.6	36.6		476.5	0.0	0.0	0.0	0.0	1.5	0.0	1.5	478.0
Mar-78	-3.9	0.0		0.0	30.6	0.0	78.0	78.0		554.5	0.0	0.0	0.0	0.0	0.8	0.0	0.8	555.3
Apr-78	2.9	0.4		0.5	33.9	17.0	79.6	62.7		75.0	0.0	17.0	0.0	62.7	31.3	30.8	62.1	384.3
May-78	13.0	4.3		2.3	38.4	88.3	19.4	-68.9	-68.9	29.0	-46.0	65.4	22.9	0.0	15.7	138.6	154.3	183.3
Jun-78	15.9	5.8		2.8	38.7	108.4	86.4	-22.0	-90.9	21.0	-8.0	94.4	14.0	0.0	7.8	69.3	77.1	98.1
Jul-78	19.2	7.7		3.3	39.3	129.7	67.1	-62.6	-153.5	9.0	-12.0	79.1	50.6	0.0	3.9	34.7	38.6	47.6
Aug-78	18.7	7.4		3.2	36.3	116.2	44.7	-71.5	-224.9	3.0	-6.0	50.7	65.5	0.0	2.0	17.3	19.3	22.3
Sep-78	10.9	3.3		1.9	31.2	59.3	83.3	24.0		27.0	24.0	59.3	0.0	0.0	1.0	8.7	9.6	36.7
Oct-78	6.6	1.5		1.1	28.2	31.0	149.7	118.7		75.0	48.0	31.0	0.0	48.0	24.5	4.3	28.8	103.8
Nov-78	-0.8	0.0		0.0	23.7	0.0	38.8	38.8		113.8	0.0	0.0	0.0	0.0	12.2	0.0	12.2	130.4
Dec-78	-7.1	0.0	30.3	0.0	22.5	0.0	78.8	78.8		192.6	0.0	0.0	0.0	0.0	6.1	0.0	6.1	203.1
Jan-79	-6.8	0.0		0.0	24.0	0.0	236.8	236.8		413.4	0.0	0.0	0.0	0.0	13.5	0.0	13.5	426.9
Feb-79	-10.1	0.0		0.0	24.3	0.0	111.9	111.9		525.3	0.0	0.0	0.0	0.0	6.8	0.0	6.8	532.1
Mar-79	0.8	0.1		0.1	30.6	3.1	136.9	133.8		75.0	0.0	3.1	0.0	133.8	66.9	18.8	85.7	317.9
Apr-79	5.0	1.0		0.8	33.9	27.1	128.1	101.0		75.0	0.0	27.1	0.0	101.0	84.0	84.6	168.6	243.6
May-79	12.5	4.0		2.0	38.4	76.8	207.3	130.5		75.0	0.0	76.8	0.0	130.5	107.2	42.3	149.5	224.5
Jun-79	16.7	6.2		2.8	38.7	108.4	34.1	-74.3	-74.3	27.0	-48.0	82.1	26.3	0.0	53.6	21.2	74.8	101.8
Jul-79	21.3	9.0		3.6	39.3	141.5	79.0	-62.5	-136.7	11.0	-16.0	95.0	48.5	0.0	26.8	10.6	37.4	48.4
Aug-79	17.7	6.8		3.0	36.3	108.9	170.0	61.1		72.1	61.1	108.9	0.0	0.0	13.4	5.3	18.7	90.8
Sep-79	13.3	4.4		2.2	31.2	68.6	70.4	1.8		73.9	1.8	68.6	0.0	0.0	6.7	2.6	9.3	83.2
Oct-79	8.0	2.0		1.3	28.2	36.7	126.2	89.5		75.0	1.1	36.7	0.0	1.1	3.9	1.3	5.2	80.2
Nov-79	4.1	0.7		0.6	23.7	14.2	118.4	104.2		75.0	0.0	14.2	0.0	104.2	54.1	0.7	54.7	129.7
Dec-79	-4.5	0.0	34.2	0.0	22.5	0.0	101.6	101.6		176.6	0.0	0.0	0.0	0.0	27.0	0.0	27.0	204.3
Jan-80	-7.2	0.0		0.0	24.0	0.0	48.3	48.3		221.2	0.0	0.0	0.0	0.0	20.8	0.0	20.8	242.0
Feb-80	-8.7	0.0		0.0	24.3	0.0	29.6	29.6		250.8	0.0	0.0	0.0	0.0	10.4	0.0	10.4	261.2
Mar-80	-2.8	0.0		0.0	30.6	0.0	110.1	110.1		360.9	0.0	0.0	0.0	0.0	5.2	0.0	5.2	366.1
Apr-80	5.8	1.3		1.0	33.9	33.9	96.6	62.7		75.0	0.0	33.9	0.0	62.7	31.4	21.0	52.4	300.5
May-80	10.7	3.2		1.9	38.4	73.0	38.4	-34.6	-34.6	46.0	-29.0	67.4	5.6	0.0	15.7	94.5	110.2	156.2
Jun-80	15.4	5.5		2.7	38.7	104.5	83.1	-21.4	-56.0	35.0	-11.0	94.1	10.4	0.0	7.8	47.3	55.1	90.1
Jul-80	19.2	7.7		3.3	39.3	129.7	170.3	40.6		75.0	40.0	129.7	0.0	0.0	3.9	23.6	27.5	102.5
Aug-80	19.6	7.9		3.3	36.3	119.8	114.4	-5.4	-5.4	70.0	-5.0	119.4	0.4	0.0	2.0	11.8	13.8	83.8
Sep-80	12.1	3.8		2.1	31.2	65.5	123.6	58.1		75.0	5.0	65.5	0.0	5.0	3.5	5.9	9.4	84.4
Oct-80	5.9	1.3		1.1	28.2	31.0	129.5	98.5		75.0	0.0	31.0	0.0	98.5	51.0	3.0	53.9	128.9
Nov-80	0.6	0.0		0.1	23.7	2.4	117.7	115.3		75.0	0.0	2.4	0.0	115.3	83.2	1.5	84.6	159.6
Dec-80	-9.9	0.0	30.6	0.0	22.5	0.0	97.9	97.9		172.9	0.0	0.0	0.0	0.0	41.6	0.0	41.6	216.0

Table A.1H Results of the PE and water balance calculations (Thornthwaite and Mather).

	Line1		Line 2	Line 3		Line 4	Line 5	Line 6	Line 7	Line 8	Line 9	Line 10	Line 11	Line 12	Line 13	Line 14	Line 15	Line 16
	Mean			Un-Adj	Corr.	Adj-			Acc Pot		Change						Tot	
Date	Temp			PE	45 deg.	PE	P	P- PE	WL	ST	in ST	AE	D	S	RO	SMRO	RO	DT
M / Y	(°C)	(i)	(I)	(mm)	Lat. N	(mm)	(mm)	(mm)	(mm)	(mm)	(mm)	(mm)	(mm)	(mm)	(mm)	(mm)	(mm)	(mm)
Jan-81	-12.8	0.0		0.0	24.0	0.0	98.6	98.6		345.0	0.0	0.0	0.0	0.0	21.9	0.0	21.9	366.9
Feb-81	-2.0	0.0		0.0	24.3	0.0	81.7	81.7		426.7	0.0	0.0	0.0	0.0	10.9	0.0	10.9	437.6
Mar-81	-0.5	0.0		0.0	30.6	0.0	92.1	92.1		518.8	0.0	0.0	0.0	0.0	5.5	0.0	5.5	524.3
Apr-81	5.1	1.0		0.8	33.9	27.1	114.1	87.0		75.0	0.0	27.1	0.0	87.0	43.5	24.9	68.4	348.1
May-81	11.9	3.7		2.0	38.4	76.8	141.0	64.2		75.0	0.0	76.8	0.0	64.2	53.8	112.1	165.9	240.9
Jun-81	16.1	5.9		2.7	38.7	104.5	141.8	37.3		75.0	0.0	104.5	0.0	37.3	45.8	56.0	101.6	176.6
Jul-81	19.6	7.9		3.3	39.3	129.7	52.7	-77.0	-77.0	26.0	-49.0	101.7	28.0	0.0	22.8	28.0	50.8	76.8
Aug-81	18.4	7.2		3.1	36.3	112.5	152.6	40.1		66.1	40.1	112.5	0.0	0.0	11.4	14.0	25.4	91.5
Sep-81	12.7	4.1		2.1	31.2	65.5	150.5	85.0		75.0	8.9	65.5	0.0	8.9	10.2	7.0	17.2	92.2
Oct-81	6.8	1.6		1.1	28.2	31.0	169.1	138.1		75.0	0.0	31.0	0.0	138.1	74.1	3.5	77.6	152.6
Nov-81	1.9	0.2		0.3	23.7	7.1	108.0	100.9		75.0	0.0	7.1	0.0	100.9	87.5	1.8	89.3	164.3
Dec-81	-3.0	0.0	31.6	0.0	22.5	0.0	171.4	171.4		246.4	0.0	0.0	0.0	0.0	43.8	0.0	43.8	291.9
Jan-82	-13.5	0.0		0.0	24.0	0.0	103.0	103.0		248.4	0.0	0.0	0.0	0.0	16.4	0.0	16.4	264.8
Feb-82	-9.7	0.0		0.0	24.3	0.0	128.9	128.9		377.3	0.0	0.0	0.0	0.0	8.2	0.0	8.2	385.5
Mar-82	-2.9	0.0		0.0	30.6	0.0	82.7	82.7		460.0	0.0	0.0	0.0	0.0	4.1	0.0	4.1	464.1
Apr-82	3.5	0.6		0.6	33.9	20.3	73.8	53.5		75.0	0.0	20.3	0.0	53.5	26.7	29.6	56.3	372.2
May-82	10.8	3.2		1.9	38.4	73.0	22.1	-50.9	-50.9	37.0	-38.0	60.1	12.9	0.0	13.4	133.2	146.6	163.6
Jun-82	15.4	5.5		2.7	38.7	104.5	131.8	27.3		64.3	27.3	104.5	0.0	0.0	6.7	66.6	73.3	137.6
Jul-82	19.6	7.9		3.3	39.3	129.7	137.8	8.1		72.4	8.1	129.7	0.0	0.0	3.3	33.3	36.6	109.1
Aug-82	16.1	5.9		2.8	36.3	101.6	143.9	42.3		75.0	2.6	101.6	0.0	2.6	3.0	16.7	19.6	94.6
Sep-82	14.1	4.8		2.4	31.2	74.9	89.3	14.4		75.0	0.0	74.9	0.0	14.4	8.7	8.3	17.0	92.0
Oct-82	7.5	1.9		1.3	28.2	36.7	58.0	21.3		75.0	0.0	36.7	0.0	21.3	15.0	4.2	19.2	94.2
Nov-82	2.6	0.4		0.4	23.7	9.5	125.3	115.6		75.0	0.0	9.5	0.0	115.8	65.4	2.1	67.5	142.5
Dec-82	-3.2	0.0	30.1	0.0	22.5	0.0	70.4	70.4		145.4	0.0	0.0	0.0	0.0	32.7	0.0	32.7	180.2
Jan-83	-7.3	0.0		0.0	24.0	0.0	71.6	71.6		273.5	0.0	0.0	0.0	0.0	8.0	0.0	8.0	281.5
Feb-83	-7.3	0.0		0.0	24.3	0.0	70.7	70.7		344.2	0.0	0.0	0.0	0.0	4.0	0.0	4.0	348.2
Mar-83	-0.4	0.0		0.0	30.6	0.0	133.4	133.4		477.6	0.0	0.0	0.0	133.4	66.7	0.0	66.7	544.3
Apr-83	5.6	1.2		0.9	33.9	30.5	125.8	95.3		75.0	0.0	30.5	0.0	95.3	81.0	18.1	99.1	318.9
May-83	10.4	3.0		1.8	38.4	69.1	174.6	105.5		75.0	0.0	69.1	0.0	105.5	93.2	81.5	174.7	249.7
Jun-83	16.9	6.3		2.9	38.7	112.2	29.2	-83.0	-83.0	23.0	-52.0	81.2	31.0	0.0	46.6	40.7	87.3	110.3
Jul-83	19.2	7.7		3.2	39.3	125.8	94.0	-31.8	-114.8	18.0	-5.0	99.0	26.8	0.0	23.3	20.4	43.7	61.7
Aug-83	18.7	7.4		3.2	36.3	116.2	60.5	-55.7	-170.5	7.0	-11.0	71.5	44.7	0.0	11.7	10.2	21.8	28.8
Sep-83	15.2	5.4		2.6	31.2	81.1	52.0	-29.1	-199.6	5.0	-2.0	54.0	27.1	0.0	5.8	5.1	10.9	15.9
Oct-83	7.7	1.9		1.3	28.2	36.7	45.4	8.7		13.7	8.7	36.7	0.0	0.0	2.9	2.5	5.5	19.2
Nov-83	2.3	0.3		0.3	23.7	7.1	207.2	200.1		75.0	61.3	7.1	0.0	61.3	32.1	1.3	33.4	108.4
Dec-83	-6.2	0.0	33.2	0.0	22.5	0.0	126.9	126.9		201.9	0.0	0.0	0.0	0.0	16.0	0.0	16.0	219.2
Jan-84	-10.9	0.0		0.0	24.0	0.0	108.6	108.6		287.5	0.0	0.0	0.0	0.0	3.2	0.0	3.2	290.7
Feb-84	-3.3	0.0		0.0	24.3	0.0	133.1	133.1		420.6	0.0	0.0	0.0	0.0	1.6	0.0	1.6	422.2
Mar-84	-5.1	0.0		0.0	30.6	0.0	158.2	158.2		578.8	0.0	0.0	0.0	0.0	0.8	0.0	0.8	579.6
Apr-84	4.1	0.7		0.6	33.9	20.3	115.5	95.2		75.0	0.0	20.3	0.0	95.2	47.6	33.2	80.8	422.2
May-84	10.8	3.2		1.8	38.4	69.1	127.9	58.8		75.0	0.0	69.1	0.0	58.8	53.2	149.4	202.6	277.6
Jun-84	15.9	5.8		2.7	38.7	104.5	166.1	61.6		75.0	0.0	104.5	0.0	61.6	57.4	74.7	132.1	207.1
Jul-84	20.0	8.2		3.4	39.3	133.6	141.0	7.4		75.0	0.0	133.6	0.0	7.4	32.4	37.4	69.7	144.7
Aug-84	20.3	8.3		3.4	36.3	123.4	110.9	-12.5	-12.5	62.0	-13.0	123.9	-0.5	0.0	16.2	18.7	34.9	96.9
Sep-84	12.3	3.9		2.0	31.2	62.4	42.7	-19.7	-32.2	48.0	-14.0	56.7	5.7	0.0	8.1	9.3	17.4	65.4
Oct-84	7.6	1.9		1.2	28.2	33.8	39.2	5.4		53.4	5.4	33.8	0.0	0.0	4.0	4.7	8.7	62.1
Nov-84	2.5	0.4		0.4	23.7	9.5	41.2	31.7		75.0	21.6	9.5	0.0	21.6	12.8	2.3	15.2	90.2
Dec-84	-5.4	0.0	32.4	0.0	22.5	0.0	103.9	103.9		178.9	0.0	0.0	0.0	0.0	6.4	0.0	6.4	187.7

Table A.1l Results of the PE and water balance calculations (Thornthwaite and Mather).

	Line 1		Line 2	Line 3		Line 4	Line 5	Line 6	Line 7	Line 8	Line 9	Line 10	Line 11	Line 12	Line 13	Line 14	Line 15	Line 16
	Mean			Un-Adj	Corr.	Adj-			Acc Pot		Change						Tot	
Date	Temp			PE	45 deg.	PE	P	P- PE	WL	ST	in ST	AE	D	S	RO	SMRO	RO	DT
M / Y	(°C)	(i)	(I)	(mm)	Lat. N	(mm)	(mm)	(mm)	(mm)	(mm)	(mm)	(mm)	(mm)	(mm)	(mm)	(mm)	(mm)	(mm)
Jan-85	-12.3	0.0		0.0	24.0	0.0	22.0	22.0		173.4	0.0	0.0	0.0	0.0	4.7	0.0	4.7	178.1
Feb-85	-6.5	0.0		0.0	24.3	0.0	69.7	69.7		243.1	0.0	0.0	0.0	0.0	2.3	0.0	2.3	245.4
Mar-85	-2.8	0.0		0.0	30.6	0.0	56.9	56.9		300.0	0.0	0.0	0.0	0.0	1.2	0.0	1.2	301.2
Apr-85	3.8	0.7		0.6	33.9	20.3	33.3	13.0		75.0	0.0	20.3	0.0	13.0	6.5	19.8	26.3	260.8
May-85	10.3	3.0		1.8	38.4	69.1	134.8	65.7		75.0	0.0	69.1	0.0	65.7	36.1	89.1	125.2	200.2
Jun-85	15.3	5.4		2.6	38.7	100.6	181.2	80.6		75.0	0.0	100.6	0.0	80.6	58.3	44.6	102.9	177.9
Jul-85	19.3	7.7		3.3	39.3	129.7	54.5	-75.2	-75.2	27.0	-48.0	102.5	27.2	0.0	29.2	22.3	51.4	78.4
Aug-85	17.4	6.6		3.0	36.3	108.9	73.3	-35.6	-110.8	19.0	-8.0	81.3	27.6	0.0	14.6	11.1	25.7	44.7
Sep-85	13.9	4.7		2.4	31.2	74.9	52.0	-22.9	-133.7	12.0	-7.0	59.0	15.9	0.0	7.3	5.6	12.9	24.9
Oct-85	7.4	1.8		1.3	28.2	36.7	65.9	29.2		41.2	29.2	36.7	0.0	0.0	3.6	2.8	6.4	47.7
Nov-85	0.2	0.0		0.0	23.7	0.0	129.1	129.1		75.0	33.8	0.0	0.0	33.8	18.7	1.4	20.1	95.1
Dec-85	-10.0	0.0	30.0	0.0	22.5	0.0	76.4	76.4		151.4	0.0	0.0	0.0	0.0	9.4	0.0	9.4	162.1
Jan-86	-8.2	0.0		0.0	24.0	0.0	123.4	123.4		373.5	0.0	0.0	0.0	0.0	0.5	0.0	0.5	374.0
Feb-86	-8.7	0.0		0.0	24.3	0.0	36.4	36.4		409.9	0.0	0.0	0.0	0.0	0.2	0.0	0.2	410.1
Mar-86	-3.5	0.0		0.0	30.6	0.0	143.7	143.7		553.6	0.0	0.0	0.0	0.0	0.1	0.0	0.1	553.7
Apr-86	5.6	1.2		1.1	33.9	37.3	111.3	74.0		75.0	0.0	37.3	0.0	74.0	37.0	26.0	63.0	346.1
May-86	10.7	3.2		2.0	38.4	76.8	71.5	-5.3	-5.3	70.0	-5.0	76.5	0.3	0.0	18.5	117.0	135.5	205.5
Jun-86	14.4	5.0		2.5	38.7	96.8	50.8	-46.0	-51.3	37.0	-33.0	83.8	13.0	0.0	9.3	58.5	67.8	104.8
Jul-86	17.5	6.7		3.0	39.3	117.9	83.3	-34.6	-85.9	23.0	-14.0	97.3	20.6	0.0	4.6	29.3	33.9	56.9
Aug-86	16.8	6.3		2.9	36.3	105.3	143.9	38.6		61.6	38.6	105.3	0.0	0.0	2.3	14.6	16.9	78.6
Sep-86	11.0	3.3		2.0	31.2	62.4	83.3	20.9		75.0	13.4	62.4	0.0	13.4	7.8	7.3	15.2	90.2
Oct-86	5.9	1.3		1.2	28.2	33.8	30.1	-3.7	-3.7	71.0	-4.0	34.1	-0.3	0.0	3.9	3.7	7.6	78.6
Nov-86	-1.5	0.0		0.0	23.7	0.0	116.4	116.4		187.4	0.0	0.0	0.0	0.0	2.0	0.0	2.0	193.0
Dec-86	-6.8	0.0	26.8	0.0	22.5	0.0	62.7	62.7		250.1	0.0	0.0	0.0	0.0	1.0	0.0	1.0	254.7
Jan-87	-10.4	0.0		0.0	24.0	0.0	127.3	127.3		328.4	0.0	0.0	0.0	0.0	12.5	0.0	12.5	340.9
Feb-87	-8.5	0.0		0.0	24.3	0.0	42.4	42.4		370.8	0.0	0.0	0.0	0.0	6.3	0.0	6.3	377.1
Mar-87	-2.3	0.0		0.0	30.6	0.0	92.9	92.9		463.7	0.0	0.0	0.0	0.0	3.1	0.0	3.1	466.8
Apr-87	6.5	1.5		1.1	33.9	37.3	52.1	14.8		75.0	0.0	37.3	0.0	14.8	7.4	37.2	44.6	420.3
May-87	11.3	3.4		1.9	38.4	73.0	70.8	-2.2	-2.2	73.0	-2.0	72.8	0.2	0.0	3.7	167.4	171.1	244.1
Jun-87	15.9	5.8		2.8	38.7	108.4	95.8	-12.6	-14.7	60.0	-13.0	108.8	-0.4	0.0	1.9	83.7	85.6	145.6
Jul-87	18.7	7.4		3.2	39.3	125.8	28.1	-97.7	-112.4	16.0	-44.0	72.1	53.7	0.0	0.9	41.9	42.8	58.8
Aug-87	17.2	6.5		2.9	36.3	105.3	46.8	-58.5	-170.9	7.0	-9.0	55.8	49.5	0.0	0.5	20.9	21.4	28.4
Sep-87	13.4	4.5		2.3	31.2	71.8	161.3	89.5		75.0	68.0	71.8	0.0	68.0	34.2	10.5	44.7	119.7
Oct-87	7.4	1.8		1.3	28.2	36.7	69.9	33.2		75.0	0.0	36.7	0.0	33.2	33.7	5.2	39.0	114.0
Nov-87	0.2	0.0		0.0	23.7	0.0	66.4	66.4		75.0	0.0	0.0	0.0	66.4	50.1	2.6	52.7	127.7
Dec-87	-6.1	0.0	30.8	0.0	22.5	0.0	126.1	126.1		201.1	0.0	0.0	0.0	0.0	25.0	0.0	25.0	228.7
Jan-88	-9.6	0.0		0.0	24.0	0.0	92.1	92.1		205.0	0.0	0.0	0.0	0.0	18.5	0.0	18.5	223.5
Feb-88	-8.6	0.0		0.0	24.3	0.0	118.1	118.1		323.1	0.0	0.0	0.0	0.0	9.3	0.0	9.3	332.4
Mar-88	-2.6	0.0		0.0	30.6	0.0	36.4	36.4		359.5	0.0	0.0	0.0	0.0	4.6	0.0	4.6	364.1
Apr-88	4.2	0.8		0.7	33.9	23.7	76.3	52.6		75.0	0.0	23.7	0.0	52.6	26.3	22.8	49.1	311.1
May-88	11.8	3.7		1.9	38.4	73.0	98.2	25.2		75.0	0.0	73.0	0.0	25.2	25.8	102.6	128.4	203.4
Jun-88	15.1	5.3		2.6	38.7	100.6	48.8	-51.8	-51.8	38.0	-39.0	67.8	12.8	0.0	12.9	51.3	64.2	100.2
Jul-88	20.2	8.3		3.5	39.3	137.6	60.0	-77.6	-129.4	13.0	-23.0	83.0	54.6	0.0	6.4	25.7	32.1	45.1
Aug-88	19.3	7.7		3.3	36.3	119.8	128.2	8.4		21.4	8.4	119.8	0.0	0.0	3.2	12.8	16.0	37.5
Sep-88	12.2	3.9		2.1	31.2	65.5	75.9	10.4		31.8	10.4	65.5	0.0	0.0	1.6	6.4	8.0	39.8
Oct-88	5.9	1.3		1.1	28.2	31.0	99.1	68.1		75.0	43.2	31.0	0.0	43.2	22.4	3.2	25.6	100.6
Nov-88	2.8	0.4		0.5	23.7	11.9	137.7	125.9		75.0	0.0	11.9	0.0	125.9	74.1	1.6	75.7	150.7
Dec-88	-7.6	0.0	31.4	0.0	22.5	0.0	37.9	37.9		112.9	0.0	0.0	0.0	0.0	37.1	0.0	37.1	151.6

Table A.1J Results of the PE and water balance calculations (Thornthwaite and Mather).

	Line 1		Line 2	Line 3		Line 4	Line 5	Line 6	Line 7	Line 8	Line 9	Line 10	Line 11	Line 12	Line 13	Line 14	Line 15	Line 16
	Mean			Un-Adj	Corr.	Adj-			Acc Pot		Change						Tot	
Date	Temp			PE	45 deg.	PE	P	P- PE	WL	ST	in ST	AE	D	S	RO	SMRO	RO	DT
M / Y	(°C)	(i)	(I)	(mm)	Lat. N	(mm)	(mm)	(mm)	(mm)	(mm)	(mm)	(mm)	(mm)	(mm)	(mm)	(mm)	(mm)	(mm)
Jan-89	-8.4	0.0		0.0	24.0	0.0	69.1	69.1		361.2	0.0	0.0	0.0	0.0	2.6	0.0	2.6	363.8
Feb-89	-9.4	0.0		0.0	24.3	0.0	73.7	73.7		434.9	0.0	0.0	0.0	0.0	1.3	0.0	1.3	436.2
Mar-89	-4.9	0.0		0.0	30.6	0.0	73.8	73.8		508.7	0.0	0.0	0.0	0.0	0.7	0.0	0.7	509.4
Apr-89	3.2	0.5		0.6	33.9	20.3	114.1	93.8		75.0	0.0	20.3	0.0	93.8	46.9	35.1	82.0	438.4
May-89	13.5	4.5		2.3	38.4	88.3	116.0	27.7		75.0	0.0	88.3	0.0	27.7	37.3	158.0	195.2	270.2
Jun-89	16.3	6.0		2.8	38.7	108.4	60.8	-47.6	-47.6	38.0	-37.0	97.8	10.6	0.0	18.6	79.0	97.6	135.6
Jul-89	18.3	7.1		3.1	39.3	121.8	78.8	-43.0	-90.6	21.0	-17.0	95.8	26.0	0.0	9.3	39.5	48.8	69.8
Aug-89	17.8	6.8		3.0	36.3	108.9	233.4	124.5		75.0	54.0	108.9	0.0	54.0	31.7	19.7	51.4	126.4
Sep-89	12.9	4.2		2.3	31.2	71.8	82.8	11.0		75.0	0.0	71.8	0.0	11.0	21.4	9.9	31.2	106.2
Oct-89	7.4	1.8		1.3	28.2	36.7	57.7	21.0		75.0	0.0	36.7	0.0	21.0	21.2	4.9	26.1	101.1
Nov-89	-0.5	0.0		0.0	23.7	0.0	139.1	139.1		214.1	0.0	0.0	0.0	0.0	10.6	0.0	10.6	229.6
Dec-89	-14.4	0.0	31.0	0.0	22.5	0.0	78.0	78.0		292.1	0.0	0.0	0.0	0.0	5.3	0.0	5.3	302.3
Jan-90	-5.6	0.0		0.0	24.0	0.0		0.0		267.8	0.0	0.0	0.0	0.0	16.5	0.0	16.5	284.3
Feb-90	-9.3	0.0		0.0	24.3	0.0	84.5	84.5		352.3	0.0	0.0	0.0	0.0	8.3	0.0	8.3	360.6
Mar-90	-2.6	0.0		0.0	30.6	0.0	59.2	59.2		411.5	0.0	0.0	0.0	0.0	4.1	0.0	4.1	415.6
Apr-90	5.0	1.0		0.8	33.9	27.1	101.4	74.3		75.0	0.0	27.1	0.0	74.3	37.1	13.9	51.0	241.4
May-90	9.4	2.6		1.6	38.4	61.4	187.6	126.2		75.0	0.0	61.4	0.0	126.2	81.7	62.6	144.2	219.2
Jun-90	16.9	6.3		2.9	38.7	112.2	51.4	-60.8	-60.8	33.0	-42.0	93.4	18.8	0.0	40.8	31.3	72.1	105.1
Jul-90	19.7	8.0		3.3	39.3	129.7	89.2	-40.5	-101.3	19.0	-14.0	103.2	26.5	0.0	20.4	15.6	36.1	55.1
Aug-90	20.0	8.2		3.4	36.3	123.4	99.4	-24.0	-125.3	13.0	-6.0	105.4	18.0	0.0	10.2	7.8	18.0	31.0
Sep-90	12.9	4.2		2.2	31.2	68.6	83.0	14.4		27.4	14.4	68.6	0.0	0.0	5.1	3.9	9.0	36.4
Oct-90	8.7	2.3		1.5	28.2	42.3	125.3	83.0		75.0	47.6	42.3	0.0	47.6	26.4	2.0	28.3	103.3
Nov-90	1.7	0.2		0.3	23.7	7.1	113.1	106.0		75.0	0.0	7.1	0.0	106.0	66.2	1.0	67.2	142.2
Dec-90	-2.9	0.0	32.8	0.0	22.5	0.0	192.8	192.8		267.8	0.0	0.0	0.0	0.0	33.1	0.0	33.1	301.9
Jan-91	-11.6	0.0		0.0	24.0	0.0	98.6	98.6		246.5	0.0	0.0	0.0	0.0	16.2	0.0	16.2	262.7
Feb-91	-7.3	0.0		0.0	24.3	0.0	27.5	27.5		274.0	0.0	0.0	0.0	0.0	8.1	0.0	8.1	282.1
Mar-91	-1.3	0.0		0.0	30.6	0.0	126.3	126.3		400.3	0.0	0.0	0.0	0.0	4.0	0.0	4.0	404.3
Apr-91	4.5	0.9		0.7	33.9	23.7	86.6	62.9		75.0	0.0	23.7	0.0	62.9	31.4	26.2	57.6	346.3
May-91	12.2	3.9		2.0	38.4	76.8	88.9	12.1		75.0	0.0	76.8	0.0	12.1	21.8	117.9	139.7	214.7
Jun-91	16.5	6.1		2.8	38.7	108.4	67.2	-41.2	-41.2	43.0	-32.0	99.2	9.2	0.0	10.9	59.0	69.8	112.8
Jul-91	19.2	7.7		3.2	39.3	125.8	59.5	-66.3	-107.4	17.0	-26.0	85.5	40.3	0.0	5.4	29.5	34.9	51.9
Aug-91	19.1	7.6		3.2	36.3	116.2	181.4	65.2		75.0	58.0	116.2	0.0	58.0	31.7	14.7	46.5	121.5
Sep-91	12.3	3.9		2.0	31.2	62.4	143.4	81.0		75.0	0.0	62.4	0.0	81.0	56.4	7.4	63.7	138.7
Oct-91	8.5	2.2		1.4	28.2	39.5	108.6	69.1		75.0	0.0	39.5	0.0	69.1	62.7	3.7	66.4	141.4
Nov-91	2.5	0.4		0.4	23.7	9.5	76.1	66.6		75.0	0.0	9.5	0.0	66.6	64.7	1.8	66.5	141.5
Dec-91	-8.3	0.0	32.6	0.0	22.5	0.0	72.9	72.9		147.9	0.0	0.0	0.0	0.0	32.3	0.0	32.3	182.1
Jan-92	-9.7	0.0		0.0	24.0	0.0	94.5	94.5		322.9	0.0	0.0	0.0	0.0	12.0	0.0	12.0	334.9
Feb-92	-9.5	0.0		0.0	24.3	0.0	104.9	104.9		427.8	0.0	0.0	0.0	0.0	6.0	0.0	6.0	433.8
Mar-92	-4.7	0.0		0.0	30.6	0.0	67.4	67.4		495.2	0.0	0.0	0.0	0.0	3.0	0.0	3.0	498.2
Apr-92	3.4	0.6		0.6	33.9	20.3	25.8	5.5		75.0	0.0	20.3	0.0	5.5	2.7	21.1	23.8	270.6
May-92	11.0	3.3		1.9	38.4	73.0	32.2	-40.8	-40.8	43.0	-32.0	64.2	8.8	0.0	1.4	95.0	96.3	139.3
Jun-92	15.8	5.7		2.7	38.7	104.5	119.8	15.3		58.3	15.3	104.5	0.0	0.0	0.7	47.5	48.2	106.5
Jul-92	16.7	6.2		2.9	39.3	114.0	125.7	11.7		70.0	11.7	114.0	0.0	0.0	0.3	23.7	24.1	94.1
Aug-92	18.3	7.1		3.1	36.3	112.5	88.0	-24.5	-24.5	53.0	-17.0	105.0	7.5	0.0	0.2	11.9	12.0	65.0
Sep-92	14.0	4.8		2.4	31.2	74.9	20.4	-54.5	-79.0	25.0	-28.0	48.4	26.5	0.0	0.1	5.9	6.0	31.0
Oct-92	6.5	1.5		1.1	28.2	31.0	162.6	131.6		75.0	50.0	31.0	0.0	50.0	25.0	3.0	28.0	103.0
Nov-92	-0.4	0.0		0.0	23.7	0.0	71.0	71.0		146.0	0.0	0.0	0.0	71.0	48.0	0.0	48.0	197.0
Dec-92	-5.1	0.0	29.2	0.0	22.5	0.0	82.4	82.4		228.4	0.0	0.0	0.0	0.0	24.0	0.0	24.0	255.4

Table A.1K Results of the PE and water balance calculations (Thornthwaite and Mather).

	Line 1		Line 2	Line 3		Line 4	Line 5	Line 6	Line 7	Line 8	Line 9	Line 10	Line 11	Line 12	Line 13	Line 14	Line 15	Line 16
	Mean			Un-Adj	Corr.	Adj-			Acc Pot		Change						Tot	
Date	Temp			PE	45 deg.	PE	P	P- PE	WL	ST	in ST	AE	D	S	RO	SMRO	RO	DT
M / Y	(°C)	(i)	(I)	(mm)	Lat. N	(mm)	(mm)	(mm)	(mm)	(mm)	(mm)	(mm)	(mm)	(mm)	(mm)	(mm)	(mm)	(mm)
Jan-93	-9.7	0.0		0.0	24.0	0.0	61.0	61.0		279.1	0.0	0.0	0.0	0.0	15.9	0.0	15.9	295.0
Feb-93	-12.9	0.0		0.0	24.3	0.0	74.4	74.4		353.5	0.0	0.0	0.0	0.0	7.9	0.0	7.9	361.4
Mar-93	-3.9	0.0		0.0	30.6	0.0	78.1	78.1		431.6	0.0	0.0	0.0	0.0	4.0	0.0	4.0	435.6
Apr-93	4.8	0.9		0.8	33.9	27.1	106.2	79.1		75.0	0.0	27.1	0.0	79.1	39.5	21.2	60.7	309.3
May-93	10.8	3.2		1.9	38.4	73.0	103.2	30.2		75.0	0.0	73.0	0.0	30.2	34.9	95.4	130.3	205.3
Jun-93	15.7	5.7		2.7	38.7	104.5	123.7	19.2		75.0	0.0	104.5	0.0	19.2	27.1	47.7	74.8	149.8
Jul-93	18.8	7.4		3.2	39.3	125.8	61.6	-64.2	-64.2	31.0	-44.0	105.6	20.2	0.0	13.5	23.9	37.4	68.4
Aug-93	19.1	7.6		3.2	36.3	116.2	34.2	-82.0	-146.1	10.0	-21.0	55.2	61.0	0.0	6.8	11.9	18.7	28.7
Sep-93	13.7	4.6		2.4	31.2	74.9	93.0	18.1		28.1	18.1	74.9	0.0	0.0	3.4	6.0	9.3	37.5
Oct-93	5.3	1.1		0.9	28.2	25.4	158.8	133.4		75.0	46.9	25.4	0.0	46.9	25.1	3.0	28.1	103.1
Nov-93	0.8	0.1		0.1	23.7	2.4	104.2	101.8		75.0	0.0	2.4	0.0	101.8	63.5	1.5	65.0	140.0
Dec-93	-4.3	0.0	30.6	0.0	22.5	0.0	143.1	143.1		218.1	0.0	0.0	0.0	0.0	31.7	0.0	31.7	251.3
Jan-94	-14.7	0.0		0.0	24.0	0.0	128.7	128.7		279.1	0.0	0.0	0.0	0.0	4.3	0.0	4.3	283.4
Feb-94	-10.5	0.0		0.0	24.3	0.0	40.5	40.5		319.6	0.0	0.0	0.0	0.0	2.1	0.0	2.1	321.7
Mar-94	-2.1	0.0		0.0	30.6	0.0	167.0	167.0		486.6	0.0	0.0	0.0	0.0	1.1	0.0	1.1	487.7
Apr-94	4.6	0.9		0.7	33.9	23.7	113.7	90.0		75.0	0.0	23.7	0.0	90.0	45.0	25.0	70.0	346.1
May-94	9.6	2.7		1.6	38.4	61.4	149.1	87.7		75.0	0.0	61.4	0.0	87.7	66.3	112.5	178.8	253.8
Jun-94	17.3	6.6		2.9	38.7	112.2	96.5	-15.7	-15.7	60.0	-15.0	111.5	0.7	0.0	33.2	56.3	89.4	149.4
Jul-94	20.9	8.7		3.6	39.3	141.5	45.8	-95.7	-111.4	16.0	-44.0	89.8	51.7	0.0	16.6	28.1	44.7	60.7
Aug-94	18.3	7.1		3.1	36.3	112.5	41.8	-70.7	-182.1	6.0	-10.0	51.8	60.7	0.0	8.3	14.1	22.4	28.4
Sep-94	13.0	4.3		2.3	31.2	71.8	63.4	-8.4	-190.5	6.0	0.0	63.4	8.4	0.0	4.1	7.0	11.2	17.2
Oct-94	8.0	2.0		1.4	26.2	39.5	76.2	36.7		42.7	36.7	39.5	0.0	0.0	2.1	3.5	5.6	48.3
Nov-94	2.6	0.4		0.4	23.7	9.5	118.8	109.3		75.0	32.3	9.5	0.0	32.3	17.2	1.8	18.9	93.9
Dec-94	-4.9	0.0	32.6	0.0	22.5	0.0	75.4	75.4		150.4	0.0	0.0	0.0	0.0	8.6	0.0	8.6	160.7
Jan-95	-7.2	0.0		0.0	24.0	0.0	169.2	169.2		300.9	0.0	0.0	0.0	0.0	21.0	0.0	21.0	321.9
Feb-95	-10.9	0.0		0.0	24.3	0.0	84.0	84.0		384.9	0.0	0.0	0.0	0.0	10.5	0.0	10.5	395.4
Mar-95	-2.1	0.0		0.0	30.6	0.0	81.9	81.9		466.8	0.0	0.0	0.0	0.0	5.3	0.0	5.3	472.1
Apr-95	2.9	0.4		0.5	33.9	17.0	73.2	56.3		75.0	0.0	17.0	0.0	56.3	28.1	29.4	57.5	373.0
May-95	10.2	2.9		1.7	38.4	65.3	94.4	29.1		75.0	0.0	65.3	0.0	29.1	28.6	132.3	160.9	235.9
Jun-95	17.3	6.6		2.9	38.7	112.2	41.6	-70.6	-70.6	28.0	-47.0	88.6	23.6	0.0	14.3	66.2	80.5	108.5
Jul-95	20.6	8.5		3.5	39.3	137.6	94.2	-43.4	-114.0	15.0	-13.0	107.2	30.4	0.0	7.2	33.1	40.2	55.2
Aug-95	18.6	7.3		3.1	36.3	112.5	64.6	-47.9	-161.9	8.0	-7.0	71.6	40.9	0.0	3.6	16.5	20.1	28.1
Sep-95	11.3	3.4		1.9	31.2	59.3	64.9	5.6		13.6	5.6	59.3	0.0	0.0	1.8	8.3	10.1	23.7
Oct-95	9.8	2.8		1.6	28.2	45.1	153.4	108.3		75.0	61.4	45.1	0.0	61.4	31.6	4.1	35.7	110.7
Nov-95	0.4	0.0		0.1	23.7	2.4	139.1	136.7		75.0	0.0	2.4	0.0	136.7	84.2	2.1	86.2	161.2
Dec-95	-7.8	0.0	32.0	0.0	22.5	0.0	56.7	56.7		131.7	0.0	0.0	0.0	0.0	42.1	0.0	42.1	175.8
Jan-96	-8.8	0.0		0.0	24.0	0.0	91.5	91.5		299.0	0.0	0.0	0.0	0.0	14.3	0.0	14.3	313.3
Feb-96	-7.3	0.0		0.0	24.3	0.0	78.5	78.5		377.5	0.0	0.0	0.0	0.0	7.1	0.0	7.1	384.6
Mar-96	-3.2	0.0		0.0	30.6	0.0	60.0	60.0		437.5	0.0	0.0	0.0	0.0	3.6	0.0	3.6	441.1
Apr-96	4.4	0.8		0.8	33.9	27.1	72.7	45.6		75.0	0.0	27.1	0.0	45.6	22.8	20.6	43.4	286.8
May-96	9.7	2.7		1.7	38.4	65.3	98.9	33.6		75.0	0.0	65.3	0.0	33.6	28.2	92.7	120.9	195.9
Jun-96	16.4	6.0		2.8	38.7	108.4	62.3	-46.1	-46.1	39.0	-36.0	98.3	10.1	0.0	14.1	46.4	60.5	99.5
Jul-96	18.3	7.1		3.1	39.3	121.8	161.2	39.4		75.0	36.0	121.8	0.0	36.0	25.1	23.2	48.2	123.2
Aug-96	18.6	7.3		3.2	36.3	116.2	21.5	-94.7	-94.7	20.0	-55.0	76.5	39.7	0.0	12.5	11.6	24.1	44.1
Sep-96	13.7	4.6		2.4	31.2	74.9	89.3	14.4		34.4	14.4	74.9	0.0	0.0	6.3	5.8	12.1	46.5
Oct-96	6.6	1.5		1.1	28.2	31.0	76.8	45.8		75.0	40.6	31.0	0.0	40.6	23.4	2.9	26.3	101.3
Nov-96	0.1	0.0		0.0	23.7	0.0	90.6	90.6		75.0	0.0	0.0	0.0	90.6	57.0	1.4	58.5	133.5
Dec-96	-1.2	0.0	30.2	0.0	22.5	0.0	132.5	132.5		207.5	0.0	0.0	0.0	0.0	28.5	0.0	28.5	237.5

Table A.1L Results of the PE and water balance calculations (Thornthwaite and Mather).

	Line 1		Line 2	Line 3		Line 4	Line 5	Line 6	Line 7	Line 8	Line 9	Line 10	Line 11	Line 12	Line 13	Line 14	Line 15	Line 16
	Mean			Un-Adj	Corr.	Adj-			Acc Pot		Change						Tot	
Date	Temp			PE	45 deg.	PE	P	P- PE	WL	ST	in ST	AE	D	S	RO	SMRO	RO	DT
M / Y	(°C)	(i)	(I)	(mm)	Lat. N	(mm)	(mm)	(mm)	(mm)	(mm)	(mm)	(mm)	(mm)	(mm)	(mm)	(mm)	(mm)	(mm)
Jan-97	-9.3	0.0		0.0	24.0	0.0	84.7	84.7		307.4	0.0	0.0	0.0	0.0	9.4	0.0	9.4	316.8
Feb-97	-8.9	0.0		0.0	24.3	0.0	59.8	59.8		367.2	0.0	0.0	0.0	0.0	4.7	0.0	4.7	371.9
Mar-97	-5.3	0.0		0.0	30.6	0.0	97.0	97.0		464.2	0.0	0.0	0.0	0.0	2.4	0.0	2.4	466.6
Apr-97	2.9	0.4		0.5	33.9	17.0	42.1	25.2		75.0	0.0	17.0	0.0	25.2	12.6	34.8	47.4	403.1
May-97	9.6	2.7		1.6	38.4	61.4	111.8	50.4		75.0	0.0	61.4	0.0	50.4	31.5	156.6	188.1	263.1
Jun-97	15.8	5.7		2.7	38.7	104.5	83.3	-21.2	-21.2	56.0	-19.0	102.3	2.2	0.0	15.7	78.3	94.0	150.0
Jul-97	19.4	7.8		3.3	39.3	129.7	75.2	-54.5	-75.7	26.0	-30.0	105.2	24.5	0.0	7.9	39.2	47.0	73.0
Aug-97	17.5	6.7		3.0	36.3	108.9	34.7	-74.2	-149.9	10.0	-16.0	50.7	58.2	0.0	3.9	19.6	23.5	33.5
Sep-97	13.6	4.6		2.3	31.2	71.8	77.5	5.7		15.7	5.7	71.8	0.0	0.0	2.0	9.8	11.8	27.5
Oct-97	6.2	1.4		1.1	28.2	31.0	21.0	-10.0	-10.0	65.0	49.3	-28.3	59.3	0.0	1.0	4.9	5.9	70.9
Nov-97	-0.3	0.0		0.0	23.7	0.0	74.3	74.3		139.3	74.3	0.0	0.0	74.3	37.6	0.0	37.6	181.8
Dec-97	-7.1	0.0	29.2	0.0	22.5	0.0	83.4	83.4		222.7	0.0	0.0	0.0	0.0	18.8	0.0	18.8	246.4
Jan-98	-7.3	0.0		0.0	24.0	0.0	148.8	148.8		274.6	0.0	0.0	0.0	0.0	8.5	0.0	8.5	283.1
Feb-98	-4.9	0.0		0.0	24.3	0.0	90.7	90.7		365.3	0.0	0.0	0.0	0.0	4.2	0.0	4.2	369.5
Mar-98	-1.2	0.0		0.0	30.6	0.0	114.6	114.6		479.9	0.0	0.0	0.0	0.0	2.1	0.0	2.1	482.0
Apr-98	5.9	1.3		1.0	33.9	33.9	87.8	53.9		75.0	0.0	33.9	0.0	53.9	27.0	21.9	48.9	301.2
May-98	13.5	4.5		2.3	38.4	88.3	74.5	-13.8	-13.8	61.0	-14.0	88.5	-0.2	0.0	13.5	98.6	112.0	173.0
Jun-98	15.6	5.6		2.6	38.7	100.6	64.9	-35.7	-49.5	38.0	-23.0	87.9	12.7	0.0	6.7	49.3	56.0	94.0
Jul-98	19.6	7.9		3.3	39.3	129.7	74.2	-55.5	-105.0	18.0	-20.0	94.2	35.5	0.0	3.4	24.6	28.0	46.0
Aug-98	18.6	7.3		3.1	36.3	112.5	59.2	-53.3	-158.4	9.0	-9.0	68.2	44.3	0.0	1.7	12.3	14.0	23.0
Sep-98	13.9	4.7		2.3	31.2	71.8	103.2	31.4		40.4	31.4	71.8	0.0	0.0	0.8	6.2	7.0	47.4
Oct-98	7.2	1.7		1.2	28.2	33.8	113.2	79.4		75.0	34.6	33.8	0.0	34.6	17.7	3.1	20.8	95.8
Nov-98	0.9	0.1		0.2	23.7	4.7	55.0	50.3		75.0	0.0	4.7	0.0	50.3	34.0	1.5	35.5	110.5
Dec-98	-3.7	0.0	33.1	0.0	22.5	0.0	50.8	50.8		125.8	0.0	0.0	0.0	0.0	17.0	0.0	17.0	144.3
Jan-99	-9.2	0.0		0.0	24.0	0.0	122.2	122.2		312.1	0.0	0.0	0.0	0.0	17.5	0.0	17.5	329.6
Feb-99	-4.1	0.0		0.0	24.3	0.0	55.8	55.8		367.9	0.0	0.0	0.0	0.0	8.7	0.0	8.7	376.6
Mar-99	0.4	0.0		0.1	30.6	3.1	125.0	121.9		75.0	0.0	3.1	0.0	121.9	61.0	22.5	83.5	347.2
Apr-99	5.3	1.1		0.8	33.9	27.1	30.7	3.6		75.0	0.0	27.1	0.0	3.6	32.3	101.3	133.5	208.5
May-99	14.2	4.9		2.3	38.4	88.3	36.1	-52.2	-52.2	36.0	-39.0	75.1	13.2	0.0	16.1	50.6	66.8	102.8
Jun-99	18.5	7.3		3.1	38.7	120.0	26.4	-93.6	-145.8	10.0	-26.0	52.4	67.6	0.0	8.1	25.3	33.4	43.4
Jul-99	20.2	8.3		3.4	39.3	133.6	98.2	-35.4	-181.2	6.0	-4.0	102.2	31.4	0.0	4.0	12.7	16.7	22.7
Aug-99	18.4	7.2		3.1	36.3	112.5	45.6	-66.9	-248.1	3.0	-3.0	48.6	63.9	0.0	2.0	6.3	8.3	11.3
Sep-99	17.2	6.5		2.8	31.2	87.4	271.2	183.8		75.0	72.0	87.4	0.0	72.0	37.0	3.2	40.2	115.2
Oct-99	6.3	1.4		0.9	28.2	25.4	61.9	36.5		75.0	0.0	25.4	0.0	36.5	36.8	1.6	38.3	113.3
Nov-99	3.3	0.5		0.5	23.7	11.9	115.0	103.2		75.0	0.0	11.9	0.0	103.2	70.0	0.8	70.7	145.7
Dec-99	-3.1	0.0	37.1	0.0	22.5	0.0	114.9	114.9		189.9	0.0	0.0	0.0	0.0	35.0	0.0	35.0	225.7
Jan-00	-8.6	0.0		0.0	24.0	0.0	173.1	173.1		364.4	0.0	0.0	0.0	0.0	1.3	0.0	1.3	365.7
Feb-00	-7.8	0.0		0.0	24.3	0.0	75.1	75.1		439.5	0.0	0.0	0.0	0.0	0.6	0.0	0.6	440.1
Mar-00	0.8	0.1		0.1	30.6	3.1	89.2	86.1		75.0	0.0	3.1	0.0	86.1	43.1	30.0	73.1	388.7
Apr-00	4.6	0.9		0.8	33.9	27.1	154.7	127.6		75.0	0.0	27.1	0.0	127.6	85.3	135.0	220.3	295.3
May-00	10.1	2.9		1.7	38.4	65.3	74.2	8.9		75.0	0.0	65.3	0.0	8.9	47.1	67.5	114.6	189.6
Jun-00	15.7	5.7		2.7	38.7	104.5	45.8	-58.7	-58.7	33.0	-42.0	87.8	16.7	0.0	23.6	33.8	57.3	90.3
Jul-00	18.3	7.1		3.1	39.3	121.8	98.1	-23.7	-82.4	24.0	-9.0	107.1	14.7	0.0	11.8	16.9	28.7	52.7
Aug-00	18.2	7.1		3.1	36.3	112.5	70.6	-41.9	-124.4	13.0	-11.0	81.6	30.9	0.0	5.9	8.4	14.3	27.3
Sep-00	12.7	4.1		2.2	31.2	68.6	67.8	-0.8	-125.2	13.0	0.0	67.8	0.8	0.0	2.9	4.2	7.2	20.2
Oct-00	7.2	1.7		1.3	28.2	36.7	89.8	53.1		66.1	53.1	36.7	0.0	0.0	1.5	2.1	3.6	69.7
Nov-00	2.7	0.4		0.5	23.7	11.9	67.3	55.5		75.0	8.9	11.9	0.0	8.9	5.2	1.1	6.2	81.2
Dec-00	-7.3	0.0	29.9	0.0	22.5	0.0	116.3	116.3		191.3	0.0	0.0	0.0	0.0	2.6	0.0	2.6	194.9

Table A.1M Results of the PE and water balance calculations (Thornthwaite and Mather).

	Line 1		Line 2	Line 3		Line 4	Line 5	Line 6	Line 7	Line 8	Line 9	Line 10	Line 11	Line 12	Line 13	Line 14	Line 15	Line 16
	Mean			Un-Adj	Corr.	Adj-			Acc Pot		Change						Tot	
Date	Temp			PE	45 deg.	PE	P	P- PE	WL	ST	in ST	AE	D	S	RO	SMRO	RO	DT
M / Y	(°C)	(i)	(I)	(mm)	Lat. N	(mm)	(mm)	(mm)	(mm)	(mm)	(mm)	(mm)	(mm)	(mm)	(mm)	(mm)	(mm)	(mm)
Jan-01	-10.3	0.0		0.0	24.0	0.0	44.8	44.8		150.9	0.0	0.0	0.0	0.0	0.1	0.0	0.1	150.9
Feb-01	-9.2	0.0		0.0	24.3	0.0	75.2	75.2		226.1	0.0	0.0	0.0	0.0	0.0	0.0	0.0	226.1
Mar-01	-3.2	0.0		0.0	30.6	0.0	69.4	69.4		295.5	0.0	0.0	0.0	0.0	0.0	0.0	0.0	295.5
Apr-01	3.3	0.5		0.5	33.9	17.0	40.0	23.1		75.0	0.0	17.0	0.0	23.1	11.5	28.8	40.3	345.7
May-01	12.4	4.0		2.0	38.4	76.8	96.9	20.1		75.0	0.0	76.8	0.0	20.1	15.8	129.6	145.4	220.4
Jun-01	18.2	7.1		3.1	38.7	120.0	81.5	-38.5	-38.5	44.0	-31.0	112.5	7.5	0.0	7.9	64.8	72.7	116.7
Jul-01	18.5	7.3		3.1	39.3	121.8	63.5	-58.3	-96.8	20.0	-24.0	87.5	34.3	0.0	4.0	32.4	36.4	56.4
Aug-01	20.0	8.2		3.4	36.3	123.4	22.9	-100.5	-197.3	5.0	-15.0	37.9	85.5	0.0	2.0	16.2	18.2	23.2
Sep-01	14.7	5.1		2.4	31.2	74.9	41.7	-33.2	-230.5	3.0	-2.0	43.7	31.2	0.0	1.0	8.1	9.1	12.1
Oct-01	8.7	2.3		1.4	28.2	39.5	47.2	7.7		10.7	7.7	39.5	0.0	0.0	0.5	4.1	4.5	15.3
Nov-01	3.4	0.6		0.5	23.7	11.9	66.9	55.1		65.8	55.1	11.9	0.0	0.0	0.2	2.0	2.3	68.0
Dec-01	-2.3	0.0	35.0	0.0	22.5	0.0	40.3	40.3		106.1	40.3	0.0	0.0	0.0	0.1	0.0	0.1	108.2

Table A.2 Yearly totals for results of the Thornthwaite and Mather (1957) method.

	Year Total Adj-PE (mm)	Year Total P- PE (mm)	Year Change ST (mm)	Year Total AE (mm)	Seasonal* low / high AE (mm)	Year Total Snow (mm)	Year Total SMRO (mm)	Year Total RO (mm)
1953	575	594	-20	546	51 / 495	142	141	334
1954	541	863	0	534	52 / 483	304	302	709
1955	558	261	16	456	35 / 421	279	277	319
1956	530	512	0	482	49 / 433	302	300	446
1957	561	304	0	389	39 / 350	205	204	344
1958	554	611	0	569	45 / 525	282	281	545
1959	573	652	0	578	44 / 534	196	195	471
1960	578	498	0	468	40 / 428	263	261	355
1961	574	568	0	498	54 / 443	333	331	639
1962	540	403	0	528	47 / 481	267	266	502
1963	552	691	0	523	59 / 463	329	327	628
1964	541	479	60	458	40 / 419	364	359	508
1965	535	255	0	455	31 / 424	235	232	297
1966	553	244	0	419	51 / 368	229	228	404
1967	539	642	0	447	41 / 406	468	465	778
1968	555	353	164	394	45 / 349	244	241	261
1969	552	534	0	522	41 / 482	254	252	483
1970	563	615	0	549	47 / 502	343	341	612
1971	553	488	0	503	42 / 460	348	346	452
1972	537	827	0	511	25 / 485	469	462	536
1973	573	639	92	527	34 / 493	230	228	538
1974	532	514	0	445	28 / 417	270	268	607
1975	558	570	0	467	41 / 427	379	376	634
1976	554	758	0	534	31 / 503	360	355	478
1977	551	711	0	511	49 / 462	330	329	554
1978	550	460	0	397	31 / 366	308	304	414
1979	585	935	0	513	54 / 459	188	187	651
1980	560	600	0	543	33 / 510	210	209	485
1981	554	919	0	526	38 / 488	249	247	678
1982	550	617	0	537	46 / 491	296	294	497
1983	579	613	0	449	44 / 405	181	180	571
1984	557	732	0	551	43 / 508	332	330	573
1985	540	409	0	470	37 / 433	198	197	388
1986	530	527	-4	497	34 / 463	260	256	344
1987	558	422	0	455	37 / 419	372	369	549
1988	563	446	0	496	43 / 453	228	226	469
1989	556	621	0	520	37 / 483	351	346	553
1990	572	615	0	509	49 / 459	139	138	488
1991	562	575	0	513	49 / 464	262	260	606
1992	530	465	0	487	31 / 456	211	208	331
1993	549	592	0	468	28 / 440	212	211	484
1994	572	545	0	451	49 / 402	250	248	457
1995	551	566	0	456	48 / 409	294	292	570
1996	545	491	0	495	31 / 464	206	205	447
1997	524	321	64	380	-28 / 408	348	343	491
1998	575	462	0	483	39 / 444	219	217	354
1999	609	494	0	433	40 / 393	225	224	553
2000	551	571	0	488	52 / 437	300	299	530
2001	585	105	31	427	51 / 375	288	286	329

Adj-PE = Adjusted potential evapotranspiration, P = Precipitation, PE = Potential Evapotranspiration

ST = Storage, AE = Actual Evapotranspiration, SMRO = Snow Melt Runoff, RO = Runoff

*low seasonal AE includes months Jan, Feb, Mar, Oct, Nov, Dec

*high seasonal AE includes months April, May, June, July, Aug, Sept

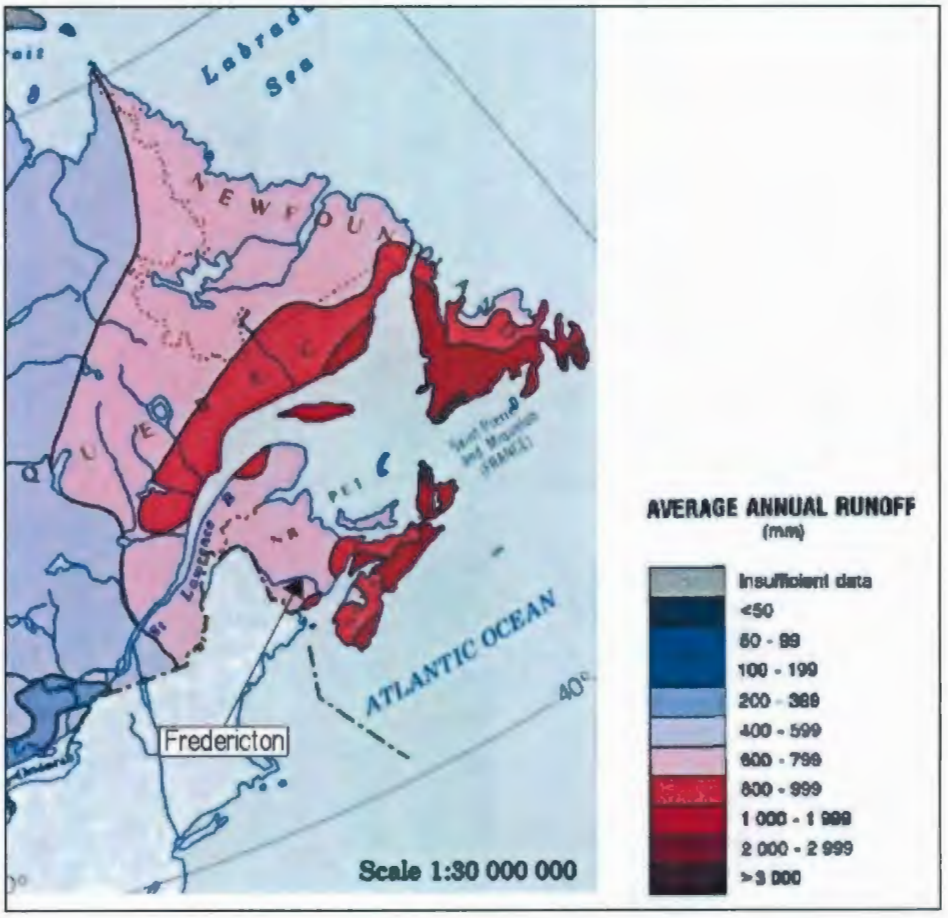

Figure A.4. Average annual runoff (total surface runoff) for New Brunswick between 600 – 799 mm / yr (The National Atlas of Canada, 1974).

A.4 Meyboom method example calculation using data from the Nashwaaksis Stream discharge (1997 – 1998).

$$Q_{tp} = Q_o \times t_1 / 2.3 \qquad \text{(Equation 2.1)}$$

Where Q_{tp} = total potential groundwater discharge
Q_o = baseflow at start of recession curve
T_1 = time for baseflow to drop from Q_o to $0.1Q_o$

and

$$Q_t = Q_{tp} / 10^{(t/t_1)} \qquad \text{(Equation 2.2)}$$

Where Q_t = potential baseflow remaining some time (t) after the start of the baseflow recession
t = time of interest

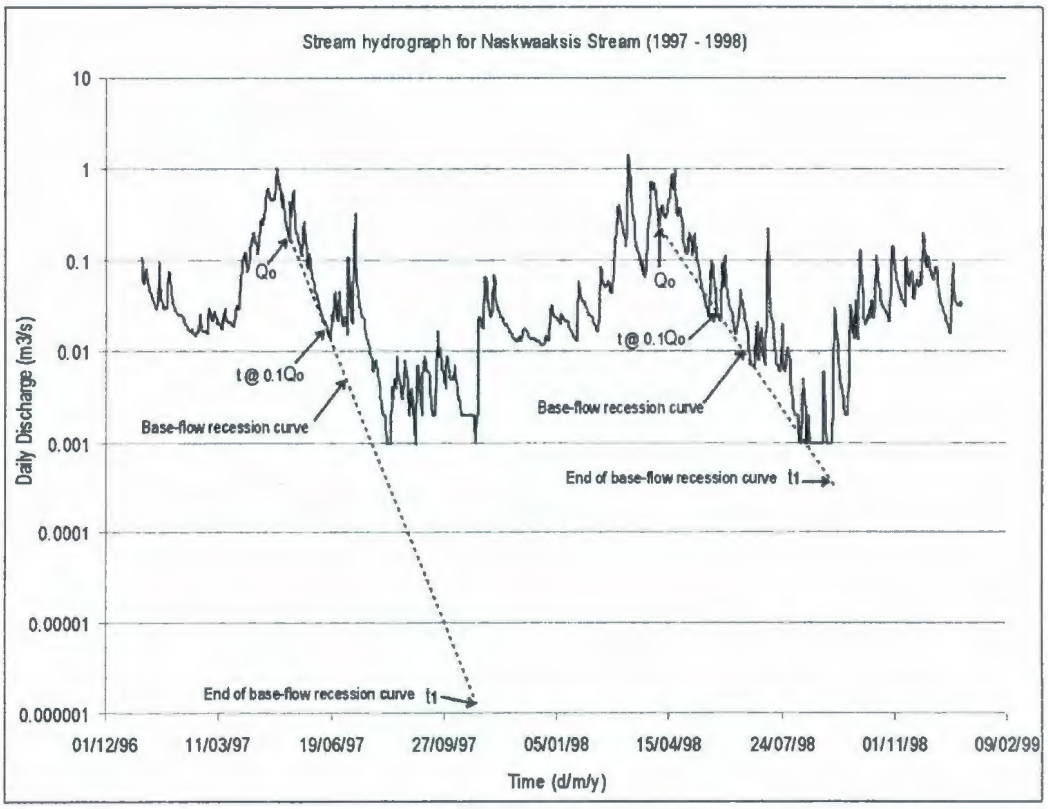

Figure A.5. Stream hydrograph for the Naskwaaksis Stream showing baseflow recession curves for years 1997 – 1998.

Table A.3 Data used for recharge and discharge analysis from hydrograph analysis of Nashwaaksis Stream.

Year	Date start for rec.curve	Qo (m^3/s)	Date@ 0.1Qo	t@0.1Qo (days)	Date@ t after start	t (days)
1978	Apr-24	0.45	May-25	31	Sep-06	135
1979	Apr-19	0.238	Jun-20	62	Jul-26	98
1980	Apr-07	0.151	Jun-07	61	Jun-25	155
1981	Apr-17	0.138	Jul-20	94	Aug-05	154
1982	Apr-11	0.11	May-30	49	Jul-12	101
1997	May-13	0.161	Jun-16	34	Oct-25	165
1998	Apr-07	0.238	May-30	53	Sep-07	153
1999	Apr-15	0.225	May-15	30	Sep-10	148
2000	Apr-21	0.139	Jun-18	58	Sep-23	155
2001	Apr-20	0.259	Jun-15	56	Sep-20	153
2002	Apr-08	0.214	Jun-21	74	Sep-03	148
2003	Apr-19	0.252	Jun-18	60	Oct-12	176
2004	Apr-13	0.187	Jun-06	54	Aug-12	121

Table A.4 Results of recharge and discharge analysis from hydrograph analysis of Nashwaaksis Stream.

	Total Potential Discharge (m^3)	Discharge at end of recession (m^3)	Recharge b/t recessions (m^3)	Groundwater Recharge (mm/yr)	Total stream annual Discharge (m^3/s)	Total stream annual Discharge (m^3/yr)
1978	524035	23	524012	92	28	8.8E+08
1979	554312	14558	539754	95	50	1.6E+09
1980	346013	996	345018	61	31	9.9E+08
1981	487296	11207	476089	84	44	1.4E+09
1982	202477	1759	200718	35	33	1.0E+09
1997	205632	3	205629	36	25	8.0E+08
1998	473848	615	473233	83	34	1.1E+09
1999	253565	3	253562	44	29	9.3E+08
2000	302851	644	302207	53	28	8.9E+08
2001	544846	1010	543836	95	20	6.4E+08
2002	594883	5949	588934	103	32	1.0E+09
2003	567986	662	567324	100	40	1.3E+09
2004	379334	2179	377154	66	19	6.0E+08

Example calculation for groundwater recharge and discharge using streamflow data from the Naskwaaksis Stream. Refer to Figure A.5, years 1997 and 1998.

Q_{tp} $= Q_o \times t_l / 2.3$ (Equation 2.1)
Q_{tp} $= (0.161\ m^3/s \times 34\ d \times 1440\ min/d \times 60\ s/min) / 2.3$
Q_{tp} $= 205632\ m^3$ = the total potential discharge

Q_t $= Q_{tp} / 10^{(t/t_l)}$ (Equation 2.2)
Q_t $= (205632\ m^3) / 10^{(165/34)}$
Q_t $= 3\ m^3$ = discharge remaining at the end of the recession

Q_{tp}-Q_t $= 205632\ m^3 - 3\ m^3$
Q_{tp}-Q_t $= 205629\ m^3$ = Groundwater recharge available between recessions for the year

Drainage area $= 5.7\ km^2 = 5700000\ m^2$
Groundwater recharge for the year $= (205629\ m^3/s\ /\ 5700000\ m^2) \times 1000$ mm/m
$= 36$ mm for the year

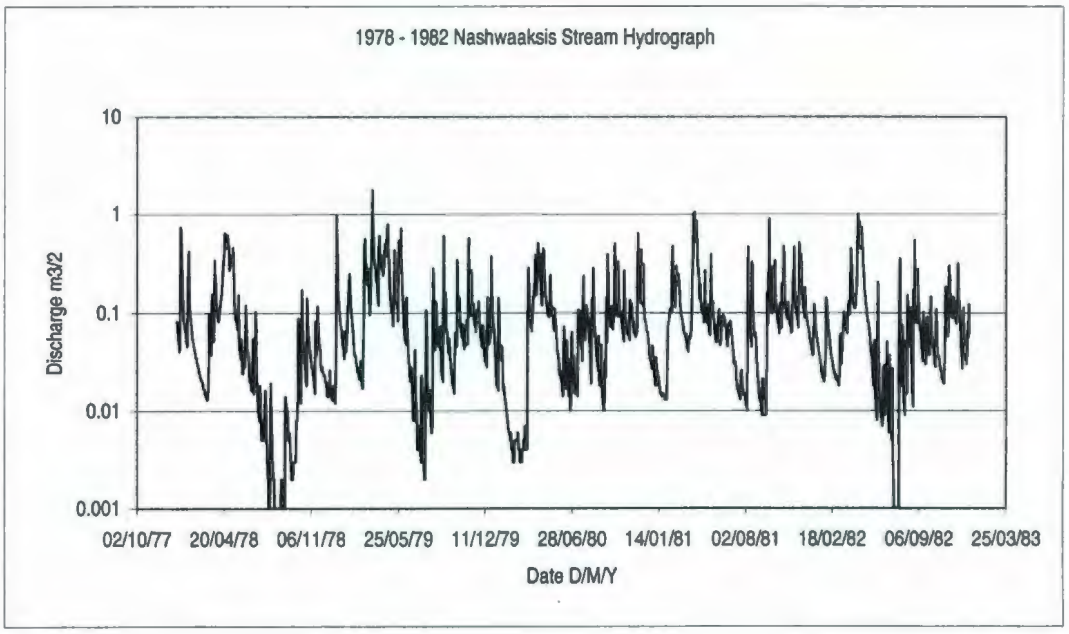

Figure A.6. Stream hydrograph for the Naskwaaksis Stream showing baseflow recession curves for years 1978 – 1982.

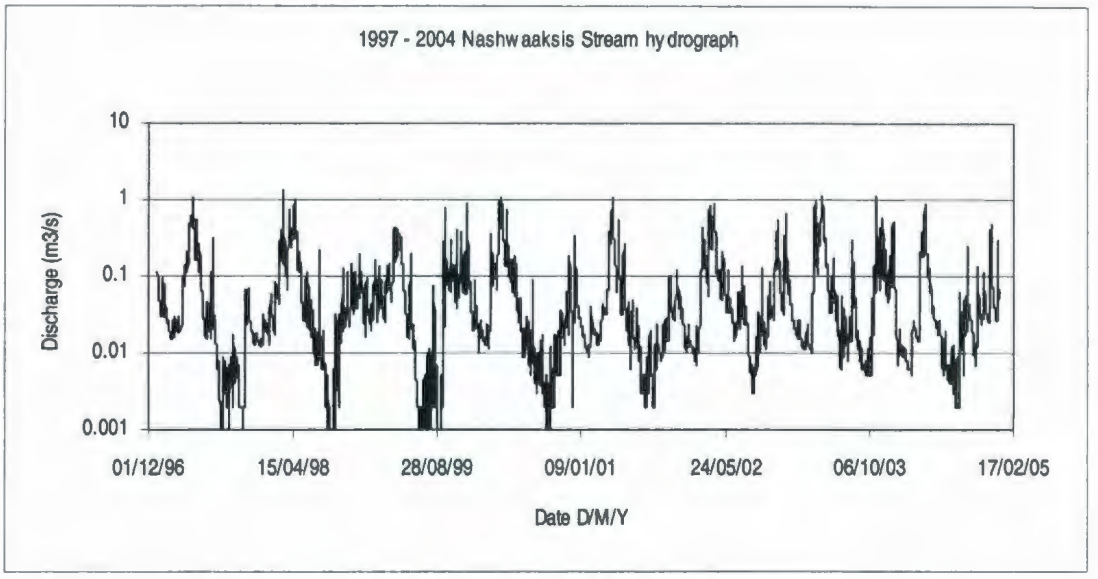

Figure A.7. Stream hydrograph for the Naskwaaksis Stream showing baseflow recession curves for years 1997 –2004.

Duration and Daily Discharge Curves

Another method of viewing stream discharge data is by means of the duration curve. This shows how often a streams particular discharge occurs in a given year (Fetter, 2001). The graph is constructed by showing the percentage of time that the probability of a given flow of a stream will be equalled or exceeded. Equation A.1 is used to graphically represent the data.

$$P = 100\ m / n = 1 \qquad \text{(Equation A.1)}$$

Where P = probability
m = serial rank
n = number of data values

Figure A.8 shows that for 1% of the time, the flowrate is at its highest, approximately 0.4 to 1.0 m^3/s. A flowrate of approximately 0.01 m^3/s will occur equal to or greater than 80% of the time.

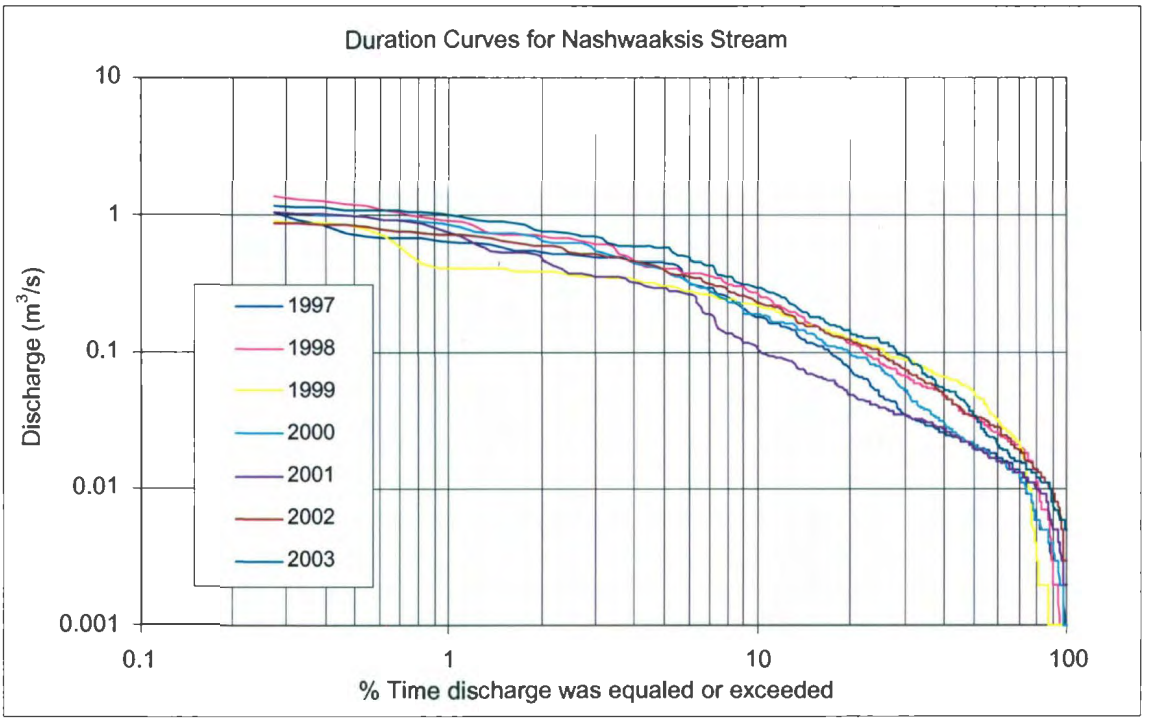

Figure A.8. Duration curves for Nashwaaksis Stream.

APPENDIX B GEOLOGICAL LOG DATA

B.1 Photo Logs

Plate B.1. Photographed core log of BH01.

Plate B.2. Photographed core log of BH02.

Plate B.3. Photographed core log of BH03.

B.2 Large-Scale Fracture Mapping

Fracture mapping locations throughout the Fredericton area were done in Odell Park, the southeast corner of Bishop Drive and Lien Street, and along the Trans Canada Highway outside of Fredericton. Results from the mapping are listed below in Table B.1.

Table B.1 Outcrop fracture mapping details.

Fracture Location	Geology	Dip and Plunge
Odell Park outcrop	Massive red fine-med sandstone	316° NW / 70°
Odell Park outcrop	Massive red fine-med sandstone	322° NW / 72°
Odell Park outcrop	Massive red fine-med sandstone	74° NEE / 90°
Odell Park outcrop	Massive red fine-med sandstone	70° NEE / 90°
Odell Park outcrop	Massive red fine-med sandstone	344° NW / 90°
Odell Park outcrop	Massive red fine-med sandstone	340° NW / 85°
Odell Park outcrop	Massive red fine-med sandstone	66° NE / 90°
Odell Park outcrop	Massive red fine-med sandstone	70° NE / 90°
Odell Park outcrop	Massive red fine-med sandstone	66° NE / 90°
Odell Park outcrop	Massive red fine-med sandstone	68° NE / 90°
Odell Park outcrop	Massive red fine-med sandstone	6° N / 45°

B.3 Inclined Borehole Fracture Details and Angle Frequency

Table B.2 An example of detailed fracture logging using BH01.

Length (m)	Strata type	N/I/U/O/C	P/C/I	Roughness (1 - 5)	Weathering Y / N	Weathering Type	Fracture Colour	Hardness R1 - R5	Length (m)	Strata type	N/I/U/O/C	P/C/I	Roughness (1 - 5)	Weathering Y / N	Weathering Type	Fracture Colour	Hardness (R1 - R5)
15.60	sandstone	I/O	I	5	Y		LG	R3	32.81	sandstone	N/O	I	5	Y	Fe, coal	R, C	R3
15.68	sandstone	N/O	P	4	N		LG	R3	32.88	sandstone	N/O	I	4	Y	Fe	R, G	R3
15.81	sandstone	I/O	I	5	N		LG	R3	33.31	sandstone	N/O	P	3	Y	Fe	R	R3
16.02	sandstone	N/O	P	4	N		LG	R3	33.33	sandstone	N/O	P	3	Y	Fe	R, G	R3
16.05	sandstone	N/O	I	5	N		LG	R3	33.46	sandstone	N/O	I	3	Y	Fe	R, Y	R3
16.25	sandstone	N/O	I	5	N		LG	R3	34.19	sandstone	N/O	I	5	Y	Fe	R	R3
16.29	sandstone	N/O	I	5	N		LG	R3	34.23	sandstone	N/O	I	5	Y	Fe	P, R	R3
16.47	sandstone	I/O	P	5	N		LG	R3	38.16	sandstone	I/O	I	5	N		G	R3
16.82	sandstone	N/O	I	5	N		LG	R3	38.25	sandstone	I/O	P	3	N		G	R3
17.17	sandstone	N/O	I	5	N		LG	R3	38.33	sandstone	N/O	P	4	Y		B, G	R3
17.50	sandstone	I/O	P	4	N		LG	R3	38.38	sandstone	N/O	I	5	Y		B, G	R3
17.64	sandstone	I/O	C	4	N		LG	R3	38.52	sandstone	N/O	I	5	N		G	R3
17.66	sandstone	I/O	I	5	N		LG	R3	39.09	sandstone	I/O	I	5	N		G	R3
17.83	sandstone	N/O	P	5	N		LG	R3	39.31	sandstone	I/O	I	5	N		G	R3
18.15	sandstone	U/O	I	5	N		LG	R3	39.41	sandstone	I/O	I	5	N		G	R3
18.58	sandstone	N/O	I	5	N		LG	R3	39.54	sandstone	I/O	P	5	N		G	R3
18.84	sandstone	I/O	I	4	N		LG	R3	39.71	sandstone	I/O	I	5	N		G	R3
19.21	sandstone	N/O	I	5	N		LG	R3	39.81	sandstone	I/O	I	5	N		G	R3
19.32	sandstone	N/O	I	5	N		LG	R3	40.23	sandstone	I/O	I	5	N		P, G	R3
20.05	sandstone	N/O	I	4	N		LG	R3	40.66	sandstone	I/O	I	5	N		G	R3
20.08	sandstone	N/O	I	5	N	Fe	LG	R3	40.76	sandstone	N/O	I	4	Y		Y, B, G	R3
20.41	sandstone	N/O	I	5	N	Fe, coal	LG	R3	40.83	sandstone	N/O	I	5	Y	Fe	Y, B, G	R3
20.45	sandstone	N/O	I	4	N		LG	R3	41.78	sandstone	N/O	P	2	N		G	R3
20.55	sandstone	N/C	C	4	N	Fe	LG	R3	43.64	sandstone	I/O	P	3	N		G	R3
20.64	sandstone	N/O	I	5	N	Cl	LG	R3	44.35	sandstone	N/O	I	5	N		C, G	R3
20.72	sandstone	N/O	P	5	N	Coal	LG	R3	45.04	sandstone	N/O	I	5	N		C, G	R2
20.80	sandstone	N/O	P	4	Y	Fe, coal	LG	R3	45.52	sst/siltst	U/O	I	5	N		G	R2
20.86	sandstone	N/O	P	5	Y	Fe, coal	LG	R3	46.17	sandstone	I/O	I	5	N		G	R3
20.91	sandstone	N/O	I	5	Y		LG	R3	46.58	sandstone	I/O	I	5	N		G	R3
21.03	sandstone	N/O	I	5	N		LG	R3	46.07	siltstone	N/O	P	2	N		RED	R2
21.36	sandstone	N/O	P	4	Y		LG	R3	48.32	siltstone	N/O	P	4	N		RED	R2
21.62	sandstone	I/O	P	4	N		LG	R3	48.59	siltstone	N/O	P	2	N		RED	R2
21.83	sandstone	N/O	I	5	Y	Fe, coal	LG	R3	48.85	siltstone	N/O	I	4	N		RED	R2
22.07	sandstone	N/O	P	3	Y	Fe, coal	LG	R3	50.98	siltstone	N/O	I	5	N		RED	R1
22.13	sandstone	I/O	P	2	N		LG	R3	51.92	siltstone	I/O	I	5	N		RED/GRE	R2
22.33	sandstone	I/O	C	4	N		LG	R3	52.11	siltstone	N/O	P	4	N		RED	R2
22.75	sandstone	N/O	I	4	Y	Fe, coal	LG	R3	52.14	siltstone	N/O	P	4	N		RED	R2
22.79	sandstone	N/O	C	4	Y	Fe	LG	R3	52.78	siltstone	N/O	P	3	N		RED	R2
22.93	sandstone	N/O	I	5	Y	Fe	LG	R3	53.03	sandstone	N/O	I	5	N		RED	R3
23.03	sandstone	N/O	P	2	Y	coal seam	LG	R2	53.13	sandstone	N/O	I	3	N		RED	R3
23.08	sandstone	N/O	P	3	Y	Fe	LG	R2	54.10	siltstone	N/O	I	5	N		RED	R2
23.12	sandstone	N/O	P	3	Y	Fe	LG	R2	55.27	siltstone	N/O	I	3	N		RED	R2
23.18	sandstone	N/O	P	3	Y	coal	LG	R2	55.53	siltstone	N/O	I	5	N		RED	R2
23.36	sandstone	I/O	I	5	N		LG	R3	55.60	siltstone	N/O	I	5	N		RED	R2
23.51	sandstone	I/O	I	5	N		LG	R3	56.03	siltstone	N/O	I	5	N		RED	R2
23.64	sandstone	N/O	P	2	N	coal	LG	R3	56.54	siltstone	N/O	I	5	N		RED	R2
23.77	sandstone	I/O	P	2	N		C, LG	R3	56.94	siltstone	N/O	I	5	N		RED	R1
23.96	sandstone	I/O	P	3	N		LG	R3	57.07	siltstone	N/O	I	5	N		RED	R2
24.37	sandstone	I/O	C	4	N		C, LG	R3	60.55	siltstone	N/O	C	3	N		RED/GRE	R1
24.55	sandstone	I/O	P	4	N		C, LG	R3	60.91	siltstone	N/O	I	5	N		RED/GRE	R1
24.63	sandstone	I/O	C	4	N		C, LG	R3	61.09	siltstone	N/O	I	5	N		RED/GRE	R1
24.87	sandstone	N/O	P	3	Y	Fe, coal	R, C	R3	61.72	siltstone	N/O	P	2	N		RED	R1
24.96	sandstone	N/O	P	2	Y	Fe	P, G	R3	61.88	siltstone	N/O	P	4	N		RED	R1
26.31	sandstone	I/O	P	3	N		G	R3	63.09	siltstone	N/O	I	5	N		RED	R2
26.92	sandstone	N/O	C	4	N		G	R3	64.92	siltstone	N/O	I	5	N		RED	R2
27.17	sandstone	N/O	I	5	Y	Fe	P, G	R3	68.58	siltstone	N/O	I	5	N		RED	R2
27.30	mudstone	N/O	C	2	Y		G	R2	68.69	siltstone	N/O	I	5	N		RED	R2
28.65	sandstone	N/O	P	5	N		P, G	R3	68.77	siltstone	N/O	I	5	N		RED	R2
29.56	sandstone	I/O	C	4	N		G	R3	68.87	siltstone	N/O	I	5	N		RED	R2
31.75	sandstone	N/O	P	3	Y	Fe	R, G	R3	69.05	siltstone	N/O	I	5	N		RED	R2
32.02	sandstone	N/O	P	4	Y		C, G	R3	70.00	siltstone	N/O	I	5	N		RED	R2
32.31	sandstone	N/O	P	3	Y	Fe	R, G	R3	72.03	siltstone	N/O	I	5	N		RED	R2
32.61	sandstone	N/O	I	5	N		G	R2									

Notes: Breaks = natural (N), induced (I), uncertain (U), opened (O), closed (C)

Fracture = planar (P), curved (C), irregular (I)

Colour = LG=light grey, C=coal, P=pink, R=rust, Y=yellow, B=brown, G=grey, RED = red, GREEN = green.

Each borehole was logged for fracture alpha and beta angles (Figure B.1) and put into fracture angle frequency and fracture occurrence frequency with length graphs as viewed below in Figures B.5 to B.9.

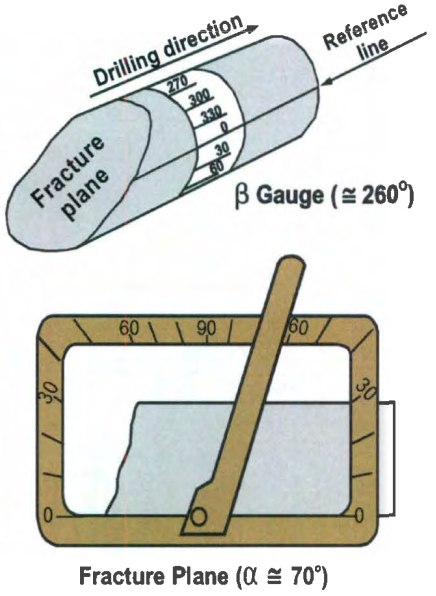

Figure B.1. Logging fracture alpha and beta angles on the core.

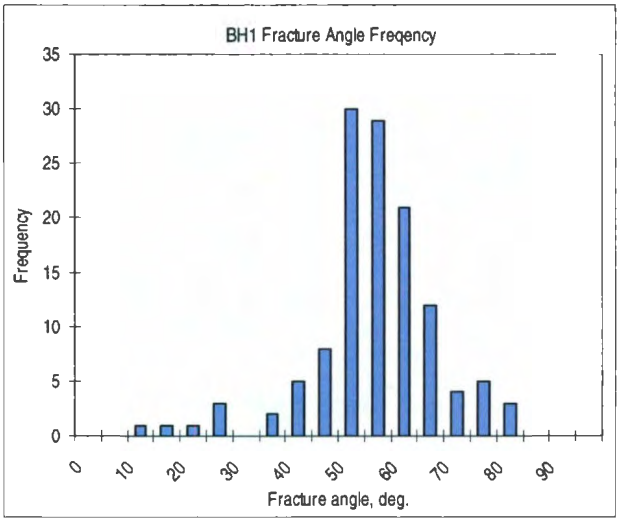

Figure B.2. Fracture angle frequency for BH01. Note angles not corrected for incline of 51^0.

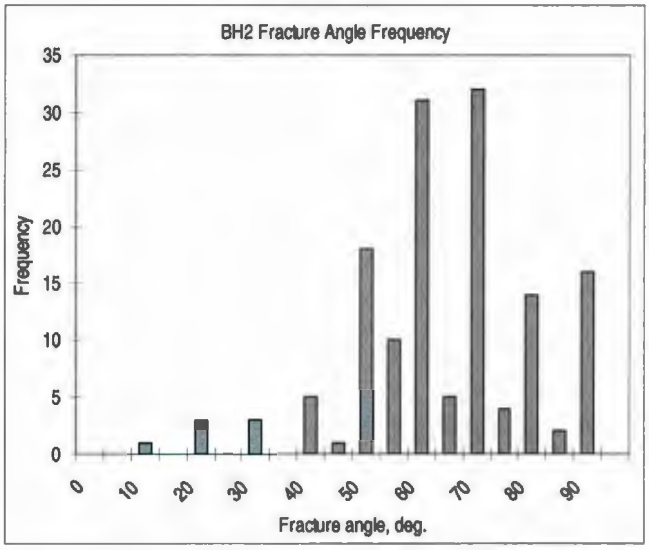

Figure B.3. Fracture angle frequency for BH02. Note angles not corrected for incline of 51^0.

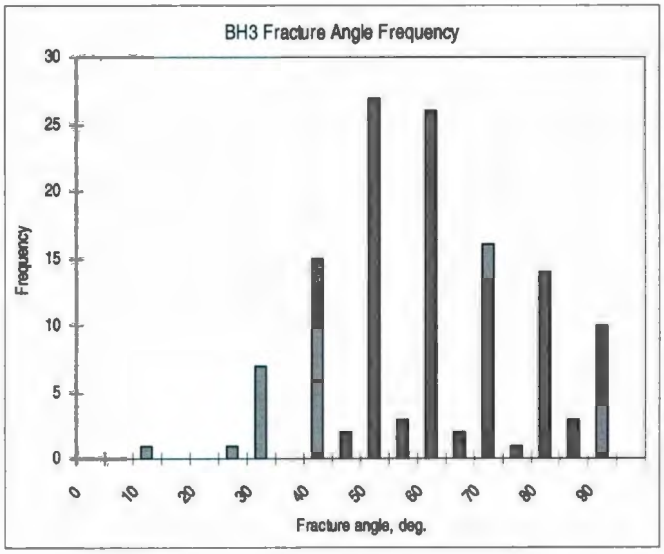

Figure B.4. Fracture angle frequency for BH03. Note angles not corrected for incline of 51^0.

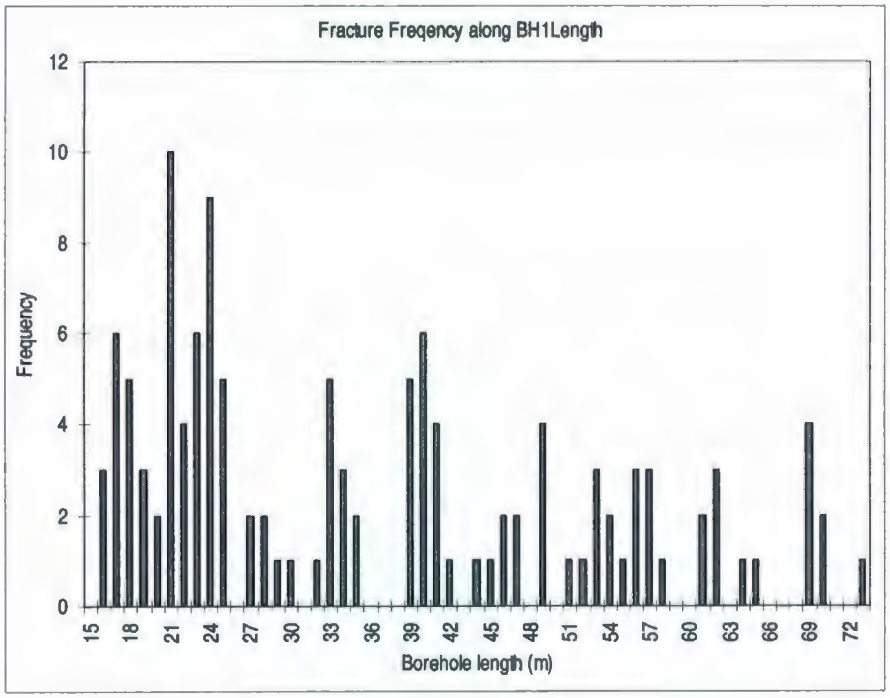

Figure B.5. Fracture frequency along BH01 length.

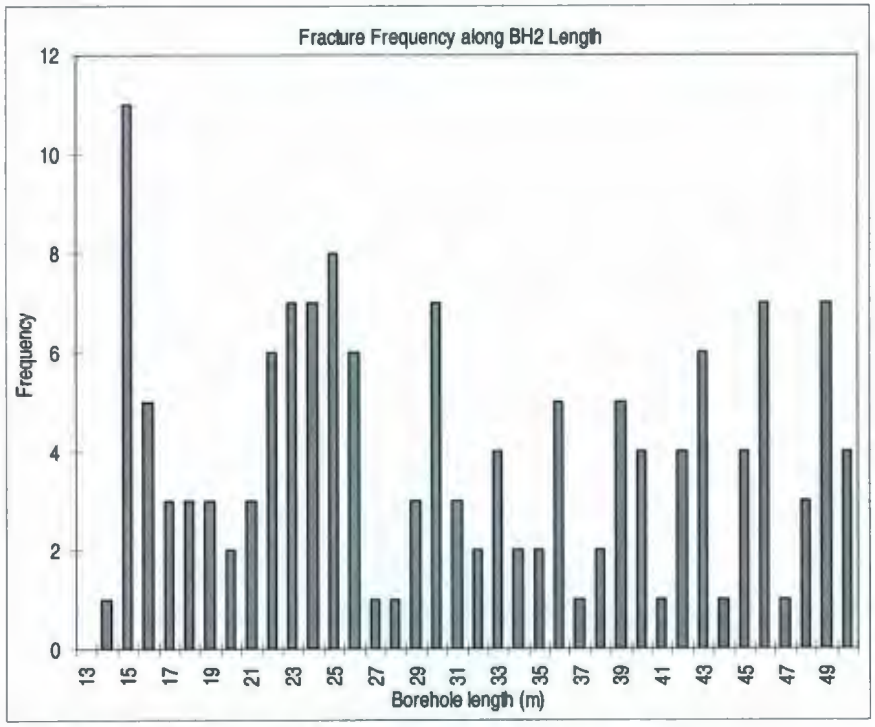

Figure B.6. Fracture frequency along BH02 length.

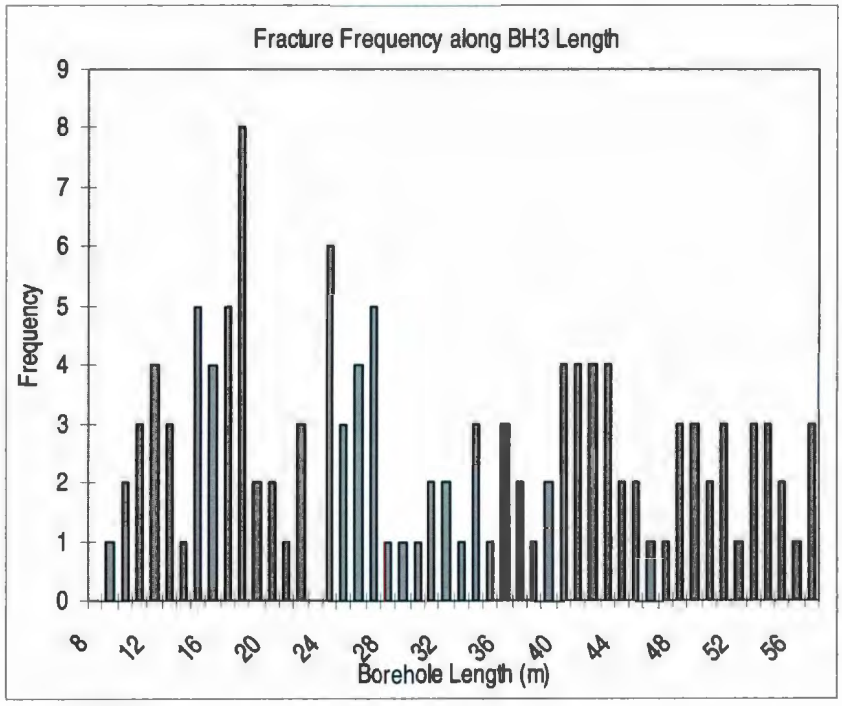

Figure B.7. Fracture frequency along BH03 length.

APPENDIX C BOREHOLE PACKER TEST DATA

Plate C.1. Boart Longyear 538 diesel drill rig with an NQ / NW triple tube core barrel used for drilling the inclined boreholes.

Plate C.2. Downhole packer test system set-up.

Plate C.3. Downhole packer test system using drillers set-up.

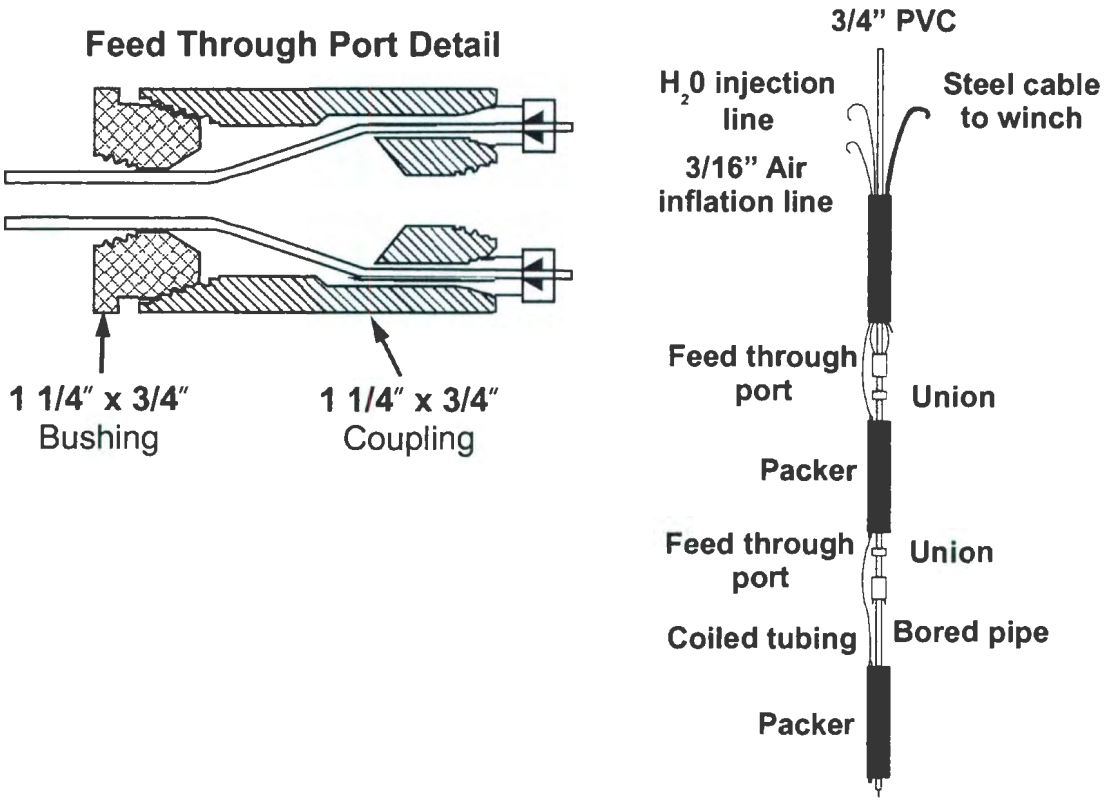

Figure C.1. Inflatable packer details.

Example Calculation of Transmissivity and Results from Packer Tests

Example C.1 calculation for transmissivity using data from BH1 – length 17.39m
Transmissivity (T) using the Thiem (1906) equation.

$$T = \frac{Q \times (\ln Ri - \ln Rw)}{(2\pi \times (Hw - Hi))} \qquad \text{(Equation 3.1)}$$

Where:

Q	=	flowrate (m^3/sec)
Ri	=	radius of well influence (m)
Rw	=	radius of borehole (m)
H_w	=	hydraulic head of borehole during test interval (m)
H_i	=	initial hydraulic head of well (m)

Conversions:
L/min = 1 / 60000 m^3/sec
1 kpa = 0.145 psi absolute
1 psi = 0.7031 m head of water
1 psi = 2.3068 ft head of water
1 kpa = 0.102 m

Q = 4.98 L/min x 1/60000 m^3/sec = 8.31 x 10^{-5} m^3/sec
Ri = 10 m
Rw = 0.0381 m
H_w = 13 kpa x 0.102 m = 1.326 m
H_i = 11 kpa x 0.102 m = 1.122 m

T = Q * ln Ri - ln Rw / 2 π * Hw – Hi
T = 8.31 x 10^{-5} m^3/sec * (ln (10 m) – ln (0.0381 m)) / (2*3.14*(1.326 m – 1.122 m))
T = 3.61 x 10^{-4} m^2/sec

Table C.1A Borehole packer test observations and transmissivity calculations for BH1 2003.							
Length (m)	Depth (m)	Elevation (m)	Flowrate (L/min)	Flowrate (m^3/sec)	Δ head (kpa)	Δ head (m)	T (m^2/s)
17.39	13.51	12.44	4.98	8.31E-05	2	0.20	3.61E-04
17.39	13.51	12.44	12.47	2.08E-04	3	0.31	6.03E-04
17.39	13.51	12.44	16.42	2.74E-04	11.5	1.17	2.07E-04
19.04	14.79	11.16	5.26	8.77E-05	6	0.61	1.27E-04
19.04	14.79	11.16	6.76	1.13E-04	22	2.24	4.45E-05
19.04	14.79	11.16	8.82	1.47E-04	48	4.90	2.66E-05
20.76	16.13	9.82	0.48	7.95E-06	42	4.28	1.65E-06
20.76	16.13	9.82	0.51	8.58E-06	90	9.18	8.29E-07
20.76	16.13	9.82	2.13	3.56E-05	124	12.65	2.49E-06
22.51	17.49	8.46	0.19	3.15E-06	97	9.89	2.83E-07
22.51	17.49	8.46	0.34	5.61E-06	145	14.79	3.36E-07
22.51	17.49	8.46	0.14	2.25E-06	50	5.10	3.92E-07
22.51	17.49	8.46	0.34	5.59E-06	130	13.26	3.74E-07
22.51	17.49	8.46	0.35	5.89E-06	150	15.30	3.41E-07
24.24	18.84	7.11	0.03	4.60E-07	40	4.08	1.00E-07
24.24	18.84	7.11	0.06	9.99E-07	70	7.14	1.24E-07
24.24	18.84	7.11	0.11	1.91E-06	120	12.24	1.38E-07
24.24	18.84	7.11	0.04	6.72E-07	20	2.04	2.92E-07
24.24	18.84	7.11	0.18	2.96E-06	70	7.14	3.67E-07
24.24	18.84	7.11	0.25	4.18E-06	115	11.73	3.16E-07
25.96	20.17	5.78	0.09	1.47E-06	18	1.84	7.11E-07
25.96	20.17	5.78	0.18	2.94E-06	30	3.06	8.53E-07
25.96	20.17	5.78	0.80	1.34E-05	133	13.57	8.77E-07
25.96	20.17	5.78	0.17	2.84E-06	20	2.04	1.24E-06
27.69	21.52	4.43	0.90	1.49E-05	50	5.10	2.60E-06
27.69	21.52	4.43	0.24	4.07E-06	15	1.53	2.36E-06
27.69	21.52	4.43	0.78	1.30E-05	55	5.61	2.06E-06
27.69	21.52	4.43	1.58	2.64E-05	125	12.75	1.84E-06
29.42	22.86	3.09	0.01	2.10E-07	120	12.24	1.52E-08
29.42	22.86	3.09	0.01	1.26E-07	87	8.87	1.26E-08
31.15	24.21	1.74	0.29	4.89E-06	20	2.04	2.13E-06
31.15	24.21	1.74	0.90	1.50E-05	70	7.14	1.86E-06
31.15	24.21	1.74	1.38	2.30E-05	120	12.24	1.66E-06
32.88	25.55	0.40	0.51	8.50E-06	35	3.57	2.11E-06
32.88	25.55	0.40	1.11	1.85E-05	85	8.67	1.90E-06
32.88	25.55	0.40	1.62	2.70E-05	125	12.75	1.88E-06
34.61	26.90	-0.95	0.02	3.27E-07	121	12.34	2.35E-08
36.34	28.24	-2.29	0.24	3.94E-06	30	3.06	1.14E-06
36.34	28.24	-2.29	0.43	7.15E-06	60	6.12	1.04E-06
36.34	28.24	-2.29	0.72	1.20E-05	100	10.20	1.05E-06
36.34	28.24	-2.29	0.48	7.93E-06	65	6.63	1.06E-06
36.34	28.24	-2.29	0.95	1.58E-05	115	11.73	1.19E-06
38.07	29.59	-3.64	0.08	1.26E-06	30	3.06	3.66E-07
38.07	29.59	-3.64	0.20	3.36E-06	70	7.14	4.18E-07
38.07	29.59	-3.64	0.36	6.06E-06	110	11.22	4.79E-07
38.07	29.59	-3.64	0.04	6.05E-07	17	1.73	3.09E-07
38.07	29.59	-3.64	0.26	4.39E-06	90	9.18	4.24E-07
39.80	30.93	-4.98	1.57	2.61E-05	80	8.16	2.84E-06
39.80	30.93	-4.98	5.33	8.89E-05	100	10.20	7.73E-06
39.80	30.93	-4.98	9.47	1.58E-04	150	15.30	9.15E-06
41.53	32.27	-6.32	0.00	6.72E-08	116	11.83	5.04E-09
41.53	32.27	-6.32	0.03	4.89E-07	140	14.28	3.04E-08
41.54	32.28	-6.33	0.06	9.46E-07	105	10.71	7.84E-08
41.54	32.28	-6.33	0.09	1.42E-06	150	15.30	8.23E-08
43.30	33.65	-7.70	0.29	4.84E-06	110	11.22	3.82E-07

Table C.1B Borehole packer test observations and transmissivity calculations for BH1 2003.							
Length	Depth	Elevation	Flowrate	Flowrate	Δ head	Δ head	T
(m)	(m)	(m)	(L/min)	(m^3/sec)	(kpa)	(m)	(m^2/s)
43.30	33.65	-7.70	0.44	7.36E-06	160	16.32	4.00E-07
43.30	33.65	-7.70	0.30	4.97E-06	60	6.12	7.21E-07
43.30	33.65	-7.70	0.72	1.21E-05	141	14.38	7.44E-07
45.02	34.99	-9.04	0.03	4.91E-07	60	6.12	7.11E-08
45.02	34.99	-9.04	0.01	1.49E-07	118	12.04	1.10E-08
45.02	34.99	-9.04	0.01	1.61E-07	143	14.59	9.81E-09
46.79	36.36	-10.41	0.09	1.58E-06	20	2.04	6.86E-07
46.79	36.36	-10.41	0.10	1.62E-06	80	8.16	1.76E-07
46.79	36.36	-10.41	0.10	1.63E-06	105	10.71	1.35E-07
46.80	36.37	-10.42	0.07	1.12E-06	20	2.04	4.87E-07
46.80	36.37	-10.42	0.16	2.71E-06	100	10.20	2.36E-07
48.53	37.71	-11.76	0.01	9.26E-08	20	2.04	4.03E-08
48.53	37.71	-11.76	0.03	4.85E-07	100	10.20	4.21E-08
50.27	39.07	-13.12	0.05	7.89E-07	150	15.30	4.57E-08
50.27	39.07	-13.12	0.05	8.66E-07	85	8.67	8.86E-08
52.01	40.42	-14.47	0.10	1.71E-06	150	15.30	9.92E-08
52.03	40.43	-14.48	0.02	2.80E-07	120	12.24	2.03E-08
53.81	41.82	-15.87	0.13	2.10E-06	60	6.12	3.05E-07
53.81	41.82	-15.87	0.10	1.60E-06	105	10.71	1.32E-07
53.81	41.82	-15.87	0.09	1.58E-06	155	15.81	8.85E-08
53.90	41.89	-15.94	0.02	3.36E-07	125	12.75	2.34E-08
55.64	43.24	-17.29	0.09	1.42E-06	75	7.65	1.65E-07
55.64	43.24	-17.29	0.09	1.58E-06	105	10.71	1.31E-07
55.73	43.31	-17.36	0.08	1.28E-06	25	2.55	4.44E-07
55.73	43.31	-17.36	0.17	2.78E-06	80	8.16	3.02E-07
55.73	43.31	-17.36	0.18	3.05E-06	100	10.20	2.65E-07
57.38	44.59	-18.64	0.04	6.00E-07	70	7.14	7.46E-08
57.38	44.59	-18.64	0.05	8.07E-07	120	12.24	5.84E-08
57.39	44.60	-18.65	0.02	3.51E-07	40	4.08	7.62E-08
57.39	44.60	-18.65	0.03	4.21E-07	100	10.20	3.66E-08
57.39	44.60	-18.65	0.03	5.61E-07	140	14.28	3.48E-08
58.55	45.50	-19.55	0.03	5.78E-07	135	13.77	3.73E-08
58.55	45.50	-19.55	0.02	3.70E-07	25	2.55	1.29E-07
58.55	45.50	-19.55	0.02	4.03E-07	40	4.08	8.77E-08
58.55	45.50	-19.55	0.03	5.38E-07	130	13.26	3.60E-08
Elevation 25.95 BH1 TOC							

Table C.2 Borehole packer test observations and transmissivity calculations for BH1 2004.							
Length	Depth	Elevation	Flowrate	Flowrate	Δ head	Δ head	T
(m)	(m)	(m)	(L/min)	(m^3/sec)	(kpa)	(m)	(m^2/s)
18.00	13.99	11.96	2.80	4.67E-05	1	0.10	4.06E-04
18.00	13.99	11.96	7.00	1.17E-04	56	5.712	1.81E-05
16.00	13.99	11.96	9.36	1.56E-04	96	9.792	1.41E-05
33.75	26.23	-0.28	0.28	4.63E-06	17	1.734	2.37E-06
33.75	26.23	-0.28	0.95	1.58E-05	90	9.180	1.52E-06
33.75	26.23	-0.28	1.45	2.42E-05	175	17.850	1.20E-06
35.48	27.57	-1.62	0.25	4.21E-06	41	4.182	8.92E-07
35.48	27.57	-1.62	0.36	6.06E-06	83	8.466	6.35E-07
35.48	27.57	-1.62	0.50	8.41E-06	152	15.504	4.81E-07
37.21	28.91	-2.96	0.20	3.41E-06	42	4.284	7.05E-07
37.21	28.91	-2.96	0.76	1.26E-05	90	9.180	1.22E-06
37.21	28.91	-2.96	1.26	2.10E-05	166	16.932	1.10E-06
38.45	29.88	-3.93	0.30	5.05E-06	42	4.284	1.04E-06
38.45	29.88	-3.93	0.76	1.26E-05	90	9.180	1.22E-06
38.45	29.88	-3.93	1.30	2.17E-05	159	16.218	1.18E-06
39.69	30.84	-4.89	0.18	2.94E-06	28	2.856	9.14E-07
39.69	30.84	-4.89	4.04	6.73E-05	55	5.610	1.06E-05
39.69	30.84	-4.89	8.08	1.35E-04	87	8.874	1.35E-05
40.93	31.81	-5.86	0.38	6.31E-06	54	5.508	1.02E-06
40.93	31.81	-5.86	0.53	8.83E-06	97	9.894	7.92E-07
40.93	31.81	-5.86	0.76	1.26E-05	169	17.238	6.49E-07
42.17	32.77	-6.82	0.40	6.73E-06	49	4.998	1.19E-06
42.17	32.77	-6.82	0.69	1.16E-05	97	9.894	1.04E-06
42.17	32.77	-6.82	1.01	1.68E-05	173	17.646	8.46E-07
43.41	33.74	-7.79	0.32	5.26E-06	44	4.488	1.04E-06
43.41	33.74	-7.79	0.72	1.20E-05	97	9.894	1.07E-06
43.41	33.74	-7.79	1.05	1.75E-05	169	17.238	8.98E-07
44.65	34.70	-8.75	0.21	3.58E-06	54	5.508	5.76E-07
44.65	34.70	-8.75	0.32	5.41E-06	97	9.894	4.85E-07
44.65	34.70	-8.75	0.53	8.83E-06	169	17.238	4.54E-07
47.66	37.04	-11.09	0.28	4.73E-06	75	7.650	5.49E-07
47.66	37.04	-11.09	0.38	6.31E-06	105	10.710	5.22E-07
47.66	37.04	-11.09	0.47	7.78E-06	185	18.870	3.66E-07
49.40	38.39	-12.44	0.28	4.63E-06	56	5.712	7.18E-07
49.40	38.39	-12.44	0.35	5.89E-06	97	9.894	5.28E-07
49.40	38.39	-12.44	0.76	1.26E-05	173	17.646	6.34E-07
51.15	39.75	-13.80	0.28	4.63E-06	62	6.324	6.49E-07
51.15	39.75	-13.80	0.35	5.89E-06	104	10.608	4.92E-07
51.15	39.75	-13.80	0.68	1.14E-05	173	17.646	5.71E-07
54.72	42.53	-16.58	0.25	4.21E-06	62	6.324	5.90E-07
54.72	42.53	-16.58	0.33	5.55E-06	111	11.322	4.35E-07
54.72	42.53	-16.58	0.47	7.78E-06	173	17.646	3.91E-07
56.51	43.92	-17.97	0.25	4.21E-06	69	7.038	5.30E-07
56.51	43.92	-17.97	0.34	5.68E-06	111	11.322	4.45E-07
56.51	43.92	-17.97	0.53	8.83E-06	180	18.360	4.27E-07
59.79	46.47	-20.52	0.26	4.29E-06	75	7.650	4.97E-07
59.79	46.47	-20.52	0.28	4.63E-06	117	11.934	3.44E-07
59.79	46.47	-20.52	0.42	6.94E-06	186	18.972	3.24E-07
61.03	47.43	-21.48	0.38	6.31E-06	62	6.324	8.85E-07
61.03	47.43	-21.48	0.59	9.88E-06	104	10.608	8.26E-07
61.03	47.43	-21.48	0.86	1.43E-05	173	17.646	7.19E-07
62.27	48.39	-22.44	2.57	4.29E-05	41	4.182	9.10E-06
62.27	48.39	-22.44	3.41	5.68E-05	103	10.506	4.79E-06
62.27	48.39	-22.44	3.79	6.31E-05	172	17.544	3.19E-06
63.51	49.36	-23.41	0.23	3.79E-06	28	2.856	1.18E-06
63.51	49.36	-23.41	0.25	4.21E-06	83	8.466	4.41E-07
63.51	49.36	-23.41	0.76	1.26E-05	159	18.218	6.90E-07
Elevation 25.95 m TOC							

Table C.3 Borehole packer test observations and transmissivity calculations for BH2 2003.

Length (m)	Depth (m)	Elevation (m)	Flowrate (L/min)	Flowrate (m^3/sec)	Δ head (kpa)	Δ head (m)	T (m^2/s)
14.62	11.36	14.30	2.70	4.50E-05	30	3.06	1.30E-05
14.62	11.36	14.30	6.50	1.08E-04	90	9.18	1.05E-05
14.62	11.36	14.30	11.41	1.90E-04	145	14.79	1.14E-05
16.34	12.70	12.97	7.50	1.25E-04	16	1.632	6.79E-05
16.34	12.70	12.97	12.45	2.07E-04	46	4.692	3.92E-05
16.34	12.70	12.97	18.17	3.03E-04	81	8.262	3.25E-05
18.09	14.06	11.61	6.61	1.10E-04	27	2.754	3.55E-05
18.09	14.06	11.61	9.45	1.57E-04	47	4.794	2.91E-05
18.09	14.06	11.61	18.08	3.01E-04	105	10.71	2.50E-05
19.82	15.40	10.26	0.38	6.31E-06	29	2.958	1.89E-06
19.82	15.40	10.26	0.62	1.04E-05	59	6.018	1.53E-06
19.82	15.40	10.26	1.25	2.08E-05	129	13.158	1.40E-06
21.54	16.74	8.93	0.18	2.97E-06	28	2.856	9.21E-07
21.54	16.74	8.93	0.20	3.35E-06	48	4.896	6.07E-07
21.54	16.74	8.93	0.48	8.04E-06	108	11.016	6.48E-07
23.28	18.09	7.57	0.72	1.20E-05	23	2.346	4.53E-06
23.28	18.09	7.57	1.26	2.10E-05	38	3.876	4.81E-06
23.28	18.09	7.57	2.70	4.51E-05	113	11.526	3.47E-06
25.00	19.43	6.23	0.01	8.96E-08	19	1.938	4.10E-08
25.00	19.43	6.23	0.01	2.26E-07	144	14.688	1.37E-08
26.74	20.78	4.88	0.11	1.89E-06	28	2.856	5.88E-07
26.74	20.78	4.88	0.28	4.63E-06	63	6.426	6.39E-07
26.74	20.78	4.88	0.51	8.52E-06	128	13.056	5.79E-07
26.74	20.78	4.88	0.41	6.91E-06	75	7.65	8.01E-07
26.74	20.78	4.88	0.69	1.15E-05	125	12.75	8.01E-07
28.46	22.12	3.55	0.22	3.65E-06	28	2.856	1.13E-06
28.46	22.12	3.55	0.44	7.29E-06	58	5.916	1.09E-06
28.46	22.12	3.55	0.80	1.34E-05	118	12.036	9.88E-07
28.46	22.12	3.55	0.60	1.00E-05	41	4.182	2.12E-06
28.46	22.12	3.55	1.19	1.99E-05	101	10.302	1.71E-06
30.18	23.45	2.21	0.29	4.84E-06	30	3.06	1.40E-06
30.18	23.45	2.21	0.40	6.70E-06	70	7.14	8.33E-07
30.18	23.45	2.21	0.97	1.61E-05	145	14.79	9.67E-07
31.92	24.80	0.86	0.13	2.10E-06	28	2.856	6.53E-07
31.92	24.80	0.86	0.28	4.58E-06	68	6.936	5.86E-07
31.92	24.80	0.86	0.41	6.90E-06	118	12.036	5.09E-07
33.65	26.15	-0.48	0.52	8.67E-06	21	2.142	3.59E-06
33.65	26.15	-0.48	0.98	1.63E-05	51	5.202	2.78E-06
33.65	26.15	-0.48	1.92	3.20E-05	106	10.812	2.62E-06
35.37	27.49	-1.82	0.02	3.32E-07	45	4.59	6.41E-08
35.37	27.49	-1.82	0.07	1.22E-06	125	12.75	8.51E-08
35.37	27.49	-1.83	0.01	8.41E-08	51	5.202	1.43E-08
35.37	27.49	-1.83	0.01	1.58E-07	111	11.322	1.24E-08
37.11	28.84	-3.17	0.76	1.26E-05	14	1.428	7.84E-06
37.11	28.84	-3.17	2.34	3.90E-05	44	4.488	7.70E-06
37.11	28.84	-3.17	5.68	9.46E-05	94	9.588	8.75E-06
38.83	30.18	-4.51	0.01	1.26E-07	89	9.078	1.23E-08
38.83	30.18	-4.51	0.01	1.34E-07	44	4.488	2.66E-08
38.83	30.18	-4.51	0.02	2.81E-07	104	10.608	2.35E-08
40.57	31.53	-5.86	0.02	3.15E-07	71	7.242	3.86E-08
40.57	31.53	-5.86	0.08	1.26E-06	116	11.832	9.46E-08
40.57	31.53	-5.86	0.04	6.65E-07	37	3.774	1.56E-07
40.57	31.53	-5.86	0.14	2.33E-06	115	11.73	1.76E-07
42.29	32.87	-7.20	0.54	8.99E-06	21	2.142	3.72E-06
42.29	32.87	-7.20	1.37	2.29E-05	51	5.202	3.90E-06
42.29	32.87	-7.20	2.97	4.96E-05	111	11.322	3.88E-06
43.66	33.93	-8.27	0.59	9.88E-06	16	1.632	5.37E-06
43.66	33.93	-8.27	1.67	2.78E-05	56	5.712	4.31E-06
43.66	33.93	-8.27	3.19	5.32E-05	111	11.322	4.17E-06
Elevation of BH2 25.665 m TOC							

Table C.4 Borehole packer test observations and transmissivity calculations for BH2 2004.							
Length	Depth	Elevation	Flowrate	Flowrate	Δ head	Δ head	T
(m)	(m)	(m)	(L/min)	(m^3/sec)	(kpa)	(m)	(m^2/s)
16.7	13.01	12.66	2.25	3.75E-05	9	0.918	3.62E-05
16.7	13.01	12.66	6.44	1.07E-04	41	4.182	2.27E-05
16.7	13.01	12.66	10.69	1.78E-04	72	7.344	2.15E-05
18.5	14.34	11.32	4.49	7.48E-05	1	0.102	6.50E-04
18.5	14.34	11.32	10.13	1.69E-04	19	1.938	7.72E-05
18.5	14.34	11.32	12.54	2.09E-04	34	3.468	5.34E-05
19.8	15.36	10.31	0.26	4.34E-06	39	3.978	9.67E-07
19.8	15.36	10.31	0.47	7.84E-06	89	9.078	7.66E-07
19.8	15.36	10.31	0.71	1.18E-05	159	16.218	6.47E-07
21.0	16.32	9.34	0.82	1.37E-05	1	0.102	1.19E-04
21.0	16.32	9.34	1.32	2.21E-05	41	4.182	4.68E-06
21.0	16.32	9.34	1.95	3.26E-05	121	12.342	2.34E-06
22.2	17.28	8.38	0.22	3.61E-06	1	0.102	3.13E-05
22.2	17.28	8.38	0.53	8.83E-06	17	1.734	4.52E-06
22.2	17.28	8.38	0.95	1.58E-05	107	10.914	1.28E-06
23.7	18.38	7.28	0.76	1.26E-05	26	2.652	4.22E-06
23.7	18.38	7.28	1.29	2.15E-05	76	7.752	2.45E-06
23.7	18.38	7.28	2.21	3.68E-05	166	16.932	1.93E-06
25.4	19.72	5.94	0.97	1.62E-05	1	0.102	1.41E-04
25.4	19.72	5.94	1.74	2.90E-05	15	1.53	1.68E-05
25.4	19.72	5.94	2.21	3.68E-05	100	10.2	3.20E-06
28.8	22.41	3.25	0.19	3.15E-06	2	0.204	1.37E-05
28.8	22.41	3.25	0.38	6.31E-06	27	2.754	2.03E-06
28.8	22.41	3.25	0.45	7.57E-06	142	14.484	4.64E-07
30.6	23.75	1.92	0.23	3.79E-06	1	0.102	3.29E-05
30.6	23.75	1.92	0.97	1.62E-05	9	0.918	1.57E-05
30.6	23.75	1.92	1.39	2.31E-05	78	7.956	2.57E-06
34.0	26.44	-0.77	0.19	3.15E-06	1	0.102	2.74E-05
34.0	26.44	-0.77	0.38	6.31E-06	16	1.632	3.43E-06
34.0	26.44	-0.77	0.59	9.78E-06	85	8.67	1.00E-06
35.8	27.78	-2.12	0.85	1.42E-05	1	0.102	1.23E-04
35.8	27.78	-2.12	1.83	3.05E-05	30	3.06	8.84E-06
35.8	27.78	-2.12	2.75	4.58E-05	99	10.098	4.02E-06
37.5	29.13	-3.46	0.09	1.50E-06	1	0.102	1.30E-05
37.5	29.13	-3.46	0.14	2.37E-06	57	5.814	3.61E-07
38.7	30.09	-4.43	1.07	1.78E-05	1	0.102	1.55E-04
38.7	30.09	-4.43	4.47	7.45E-05	14	1.428	4.63E-05
38.7	30.09	-4.43	7.44	1.24E-04	24	2.448	4.50E-05
40.0	31.05	-5.39	0.14	2.31E-06	72	7.344	2.79E-07
41.2	32.03	-6.36	0.07	1.10E-06	7	0.714	1.37E-06
41.2	32.03	-6.36	0.14	2.37E-06	52	5.304	3.96E-07
42.5	32.99	-7.32	0.09	1.58E-06	1	0.102	1.37E-05
42.5	32.99	-7.32	0.14	2.27E-06	7	0.714	2.82E-06
42.5	32.99	-7.32	0.19	3.15E-06	72	7.344	3.81E-07
Elevation 25.665 m TOC							

Table C.5 Borehole packer test observations and transmissivity calculations for BH3 2003.

Length (m)	Depth (m)	Elevation (m)	Flowrate (L/min)	Flowrate (m^3/sec)	Δ head (kpa)	Δ head (m)	T (m^2/s)
10.53	7.45	6.25	8.15	1.36E-04	63	6.43	1.88E-05
10.53	7.45	6.25	11.31	1.89E-04	128	13.06	1.28E-05
10.53	7.45	6.25	11.15	1.86E-04	75	7.65	2.15E-05
31.79	22.48	-8.78	0.46	7.67E-06	19	1.94	3.51E-06
31.79	22.48	-8.78	0.86	1.43E-05	144	14.69	8.66E-07
31.79	22.48	-8.78	1.20	2.00E-05	28	2.86	6.21E-06
34.87	24.66	-10.96	0.76	1.27E-05	28	2.86	3.93E-06
34.87	24.66	-10.96	0.68	1.14E-05	68	6.94	1.46E-06
34.87	24.66	-10.96	0.62	1.03E-05	128	13.06	6.98E-07
37.81	26.74	-13.04	0.16	2.67E-06	23	2.35	1.01E-06
37.81	26.74	-13.04	0.98	1.63E-05	38	3.88	3.74E-06
37.81	26.74	-13.04	0.45	7.50E-06	113	11.53	5.77E-07
40.78	28.84	-15.14	0.62	1.03E-05	28	2.86	3.21E-06
40.78	28.84	-15.14	0.60	1.00E-05	48	4.90	1.81E-06
40.78	28.84	-15.14	0.64	1.07E-05	108	11.02	8.65E-07
43.77	30.95	-17.26	0.02	3.33E-07	29	2.96	1.00E-07
43.77	30.95	-17.26	0.34	5.67E-06	59	6.02	8.35E-07
43.77	30.95	-17.26	0.42	7.00E-06	129	13.16	4.72E-07
46.88	33.15	-19.45	1.20	2.00E-05	27	2.75	6.44E-06
46.88	33.15	-19.45	2.25	3.75E-05	47	4.79	6.94E-06
46.88	33.15	-19.45	2.92	4.86E-05	105	10.71	4.03E-06
47.396	33.51	-19.82	1.55	2.58E-05	16	1.63	1.40E-05
47.396	33.51	-19.82	0.86	1.43E-05	46	4.69	2.70E-06
47.396	33.51	-19.82	0.97	1.61E-05	81	8.26	1.73E-06
53.035	37.50	-23.81	0.26	4.35E-06	30	3.06	1.26E-06
53.035	37.50	-23.81	0.37	6.17E-06	90	9.18	5.96E-07
53.035	37.50	-23.81	0.46	7.64E-06	145	14.79	4.58E-07
Elevation 13.695 m TOC							

Table C.6A Packer test observations and transmissivity calculations for BH3 2004.

Length (m)	Depth (m)	Elevation (m)	Flowrate (L/min)	Flowrate (m^3/sec)	Δ head (kpa)	Δ head (m)	T (m^2/s)
16.48	11.65	2.04	0.27	4.51E-06	14	1.43	2.80E-06
16.48	11.65	2.04	0.58	9.59E-06	62	6.32	1.34E-06
16.48	11.65	2.04	0.82	1.37E-05	124	12.65	9.59E-07
17.72	12.53	1.17	0.62	1.03E-05	28	2.86	3.18E-06
17.72	12.53	1.17	0.69	1.16E-05	69	7.04	1.46E-06
17.72	12.53	1.17	1.01	1.68E-05	159	16.22	9.20E-07
18.96	13.41	0.29	0.44	7.36E-06	14	1.43	4.57E-06
18.96	13.41	0.29	0.76	1.26E-05	69	7.04	1.59E-06
18.96	13.41	0.29	1.07	1.79E-05	131	13.36	1.19E-06
20.20	14.28	-0.59	0.68	1.14E-05	48	4.90	2.06E-06
20.20	14.28	-0.59	0.99	1.65E-05	124	12.65	1.16E-06
20.20	14.28	-0.59	1.18	1.96E-05	193	19.69	8.84E-07
21.44	15.16	-1.47	0.11	1.80E-06	13	1.33	1.21E-06
21.44	15.16	-1.47	0.83	1.39E-05	41	4.18	2.94E-06
21.44	15.16	-1.47	1.21	2.02E-05	103	10.51	1.70E-06
22.68	16.04	-2.34	0.43	7.21E-06	27	2.75	2.32E-06
22.68	16.04	-2.34	0.67	1.11E-05	82	8.36	1.18E-06
22.68	16.04	-2.34	1.07	1.79E-05	179	18.26	8.68E-07
23.92	16.91	-3.22	0.57	9.46E-06	34	3.47	2.42E-06
23.92	16.91	-3.22	1.24	2.07E-05	110	11.22	1.64E-06
23.92	16.91	-3.22	1.45	2.42E-05	179	18.26	1.17E-06
25.16	17.79	-4.10	0.72	1.20E-05	69	7.04	1.51E-06
25.16	17.79	-4.10	0.83	1.39E-05	97	9.89	1.24E-06
25.16	17.79	-4.10	1.39	2.31E-05	166	16.93	1.21E-06
26.39	18.66	-4.97	0.65	1.08E-05	62	6.32	1.52E-06
26.39	18.66	-4.97	0.78	1.30E-05	97	9.89	1.17E-06
26.39	18.66	-4.97	1.05	1.75E-05	152	15.50	9.99E-07
27.64	19.54	-5.85	1.05	1.75E-05	62	6.32	2.45E-06
27.64	19.54	-5.85	1.48	2.47E-05	90	9.18	2.39E-06
27.64	19.54	-5.85	1.89	3.15E-05	166	16.93	1.65E-06
28.88	20.42	-6.73	0.63	1.05E-05	55	5.61	1.66E-06
28.88	20.42	-6.73	0.76	1.26E-05	90	9.18	1.22E-06
28.88	20.42	-6.73	0.97	1.62E-05	152	15.50	9.26E-07
30.12	21.30	-7.60	0.63	1.05E-05	35	3.57	2.61E-06
30.12	21.30	-7.60	0.76	1.26E-05	48	4.90	2.29E-06
30.12	21.30	-7.60	1.14	1.89E-05	152	15.50	1.08E-06
31.36	22.17	-8.48	0.76	1.26E-05	62	6.32	1.77E-06
31.36	22.17	-8.48	1.01	1.68E-05	76	7.75	1.92E-06
31.36	22.17	-8.48	1.14	1.89E-05	117	11.93	1.41E-06
32.60	23.05	-9.36	1.22	2.04E-05	55	5.61	3.23E-06
32.60	23.05	-9.36	1.51	2.52E-05	124	12.65	1.77E-06
32.60	23.05	-9.36	2.02	3.36E-05	173	17.65	1.69E-06
33.84	23.93	-10.23	0.76	1.26E-05	72	7.34	1.52E-06
33.84	23.93	-10.23	0.81	1.35E-05	112	11.42	1.05E-06
33.84	23.93	-10.23	1.03	1.71E-05	172	17.54	8.66E-07
35.08	24.81	-11.11	0.57	9.46E-06	56	5.71	1.47E-06
35.08	24.81	-11.11	0.85	1.41E-05	118	12.04	1.04E-06
35.08	24.81	-11.11	1.17	1.96E-05	187	19.07	9.09E-07
36.32	25.68	-11.99	0.82	1.37E-05	7	0.71	1.70E-05
36.32	25.68	-11.99	1.10	1.83E-05	14	1.43	1.14E-05
36.32	25.68	-11.99	1.26	2.10E-05	28	2.86	6.53E-06
37.56	26.56	-12.86	1.01	1.68E-05	49	5.00	2.99E-06
37.56	26.56	-12.86	1.07	1.79E-05	69	7.04	2.25E-06
37.56	26.56	-12.86	1.26	2.10E-05	104	10.61	1.76E-06
38.80	27.44	-13.74	0.59	9.88E-06	49	5.00	1.75E-06
38.80	27.44	-13.74	0.95	1.58E-05	76	7.75	1.80E-06
38.80	27.44	-13.74	1.14	1.89E-05	186	18.97	8.85E-07

Table C.6B Packer test observations and transmissivity calculations for BH3 2004.							
Length	Depth	Elevation	Flowrate	Flowrate	Δ head	Δ head	T
(m)	(m)	(m)	(L/min)	(m^3/sec)	(kpa)	(m)	(m^2/s)
40.04	28.31	-14.62	0.69	1.16E-05	69	7.04	1.46E-06
40.04	28.31	-14.62	0.79	1.32E-05	90	9.18	1.28E-06
40.04	28.31	-14.62	1.05	1.75E-05	187	19.07	8.12E-07
41.28	29.19	-15.49	0.57	9.46E-06	56	5.71	1.47E-06
41.28	29.19	-15.49	0.76	1.26E-05	104	10.61	1.06E-06
41.28	29.19	-15.49	1.14	1.89E-05	187	19.07	8.80E-07
42.52	30.07	-16.37	0.53	8.83E-06	48	4.90	1.60E-06
42.52	30.07	-16.37	0.88	1.47E-05	104	10.61	1.23E-06
42.52	30.07	-16.37	1.14	1.89E-05	159	16.22	1.04E-06
43.76	30.94	-17.25	0.56	9.34E-06	96	9.79	8.46E-07
43.76	30.94	-17.25	0.76	1.26E-05	131	13.36	8.38E-07
43.76	30.94	-17.25	1.01	1.68E-05	200	20.40	7.31E-07
45.00	31.82	-18.12	0.50	8.33E-06	76	7.75	9.53E-07
45.00	31.82	-18.12	0.82	1.37E-05	145	14.79	8.20E-07
45.00	31.82	-18.12	1.07	1.79E-05	194	19.79	8.01E-07
46.24	32.70	-19.00	0.82	1.37E-05	56	5.71	2.13E-06
46.24	32.70	-19.00	1.14	1.89E-05	111	11.32	1.48E-06
46.24	32.70	-19.00	1.51	2.52E-05	173	17.65	1.27E-06
47.48	33.57	-19.88	0.76	1.26E-05	42	4.28	2.61E-06
47.48	33.57	-19.88	1.20	2.00E-05	111	11.32	1.57E-06
47.48	33.57	-19.88	1.68	2.80E-05	180	18.36	1.35E-06
48.72	34.45	-20.76	0.57	9.46E-06	48	4.90	1.71E-06
48.72	34.45	-20.76	0.76	1.26E-05	90	9.18	1.22E-06
48.72	34.45	-20.76	0.88	1.47E-05	166	16.93	7.71E-07
49.96	35.33	-21.63	2.46	4.10E-05	49	5.00	7.28E-06
49.96	35.33	-21.63	3.03	5.05E-05	111	11.32	3.95E-06
49.96	35.33	-21.63	3.47	5.78E-05	180	18.36	2.79E-06
51.20	36.20	-22.51	2.02	3.36E-05	62	6.32	4.72E-06
51.20	36.20	-22.51	2.90	4.84E-05	124	12.65	3.39E-06
51.20	36.20	-22.51	3.28	5.47E-05	193	19.69	2.46E-06
52.44	37.08	-23.39	0.50	8.41E-06	49	5.00	1.49E-06
52.44	37.08	-23.39	0.76	1.26E-05	125	12.75	8.78E-07
52.44	37.08	-23.39	0.95	1.58E-05	187	19.07	7.33E-07
53.68	37.96	-24.26	0.57	9.46E-06	62	6.32	1.33E-06
53.68	37.96	-24.26	0.76	1.26E-05	104	10.61	1.06E-06
53.68	37.96	-24.26	1.04	1.73E-05	186	18.97	8.11E-07
54.92	36.83	-25.14	0.69	1.16E-05	82	8.36	1.23E-06
54.92	38.83	-25.14	0.76	1.26E-05	124	12.65	8.85E-07
54.92	38.83	-25.14	1.01	1.68E-05	200	20.40	7.31E-07
Elevation 13.695 m TOC							

Table C.7 Average transmissivity (T) summary from the packer tests.

BH1				BH2				BH3			
BH1-2003		BH1-2004		BH2-2003		BH2-2004		BH3-2003		BH3-2004	
Length	T	Length	T	Length	T	Length	T	Length	T	Length	T
(m)	(m2/s)	(m)	(m2/s)	(m)	(m2/s)	(m)	(m2/s)	(m)	(m2/s)	(m)	(m2/s)
17.4	3.90E-04	18.0	1.46E-04	14.6	1.16E-05	17	2.68E-05	10.5	1.77E-05	16.5	1.70E-06
19.0	6.61E-05	33.8	1.70E-06	16.3	4.66E-05	18	2.60E-04	31.8	3.53E-06	17.7	1.85E-06
20.8	1.66E-06	35.5	6.69E-07	18.1	2.99E-05	20	7.93E-07	34.9	2.03E-06	19.0	2.45E-06
22.5	3.45E-07	37.2	1.01E-06	19.8	1.61E-06	21	4.21E-05	37.8	1.77E-06	20.2	1.37E-06
24.2	2.23E-07	38.5	1.15E-06	21.5	7.25E-07	22	1.24E-05	40.8	1.96E-06	21.4	1.95E-06
26.0	9.19E-07	39.7	8.34E-06	23.3	4.27E-06	24	2.87E-06	43.8	4.69E-07	22.7	1.46E-06
27.7	2.21E-06	40.9	8.19E-07	25.0	2.73E-08	28	5.35E-05	46.9	5.80E-06	23.9	1.74E-06
29.4	1.39E-08	42.2	1.03E-06	26.7	6.81E-07	29	5.40E-06	47.4	6.16E-06	25.2	1.32E-06
31.2	1.88E-06	43.4	1.00E-06	28.5	1.41E-06	33	1.71E-05	53.0	7.72E-07	26.4	1.23E-06
32.9	1.96E-06	44.7	5.05E-07	30.2	1.07E-06	35	1.06E-05			27.6	2.16E-06
34.6	2.35E-08	47.7	4.79E-07	31.9	5.83E-07	36	4.54E-05			28.9	1.27E-06
36.3	1.10E-06	49.4	6.27E-07	33.6	3.00E-06	37	6.70E-06			30.1	1.99E-06
38.1	3.99E-07	51.2	5.71E-07	35.4	4.40E-08	39	8.21E-05			31.4	1.70E-06
39.8	6.57E-06	54.7	4.72E-07	37.1	8.10E-06	40	2.79E-07			32.6	2.23E-06
41.5	4.90E-08	56.5	4.67E-07	38.8	2.08E-08	41	8.84E-07			33.8	1.15E-06
43.3	5.62E-07	59.8	3.89E-07	40.6	1.16E-07	42	5.64E-06			35.1	1.14E-06
45.0	3.06E-08	61.0	8.10E-07	42.3	3.84E-06					36.3	1.16E-05
46.8	3.44E-07	62.3	5.69E-06	43.7	4.62E-06					37.6	2.33E-06
48.5	4.12E-08	63.5	7.69E-07							38.8	1.48E-06
50.3	6.72E-08									40.0	1.18E-06
52.0	5.98E-08									41.3	1.13E-06
53.9	1.37E-07									42.5	1.29E-06
55.7	2.61E-07									43.8	8.05E-07
57.4	5.61E-08									45.0	8.58E-07
58.6	6.49E-08									46.2	1.63E-06
										47.5	1.84E-06
										48.7	1.23E-06
										50.0	4.68E-06
										51.2	3.52E-06
										52.4	1.03E-06
										53.7	1.06E-06
										55.0	9.48E-07

Example Calculation of Hydraulic Conductivity and Results from Packer Tests

An example calculation for hydraulic conductivity using 2003 BH1 – length 17.39m:
Equivalent porous media hydraulic conductivity (K_e)

$$Ke = \frac{Qf \times (\ln Ri - \ln Rw)}{(2\pi L \times (Hw - Hi))} \qquad \text{(Equation 3.2)}$$

Where:

Q f	= flowrate through the fractures (m^3/s)
Ri	= radius of influence (m)
Rw	= radius of well borehole (m)
H_w	= hydraulic head of borehole during test (m)
H_i	= initial hydraulic head of well (m)
L	= length of test interval (m)

Conversions:
L/min = 1 / 60000 m^3/sec
1 kpa = 0.102 m

Q = 4.98 L/min x 1/60000 m^3/sec = 8.31 x 10^{-5} m^3/sec
Ri = 10 m
Rw = 0.0381 m
H_w = 13 kpa x 0.102 m = 1.326 m
H_i = 11 kpa x 0.102 m = 1.122 m
L = 1.73 m (2003)
L = 0.90 m (2004)

K_e = 8.31 x 10^{-5} m^3/sec * ln(10 m) – ln(0.0381 m) / 2 π 1.73 m (1.326 m – 1.122 m)
K_e = 2.26 x 10^{-4} m/s

Table C.8 Average hydraulic conductivity (K) summary from the packer tests*.

BH1				BH2				BH3			
BH1-03		BH1-04		BH2-03		BH2-04		BH3-03		BH3-04	
Length	K	Length	K	Length	K	Length	K	Length	K	Length	K
(m)	(m/s)	(m)	(m/s)	(m)	(m/s)	(m)	(m/s)	(m)	(m/s)	(m)	(m/s)
17.4	**2.26E-04**	**18.0**	**1.62E-04**	**14.6**	**6.73E-06**	**16.7**	**2.98E-05**	**10.5**	**1.02E-05**	16.5	1.89E-06
19.0	**3.82E-05**	33.8	1.89E-06	**16.3**	**2.69E-05**	**18.5**	**2.89E-04**	31.8	2.04E-06	17.7	2.06E-06
20.8	9.57E-07	35.5	7.44E-07	**18.1**	**1.73E-05**	19.8	8.82E-07	34.9	1.17E-06	19.0	2.72E-06
22.5	2.00E-07	37.2	1.12E-06	19.8	9.30E-07	**21.0**	**4.67E-05**	37.8	1.03E-06	20.2	1.52E-06
24.2	1.29E-07	38.5	1.28E-06	21.5	4.19E-07	**22.4**	**1.38E-05**	40.8	1.13E-06	21.4	2.17E-06
26.0	5.31E-07	**39.7**	**9.26E-06**	23.3	2.47E-06	24.1	3.19E-06	43.8	2.71E-07	22.7	1.62E-06
27.7	1.28E-06	40.9	9.10E-07	25.0	1.58E-08	**27.6**	**5.95E-05**	46.9	3.35E-06	23.9	1.94E-06
29.4	8.05E-09	42.2	1.14E-06	26.7	3.94E-07	**29.3**	**6.00E-06**	47.4	3.56E-06	25.2	1.47E-06
31.2	1.09E-06	43.4	1.12E-06	28.5	8.15E-07	**32.8**	**1.90E-05**	53.0	4.46E-07	26.4	1.37E-06
32.9	1.13E-06	44.7	5.61E-07	30.2	6.17E-07	**34.5**	**1.18E-05**			27.6	2.40E-06
34.6	1.36E-08	47.7	5.32E-07	31.9	3.37E-07	**36.2**	**5.05E-05**			28.9	1.41E-06
36.3	6.34E-07	49.4	6.96E-07	33.6	1.73E-06	**37.5**	**7.44E-06**			30.1	2.22E-06
38.1	2.31E-07	51.2	6.34E-07	35.4	2.54E-08	**38.7**	**9.12E-05**			31.4	1.89E-06
39.8	3.80E-06	54.7	5.24E-07	**37.1**	**4.68E-06**	40.0	3.10E-07			32.6	2.48E-06
41.5	2.83E-08	56.5	5.19E-07	38.8	1.20E-08	41.2	9.82E-07			33.8	1.27E-06
43.3	3.25E-07	59.8	4.32E-07	40.6	6.73E-08	42.5	6.27E-06			35.1	1.27E-06
45.0	1.77E-08	61.0	9.00E-07	42.3	2.22E-06					**36.3**	**1.29E-05**
46.8	1.99E-07	**62.3**	**6.33E-06**	43.7	2.67E-06					37.6	2.59E-06
48.5	2.38E-08	63.5	8.54E-07							38.8	1.65E-06
50.3	3.88E-08									40.0	1.31E-06
52.0	3.45E-08									41.3	1.26E-06
53.9	7.93E-08									42.5	1.43E-06
55.7	1.51E-07									43.8	8.94E-07
57.4	3.24E-08									45.0	9.53E-07
58.6	3.75E-08									46.2	1.81E-06
										47.5	2.05E-06
										48.7	1.37E-06
										50.0	**5.19E-06**
										51.2	3.92E-06
										52.4	1.15E-06
										53.7	1.18E-06
										55.0	1.05E-06

*2003 length interval = 1.73 m 2004 length interval = 0.90 m

Temperature Calibration of Thermistor

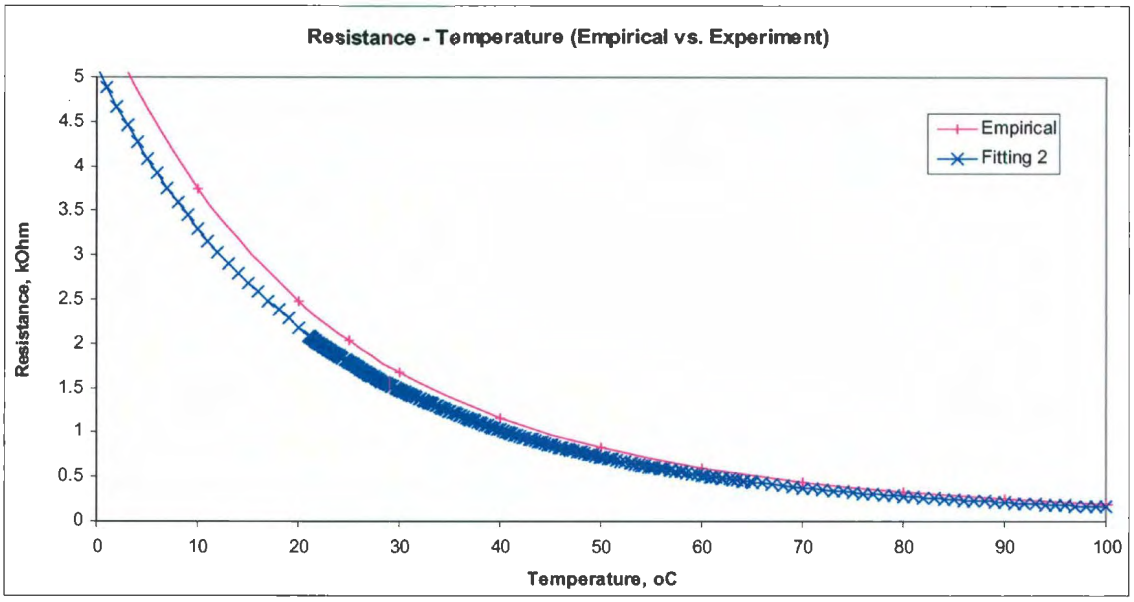

Figure C.2. Thermistor cable calibration curve.

Table C.9 Thermistor calibration sheet used for temperature determination.

O deg C	kohms	O deg C	kohms	O deg C	kohms	O deg C	kohms
0	5.121	**6**	3.925	**12**	3.036	**18**	2.387
0.1	5.0975	6.1	3.9085	12.1	3.0239	18.1	2.3772
0.2	5.074	6.2	3.892	12.2	3.0118	18.2	2.3674
0.3	5.0505	6.3	3.8755	12.3	2.9997	18.3	2.3576
0.4	5.027	6.4	3.859	12.4	2.9876	18.4	2.3478
0.5	5.0035	6.5	3.8425	12.5	2.9755	18.5	2.338
0.6	4.98	6.6	3.826	12.6	2.9634	18.6	2.3282
0.7	4.9565	6.7	3.8095	12.7	2.9513	18.7	2.3184
0.8	4.933	6.8	3.793	12.8	2.9392	18.8	2.3086
0.9	4.9095	6.9	3.7765	12.9	2.9271	18.9	2.2988
1	4.886	**7**	3.76	**13**	2.915	**19**	2.289
1.1	4.8644	7.1	3.7444	13.1	2.9036	19.1	2.2792
1.2	4.8428	7.2	3.7288	13.2	2.8922	19.2	2.2694
1.3	4.8212	7.3	3.7132	13.3	2.8808	19.3	2.2596
1.4	4.7996	7.4	3.6976	13.4	2.8694	19.4	2.2498
1.5	4.778	7.5	3.682	13.5	2.858	19.5	2.24
1.6	4.7564	7.6	3.6664	13.6	2.8466	19.6	2.2302
1.7	4.7348	7.7	3.6508	13.7	2.8352	19.7	2.2204
1.8	4.7132	7.8	3.6352	13.8	2.8238	19.8	2.2106
1.9	4.6916	7.9	3.6196	13.9	2.8124	19.9	2.2008
2	4.67	**8**	3.604	**14**	2.801	**20**	2.191
2.1	4.6495	8.1	3.5889	14.1	2.7902	20.1	2.1813
2.2	4.629	8.2	3.5738	14.2	2.7794	20.2	2.1716
2.3	4.6085	8.3	3.5587	14.3	2.7686	20.3	2.1619
2.4	4.588	8.4	3.5436	14.4	2.7578	20.4	2.1522
2.5	4.5675	8.5	3.5285	14.5	2.747	20.5	2.1425
2.6	4.547	8.6	3.5134	14.6	2.7362	20.6	2.1328
2.7	4.5265	8.7	3.4983	14.7	2.7254	20.7	2.1231
2.8	4.506	8.8	3.4832	14.8	2.7146	20.8	2.1134
2.9	4.4855	8.9	3.4681	14.9	2.7038	20.9	2.1037
3	4.465	**9**	3.453	**15**	2.693	**21**	2.094
3.1	4.446	9.1	3.4382	15.1	2.6824		
3.2	4.427	9.2	3.4234	15.2	2.6718		
3.3	4.408	9.3	3.4086	15.3	2.6612		
3.4	4.389	9.4	3.3938	15.4	2.6506		
3.5	4.37	9.5	3.379	15.5	2.64		
3.6	4.351	9.6	3.3642	15.6	2.6294		
3.7	4.332	9.7	3.3494	15.7	2.6188		
3.8	4.313	9.8	3.3346	15.8	2.6082		
3.9	4.294	9.9	3.3198	15.9	2.5976		
4	4.275	**10**	3.305	**16**	2.587		
4.1	4.257	10.1	3.291	16.1	2.5769		
4.2	4.239	10.2	3.277	16.2	2.5668		
4.3	4.221	10.3	3.263	16.3	2.5567		
4.4	4.203	10.4	3.249	16.4	2.5466		
4.5	4.185	10.5	3.235	16.5	2.5365		
4.6	4.167	10.6	3.221	16.6	2.5264		
4.7	4.149	10.7	3.207	16.7	2.5163		
4.8	4.131	10.8	3.193	16.8	2.5062		
4.9	4.113	10.9	3.179	16.9	2.4961		
5	4.095	**11**	3.165	**17**	2.486		
5.1	4.078	11.1	3.1521	17.1	2.4761		
5.2	4.061	11.2	3.1392	17.2	2.4662		
5.3	4.044	11.3	3.1263	17.3	2.4563		
5.4	4.027	11.4	3.1134	17.4	2.4464		
5.5	4.01	11.5	3.1005	17.5	2.4365		
5.6	3.993	11.6	3.0876	17.6	2.4266		
5.7	3.976	11.7	3.0747	17.7	2.4167		
5.8	3.959	11.8	3.0618	17.8	2.4068		
5.9	3.942	11.9	3.0489	17.9	2.3969		

Bedrock well 98-2 Slug Test Results

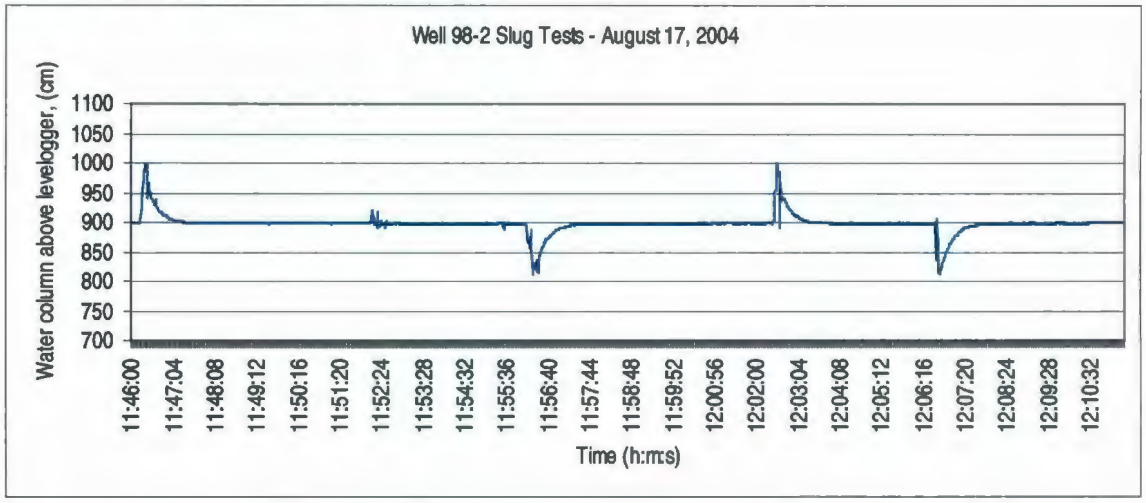

Figure C.3. Well 98-2 slug test data used in Bouwer-Rice analysis.

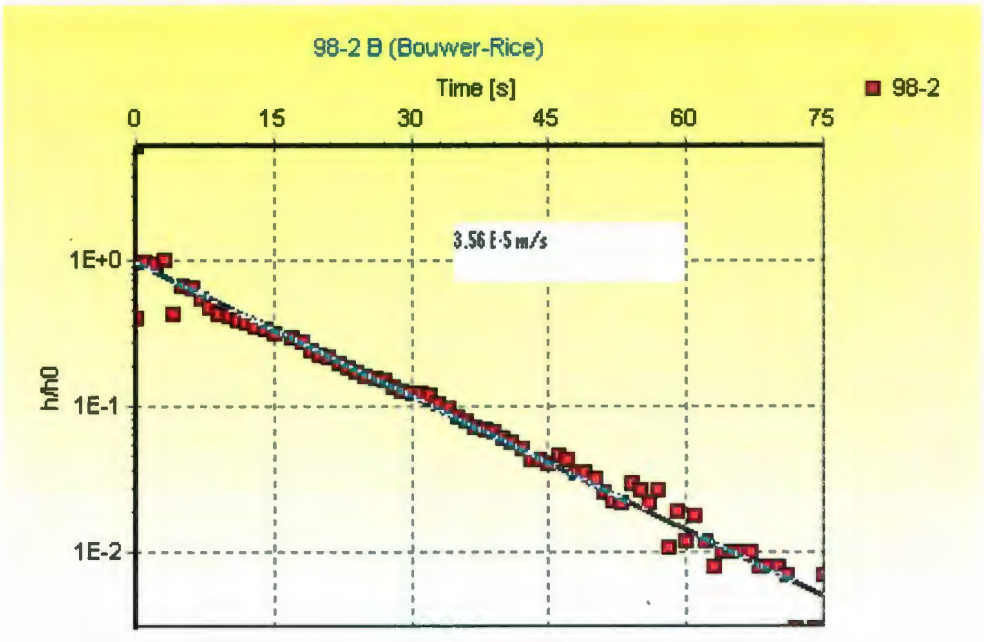

Figure C.4. Hydraulic conductivity results from Bouwer-Rice analysis.

APPENDIX D GROUNDWATER SAMPLING PROCEDURES AND GEOCHEMCIAL DATA

D.1 Groundwater Sampling Procedures

Bedrock groundwater samples were taken from three discrete intervals of each inclined borehole located in Odell Park, using the borehole packers to seal off the discrete interval. An additional bedrock groundwater sample was collected from the vertical bedrock well 98 - 2 at depth. This well is located adjacent the Saint John River in St. Anne's Point to the east of the Delta Hotel. The sampling procedure was consistent for each of the wells with the exception of the sample extraction method. For the artesian flowing wells BH01 and BH02, samples were taken after three well volumes of the packed off discrete interval had flowed from the well. Each interval volume was 12.2 L. A peristaltic pump was used to extract water samples from wells BH03 and bedrock well 98-2 at a rate of 145 ml / min. For each sample interval, the following field parameters were monitored prior to sample collection including flowrates, temperature, pH, Eh, conductivity, alkalinity and dissolved oxygen.

Sample Flowrate Monitoring

A 500 ml bottle and stopwatch was used to estimate the flowrates of the artesian flowing well samples prior to sample collection. The peristaltic pump was set to extract samples at a flowrate of 145 ml/min.

pH, Eh, Conductivity and Temperature Monitoring

A flow-through cell was used to monitor pH, Eh, conductivity and temperature prior to sample collection. The pH meter was calibrated to the standards 4.0, 7.0 and 10.0 pH solutions at every sample interval and monitored until the pH stabilized to +/- 0.02 or 30 minutes of monitoring had elapsed. The conductivity meter was calibrated to the standard solution of 14.90 uS/cm. Eh was recorded to determine whether oxidizing or

reducing conditions were occurring. Eh readings were taken in addition to the pH readings once the pH began to stabilize. The Eh meter did not require calibration. The sample temperature was recorded using the thermistor.

Dissolved Oxygen Determination

The dissolved oxygen (DO) content of each sample was recorded using the following procedure. A syringe was attached to a three-way valve connected to the sampling line. The syringe was filled twice with sample water to rinse and expel all air from the syringe. The syringe was then filled with sample water to more than 50 ml and all bubbles were knocked out and the syringe was emptied to the 50 ml line. A rubber septa was attached to the tip of the syringe for needle injection of 0.5 ml each of manganese sulphate ($MnSO_4$), azide (N_3) and sulphuric acid (H_2SO_4), in that order. The needle was filled first with $MnSO_4$, all air bubbles knocked off, expelled to 0.5 ml and injected into the syringe. The syringe was inverted slowly a couple of times for proper mixing. The needle was then filled with N_3, all air bubbles knocked off, expelled to 0.5 ml and injected into the syringe. The syringe was inverted slowly a couple of times for proper mixing. A precipitate was formed in the syringe and allowed to settle to approximately half the syringe volume. The needle was then filled with H_2SO_4, all air bubbles knocked off, expelled to 0.5 ml and injected into the syringe. The syringe was inverted slowly a couple of times for proper mixing. The syringe solution turned a clear yellow and the volume was recorded prior to titration.

The digital HACH titrator was set to zero before titration began. Each digit represented 0.00125 ml of thiosulfate. The syringe solution was transferred to a flask, with the attempt to avoid any splashing. Thiosulfate was slowly added to the flask until the solution turned a very pale yellow. Five drops of starch were then added to the solution, which turned blue. Thiosulfate was then continuously added until the solution turned clear. If less than 100 digits on the HACH meter was recorded, a lower concentration of thiosulfate was used and the test repeated on the sample. The following

equation D.1 was then used to determine the amount of dissolved oxygen (DO). The field results are in Table D.1.

$$DO = N_{TS} \times V_{TS} \times 8 \times 1000 / V_{sample} \text{ (mg/L)} \quad \text{(Equation D.1)}$$

Where;

N = normal

V = volume

V_{TS} = # of digits x 0.00125 ml

Table D.1 Dissolved Oxygen in BH1, BH2, BH3, 98-2 (2004).

Sample Number	Normal thiosulfate (mg/L)	HACH digits	Volume thiosulfate (L)	Volume sample (L)	DO (mg/L)
BH1-21	0.0149	178	2.23E-04	0.0515	0.51
BH1-21	0.0149	476	5.95E-04	0.051	1.39
BH1-21	0.0149	478	5.98E-04	0.0515	1.38
BH1-40	0.0149	164	2.05E-04	0.0515	0.47
BH1-40	0.0149	94	1.18E-04	0.0515	0.27
BH1-40	0.0149	188	2.35E-04	0.0515	0.54
BH1-63	0.0149	134	1.68E-04	0.0515	0.39
BH1-63	0.0149	324	4.05E-04	0.0515	0.94
BH1-63	0.0149	142	1.78E-04	0.0515	0.41
BH2-17	0.149	53	6.63E-05	0.0515	1.53
BH2-17	0.149	48	6.00E-05	0.0515	1.39
BH2-38	0.149	14	1.75E-05	0.051	0.41
BH2-38	0.149	9	1.13E-05	0.051	0.26
BH2-43	0.0149	217	2.71E-04	0.051	0.63
BH2-43	0.0149	194	2.43E-04	0.051	0.57
BH2-43	0.0149	151	1.89E-04	0.051	0.44
BH3-27	0.0149	101	1.26E-04	0.0515	0.29
BH3-27	0.0149	81	1.01E-04	0.0515	0.23
BH3-27	0.0149	83	1.04E-04	0.0515	0.24
BH3-31	0.0149	91	1.14E-04	0.0515	0.26
BH3-31	0.0149	64	8.00E-05	0.0515	0.19
BH3-31	0.0149	109	1.36E-04	0.0515	0.32
BH3-50	0.0149	190	2.38E-04	0.0515	0.55
BH3-50	0.0149	77	9.63E-05	0.0515	0.22
BH3-50	0.0149	107	1.34E-04	0.0515	0.31
98-2	0.0149	637	7.96E-04	0.0515	1.84
98-2	0.0149	692	8.65E-04	0.0515	2.00
98-2	0.0149	654	8.18E-04	0.0515	1.89

Alkalinity Determination

Alkalinity was measured at each sample interval using the HACH digital titration method. A measured 50 ml of sample was put into the graduated cylinder and transferred to a 100 ml erler meyer flask. Four drops of methyl red were added to the sample and the sulphuric acid (H_2SO_4) concentration being used was recorded. In this study, 0.151 normal of H_2SO_4 was used for each sample. Titration began and the number of digits at the following colour endpoints was recorded: blue/grey, grey, violet grey and pink. The calculated concentrations of $CaCO_3$ would determine which colour endpoint to use for the results. Concentrations less than 30 mg/L use the blue-grey endpoint. Concentrations between 30 – 150 mg/L use the grey endpoint. Concentrations between 150 – 500 mg/L use the violet grey endpoint. Concentrations greater than 500 mg/L use the pink endpoint. Since the calculated concentrations were between 80 mg/L and 153 mg/L, the grey endpoint was used for determining the final concentrations. The test was repeated two to three times per sample interval. Equations D.2 to D.11 were used to determine the alkalinity. The results from the field alkalinity are found in Table 3.10.

H_2SO4 vol. acid used = No. digits on HACH meter x 0.00125 (Equation D.2)

Acid ccn. = Normality of acid used / 2 (Equation D.3)

Mols of H^+ = (Acid ccn. x acid volume x 2) / 1000 (Equation D.4)

Equivalents of H^+ = Mols of H^+ x 1 (Equation D.5)

Milliequivalents of H^+ = Equivalents of H^+ x 1000 (Equation D.6)

$$\text{Milliequivalents of } H^+ \text{ per L} = \frac{\text{Milliequivalents of } H^+}{\text{Sample volume} / 1000} \quad \text{(Equation D.7)}$$

Milliequivalents of HCO_3^- = Milliequivalents of H^+ (Equation D.8)

$$\text{Ccn. of } HCO_3^- = \frac{\text{Milliequivalents of } HCO_3^-}{(\text{sample volume}/1000) \times (1.01 + 12.01 + 3 \times 15.994)/2} \quad \text{(Equation D.9)}$$

Ccn. of CO_3^{2-} = Milliequivalents of H^+ x (12.01 + 3 x 15.994)/2 (Equation D.10)

Ccn. of $CaCO_3$ = Ccn. CO3 / (100.0862 + 59.99) (Equation D.11)

Table D.2A Field alkalinity for groundwater samples BH1, BH2, BH3 and 98-2 (Summer 2004).

ID	Colour	HACH Digits	Vol. of H2SO4 acid (mL)	Sample vol. (mL)	Norm. of acid used (N)	Ccn.of acid (M)	Mols of H+ (M)	Eqs. of H+ (eqs)	Millieqs. of H+ (meqs)	Millieqs./L (meqs/L)	Millieqs.of HCO3- (meqs)	Ccn. OF HCO3- (mg/L)	Ccn. of CO3-2 (mg/L)	Ccn. of CaCO3 (mg/L)
BH2-17	BG	489	0.611	50	0.151	0.076	9.23E-05	9.23E-05	0.092	1.85	0.092	112.64	55.37	92.35
BH2-17	G	493	0.616	50	0.151	0.076	9.31E-05	9.31E-05	0.093	1.86	0.093	113.56	55.82	93.11
BH2-17	VG	503	0.629	50	0.151	0.076	9.49E-05	9.49E-05	0.095	1.90	0.095	115.86	56.96	95.00
BH2-17	P	507	0.634	50	0.151	0.076	9.57E-05	9.57E-05	0.096	1.91	0.096	116.78	57.41	95.75
BH2-17	BG	473	0.591	50	0.151	0.076	8.93E-05	8.93E-05	0.089	1.79	0.089	108.95	53.56	89.33
BH2-17	G	478	0.598	50	0.151	0.076	9.02E-05	9.02E-05	0.090	1.80	0.090	110.10	54.13	90.28
BH2-17	VG	483	0.604	50	0.151	0.076	9.12E-05	9.12E-05	0.091	1.82	0.091	111.26	54.69	91.22
BH2-17	P	487	0.609	50	0.151	0.076	9.19E-05	9.19E-05	0.092	1.84	0.092	112.18	55.15	91.98
BH2-38	BG	521	0.651	49	0.151	0.076	9.83E-05	9.83E-05	0.098	2.01	0.098	122.46	60.20	100.41
BH2-38	G	529	0.661	49	0.151	0.076	9.98E-05	9.98E-05	0.100	2.04	0.100	124.34	61.12	101.95
BH2-38	VG	533	0.666	49	0.151	0.076	1.01E-04	1.01E-04	0.101	2.05	0.101	125.28	61.59	102.72
BH2-38	P	539	0.674	49	0.151	0.076	1.02E-04	1.02E-04	0.102	2.08	0.102	126.69	62.28	103.87
BH2-38	BG	558	0.698	49	0.151	0.076	1.05E-04	1.05E-04	0.105	2.15	0.105	131.15	64.47	107.54
BH2-38	G	562	0.703	49	0.151	0.076	1.06E-04	1.06E-04	0.106	2.16	0.106	132.10	64.94	108.31
BH2-38	VG	567	0.709	49	0.151	0.076	1.07E-04	1.07E-04	0.107	2.18	0.107	133.27	65.51	109.27
BH2-38	P	571	0.714	49	0.151	0.076	1.08E-04	1.08E-04	0.108	2.20	0.108	134.21	65.98	110.04
BH2-38	BG	531	0.664	49	0.151	0.076	1.00E-04	1.00E-04	0.100	2.05	0.100	124.81	61.35	102.33
BH2-38	G	534	0.668	49	0.151	0.076	1.01E-04	1.01E-04	0.101	2.06	0.101	125.51	61.70	102.91
BH2-38	VG	540	0.675	49	0.151	0.076	1.02E-04	1.02E-04	0.102	2.08	0.102	126.92	62.39	104.07
BH2-38	P	545	0.681	49	0.151	0.076	1.03E-04	1.03E-04	0.103	2.10	0.103	128.10	62.97	105.03
BH2-43	BG	478	0.598	50	0.151	0.076	9.02E-05	9.02E-05	0.090	1.80	0.090	110.10	54.13	90.28
BH2-43	G	490	0.613	50	0.151	0.076	9.25E-05	9.25E-05	0.092	1.85	0.092	112.87	55.49	92.54
BH2-43	VG	502	0.628	50	0.151	0.076	9.48E-05	9.48E-05	0.095	1.90	0.095	115.63	56.84	94.81
BH2-43	P	512	0.640	50	0.151	0.076	9.66E-05	9.66E-05	0.097	1.93	0.097	117.94	57.98	96.70
BH2-43	BG	480	0.600	50	0.151	0.076	9.06E-05	9.06E-05	0.091	1.81	0.091	110.56	54.35	90.65
BH2-43	G	484	0.605	50	0.151	0.076	9.14E-05	9.14E-05	0.091	1.83	0.091	111.49	54.81	91.41

Table D.2B Field alkalinity for groundwater samples BH1, BH2, BH3 and 98-2 (Summer 2004).

ID	Colour	Digits	Vol. of H2SO4 acid (mL)	Sample vol. (mL)	Norm. of acid used (N)	Ccn.of acid (M)	Mols of H+ (M)	Eqs. of H+ (eqs)	Millieqs. of H+ (meqs)	Millieqs./L (meqs/L)	Millieqs.of HCO3- (meqs)	Ccn. OF HCO3- (mg/L)	Ccn. of CO3-2 (mg/L)	Ccn. of CaCO3 (mg/L)
BH2-43	VG	490	0.613	50	0.151	0.076	9.25E-05	9.25E-05	0.092	1.85	0.092	112.87	55.49	92.54
BH2-43	P	498	0.623	50	0.151	0.076	9.40E-05	9.40E-05	0.094	1.88	0.094	114.71	56.39	94.05
BH1-21	BG	480	0.600	50	0.151	0.076	9.06E-05	9.06E-05	0.091	1.81	0.091	110.56	54.35	90.65
BH1-21	G	488	0.610	50	0.151	0.076	9.21E-05	9.21E-05	0.092	1.84	0.092	112.41	55.26	92.16
BH1-21	VG	495	0.619	50	0.151	0.076	9.34E-05	9.34E-05	0.093	1.87	0.093	114.02	56.05	93.49
BH1-21	P	506	0.633	50	0.151	0.076	9.55E-05	9.55E-05	0.096	1.91	0.096	116.55	57.30	95.56
BH1-21	BG	519	0.649	50	0.151	0.076	9.80E-05	9.80E-05	0.098	1.96	0.098	119.55	58.77	98.02
BH1-21	G	523	0.654	50	0.151	0.076	9.87E-05	9.87E-05	0.099	1.97	0.099	120.47	59.22	98.77
BH1-21	VG	529	0.661	50	0.151	0.076	9.98E-05	9.98E-05	0.100	2.00	0.100	121.85	59.90	99.91
BH1-21	P	536	0.670	50	0.151	0.076	1.01E-04	1.01E-04	0.101	2.02	0.101	123.46	60.69	101.23
BH1-40	BG	563	0.704	50	0.151	0.076	1.06E-04	1.06E-04	0.106	2.13	0.106	129.68	63.75	106.33
BH1-40	G	572	0.715	50	0.151	0.076	1.08E-04	1.08E-04	0.108	2.16	0.108	131.76	64.77	108.03
BH1-40	VG	582	0.728	50	0.151	0.076	1.10E-04	1.10E-04	0.110	2.20	0.110	134.06	65.90	109.92
BH1-40	P	592	0.740	50	0.151	0.076	1.12E-04	1.12E-04	0.112	2.23	0.112	136.36	67.04	111.81
BH1-40	BG	573	0.716	50	0.151	0.076	1.08E-04	1.08E-04	0.108	2.16	0.108	131.99	64.88	108.22
BH1-40	G	580	0.725	50	0.151	0.076	1.09E-04	1.09E-04	0.109	2.19	0.109	133.60	65.68	109.54
BH1-40	VG	592	0.740	50	0.151	0.076	1.12E-04	1.12E-04	0.112	2.23	0.112	136.36	67.04	111.81
BH1-40	P	597	0.746	50	0.151	0.076	1.13E-04	1.13E-04	0.113	2.25	0.113	137.52	67.60	112.75
BH1-63	BG	715	0.894	50	0.151	0.076	1.35E-04	1.35E-04	0.135	2.70	0.135	164.70	80.96	135.04
BH1-63	G	725	0.906	50	0.151	0.076	1.37E-04	1.37E-04	0.137	2.74	0.137	167.00	82.10	136.92
BH1-63	VG	731	0.914	50	0.151	0.076	1.38E-04	1.38E-04	0.138	2.76	0.138	168.38	82.77	138.06
BH1-63	P	735	0.919	50	0.151	0.076	1.39E-04	1.39E-04	0.139	2.77	0.139	169.30	83.23	138.81
BH1-63	BG	710	0.888	50	0.151	0.076	1.34E-04	1.34E-04	0.134	2.68	0.134	163.54	80.40	134.09
BH1-63	G	716	0.895	50	0.151	0.076	1.35E-04	1.35E-04	0.135	2.70	0.135	164.93	81.08	135.22
BH1-63	VG	723	0.904	50	0.151	0.076	1.36E-04	1.36E-04	0.136	2.73	0.136	166.54	81.87	136.55
BH1-63	P	729	0.911	50	0.151	0.076	1.38E-04	1.38E-04	0.138	2.75	0.138	167.92	82.55	137.68

Table D.2C Field alkalinity for groundwater samples BH1, BH2, BH3 and 98-2 (Summer 2004).

ID	Colour	Digits	Vol. of H2SO4 acid (mL)	Sample vol. (mL)	Norm. of acid used (N)	Ccn.of acid (M)	Mols of H+ (M)	Eqs. of H+ (eqs)	Millieqs. of H+ (meqs)	Millieqs./L (meqs/L)	Millieqs.of HCO3- (meqs)	Ccn. OF HCO3- (mg/L)	Ccn. of CO3-2 (mg/L)	Ccn. of CaCO3 (mg/L)
BH3-50	BG	676	0.845	50	0.151	0.076	1.28E-04	1.28E-04	0.128	2.55	0.128	155.71	76.55	127.67
BH3-50	G	698	0.873	50	0.151	0.076	1.32E-04	1.32E-04	0.132	2.63	0.132	160.78	79.04	131.83
BH3-50	VG	707	0.884	50	0.151	0.076	1.33E-04	1.33E-04	0.133	2.67	0.133	162.85	80.06	133.53
BH3-50	P	715	0.894	50	0.151	0.076	1.35E-04	1.35E-04	0.135	2.70	0.135	164.70	80.96	135.04
BH3-50	BG	796	0.995	51	0.151	0.076	1.50E-04	1.50E-04	0.150	2.95	0.150	179.76	88.37	147.39
BH3-50	G	804	1.005	51	0.151	0.076	1.52E-04	1.52E-04	0.152	2.98	0.152	181.57	89.26	148.87
BH3-50	VG	819	1.024	51	0.151	0.076	1.55E-04	1.55E-04	0.155	3.03	0.155	184.95	90.92	151.64
BH3-50	P	829	1.036	51	0.151	0.076	1.56E-04	1.56E-04	0.156	3.07	0.156	187.21	92.03	153.50
BH3-50	BG	630	0.788	50	0.151	0.076	1.19E-04	1.19E-04	0.119	2.38	0.119	145.12	71.34	118.98
BH3-50	G	643	0.804	50	0.151	0.076	1.21E-04	1.21E-04	0.121	2.43	0.121	148.11	72.81	121.44
BH3-50	VG	658	0.823	50	0.151	0.076	1.24E-04	1.24E-04	0.124	2.48	0.124	151.57	74.51	124.27
BH3-50	P	671	0.839	50	0.151	0.076	1.27E-04	1.27E-04	0.127	2.53	0.127	154.56	75.98	126.73
BH3-31	BG	586	0.733	50	0.151	0.076	1.11E-04	1.11E-04	0.111	2.21	0.111	134.98	66.36	110.67
BH3-31	G	592	0.740	50	0.151	0.076	1.12E-04	1.12E-04	0.112	2.23	0.112	136.36	67.04	111.81
BH3-31	VG	601	0.751	50	0.151	0.076	1.13E-04	1.13E-04	0.113	2.27	0.113	138.44	68.05	113.51
BH3-31	P	610	0.763	50	0.151	0.076	1.15E-04	1.15E-04	0.115	2.30	0.115	140.51	69.07	115.21
BH3-31	BG	585	0.731	50	0.151	0.076	1.10E-04	1.10E-04	0.110	2.21	0.110	134.75	66.24	110.48
BH3-31	G	592	0.740	50	0.151	0.076	1.12E-04	1.12E-04	0.112	2.23	0.112	136.36	67.04	111.81
BH3-31	VG	599	0.749	50	0.151	0.076	1.13E-04	1.13E-04	0.113	2.26	0.113	137.98	67.83	113.13
BH3-31	P	606	0.758	50	0.151	0.076	1.14E-04	1.14E-04	0.114	2.29	0.114	139.59	68.62	114.45
BH3-27	BG	601	0.751	50	0.151	0.076	1.13E-04	1.13E-04	0.113	2.27	0.113	138.44	68.05	113.51
BH3-27	G	618	0.773	50	0.151	0.076	1.17E-04	1.17E-04	0.117	2.33	0.117	142.35	69.98	116.72
BH3-27	VG	626	0.783	50	0.151	0.076	1.18E-04	1.18E-04	0.118	2.36	0.118	144.20	70.89	118.23
BH3-27	P	633	0.791	50	0.151	0.076	1.19E-04	1.19E-04	0.119	2.39	0.119	145.81	71.68	119.55
BH3-27	BG	600	0.750	50	0.151	0.076	1.13E-04	1.13E-04	0.113	2.27	0.113	138.21	67.94	113.32
BH3-27	G	611	0.764	50	0.151	0.076	1.15E-04	1.15E-04	0.115	2.31	0.115	140.74	69.19	115.39

Table D.2D Field alkalinity for groundwater samples BH1, BH2, BH3 and 98-2 (Summer 2004).

ID	Colour	Digits	Vol. of H2SO4 acid (mL)	Sample vol. (mL)	Norm. of acid used (N)	Ccn.of acid (M)	Mols of H+ (M)	Eqs. of H+ (eqs)	Millieqs. of H+ (meqs)	Millieqs./L (meqs/L)	Millieqs.of HCO3- (meqs)	Ccn. OF HCO3- (mg/L)	Ccn. of CO3-2 (mg/L)	Ccn. of CaCO3 (mg/L)
BH3-27	VG	620	0.775	50	0.151	0.076	1.17E-04	1.17E-04	0.117	2.34	0.117	142.81	70.21	117.09
BH3-27	P	627	0.784	50	0.151	0.076	1.18E-04	1.18E-04	0.118	2.37	0.118	144.43	71.00	118.42
98-2	BG	443	0.554	50	0.151	0.076	8.36E-05	8.36E-05	0.084	1.67	0.084	102.04	50.16	83.67
98-2	G	450	0.563	50	0.151	0.076	8.49E-05	8.49E-05	0.085	1.70	0.085	103.65	50.96	84.99
98-2	VG	456	0.570	50	0.151	0.076	8.61E-05	8.61E-05	0.086	1.72	0.086	105.04	51.64	86.12
98-2	P	467	0.584	50	0.151	0.076	8.81E-05	8.81E-05	0.088	1.76	0.088	107.57	52.88	88.20
98-2	BG	426	0.533	50	0.151	0.076	8.04E-05	8.04E-05	0.080	1.61	0.080	98.13	48.24	80.46
98-2	G	432	0.540	50	0.151	0.076	8.15E-05	8.15E-05	0.082	1.63	0.082	99.51	48.92	81.59
98-2	VG	441	0.551	50	0.151	0.076	8.32E-05	8.32E-05	0.083	1.66	0.083	101.58	49.94	83.29
98-2	P	448	0.560	50	0.151	0.076	8.46E-05	8.46E-05	0.085	1.69	0.085	103.19	50.73	84.61
98-2	BG	427	0.534	50	0.151	0.076	8.06E-05	8.06E-05	0.081	1.61	0.081	98.36	48.35	80.64
98-2	G	432	0.540	50	0.151	0.076	8.15E-05	8.15E-05	0.082	1.63	0.082	99.51	48.92	81.59
98-2	VG	443	0.554	50	0.151	0.076	8.36E-05	8.36E-05	0.084	1.67	0.084	102.04	50.16	83.67
98-2	P	449	0.561	50	0.151	0.076	8.47E-05	8.47E-05	0.085	1.69	0.085	103.42	50.84	84.80

Table D.3A Ion analysis results for groundwater samples BH1, BH2, BH3 and 98-2 (Summer 2004).

Sample	Mg	Al	Si	Ar	K	Cr	Mn	Fe	Co	Ni	Cu	Zn	As	Cd	Pb	Sr	Mo	In	Sn	Be
	(mg/L)	(mg/L)	(mg/L)	(cps)	(mg/L)	(mg/L)	(mg/L)	(mg/L)	(mg/L)	(mg/L)	(mg/L)	(mg/L)	(mg/L)	(mg/L)	(mg/L)	(mg/L)	(mg/L)	(mg/L)	(mg/L)	(mg/L)
BH1-21	3.69	0.027	4.94	21286056	0.926	0.002	0.084	0.032	0.001	0.008	0.006	0.031	0.003	0.006	0.004	1.008	0.006	0.047	0.003	0.000
BH1-40	4.04	0.024	5.00	20102247	0.930	0.004	0.064	0.005	0.003	0.012	0.005	0.002	0.010	0.007	0.010	1.404	0.001	0.035	0.009	0.000
BH1-63	0.35	0.057	4.54	22479351	0.543	0.001	0.002	0.013	0.001	0.005	0.005	0.000	0.014	0.008	0.023	0.202	0.020	0.032	0.009	0.000
BH2-17	3.42	0.030	4.84	22297431	1.020	0.006	0.056	0.001	0.000	0.010	0.001	0.030	0.001	0.005	0.011	0.732	0.001	0.060	0.002	0.000
BH2-38	3.86	0.034	4.88	21901204	0.893	0.002	0.083	0.002	0.005	0.009	0.005	0.016	0.007	0.006	0.016	1.113	0.002	0.051	0.022	0.000
BH2-43	1.29	0.020	4.12	22802034	0.703	0.002	0.037	0.006	0.003	0.008	0.003	0.009	0.009	0.005	0.010	0.501	0.004	0.003	0.021	0.000
BH3-27	3.91	0.023	5.16	21173225	0.859	0.002	0.337	0.080	0.004	0.014	0.002	0.028	0.015	0.005	0.018	0.542	0.004	0.008	0.007	0.000
BH3-31	3.44	0.030	4.98	22216367	0.766	0.001	0.268	0.043	0.000	0.007	0.011	0.014	0.011	0.007	0.010	0.533	0.008	0.018	0.003	0.000
BH3-50	4.13	0.027	5.02	20870822	0.903	0.001	0.275	1.118	0.002	0.014	0.003	0.097	0.002	0.006	0.009	0.582	0.002	0.035	0.004	0.000
98-2-61	2.58	0.143	4.53	21576318	1.300	0.002	0.072	0.514	0.006	0.010	0.008	0.044	0.003	0.008	0.016	0.275	0.006	0.016	0.005	0.000

Table D.3B Ion analysis results for groundwater samples BH1, BH2, BH3 and 98-2 (Summer 2004).

Sample No	Br (mg/L)	Cl (mg/L)	F (mg/L)	NO_3 (mg/L)	SO_4 (mg/L)	HCO_3* (mg/L)	Ba (mg/L)	Sb (mg/L)	V (mg/L)	Ca (mg/L)	Na (mg/L)
BH1-21	0.04	22.9	0.23	nd	19.3	116	0.095	0.016	0.001	35.3	19.6
BH1-40	0.04	26.5	0.19	0.25	24.2	133	0.103	0.005	0.002	43.0	17.5
BH1-63	nd	12.2	1.44	nd	19.1	166	0.011	0.074	0.002	5.6	70.3
BH2-17	0.04	16.8	0.22	nd	15.2	112	0.093	0.021	0.002	29.9	18.3
BH2-38	0.05	23.1	0.20	nd	22.9	139	0.086	0.001	0.003	37.7	19.0
BH2-43	0.04	15.6	0.33	nd	16.1	125	0.063	0.002	0.004	15.8	40.2
BH3-27	nd	3.2	0.19	nd	20.1	142	0.092	0.006	0.002	31.6	19.8
BH3-31	nd	2.2	0.20	nd	20.4	136	0.086	0.040	0.001	28.3	21.5
BH3-50	nd	5.0	0.20	nd	18.0	163	0.095	0.015	0.001	30.8	23.5
98-2-61	0.04	18.5	0.25	nd	18.7	101	0.040	0.026	0.003	14.7	33.8

nd = non detect

* Alkalinity measured in the field as bicarbonate (HCO_3).

Table D.4A Trace element analysis results for groundwater samples BH1, BH2, BH3 and 98-2 (Summer 2004).

Sample	Li 6 (ppm)	B (ppm)	C (cps)	N (cps)	P (ppm)	S (ppm)	Ti (ppm)	V (ppm)	Se 77 (ppm)	Br (ppm)	Se (ppm)
BH1-21	9.24	<25.77	43268670	482973800	<2285	7612	2.06	0.26	<1.22	<169.15	<0.91
BH1-40	9.77	<25.75	43248424	489354074	<2283	8066	2.21	0.29	<1.22	181.65	<0.99
BH1-63	40.97	63.72	48130438	507169871	3184	6922	3.28	0.24	<1.22	<169.92	<0.91
BH2-17	8.21	<25.74	43136559	501743099	<2282	6576	2.10	0.39	<1.22	<168.96	<0.91
BH2-38	8.88	<26.01	43676799	485972907	<2306	6922	2.12	0.40	<1.23	<170.75	<0.92
BH2-43	19.08	28.65	53692830	52066456	<39	4520	<0.62	<0.80	<6.69	22.54	<0.54
BH3-27	7.52	<26.41	43621594	495690550	<2341	85719	2.40	<0.09	<1.24	<173.33	<0.97
BH3-31	7.68	<25.74	44036771	521572451	<2282	11910	2.04	0.09	<1.21	<168.93	<0.90
BH3-50	9.56	<22.37	54453900	52545655	<39	5883	<0.62	<0.79	<6.58	11.73	<0.54
98-2-61	7.64	<23.08	52063666	49136712	<40	4820	11.19	<0.82	<6.86	24.98	<0.56

Table D.4B Trace element analysis results for groundwater samples BH1, BH2, BH3 and 98-2 (Summer 2004).

Sample	Rb (ppm)	Ag (ppm)	Sb (ppm)	I (ppm)	Cs (ppm)	Ba (ppm)	La (ppm)	Ce (ppm)	Hg (ppm)	Tl (ppm)	Bi (ppm)	U (ppm)
BH1-21	0.98	0.45	0.03	3.73	<0.01	85.16	0.01	0.02	0.21	0.93	<0.01	1.07
BH1-40	0.89	0.01	0.03	4.12	<0.01	100.75	0.01	0.01	9.59	1.12	<0.01	1.65
BH1-63	0.49	0.02	0.07	2.95	0.02	11.40	0.06	0.14	0.32	0.38	<0.01	0.39
BH2-17	0.69	<0.01	0.03	3.58	<0.01	75.81	0.01	0.01	<0.04	0.68	<0.01	0.97
BH2-38	0.71	<0.01	0.03	3.42	<0.01	83.42	0.01	0.01	<0.04	0.93	<0.01	1.31
BH2-43	0.37	<0.02	0.01	7.02	<0.00	39.32	0.00	<0.00	0.12	0.02	<0.00	0.33
BH3-27	0.58	0.04	0.09	4.90	0.01	91.91	0.04	0.12	0.33	0.09	<0.01	0.64
BH3-31	0.57	<0.01	0.06	5.47	<0.01	81.82	0.02	0.04	<0.04	<0.09	<0.01	0.56
BH3-50	0.54	<0.02	0.07	6.58	0.00	89.43	0.01	0.01	0.05	<0.01	<0.00	0.40
98-2-61	0.62	<0.02	0.08	10.34	0.04	41.07	1.04	2.17	0.05	0.03	0.01	0.84

APPENDIX E GEOPHYSICAL DATA

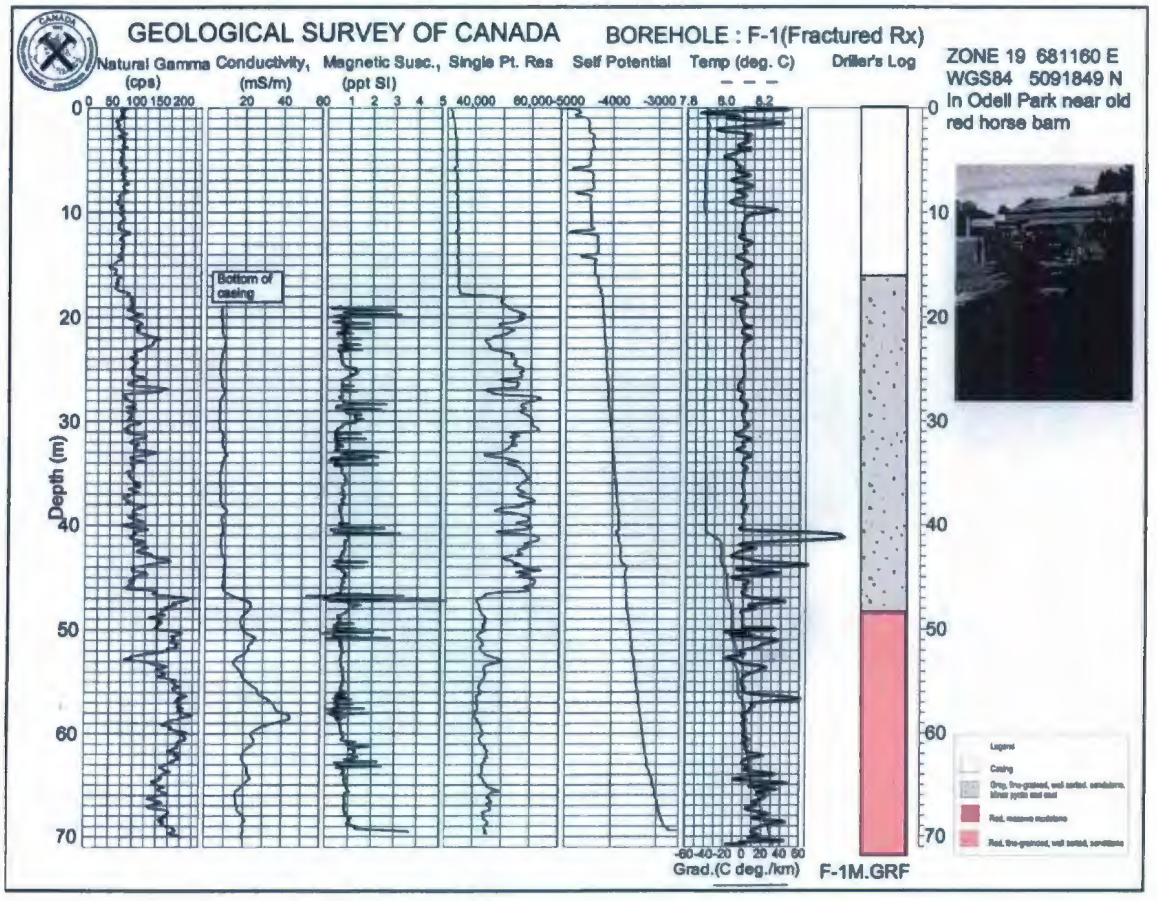

Figure E.1. Geophysical log of borehole BH01 provided by the Geological Survey of Canada (unpublished data, 2003).

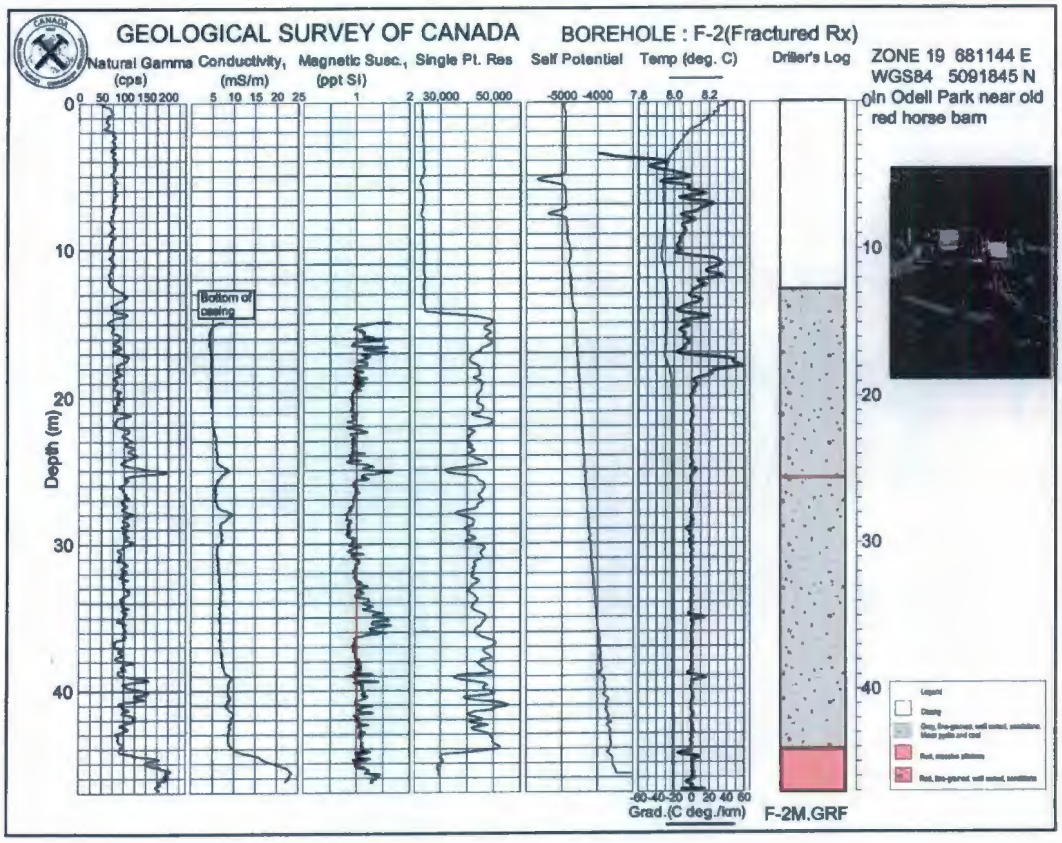

Figure E.2. Geophysical log of borehole BH02 provided by the Geological Survey of Canada (unpublished data, 2003).

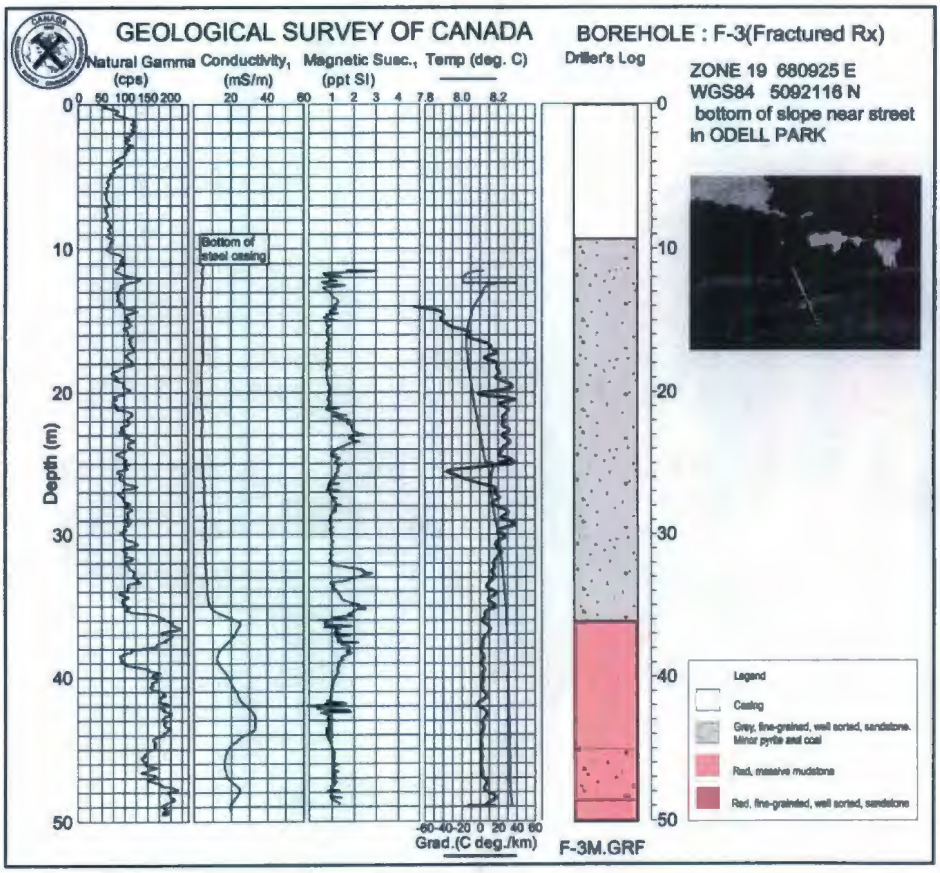

Figure E.3. Geophysical log of borehole BH03 provided by the Geological Survey of Canada (unpublished data, 2003).

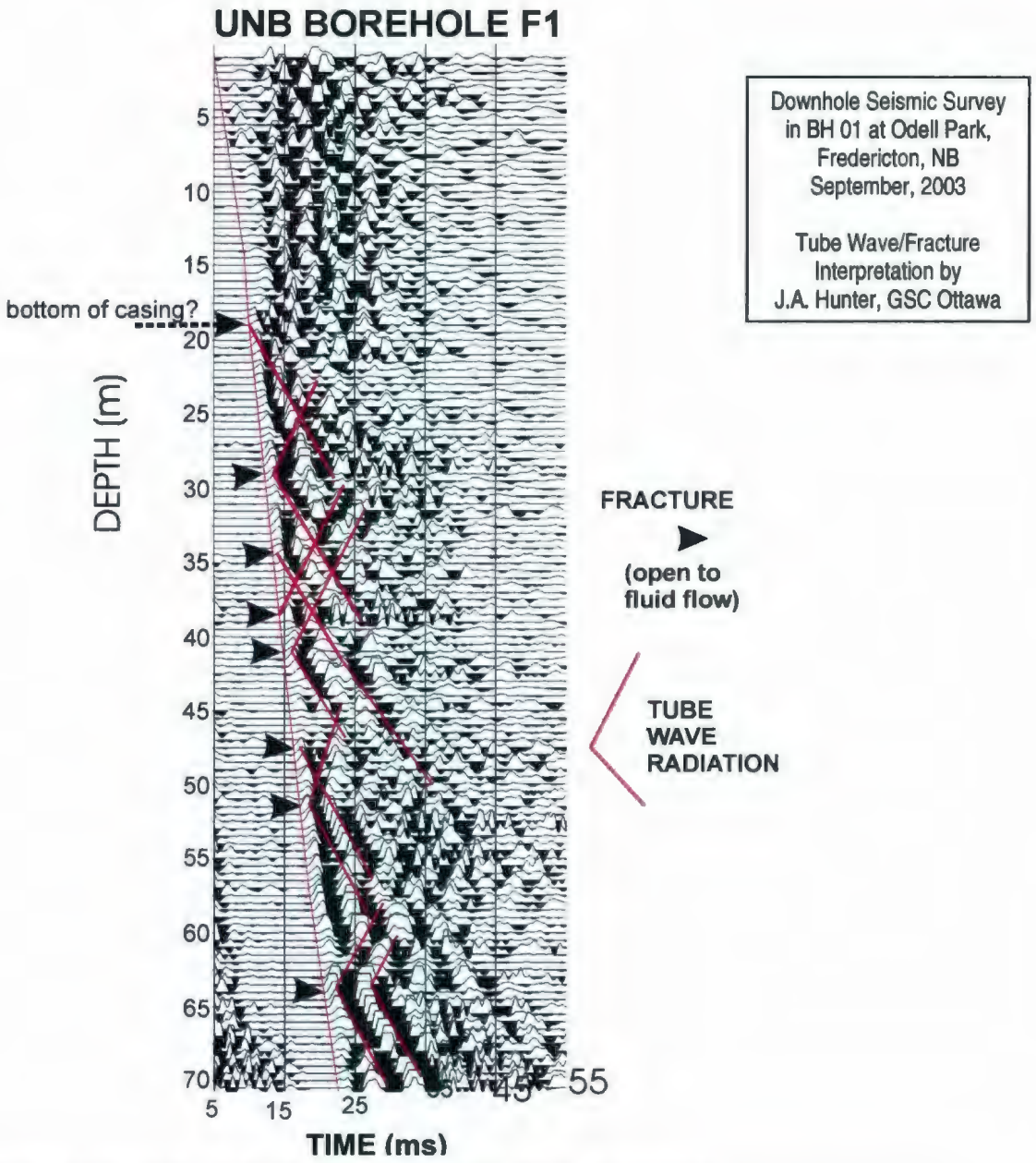

Jim Hunter's Interpretation of the Downhole Seismic Record from Borehole F-1
Shown is a filtered (50-400-800-1200 Hz) downhole seismic section acquired using a buffalo gun source at surface and a hydrophone streamer (with 0.5 m hydrophone spacing) in fractured rock borehole F-1 at Odell Park, Fredericton. The interpreted positions of cracks open to fluid flow are indicated with arrows on the depth axis. These are based on the radiation patterns of tube waves emanating from the P-wave first arrival. The interpretation must take into account interference associated with overlapping wave-trains emanating from some closely spaced fractures.

Figure E.4. Interpretation of seismic record by J. A. Hunter for BH01 provided by the Geological Survey of Canada (unpublished data, 2003).

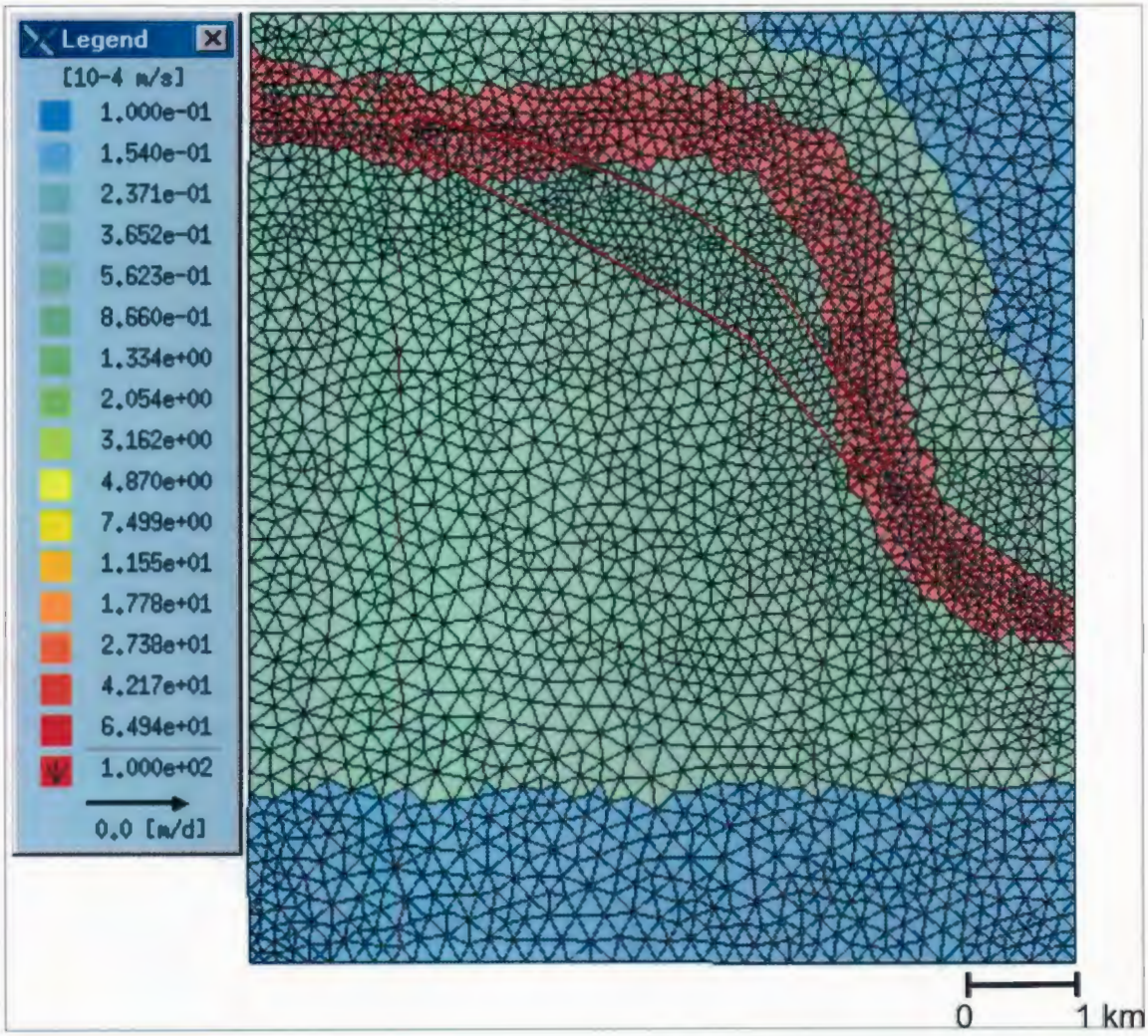

Figure F.1. Hydraulic conductivity values used for the sand and gravel Layer 1 in model.

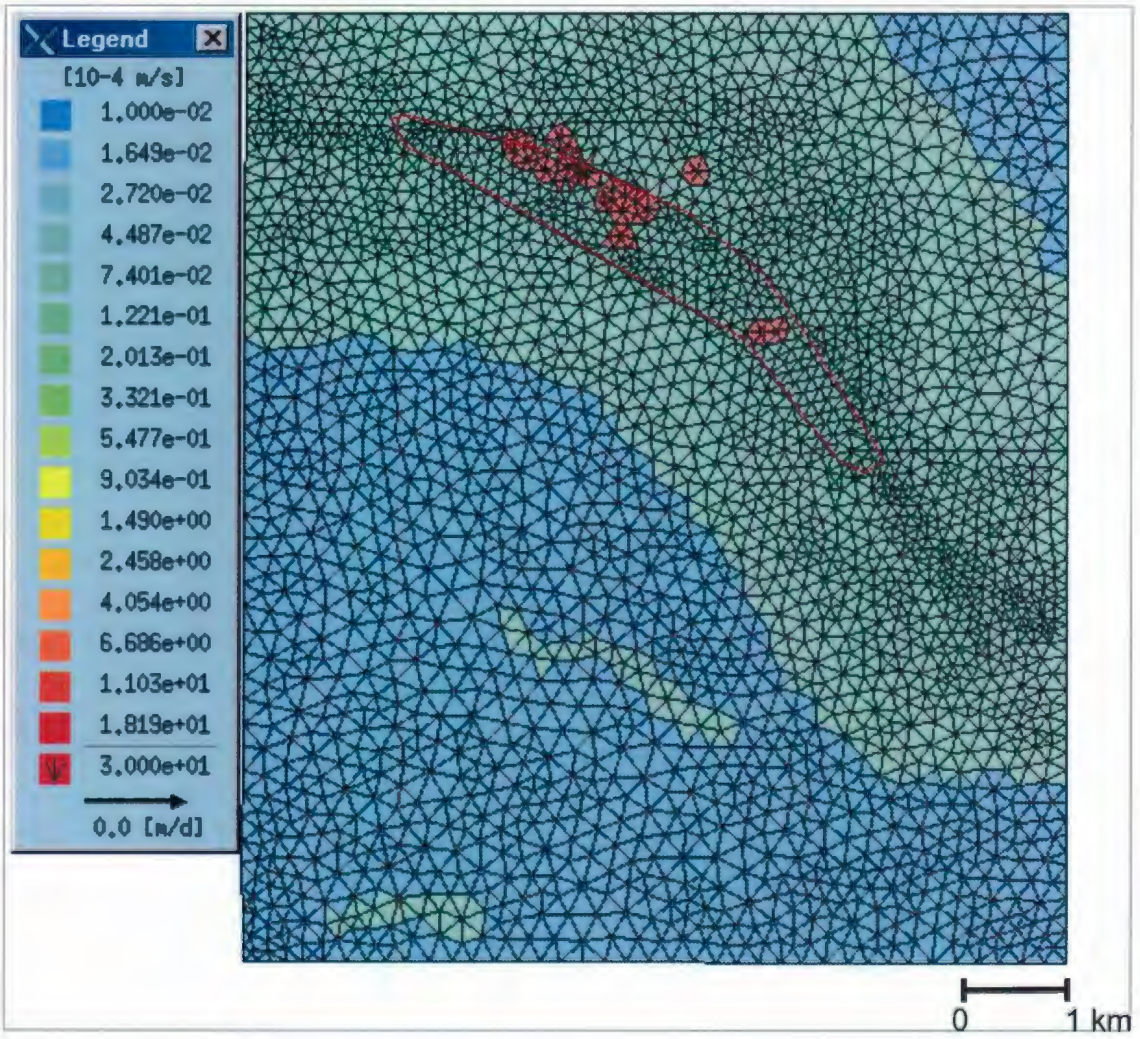

Figure F.2. Hydraulic conductivity values used for the clay Layer 2 in model.

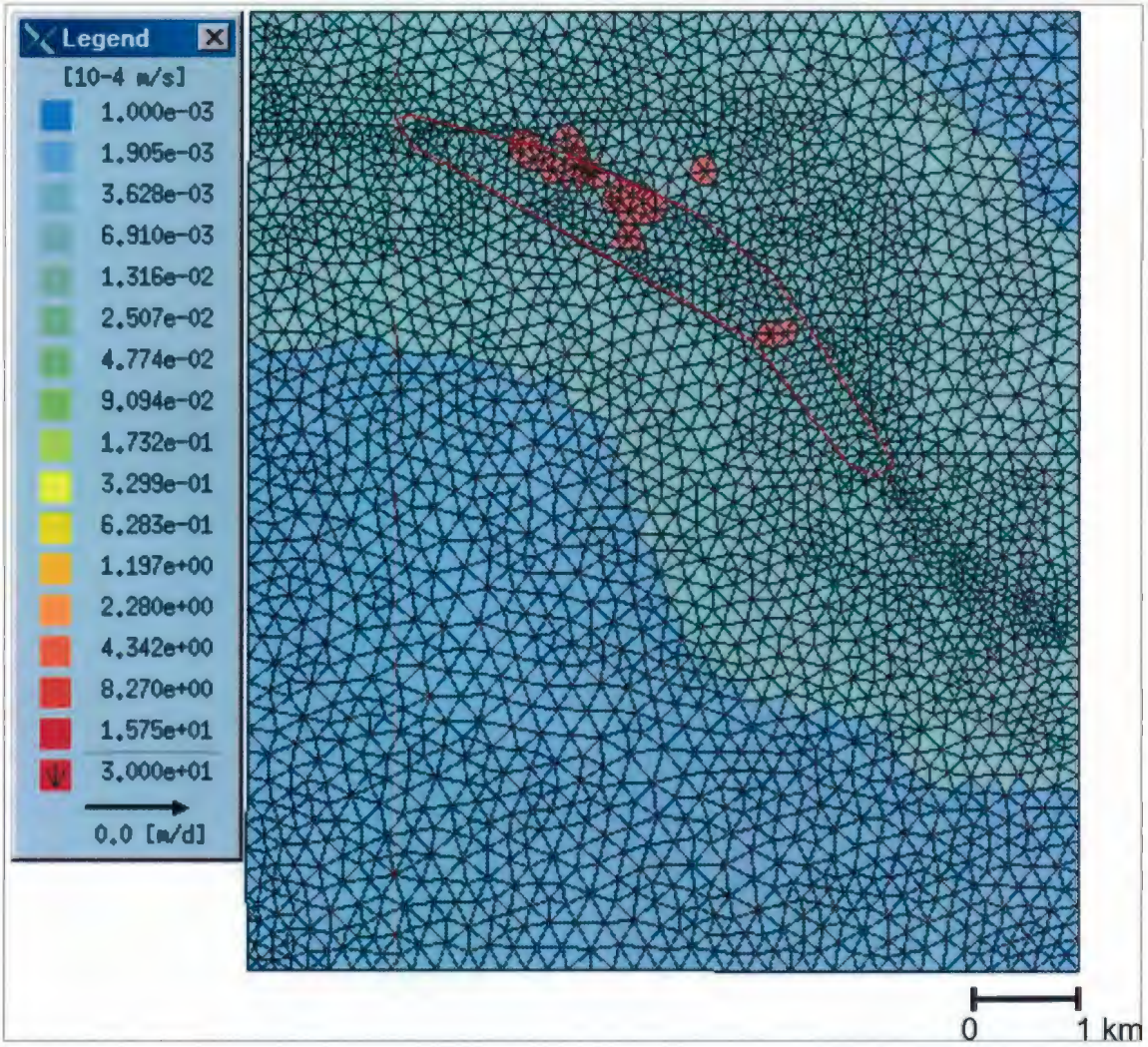

Figure F.3. Hydraulic conductivity values used for the clay Layer 3 in model.

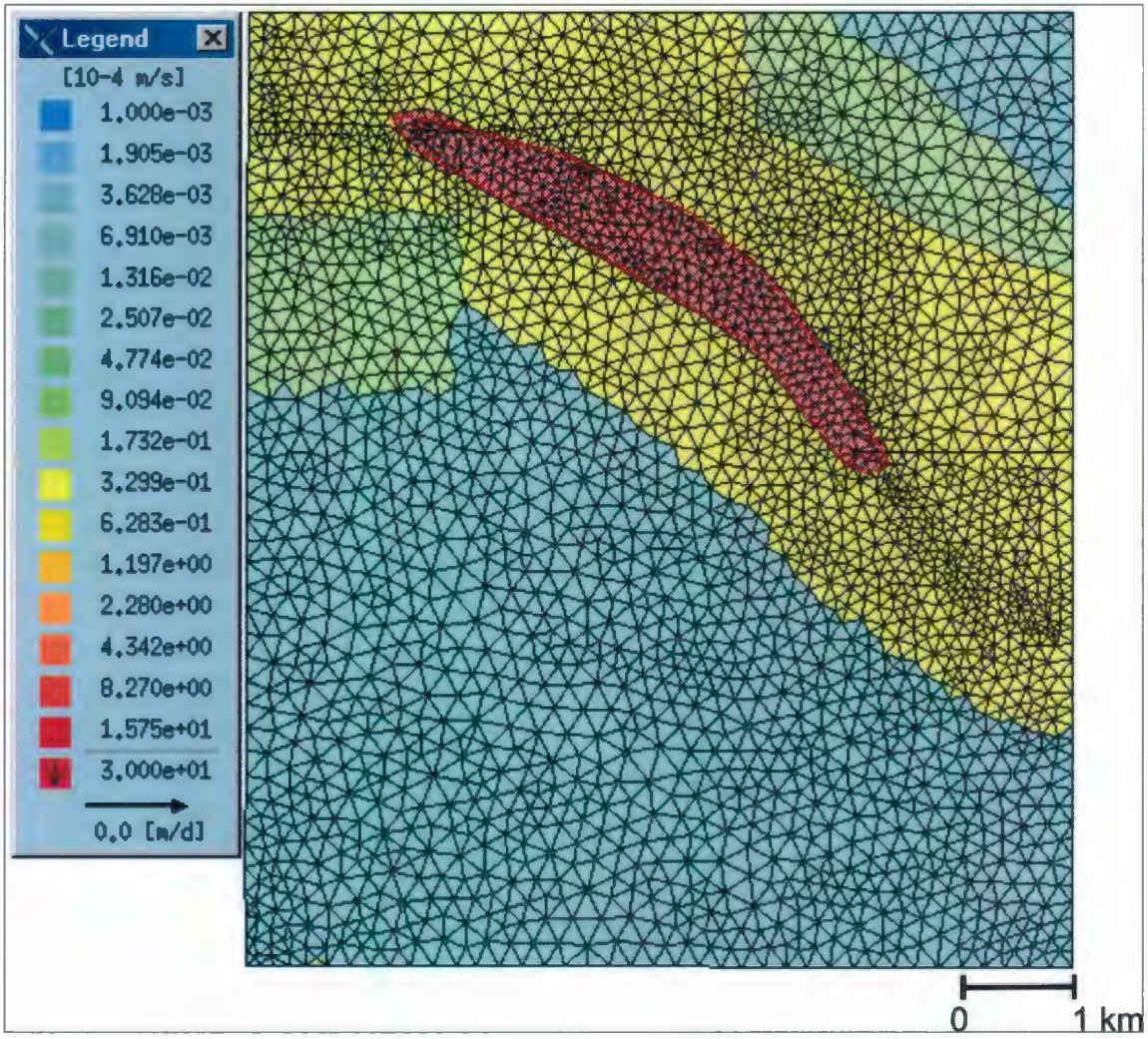

Figure F.4. Hydraulic conductivity values used for the sand and gravel aquifer Layer 4 in model.

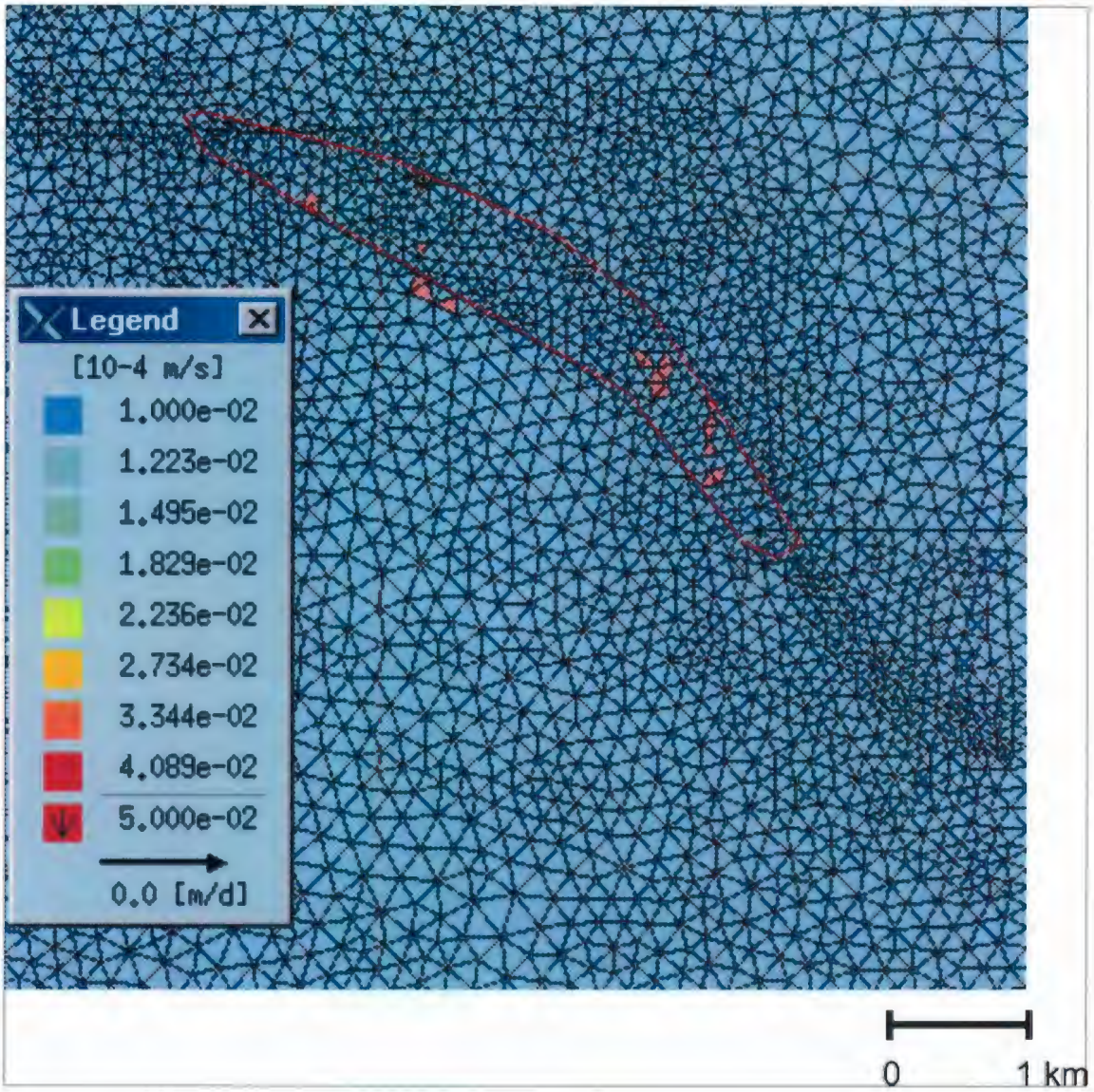

Figure F.5. Hydraulic conductivity values used for the till Layer 5 in model using the database till window information.

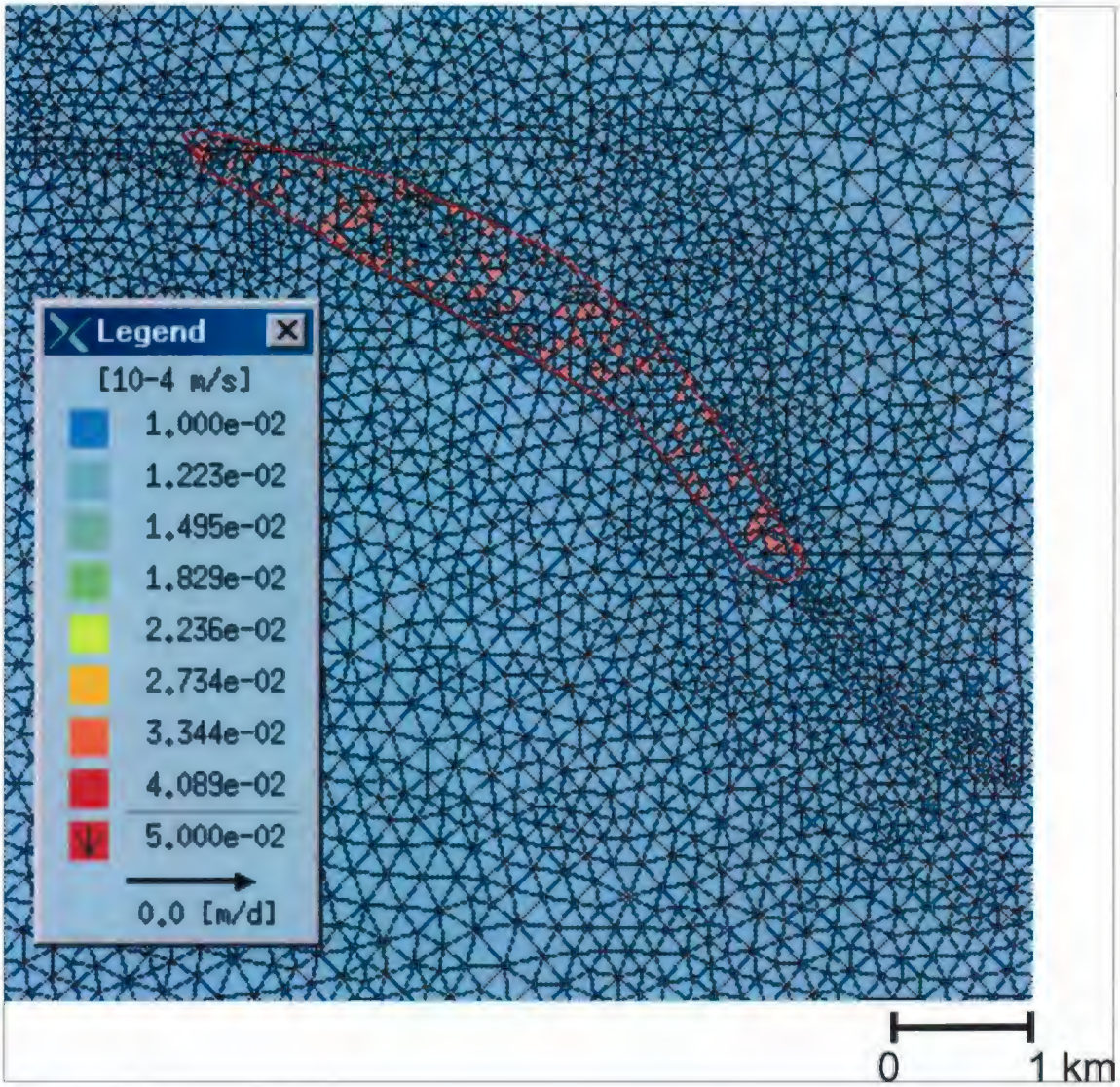

Figure F.6. Hydraulic conductivity values used for the till Layer 5 using the randomly assigned windows in the till layer.

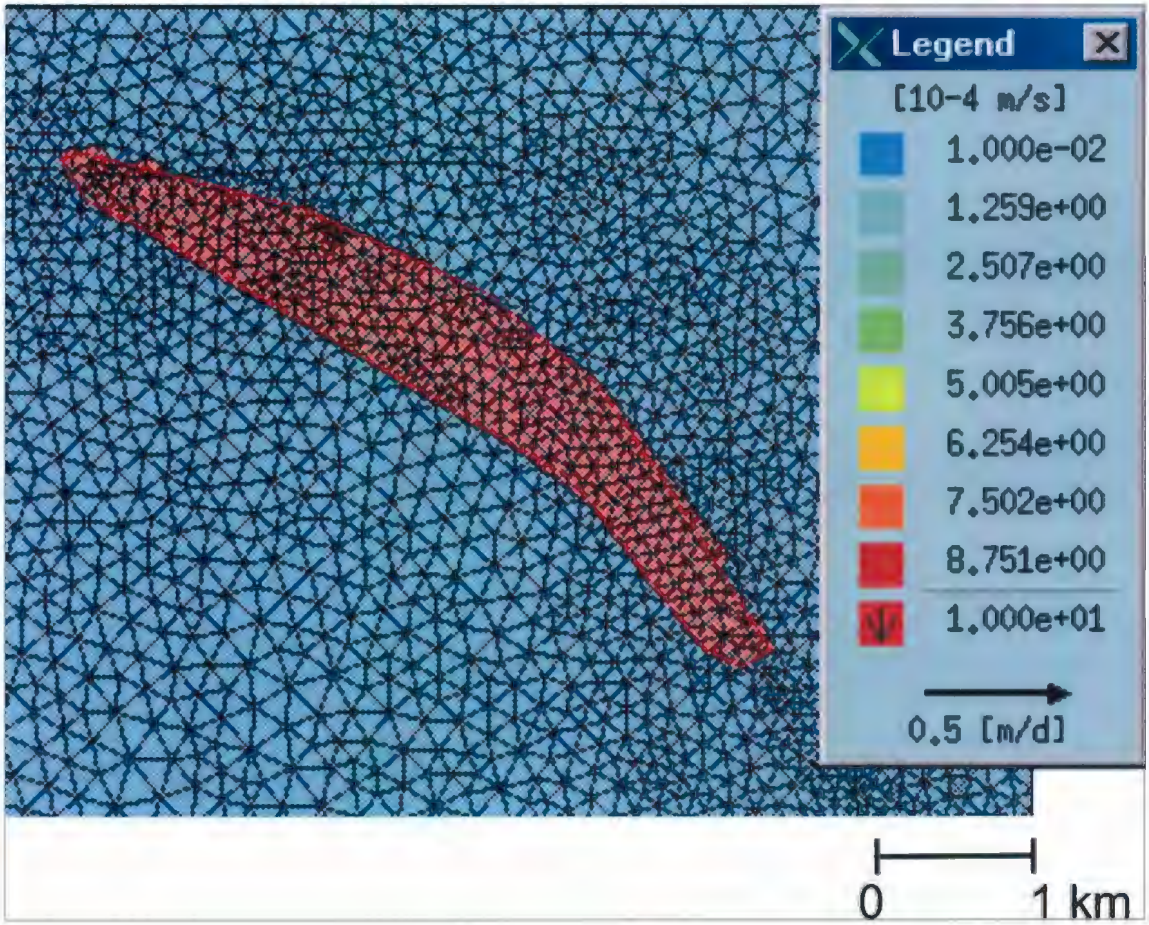

Figure F.7. Hydraulic conductivity values used for the sand and gravel Layer 6 in model.

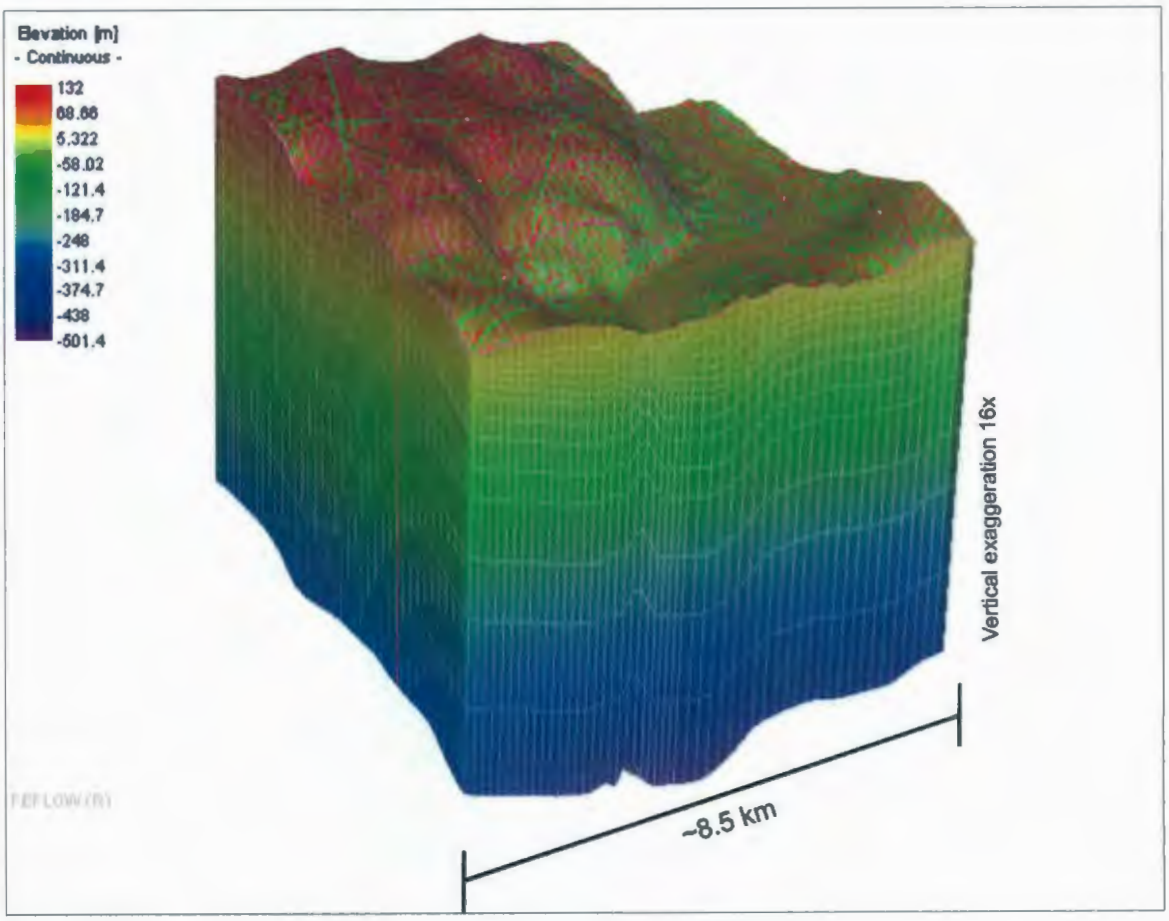

Figure F.8. Elevation range of model domain.

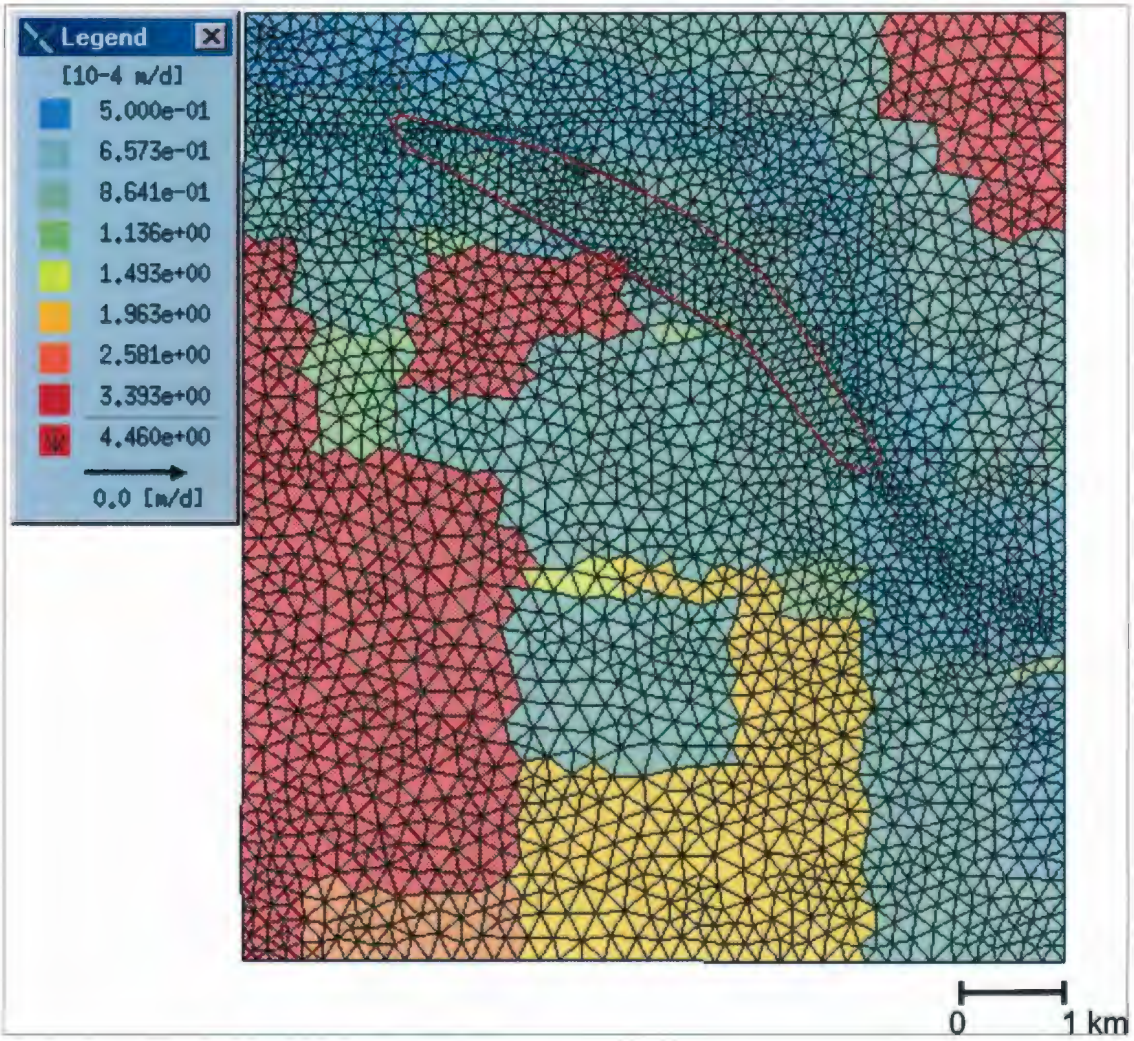

Figure F.9. Recharge values used for the top layer in model.

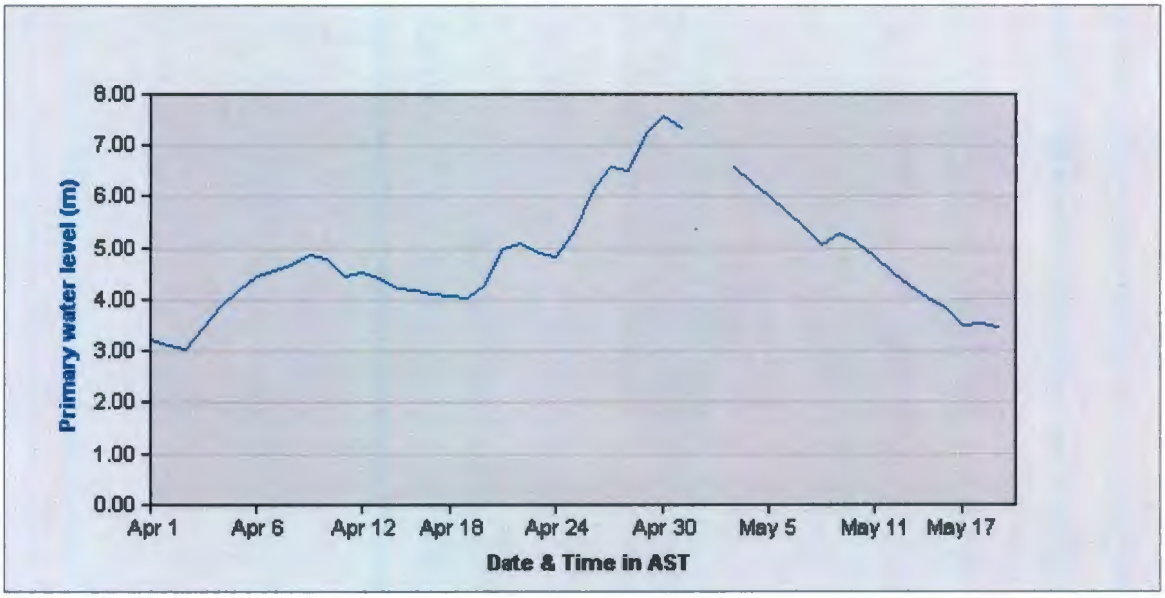

Figure F.10. Saint John River water levels during snapshot period April 1 – May 20, 2005.

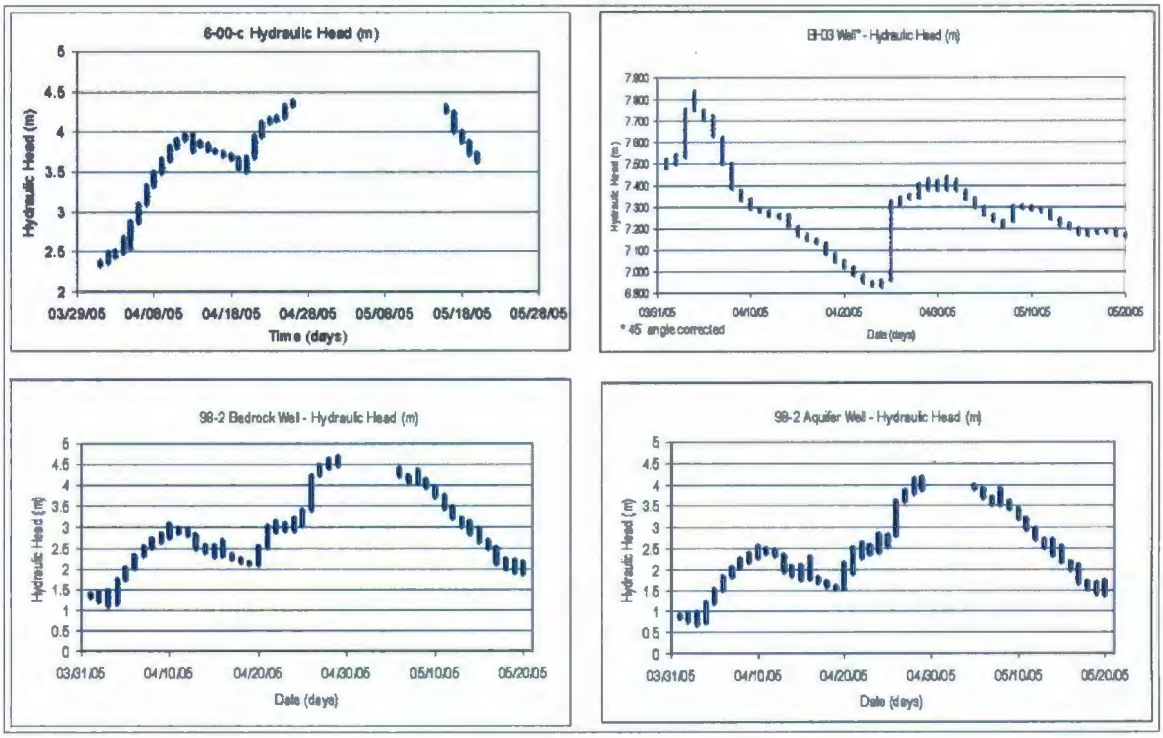

Figure F.11. Bedrock wells 6-00, BH03, 98-2 and aquifer well 98-2 water levels during snapshot period April 1 – May 20, 2005.

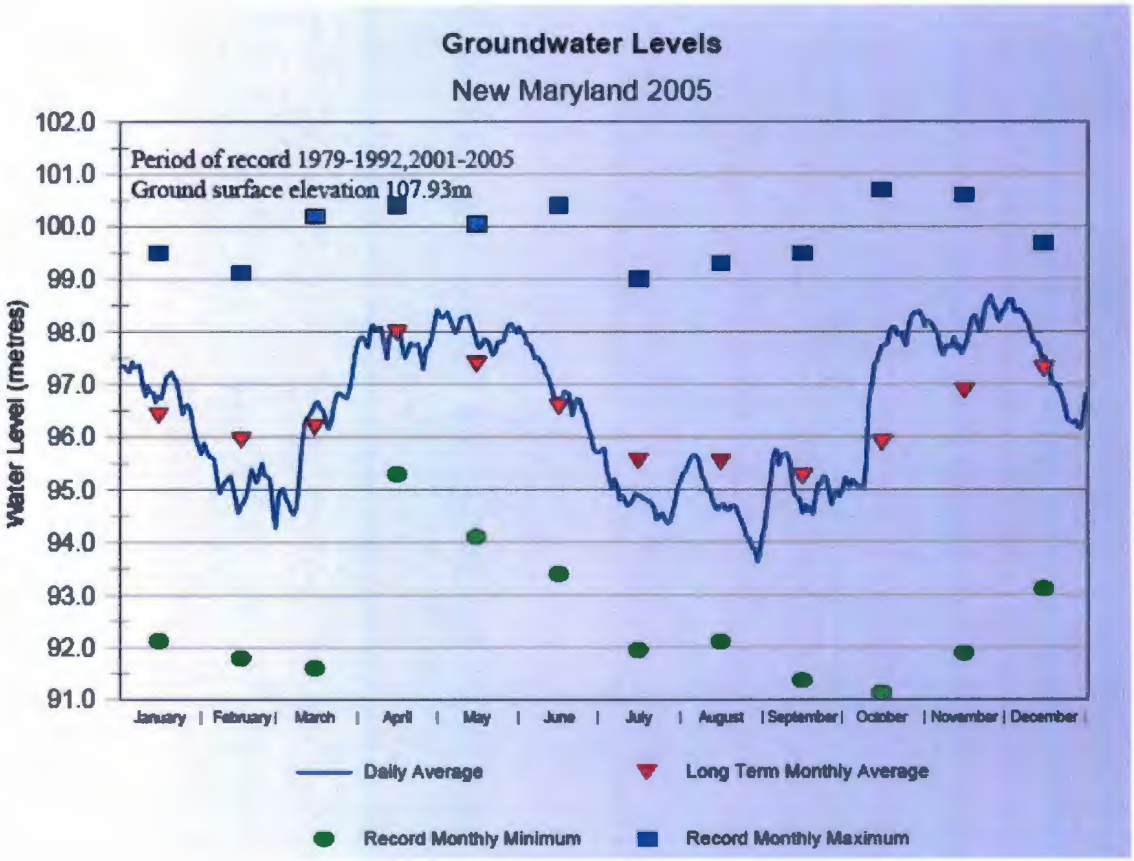

Figure F.12. New Maryland water levels from January to December, 2005 (Hydrologic Services Water Sciences Section, 2006).

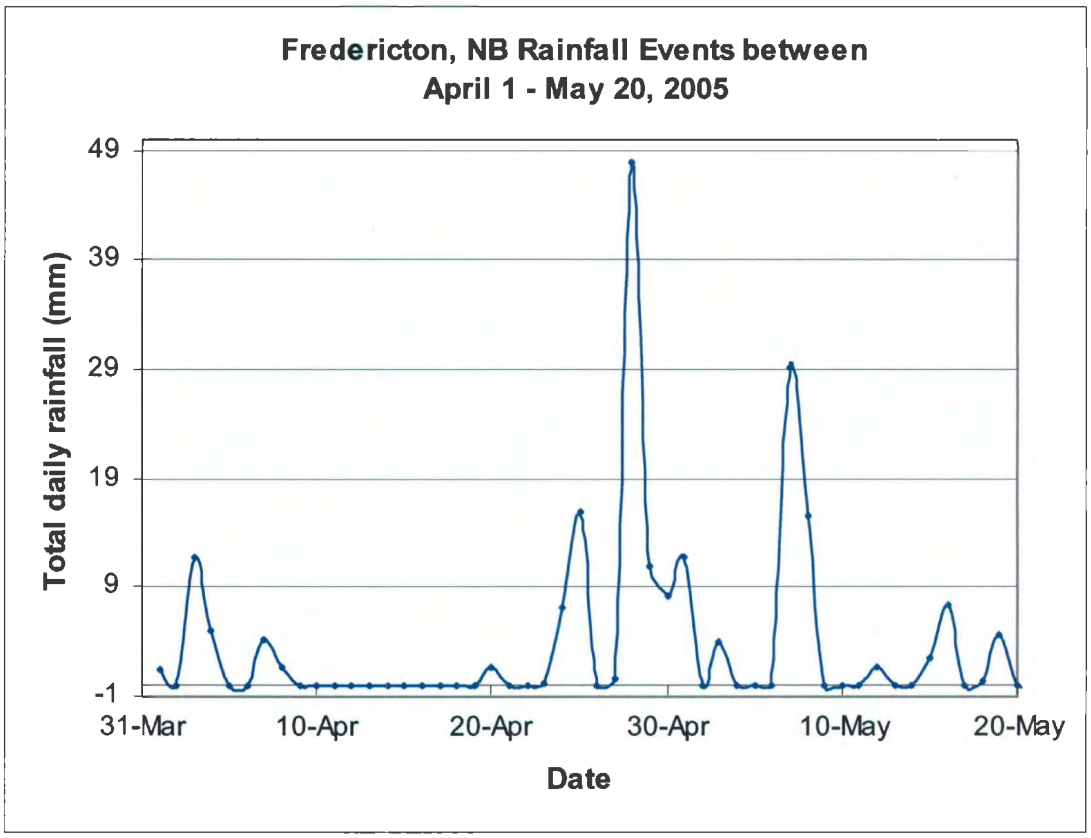

Figure F.13. Precipitation during snapshot period April 1 – May 20, 2005.

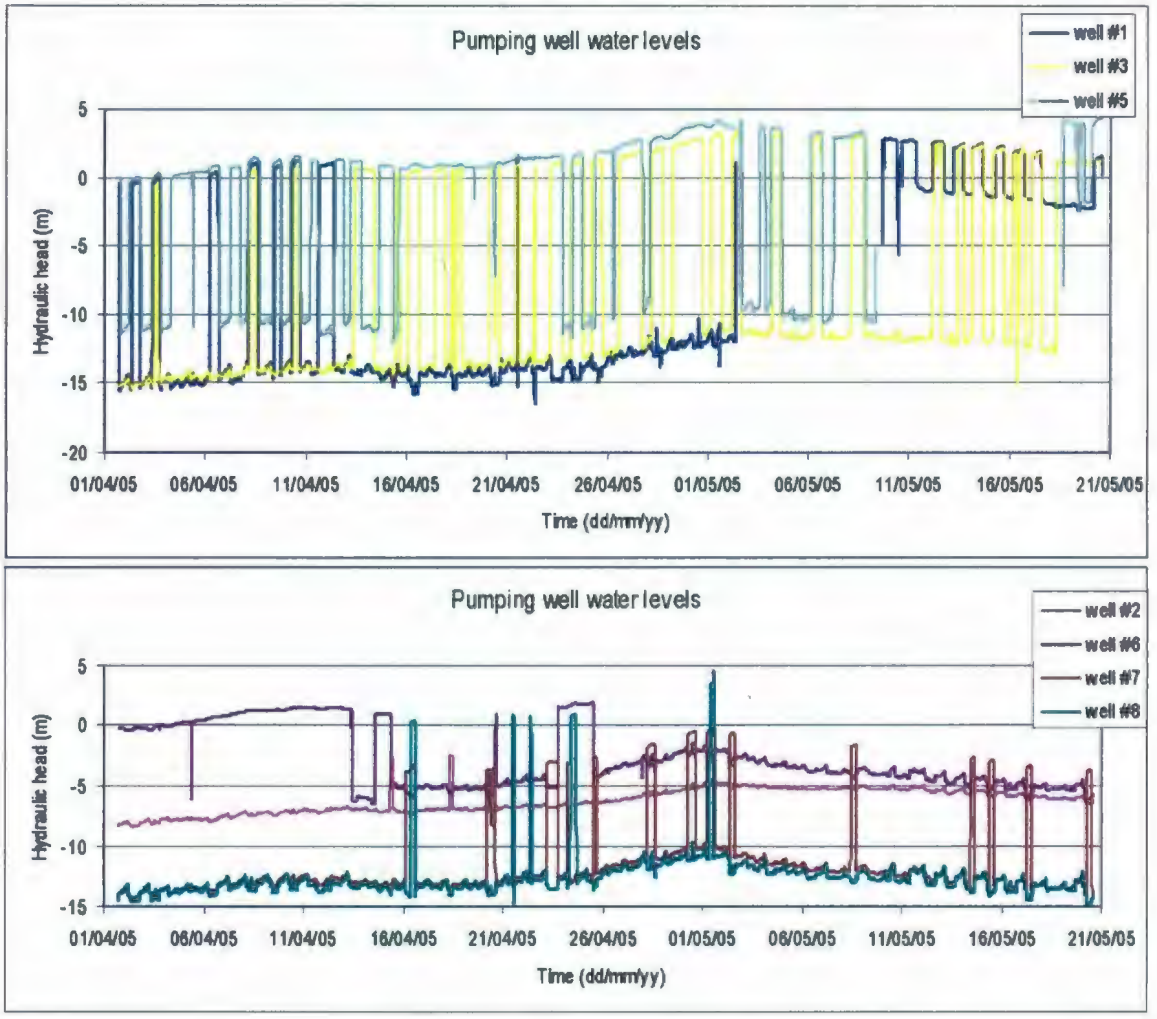

Figure F.14. Pumping well water levels during snapshot period April 1 – May 20, 2005.

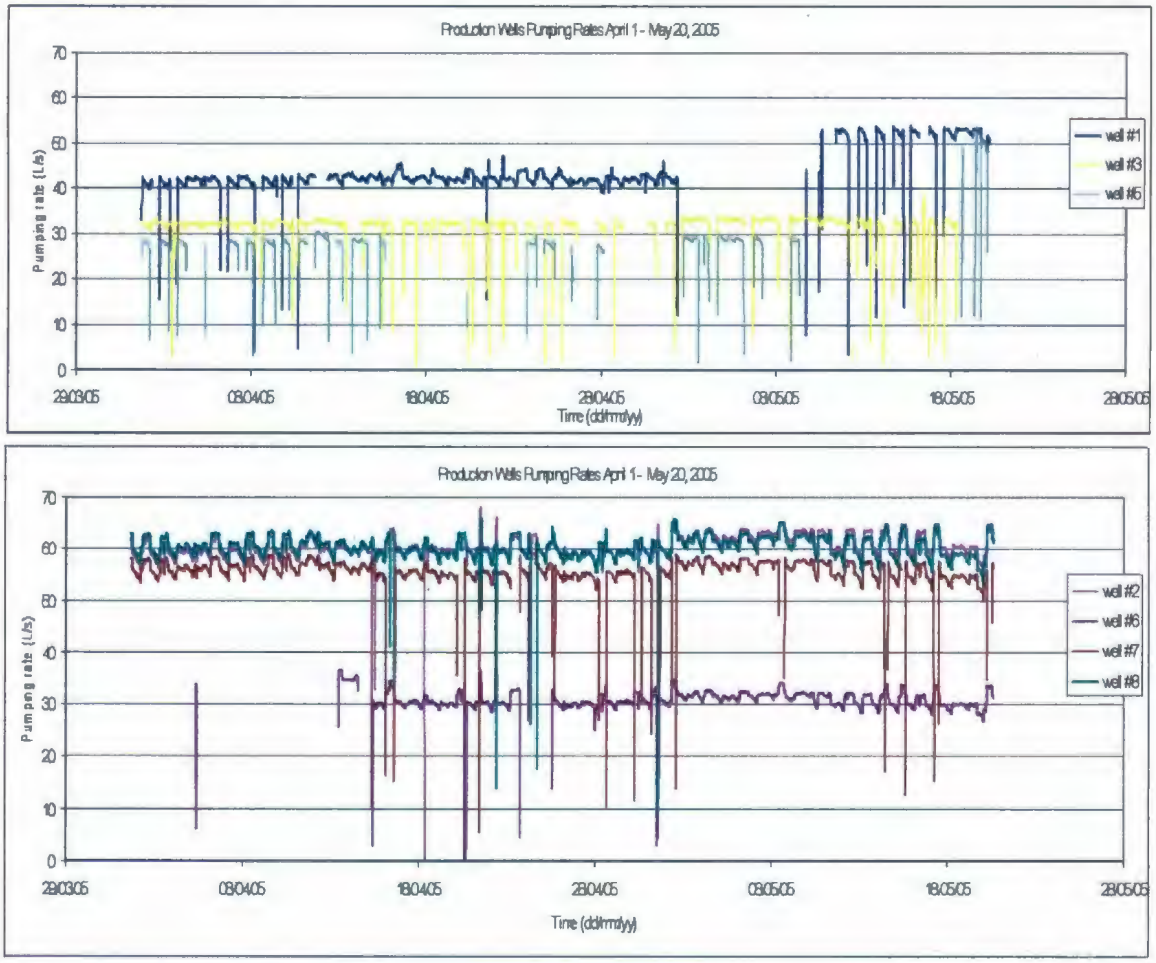

Figure F.15. Pumping well rates during snapshot period April 1 – May 20, 2005.

APPENDIX F NUMERICAL MODEL DATA - TABLES

Table F.1 Element numbers for each layer and hydraulic conductivity used for each layer of the model.

Layer	Element No.'s Range		Kx / Ky (m/s)	Kx / Ky (m/s)	Kx / Ky (m/s)	Kx / Ky (m/s)	Kx / Ky (m/d)	Kx / Ky (m/d)	Kx / Ky (m/d)	Kx / Ky (m/d)
1	1	5231	1.00E-02	1.00E-04	1.00E-05	-	864	8.64	0.864	-
2	5232	10462	3.00E-03	1.00E-05	1.00E-06	-	259	0.864	0.0864	-
3	10463	15693	3.00E-03	1.00E-06	1.00E-07	-	259	0.0864	0.00864	-
4	15694	20924	3.00E-03	8.00E-05	1.00E-05	1.00E-06	259	6.91	0.864	0.0864
5	20925	26155	5.00E-05	1.00E-06	-	-	4.3200	0.0864	-	-
6	26156	31386	1.00E-03	1.00E-06			86.4	0.0864	-	-
7	31387	36617	5.00E-06	-	-	-	0.432	-	-	-
8	36618	41848	2.50E-06	-	-	-	0.2160	-	-	-
9	41849	47079	1.00E-06	-	-	-	0.0864	-	-	-
10	47080	52310	7.50E-07	-	-	-	0.0648	-	-	-
11	52311	57541	5.00E-07	-	-	-	0.0432	-	-	-
12	57542	62772	2.50E-07	-	-	-	0.0216	-	-	-
13	62773	68003	1.00E-07	-	-	-	0.0086	-	-	-
14	68004	73234	7.50E-08	-	-	-	0.0065	-	-	-
15	73235	78465	5.00E-08	-	-	-	0.00432	-	-	-
16	78466	83696	2.50E-08	-	-	-	0.00216	-	-	-

Table F.2 Hydrostratigraphic units x, y, z coordinates.

x	y	Silty Clay	Aquifer	Till	Bedrock	x	y	Silty Clay	Aquifer	Till	Bedrock	x	y	Silty Clay	Aquifer	Till	Bedrock	x	y	Silty Clay	Aquifer	Till	Bedrock
2484523	7435516	124.9	124.4	123.9	123.4	2486500	7435516	104.0	103.5	103.0	102.5	2488484	7435516	84.0	83.5	83.0	82.5	2490505	7435516	55.3	54.8	54.3	53.8
2484523	7434006	116.5	115.8	115.0	114.3	2486500	7434006	98.5	98.0	98.0	97.2	2488484	7434006	95.4	94.7	93.9	93.2	2490505	7434006	60.5	59.7	59.0	58.2
2484523	7434496	119.5	118.8	118.0	117.3	2486500	7434496	113.0	112.3	111.5	110.8	2488484	7434496	110.0	109.3	108.5	107.8	2490505	7434496	46.5	43.3	41.1	38.9
2484523	7435003	130.5	129.5	128.5	127.5	2486500	7435003	117.8	116.9	115.9	114.9	2488484	7435003	111.0	110.0	109.0	108.0	2490505	7435003	43.5	40.6	37.5	34.5
2484523	7435493	131.5	130.5	129.5	128.5	2486500	7435493	119.0	118.0	117.0	116.0	2488484	7435493	73.5	72.5	71.5	70.5	2490505	7435493	46.5	45.6	44.5	43.5
2484523	7436000	108.6	107.4	106.2	105.0	2486500	7436000	114.8	113.4	112.2	111.0	2488484	7436000	91.6	90.4	89.2	88.0	2490505	7436000	38.0	36.8	35.6	34.4
2484523	7436506	102.5	101.3	100.1	98.9	2486500	7436506	108.1	107.9	106.7	105.5	2488484	7436506	105.1	103.9	102.7	101.5	2490505	7436506	16.8	15.8	14.4	13.2
2484523	7436996	102.2	100.8	99.4	98.0	2486500	7436996	108.2	107.8	106.4	105.0	2488484	7436996	104.7	103.3	101.9	100.5	2490505	7436996	-6.8	-10.2	-13.6	-17.0
2484523	7437503	115.2	113.8	112.4	111.0	2486500	7437503	113.7	112.3	110.8	109.5	2488484	7437503	104.7	103.3	101.9	100.6	2490505	7437503	-10.0	-35.0	-45.0	-50.0
2484523	7437993	118.1	116.5	114.8	113.2	2486500	7437993	115.4	113.8	112.2	110.6	2488484	7437993	95.3	93.7	92.1	90.5	2490505	7437993	-1.51	-23.76	-32.28	-43.87
2484523	7438500	99.3	97.7	96.1	94.5	2486500	7438500	114.8	113.2	111.6	110.0	2488484	7438500	72.7	71.1	69.5	67.9	2490505	7438500	4.0	3.0	-25.0	-40.0
2484523	7438007	96.5	93.5	91.5	89.5	2486500	7438007	92.5	90.5	88.5	86.5	2488484	7438007	27.5	24.5	21.5	18.5	2490505	7438007	5.4	-20.0	-30.0	-40.6
2484523	7438497	93.9	91.4	89.0	86.6	2486500	7438497	40.7	38.3	35.9	33.5	2488484	7438497	5.8	3.8	1.8	-0.2	2490505	7438497	-2.0	-25.0	-45.0	-66.0
2484523	7440004	89.0	67.5	66.0	64.5	2486500	7440004	9.0	4.0	2.0	0.0	2488484	7440004	-0.5	-5.5	-10.5	-15.5	2490505	7440004	5.0	3.0	-3.0	-16.0
2484523	7440494	7.0	5.0	3.0	-11.0	2486500	7440494	2.0	1.0	0.0	-12.0	2488484	7440494	5.1	-10.4	-28.55	-47.0	2490505	7440494	5.0	0.0	-5.0	-10.0
2484523	7441001	-2.0	-10.0	-15.0	-20.0	2486500	7441001	-1.0	-3.0	-5.0	-30.0	2488484	7441001	-10.0	-20.0	-45.0	-55.0	2490505	7441001	10.0	0.0	-5.0	-10.0
2484523	7441508	-5.0	-8.0	-10.0	-33.0	2486500	7441508	1.0	-6.0	-12.0	-40.0	2488484	7441508	-10.0	-15.0	-25.0	-30.0	2490505	7441508	20.0	10.0	5.0	0.0
2484523	7441964	9.0	5.0	-1.0	-26.0	2486500	7441964	7.0	5.0	3.0	-35.0	2488484	7441964	5.0	0.0	-5.0	-10.0	2490505	7441964	45.0	40.0	35.0	30.0
2484996	7435516	121.5	121.0	120.5	120.0	2487007	7435516	76.5	75.0	74.5	74.0	2488001	7435516	80.0	79.5	79.0	78.5	2490995	7435516	53.4	52.9	52.4	51.9
2484996	7434006	118.0	117.3	116.5	115.8	2487007	7434006	94.5	93.8	93.0	92.3	2488001	7434006	90.8	90.0	89.3	88.5	2490995	7434006	43.0	40.0	37.0	34.0
2484996	7434496	121.8	120.8	120.1	119.4	2487007	7434496	111.0	110.2	109.5	108.7	2488001	7434496	84.5	83.8	83.0	82.3	2490995	7434496	29.4	23.4	18.4	13.4
2484996	7435003	130.8	129.6	128.8	127.6	2487007	7435003	116.4	115.4	114.4	113.4	2488001	7435003	82.4	81.4	80.4	89.4	2490995	7435003	24.0	18.0	8.0	0.0
2484996	7435493	120.4	119.4	118.4	117.4	2487007	7435493	113.0	112.0	111.0	110.0	2488001	7435493	71.6	70.5	69.5	68.5	2490995	7435493	10.5	2.5	-5.5	-13.5
2484996	7436000	103.0	101.8	100.6	99.4	2487007	7436000	105.1	104.9	103.7	102.5	2488001	7436000	86.6	85.4	84.2	83.0	2490995	7436000	13.0	3.0	-7.0	-17.0
2484996	7436506	105.3	104.1	102.9	101.7	2487007	7436506	107.6	106.4	105.2	104.0	2488001	7436506	95.1	93.9	92.7	91.5	2490995	7436506	-11.6	-18.1	-24.6	-31.1
2484996	7436996	104.2	102.8	101.4	100.0	2487007	7436996	107.2	105.8	104.4	103.0	2488001	7436996	96.5	97.1	95.7	94.3	2490995	7436996	-18.8	-25.0	-40.0	-48.3
2484996	7437503	120.2	118.8	117.4	116.0	2487007	7437503	108.2	106.8	105.4	104.0	2488001	7437503	93.6	92.2	90.8	89.4	2490995	7437503	-10.0	-35.0	-45.0	-55.0
2484996	7437993	121.9	120.3	118.7	117.1	2487007	7437993	112.3	110.7	109.1	107.5	2488001	7437993	79.7	78.1	76.5	74.9	2490995	7437993	0.07	-11.56	-19.39	-20
2484996	7438500	112.8	111.2	109.6	108.0	2487007	7438500	104.3	102.7	101.1	99.5	2488001	7438500	43.9	28.9	33.9	28.9	2490995	7438500	6.5	6.5	-17.0	-26.0
2484996	7438007	92.3	90.3	88.3	86.3	2487007	7438007	86.5	84.5	82.5	80.5	2488001	7438007	6.8	-8	-10.4	-17.11	2490995	7438007	5.0	-15.0	-20.0	-26.0
2484996	7438497	76.7	74.3	71.9	69.5	2487007	7438497	32.7	30.3	27.9	6.0	2488001	7438497	-10.0	-20.0	-40.0	-50.0	2490995	7438497	5.0	-5.0	-15.0	-26.0
2484996	7440004	89.0	87.5	86.0	84.5	2487007	7440004	10.0	2.5	-0.5	-15.0	2488001	7440004	-3.0	-10.0	-35.0	-45.0	2490995	7440004	2.0	0.0	-5.0	-7.0
2484996	7440494	9.0	7.0	5.0	0.0	2487007	7440494	3	-15	-35	-40.0	2488001	7440494	-5.0	-15.0	-35.0	-50.0	2490995	7440494	5.0	0.0	-3.0	-5.0
2484996	7441001	-5.0	-4.0	-3.0	-20.0	2487007	7441001	-1.0	-20.0	-30.0	-38.0	2488001	7441001	-10.0	-20.0	-40.0	-50.0	2490995	7441001	15.0	5.0	0.0	-5.0
2484996	7441508	-5.0	-6.0	-7.0	-30.0	2487007	7441508	4.0	-10.0	-22.0	-30.0	2488001	7441508	-5.0	-10.0	-15.0	-20.0	2490995	7441508	25.0	15.0	10.0	5.0
2484996	7441964	11.0	5.0	0.0	-25.0	2487007	7441964	5.0	0.0	-4.0	-20.0	2488001	7441964	20.0	10.0	5.0	0.0	2490995	7441964	41.0	38.0	37.0	35.0
2485503	7435516	117.4	116.8	116.4	115.9	2487497	7435516	77.6	77.1	76.6	76.1	2488508	7435516	77.2	76.7	76.2	75.7	2491502	7435516	32.0	28.0	24.0	20.0
2485503	7434006	110.5	109.8	109.0	108.3	2487497	7434006	84.5	83.8	83.0	82.3	2488508	7434006	85.0	84.3	83.5	82.8	2491502	7434006	24.0	19.5	15.0	10.5
2485503	7434496	123.0	122.3	121.5	120.8	2487497	7434496	111.0	110.3	109.5	108.8	2488508	7434496	89.0	88.3	87.5	86.8	2491502	7434496	14.5	5.5	-3.5	-12.5
2485503	7435003	128.5	127.5	126.5	125.5	2487497	7435003	111.4	110.4	109.4	108.4	2488508	7435003	71.2	70.2	69.2	68.2	2491502	7435003	15.5	4.5	-6.5	-17.5
2485503	7435493	126.0	125.0	124.0	123.0	2487497	7435493	104.8	103.8	102.8	101.8	2488508	7435493	68.0	67.0	66.0	65.0	2491502	7435493	10.5	-0.5	-11.5	-22.5
2485503	7436000	107.6	106.4	105.2	104.0	2487497	7436000	104.8	103.7	102.5	101.3	2488508	7436000	84.1	82.8	81.7	80.5	2491502	7436000	11.5	-1.5	-14.5	-27.5
2485503	7436506	110.2	109.0	107.8	106.6	2487497	7436506	107.8	106.4	105.2	104.0	2488508	7436506	79.4	78.2	77.0	75.8	2491502	7436506	-15.0	-27.0	-36.0	-46.0
2485503	7436996	113.7	112.3	110.9	109.5	2487497	7436996	112.2	110.8	109.4	108.0	2488508	7436996	67.4	66.0	64.6	63.2	2491502	7436996	-6.0	-18.0	-40.0	-60.0
2485503	7437503	117.7	116.3	114.9	113.5	2487497	7437503	114.6	113.2	111.8	110.4	2488508	7437503	63.7	62.3	60.9	59.5	2491502	7437503	-3.0	-12.0	-45.0	-55.0
2485503	7437993	127.8	126.2	124.6	123.0	2487497	7437993	108.8	107.2	105.6	104.0	2488508	7437993	44.1	42.5	40.9	39.3	2491502	7437993	2.0	-8.0	-25.0	-40.0
2485503	7438500	108.8	107.2	105.6	104.0	2487497	7438500	95.8	94.2	92.6	91.0	2488508	7438500	5.7	4.2	2.7	1.2	2491502	7438500	4.0	-5.0	-18.0	-26.0
2485503	7438007	98.0	96.0	94.0	92.0	2487497	7438007	88.0	86.0	84.0	82.0	2488508	7438007	5.4	-31.5	-39.12	-55.6	2491502	7438007	6.0	-1.0	-18.0	-26.0
2485503	7438497	52.7	50.3	47.9	45.5	2487497	7438497	28.2	25.8	23.4	21.0	2488508	7438497	5.0	-20.0	-40.0	-50.0	2491502	7438497	1.0	-1.0	-4.0	-15.0
2485503	7440004	57.0	56.0	55.0	54.0	2487497	7440004	-0.5	-5.5	-10.5	-15.5	2488508	7440004	2.0	-10.0	-25.0	-45.0	2491502	7440004	0.0	-4.0	-8.0	-10.0
2485503	7440494	10.0	9.0	8.0	7.0	2487497	7440494	-0.5	-5.5	-10.5	-15.5	2488508	7440494	-10.0	-20.0	-30.0	-40.0	2491502	7440494	5.0	0.0	-3.0	-5.0
2485503	7441001	-1.0	-2.0	-3.0	-15.0	2487497	7441001	-10.0	-20.0	-30.0	-40.0	2488508	7441001	-5.0	-10.0	-30.0	-40.0	2491502	7441001	10.0	5.0	-5.0	-10.0
2485503	7441508	-5.0	-12.0	-20.0	-25.0	2487497	7441508	-10.0	-15.0	-32.0	-42.0	2488508	7441508	8.0	4.0	2.0	0.0	2491502	7441508	20.0	10.0	5.0	0.0
2485503	7441964	10.0	0.0	-15.0	-40.0	2487497	7441964	-10.0	-15.0	-32.0	-42.0	2488508	7441964	28.0	24.0	22.0	20.0	2491502	7441964	35.0	30.0	25.0	20.0
2485993	7435516	115.2	114.7	114.2	113.7	2488004	7435516	83.6	83.0	82.5	82.0	2488998	7435516	80.9	80.4	58.9	58.4	2491975	7435516	16.1	10.1	5.1	0.1
2485993	7434006	104.3	103.6	102.8	102.1	2488004	7434006	96.8	96.2	95.4	94.7	2488998	7434006	65.0	64.3	63.5	62.8	2491975	7434006	12.0	5.0	-2.0	-9.0
2485993	7434496	112.6	111.8	111.0	110.3	2488004	7434496	110.1	109.4	108.6	107.9	2488998	7434496	67.0	66.3	65.5	64.8	2491975	7434496	12.0	3.0	-7.0	-17.0
2485993	7435003	122.5	121.5	120.5	119.5	2488004	7435003	112.2	111.2	110.2	109.2	2488998	7435003	48.1	47.1	46.1	45.1	2491975	7435003	7.4	-3.0	-15.5	-28.0
2485993	7435493	126.5	124.5	123.5	122.5	2488004	7435493	95.0	94.0	93.0	92.0	2488998	7435493	58.0	57.0	56.0	55.0	2491975	7435493	1.0	-11.0	-23.0	-36.0
2485993	7436000	115.6	114.4	113.2	112.0	2488004	7436000	86.1	84.8	83.7	82.5	2488998	7436000	64.1	62.9	61.7	60.5	2491975	7436000	10.0	-16.5	-28.0	-39.5
2485993	7436506	108.1	106.9	105.7	104.5	2488004	7436506	107.6	106.4	105.2	104.0	2488998	7436506	64.6	63.4	62.2	61.0	2491975	7436506	-15.0	-24.0	-33.0	-42.0
2485993	7436996	108.7	107.3	105.9	104.5	2488004	7436996	112.7	111.3	109.9	108.5	2488998	7436996	59.0	57.6	56.2	54.8	2491975	7436996	-16.0	-30.0	-40.0	-50.0
2485993	7437503	114.2	112.8	111.4	110.0	2488004	7437503	114.7	113.3	111.9	110.5	2488998	7437503	21.3	19.9	18.5	17.1	2491975	7437503	-7.0	-33.0	-45.0	-55.0
2485993	7437993	119.7	118.1	116.5	114.9	2488004	7437993	85.1	83.5	81.9	80.3	2488998	7437993	-7.8	-32.59	-45.09	-48.75	2491975	7437993	9.0	-5.0	-20.0	-40.0
2485993	7438500	110.0	108.4	106.8	105.2	2488004	7438500	75.8	74.2	72.6	71.0	2488998	7438500	-0.5	-1.0	-40.0	-50.0	2491975	7438500	20.0	15.0	0.0	-10.0
2485993	7438007	80.0	78.0	76.0	74.0	2488004	7438007	43.0	41.0	39.0	37.0	2488998	7438007	5.4	-31.5	-39.12	-55.6	2491975	7438007	10.0	5.0	0.0	-5.0
2485993	7438497	62.2	59.8	57.4	55.0	2488004	7438497	12.5	12.0	11.5	11.0	2488998	7438497	-5.0	-30.0	-50.0	-60.0	2491975	7438497	8.0	6.0	3.0	-2.0
2485993	7440004	29.3	25.8	22.3	18.8	2488004	7440004	0.0	-5.0	-10.0	-15.0	2488998	7440004	-5.0	-10.0	-25.0	-35.0	2491975	7440004	0.0	-4.0	-6.0	-8.0
2485993	7440494	12.0	11.0	10.0	-10.0	2488004	7440494	0	-11.6	-38.11	-43.33	2488998	7440494	0.0	-10.0	-20.0	-30.0	2491975	7440494	0.0	-3.0	-7.0	-10.0
2485993	7441001	-1.0	-2.0	-3.0	-25.0	2488004	7441001	-10.0	-20.0	-40.0	-50.0	2488998	7441001	0.0	-10.0	-20.0	-30.0	2491975	7441001	15.0	0.0	-5.0	-10.0
2485993	7441508	0.0	-8.0	-15.0	-45.0	2488004	7441508	-10.0	-15.0	-32.0	-42.0	2488998	7441508	15.0	10.0	5.0	0.0	2491975	7441508	25.0	15.0	10.0	5.0
2485993	7441964	12.0	0.0	-5.0	-35.0	2488004	7441964	0.0	-5.0	-20.0	-30.0	2488998	7441964	35.0	24.0	22.0	20.0	2491975	7441964	23.0	20.0	15.0	10.0

Table F.3 Boreholes with window locations in Layer 5 (till) determined from borehole database.			
Well No.	Easting (m)	Northing (m)	Element No.'s
88-4-O	2486751	7440393	20943 + 20942
605	2487507	7439756	23272 + 23271
2-92	2487555	7440515	26154 + 26155
Pg 93	2487572	7440084	21135
Pg 179	2487726	7439623	23269
PZ-2	2487737	7439668	23269
PZ-1	2487744	7439617	23269
PZ-18	2487764	7439662	23269
PZ-19	2487766	7439640	23269
4-00	2489172	7439226	21190 + 21191
3-01	2489271	7439113	21204
2-01	2489310	7439205	21294 + 21205
6-00	2489336	7439069	21208 + 21203
1-00	2489659	7438756	21352 + 21158
4-92	2489687	7438559	21349
2-00	2489697	7438896	21050
5-92	2489711	7438391	21162 + 21006
3-00	2489726	7438364	21162 + 21006
		Total	21 elements

Table F.4 Random sampling of 518 esker element numbers on Layer 5 (till) to obtain 20% coverage of window location.

No.	Element No.	X	Y	No.	Element No.	X	Y
1	20926	2486098	7440914	53	21200	2488663	7439612
2	20928	2486177	7440838	54	21206	2489417	7439142
3	20933	2486357	7440667	55	21210	2488235	7439636
4	20945	2486857	7440361	56	21213	2488145	7439787
5	20947	2486967	7440286	57	21215	2488247	7439872
6	20950	2487179	7440110	58	21222	2487750	7440017
7	20951	2487145	7440159	59	21226	2487935	7439893
8	20953	2487246	7440116	60	21229	2487999	7439926
9	20957	2487494	7439943	61	21231	2488075	7440032
10	20961	2487690	7439821	62	21244	2489420	7438922
11	20970	2488189	7439534	63	21245	2489426	7438858
12	20978	2488445	7439448	64	21261	2488577	7439750
13	20979	2488589	7439321	65	21267	2489018	7439340
14	20998	2489402	7438739	66	21269	2488895	7439296
15	21001	2489527	7438552	67	21271	2489127	7439399
16	21004	2489599	7438456	68	21275	2489173	7439353
17	21026	2490148	7438027	69	21280	2488969	7439482
18	21029	2490129	7438181	70	21281	2488883	7439570
19	21030	2490089	7438083	71	21284	2488949	7439673
20	21033	2490129	7438323	72	21287	2488829	7439760
21	21037	2490030	7438535	73	21288	2488765	7439790
22	21040	2489940	7438647	74	21289	2488704	7439743
23	21051	2489671	7439017	75	21297	2487820	7440116
24	21053	2489617	7439022	76	21315	2487459	7440117
25	21056	2489487	7439255	77	21321	2488136	7440150
26	21070	2488948	7439806	78	21332	2487027	7440396
27	21076	2488808	7439890	79	21336	2486819	7440768
28	21084	2488428	7440140	80	21344	2487213	7440367
29	21085	2488310	7440253	81	21360	2487742	7440355
30	21092	2488037	7440342	82	21364	2487181	7440592
31	21093	2487897	7440453	83	21369	2487185	7440522
32	21095	2487785	7440498	84	21370	2487119	7440486
33	21104	2487407	7440649	85	21374	2486971	7440558
34	21127	2486326	7440882	86	21375	2487005	7440506
35	21129	2486276	7440884	87	21376	2487119	7440623
36	21131	2489947	7438131	88	21379	2487381	7440597
37	21132	2489955	7438199	89	21383	2487313	7440243
38	21133	2490023	7438243	90	21384	2487314	7440189
39	21137	2487615	7439969	91	21391	2488339	7439634
40	21138	2488824	7439315	92	21394	2488053	7439736
41	21139	2488815	7439374	93	21401	2488655	7439921
42	21147	2487558	7440572	94	21402	2487105	7440422
43	21150	2486903	7440429	95	21598	2485963	7440965
44	21153	2489251	7439440	96	21603	2486083	7440979
45	21155	2489541	7438763	97	21605	2486270	7440945
46	21165	2489811	7438544	98	21607	2486321	7440942
47	21167	2486528	7440634	99	21688	2490276	7438035
48	21169	2486566	7440762	100	23298	2486174	7440722
49	21173	2488013	7440145	101	23305	2485999	7440877
50	21179	2490024	7438320	102	23306	2485943	7440910
51	21196	2488555	7439530	103	26148	2487606	7440537
52	21199	2488703	7439544	104	26151	2487678	7440575

Table F.5 Pumping well hydraulic heads for April 1 – May 20, 2005.					
	Initial HH	Final HH	Average HH	Minimum HH	Maximum HH
Well #	01-Apr-05	20-May-05			
	(m)	(m)	(m)	(m)	(m)
PW01	-0.37	0.15	-8.99	-17.91	2.84
PW02	-8.39	-6.34	-6.34	-10.90	-2.48
PW03	-15.27	1.22	-8.06	-17.90	3.40
PW05	0.04	4.26	-1.72	-12.24	4.34
PW06	-0.27	-5.68	-2.68	-13.52	4.64
PW07	-14.27	-13.89	-11.58	-17.43	0.05
PW08	-14.56	-14.04	-12.57	-30.46	3.69
* Actual daily hydraulic head levels shown in Figure F.14 in Appendix F.					

Table F.6 Pumping Rates (PR) for production wells for April 1 – May 20, 2005.**					
	Initial PR	Final PR	Average PR	Minimum PR	Maximum PR
Well #	01-Apr-05	20-May-05			
	(m^3/d)	(m^3/d)	(m^3/d)	(m^3/d)	(m^3/d)
PW01	2850	0	3,785	0	4667
PW02	5353	5405	5,240	0	5899
PW03	2812	0	2,770	0	3304
PW05	0	0	2,479	0	4666
PW06	0	2692	2,676	0	3164
PW07	5006	4867	4,815	0	5122
PW08	5434	5280	5,219	0	5700
			Total = 26,983		
** Actual daily pumping rates shown in Figure F.15 in Appendix F.					

Table F.7 Production well surface and transducer elevations.			
City of Fredericton Water Treatment Plant			
Location	Geodetic Base Elevation (m)	Transducer Depth (m)	Transducer Elevation (m)
Production Well #1	10.32	27.4	-17.09
Production Well #2	10.33	20.4	-10.08
Production Well #3	10.33	27.4	-17.07
Production Well #5	9.89	21.3	-11.42
Production Well #6	10.40	23.1	-12.70
Production Well #7	9.29	25.9	-16.61
Production Well #8	9.97	39.6	-29.63

Table F.8 Results of the sensitivity analysis by increasing recharge 50% using model with randomly assigned windows in till layer, excluding the basal sand and gravel layer.					
	Calibrated		Hydraulic Head		
	Calculated (m)	Calculated (m)	Hm - Hc (m)	Hm - Hc Absolute (m)	Square Difference
Grieves Brook	23.2	25.58	-2.36	2.36	5.56
Rice Brook	10.6	10.95	-0.31	0.31	0.10
New Maryland Well	96.7	104.18	-7.49	7.49	56.09
Nashwaaksis Stream	3.1	3.07	-0.01	0.01	0.00
Corbett Brook	45.8	48.35	-2.58	2.58	6.64
Corbett Brook	85.1	97.71	-12.56	12.56	157.79
Corbett Brook	112.5	124.88	-12.37	12.37	153.05
Phyllis Creek	79.2	87.08	-7.92	7.92	62.80
Baker Brook	120.1	124.44	-4.39	4.39	19.26
BH03	7.4	8.69	-1.25	1.25	1.56
			-5.12	5.12	6.80
ME = Mean Error			ME	MAE	RMS
MAE = Mean Absolute Error					
RMS = Root Mean Square Error					

Table F.9 Results of the sensitivity analysis by decreasing recharge 50% using model with randomly assigned windows in till layer, excluding the basal sand and gravel layer.

	Calibrated		Hydraulic Head		
	Calculated	Calculated	Hm - Hc	Hm - Hc	Square
	(m)	(m)	(m)	Absolute (m)	Difference
Grieves Brook	23.2	20.88	2.34	2.34	5.48
Rice Brook	10.6	10.37	0.27	0.27	0.07
New Maryland Well	96.7	85.96	10.73	10.73	115.06
Nashwaaksis Stream	3.1	3.05	0.01	0.01	0.00
Corbett Brook	45.8	38.27	7.50	7.50	56.30
Corbett Brook	85.1	67.39	17.76	17.76	315.40
Corbett Brook	112.5	90.01	22.49	22.49	506.02
Phyllis Creek	79.2	78.34	0.81	0.81	0.66
Baker Brook	120.1	112.72	7.33	7.33	53.75
BH03	7.4	6.48	0.97	0.97	0.93
			7.02	7.02	10.26
ME = Mean Error			ME	MAE	RMS
MAE = Mean Absolute Error					
RMS = Root Mean Square Error					

Table F.10 Results of the sensitivity analysis by decreasing hydraulic conductivity 50% using model with randomly assigned windows in till layer, excluding the basal sand and gravel layer.

	Calibrated		Hydraulic Head		
	Calculated	Calculated	Hm - Hc	Hm - Hc	Square
	(m)	(m)	(m)	Absolute (m)	Difference
Grieves Brook	23.2	27.93	-4.71	4.71	22.15
Rice Brook	10.6	11.24	-0.60	0.60	0.36
New Maryland Well	96.7	113.29	-16.60	16.60	275.48
Nashwaaksis Stream	3.1	3.08	-0.02	0.02	0.00
Corbett Brook	45.8	53.39	-7.62	7.62	58.01
Corbett Brook	85.1	112.87	-27.72	27.72	768.50
Corbett Brook	112.5	142.31	-29.80	29.80	888.32
Phyllis Creek	79.2	91.45	-12.29	12.29	151.08
Baker Brook	120.1	130.30	-10.25	10.25	105.04
BH03	7.4	9.80	-2.36	2.36	5.55
			-11.20	11.20	15.08
ME = Mean Error			ME	MAE	RMS
MAE = Mean Absolute Error					
RMS = Root Mean Square Error					

Table F.11 Results of the sensitivity analysis by increasing hydraulic conductivity 50% using model with randomly assigned windows in till layer, excluding the basal sand and gravel layer.

	Calibrated		Hydraulic Head		
	Calculated	Calculated	Hm - Hc	Hm - Hc	Square
	(m)	(m)	(m)	Absolute (m)	Difference
Grieves Brook	23.2	21.67	1.56	1.56	2.42
Rice Brook	10.6	10.47	0.17	0.17	0.03
New Maryland Well	96.7	89.00	7.69	7.69	59.15
Nashwaaksis Stream	3.1	3.05	0.01	0.01	0.00
Corbett Brook	45.8	39.95	5.82	5.82	33.91
Corbett Brook	85.1	72.44	12.71	12.71	161.44
Corbett Brook	112.5	95.82	16.68	16.68	278.35
Phyllis Creek	79.2	79.80	-0.65	0.65	0.42
Baker Brook	120.1	114.67	5.38	5.38	28.93
BH03	7.4	6.85	0.60	0.60	0.36
			5.00	5.13	7.52
ME = Mean Error			ME	MAE	RMS
MAE = Mean Absolute Error					
RMS = Root Mean Square Error					

Table F.12 Results of the sensitivity analysis by increasing hydraulic conductivity 50% and decreasing recharge 50% using model with randomly assigned windows in till layer, excluding the basal sand and gravel layer.

	Calibrated		Hydraulic Head		
	Calculated	Calculated	Hm - Hc	Hm - Hc	Square
	(m)	(m)	(m)	Absolute (m)	Difference
Grieves Brook	23.2	20.15	3.08	3.08	9.47
Rice Brook	10.6	10.46	0.19	0.19	0.03
New Maryland Well	96.7	83.07	13.62	13.62	185.50
Nashwaaksis Stream	3.1	3.07	-0.01	0.01	0.00
Corbett Brook	45.8	38.86	6.92	6.92	47.83
Corbett Brook	85.1	62.61	22.54	22.54	508.13
Corbett Brook	112.5	81.44	31.06	31.06	964.96
Phyllis Creek	79.2	71.40	7.75	7.75	60.09
Baker Brook	120.1	110.83	9.22	9.22	85.06
BH03	7.4	7.74	-0.30	0.30	0.09
			9.41	9.47	13.64
ME = Mean Error			ME	MAE	RMS
MAE = Mean Absolute Error					
RMS = Root Mean Square Error					

Table F.13 Results of the sensitivity analysis by decreasing hydraulic conductivity 50% and increasing recharge 50% using model with randomly assigned windows in till layer, excluding the basal sand and gravel layer.

	Calibrated		Hydraulic Head		
	Calculated	Calculated	Hm - Hc	Hm - Hc	Square
	(m)	(m)	(m)	Absolute (m)	Difference
Grieves Brook	23.2	32.61	-9.39	9.39	88.10
Rice Brook	10.6	11.78	-1.14	1.14	1.30
New Maryland Well	96.7	138.64	-41.95	41.95	1760.05
Nashwaaksis Stream	3.1	3.10	-0.04	0.04	0.00
Corbett Brook	45.8	69.34	-23.56	23.56	555.29
Corbett Brook	85.1	157.23	-72.08	72.08	5195.36
Corbett Brook	112.5	210.60	-98.10	98.10	9622.69
Phyllis Creek	79.2	106.97	-27.81	27.81	773.54
Baker Brook	120.1	148.09	-28.03	28.03	785.93
BH03	7.4	12.20	-4.76	4.76	22.68
			-30.69	30.69	43.36
ME = Mean Error			ME	MAE	RMS
MAE = Mean Absolute Error					
RMS = Root Mean Square Error					

Table F.14 Results of the sensitivity analysis by increasing hydraulic conductivity in the Z-direction by 2 orders of magnitude, using model with randomly assigned windows in till layer, excluding the basal sand and gravel layer.

	Calibrated		Hydraulic Head		
	Calculated	Calculated	Hm - Hc	Hm - Hc	Square
	(m)	(m)	(m)	Absolute (m)	Difference
Grieves Brook	23.2	23.11	0.12	0.12	0.01
Rice Brook	10.6	11.80	-1.16	1.16	1.35
New Maryland Well	96.7	107.92	-11.23	11.23	126.17
Nashwaaksis Stream	3.1	2.99	0.07	0.07	0.00
Corbett Brook	45.8	46.92	-1.14	1.14	1.30
Corbett Brook	85.1	94.39	-9.25	9.25	85.47
Corbett Brook	112.5	123.44	-10.93	10.93	119.49
Phyllis Creek	79.2	86.97	-7.82	7.82	61.12
Baker Brook	120.1	126.85	-6.80	6.80	46.25
BH03	7.4	8.18	-0.74	0.74	0.55
			-4.89	4.93	6.65
ME = Mean Error			ME	MAE	RMS
MAE = Mean Absolute Error					
RMS = Root Mean Square Error					

Table F.15 Temporal and control data set in FEFLOW for model verification.	
Automatic time step control via: predictor corrector schemes	
Forward Adams-Bashford/backward trapezoid (AB/TR time integration scheme)	
Initial time step length (day)	0.001
Final time (day)	49.7
Initial time (day)	0
Time to switch to CN-scheme	2000 time steps
Error Tolerance	Default: 0.001%
Applied to:	Default: Euclidian L2 Integral (RMS) Norm
Maximum number of iterations per time step	12
Adaptive Mesh Error	0.001%
A posteriori error estimator	Onate-Bugeda
Upwinding to stabilize numerical results	Default: No upwind. Galerkin FEM

Table F.16 Results of the steady-state model and associated errors using the borehole database till window locations, excluding the basal sand and gravel layer.

	Hydraulic Head		Hydraulic Head		
	Measured in field (m)	Calculated (m)	Ho - Hc (m)	Ho - Hc Absolute (m)	Square Difference
Grieves Brook	22	23.28	-1.28	1.28	1.63
Rice Brook	13	10.63	2.37	2.37	5.62
New Maryland Well	97.8	95.04	2.76	2.76	7.64
Nashwaaksis Stream	4.8	3.06	1.74	1.74	3.04
Corbett Brook	44.5	43.35	1.15	1.15	1.32
Corbett Brook	79.7	82.45	-2.75	2.75	7.58
Corbett Brook	107.4	107.35	0.05	0.05	0
Phyllis Creek	85	82.74	2.26	2.26	5.11
Baker Brook	115.5	118.58	-3.08	3.08	9.49
BH03	7.5	7.37	0.13	0.13	0.02
			0.34	1.76	2.04
ME = Mean Error			ME	MAE	RMS
MAE = Mean Absolute Error					
RMS = Root Mean Square					

Table F.17 Steady-state hydraulic head results of excluding and including the basal sand and gravel layer.

		Random Windows		Database Windows	
		Sand + Gravel		Sand + Gravel	
	Field	Excluded	Included	Excluded	Included
Location	Measured	Calculated	Calculated	Calculated	Calculated
	HH (m)	HH (m)	HH (m)	HH (m)	HH (m)
Grieves Brook	22	23.23	23.23	23.28	23.28
Rice Brook	13	10.66	10.66	10.63	10.63
New Maryland Well	97.8	95.07	95.06	95.04	95.03
Nashwaaksis Stream	4.8	3.06	3.06	3.06	3.06
Corbett Brook	44.5	43.31	43.31	43.35	43.35
Corbett Brook	79.7	82.55	82.5	82.45	82.42
Corbett Brook	107.4	107.44	107.38	107.35	107.32
Phyllis Creek	85	82.71	82.68	82.74	82.72
Baker Brook	115.5	118.58	118.58	118.58	118.58
BH03	7.5	7.58	7.21	7.37	7.31

Table F.18 Vertical fluid influx and outflux between slices within the steady-state model domain including the basal sand and gravel layer with the randomly assigned windows in the till layer.

		FENCE																
		1	2	3	4	5	6	7	8	9	10	11	12	13	14	15	16	17
LAYER	SLICE	m³/d	m³/d	m³/d	m³/d	m³/d	m³/d	m³/d	m³/d	m³/d	m³/d	m³/d	m³/d	m³/d	m³/d	m³/d	m³/d	m³/d
sand/gravel	1	301	554	493	316	194	-184	-379	-25	-23	304	895	86	1496	464	-10	194	-724
clay	2	265	644	1068	451	618	-200	-252	32	86	382	906	134	1636	513	98	475	-503
clay	3	196	334	478	333	506	-81	70	23	150	400	841	132	1372	445	-47	94	-286
aquifer	4	133	309	393	257	-6	90	-74	44	131	197	476	138	915	336	-5	409	-507
till	5	60	219	262	191	1711	-102	352	1	67	204	157	114	339	175	411	796	540
sand+gravel	6	30	139	168	65	668	31	185	10	15	94	80	96	73	49	123	166	265
bedrock	7	27	130	154	56	291	173	250	0.2	15	9	67	93	36	25	173	211	299

Fluid flux in negative/downward direction.

Table F.19 Vertical fluid influx and outflux between slices within the steady-state model domain including the basal sand and gravel layer with the borehole database assigned windows in the till layer.

		FENCE																
		1	2	3	4	5	6	7	8	9	10	11	12	13	14	15	16	17
	SLICE	m³/d	m³/d	m³/d	m³/d	m³/d	m³/d	m³/d	m³/d	m³/d	m³/d	m³/d	m³/d	m³/d	m³/d	m³/d	m³/d	m³/d
sand/gravel	1	315	536	430	253	335	-186	-456	-34	-78	164	1257	30	2270	305	-4	217	-727
clay	2	268	637	991	382	946	-202	-367	-2	-56	214	1087	80	2379	349	104	453	-507
clay	3	195	326	418	268	767	-78	-37	-5	47	223	1143	80	2023	284	-47	52	-289
aquifer	4	136	303	346	230	-482	782	-260	11	25	97	606	69	1335	219	23	424	-551
till	5	54	212	245	147	3032	-678	377	20	88	62	184	67	469	111	475	857	573
sand+gravel	6	28	135	162	60	502	216	223	24	13	56	80	74	87	33	179	182	322
bedrock	7	25	126	149	53	288	215	254	11	12	15	67	75	27	26	188	218	299

Fluid flux in negative/downward direction.

Table F.20 Hydraulic head data for transient simulations using the randomly assigned windows in the till layer, basal sand and gravel layer excluded.

	Northing	Easting	26,000	26,000	52,000	52,000
			365 d	5 yr	365 d	5 yr
	(m)	(m)	(m³/d)	(m³/d)	(m³/d)	(m³/d)
Grieves B	2490576	7441293	23.21	23.20	23.19	23.16
Rice Brook	2491860	7439147	10.57	10.56	10.48	10.46
New Maryland	2487812	7433914	95.07	95.07	95.07	95.06
Nashw. Stream	2487446	7441955	3.05	3.05	3.05	3.05
Corbett Brook - low	2490570	7434674	43.31	43.30	43.31	43.30
Corbett Brook - med	2488512	7435528	82.55	82.47	82.55	82.38
Corbett Brook - high	2487141	7436128	107.44	107.34	107.44	107.23
Phyllis Creek	2485040	7439238	82.71	82.66	82.70	82.60
Baker Brook	2486092	7433536	118.58	118.58	118.58	118.58
BH03	2487232	7439898	6.81	6.75	6.04	5.91
98-a	2487527	7440598	2.71	2.70	2.07	2.07
6-00	2489347	7439094	1.04	0.93	-2.40	-2.61
98-b	2487541	7440656	2.72	2.72	2.08	2.06
PW01	2487754	7440557	1.91	1.90	0.40	0.39
PW09	2489158	7439202	0.48	0.42	-3.39	-3.51
PW10	2489347	7439094	0.55	0.49	-3.21	-3.33
PW07	2487512	7440540	2.46	2.46	1.57	1.57
PW08	2487619	7440519	2.17	2.17	0.95	0.94
PW02	2487775	7440259	1.85	1.84	0.23	0.22
PW06	2487437	7440596	2.83	2.83	2.34	2.33
PW03	2488072	7440466	-5.22	-5.23	-13.92	-13.94
PW05	2487595	7440631	2.43	2.43	1.52	1.51

Table F.21 Results of transient simulation fluid flux mass balance for pumping 26,000 m³/d using the randomly assigned windows in the till layer, basal sand and gravel excluded.

FLUX_TYPE:	Fluid flux mass balance			
BALANCE_TYPE:	Total			
CURRENT_TIME:	365 d		5 yr	
FLUX_TYPE	FLUX_IN(+)	FLUX_OUT(-)	FLUX_IN(+)	FLUX_OUT(-)
UNIT	Q [m3/d]	Q [m3/d]	Q [m3/d]	Q [m3/d]
BC123_FLUXES	39350	-27018	39497	-26944
WELL_FLUXES	0	-26001	0	-26001
AREAL_FLUXES	13312	0	13312	0
IMBALANCE	0	-357	0	-136
Total	52663	-53376	52809	-53081
Error %	-1.35		-0.52	

Table F.22 Vertical fluid influx and outflux between slices for model using randomly assigned windows in till layer, pumping 26,000 m³/d for 365 d. Basal sand and gravel layer excluded.

		FENCE																
		1	2	3	4	5	6	7	8	9	10	11	12	13	14	15	16	17
	SLICE	m³/d	m³/d	m³/d	m³/d	m³/d	m³/d	m³/d	m³/d	m³/d	m³/d	m³/d	m³/d	m³/d	m³/d	m³/d	m³/d	m³/d
sand/gravel	1	-75	303	147	-20	-2292	-219	-848	-78	288	-460	-5017	51	-9852	-352	37	307	-729
clay	2	-855	345	647	81	-6934	-226	-917	-161	-985	-527	-4659	107	-11147	-329	133	386	-499
clay	3	-788	194	145	-17	-5831	-107	-170	-138	-2070	-554	-7578	105	-8022	-383	-45	-107	-287
aquifer	4	-447	237	133	132	-5516	-713	-733	-227	-1481	-269	-3695	103	-5299	-230	8	340	-495
till	5	-49	178	173	-50	-799	1038	598	83	-444	-417	-501	111	-1391	-90	598	1008	664
sandstone	6	18	111	135	54	356	266	329	60	36	51	56	90	32	39	226	298	351

Fluid flux in negative/downward direction.

Table F.23 Vertical fluid influx and outflux between slices for model using randomly assigned windows in till layer. Pumping 26,000 m3/d for 5 yr. Basal sand and gravel layer excluded.

		FENCE																
		1	2	3	4	5	6	7	8	9	10	11	12	13	14	15	16	17
	SLICE	m³/d	m³/d	m³/d	m³/d	m³/d	m³/d	m³/d	m³/d	m³/d	m³/d	m³/d	m³/d	m³/d	m³/d	m³/d	m³/d	m³/d
sand/gravel	1	-78	295	132	-31	-2300	-214	-839	-79	286	-477	-5033	50	-9890	-370	30	300	-721
clay	2	-860	336	628	68	-6956	-222	-913	-166	-991	-547	-4674	106	-11189	-348	125	369	-496
clay	3	-792	189	131	-29	-5851	-107	-178	-140	-2079	-575	-7598	104	-8055	-402	-46	-113	-286
aquifer	4	-450	233	121	123	-5512	-730	-739	-233	-1488	-280	-3705	102	-5321	-244	4	382	-490
till	5	-51	174	164	-61	-873	1027	567	74	-453	-430	-504	110	-1398	-99	576	976	652
sandstone	6	16	108	128	45	340	242	304	50	30	47	55	90	31	35	213	282	342

Fluid flux in negative/downward direction.

Table F.24 Results of transient simulation fluid flux mass balance for pumping at 52,000 m³/d using the randomly assigned windows in the till layer, basal sand and gravel excluded.

FLUX_TYPE:	Fluid flux mass balance			
BALANCE_TYPE:	Total			
CURRENT_TIME:	365 d		5 yr	
FLUX_TYPE	FLUX_IN(+)	FLUX_OUT(-)	FLUX_IN(+)	FLUX_OUT(-)
UNIT	Q [m3/d]	Q [m3/d]	Q [m3/d]	Q [m3/d]
BC123_FLUXES	64484	-26488	64789	-26362
WELL_FLUXES	0	-52002	0	-52002
AREAL_FLUXES	13312	0	13312	0
IMBALANCE	0	-694	0	-263
Total	77796	-79185	78102	-78627
Error %	-1.8		-0.7	

Table F.25 Vertical fluid influx and outflux between slices using model with randomly assigned windows in till layer, pumping 52,000 m3/d, 5 yr. Basal sand and gravel layer excluded.

		POLYGON																
		1	2	3	4	5	6	7	8	9	10	11	12	13	14	15	16	17
	SLICE	m³/d	m³/d	m³/d	m³/d	m³/d	m³/d	m³/d	m³/d	m³/d	m³/d	m³/d	m³/d	m³/d	m³/d	m³/d	m³/d	m³/d
sand/gravel	1	-41	-138	426	6	86	-235	-925	-59	-672	13	10	-39	-285	-8	41	555	-728
clay	2	-1666	76	615	-178	-4558	-234	-1405	-320	-3042	-806	-7955	37	-11108	-653	139	317	-506
clay	3	-1774	39	-229	-401	-12198	-134	-432	-308	-4295	-1568	-16030	75	-17464	-1267	-46	-326	-286
aquifer	4	-1031	154	-161	-11	-10863	-1561	-1398	-517	-3075	-737	-7906	69	-11516	-828	-5	315	-461
till	5	-161	128	65	-318	-3561	2027	677	159	-958	-1017	-1154	108	-3093	-359	634	1048	647
sandstone	6	4	84	100	33	337	316	363	99	47	65	45	89	23	47	239	296	341
	Fluid flux in downward direction																	

Table F.26 Hydraulic head results after pumping 26,000 m³/d for various transient simulations.						
	Randomly assigned windows in till layer					Borehole Data
	Sand and Gravel Excluded				Sand Included	Sand Included
	365 d	5 yr	365 d	365 d	365 d	365 d
			50 % Increase in Recharge	50% Decrease in Recharge		
	(m)	(m)	(m)	(m)	(m)	(m)
Grieves B	23.21	23.2	25.14	21.29	23.21	23.21
Rice Brook	10.57	10.56	10.81	10.33	10.57	10.57
New Maryland	95.07	95.07	97.56	92.58	95.06	95.06
Nashw. Stream	3.05	3.05	3.06	3.04	3.05	3.05
Corbett Brook - low	43.31	43.3	44.87	41.75	43.30	43.30
Corbett Brook - med	82.55	82.47	84.76	80.33	82.50	82.50
Corbett Brook - high	107.44	107.34	110.79	104.09	107.38	107.38
Phyllis Creek	82.71	82.66	84.54	80.87	82.67	82.67
Baker Brook	118.58	118.58	120.96	116.20	118.58	118.58
BH03	6.81	6.75	7.33	6.29	6.40	6.39
98-a	2.71	2.7	2.71	2.70	2.71	2.71
6-00	1.04	0.93	1.15	0.92	1.53	1.51
98-b	2.72	2.72	2.73	2.72	2.64	2.63
PW01	1.91	1.9	1.92	1.89	1.92	1.91
PW09	0.48	0.42	0.60	0.35	0.66	0.66
PW10	0.55	0.49	0.67	0.43	0.72	0.72
PW07	2.46	2.46	2.47	2.46	2.47	2.47
PW08	2.17	2.17	2.18	2.16	2.18	2.18
PW02	1.85	1.84	1.87	1.83	1.86	1.87
PW06	2.83	2.83	2.84	2.83	2.83	2.83
PW03	-5.22	-5.23	-5.20	-5.25	-5.21	-5.21
PW05	2.43	2.43	2.44	2.43	2.44	2.44

Table F. 27 Mass balance of increasing recharge 50% while pumping 26,000 m³/d.		
#FLUX_TYPE:	Fluid flux mass balance	
#BALANCE_TYPE:	Total	
#CURRENT_TIME:	365.000000 [d]	
FLUX_TYPE	FLUX_IN(+)	FLUX_OUT(-)
UNIT	Q [m3/d]	Q [m3/d]
BC123_FLUXES	3.83E+04	-2.95E+04
WELL_FLUXES	0.00E+00	-2.60E+04
AREAL_FLUXES	2.00E+04	0.00E+00
IMBALANCE	2.76E+03	0.00E+00
Error %	5%	

Table F.28 Vertical fluid influx and outflux between slices using model with randomly assigned windows in till layer, pumping 26,000 m³/d, 365d, increasing recharge 50%. Basal sand and gravel layer excluded.

		FENCE																
		1	2	3	4	5	6	7	8	9	10	11	12	13	14	15	16	17
	SLICE	m³/d	m³/d	m³/d	m³/d	m³/d	m³/d	m³/d	m³/d	m³/d	m³/d	m³/d	m³/d	m³/d	m³/d	m³/d	m³/d	m³/d
sand/gravel	1	-67	328	206	14	-2310	-271	-901	-97	266	-429	-4955	55	-9672	-309	22	299	-863
clay	2	-837	374	782	133	-6894	-280	-955	-168	-985	-488	-4597	115	-10948	-261	125	403	-592
clay	3	-776	209	198	19	-5806	-146	-182	-143	-2060	-513	-7499	113	-7660	-341	-70	-119	-362
aquifer	4	-440	247	175	158	-5559	-729	-750	-229	-1473	-252	-3658	111	-5193	-200	-10	413	-597
till	5	-47	184	199	-29	-576	1035	626	78	-440	-402	-493	117	-1358	-77	635	1062	714
bedrock	6	18	115	148	57	387	277	342	58	36	51	57	95	34	39	234	308	363
	Fluid flux in downward direction.																	

Table F.29 Mass balance of decreasing recharge 50% while pumping 26,000 m3/d.

#FLUX_TYPE:	Fluid flux mass balance	
#BALANCE_TYPE:	Total	
#CURRENT_TIME:	365.000000 [d]	
FLUX_TYPE	FLUX_IN(+)	FLUX_OUT(-)
UNIT	Q [m3/d]	Q [m3/d]
BC123_FLUXES	4.06E+04	-2.47E+04
WELL_FLUXES	0.00E+00	-2.60E+04
AREAL_FLUXES	6.66E+03	0.00E+00
IMBALANCE	0.00E+00	-3.46E+03
Error %	7%	

Table F.30 Vertical fluid influx and outflux between slices using model with randomly assigned windows in till layer, pumping 26,000 m³/d, 365d, decreasing recharge 50%. Basal sand and gravel layer excluded.

		1	2	3	4	5	6	7	8	9	10	11	12	13	14	15	16	17
	SLICE	m³/d	m³/d	m³/d	m³/d	m³/d	m³/d	m³/d	m³/d	m³/d	m³/d	m³/d	m³/d	m³/d	m³/d	m³/d	m³/d	m³/d
sand/gravel	1	-84	278	87	-55	-2273	-166	-795	-58	309	-492	-5079	46	-10032	-395	51	314	-595
clay	2	-874	316	511	30	-6974	-173	-879	-156	-985	-566	-4721	98	-11346	-376	141	369	-405
clay	3	-799	180	91	-54	-5856	-67	-157	-129	-2081	-595	-7657	96	-8184	-425	-20	-96	-211
aquifer	4	-453	226	92	106	-5473	-698	-716	-224	-1489	-286	-3733	94	-5404	-260	26	386	-392
till	5	-50	171	147	-70	-1023	1041	570	88	-448	-433	-509	105	-1423	-103	561	954	614
bedrock	6	18	108	123	50	324	256	316	63	37	50	55	86	30	39	218	288	339

Table F.31 Results of fluid flux mass balance, pumping 26,000 m³/d, including the basal sand and gravel layer.				
FLUX_TYPE:	Fluid flux mass balance			
BALANCE_TYPE:	Total			
CURRENT_TIME:	365.000000 [d]			
	Randomly assigned windows in till layer		Borehole database assigned windows in till layer	
FLUX_TYPE	FLUX_IN(+)	FLUX_OUT(-)	FLUX_IN(+)	FLUX_OUT(-)
UNIT	Q [m3/d]	Q [m3/d]	Q [m3/d]	Q [m3/d]
BC123_FLUXES	36214	-23880	36211	-23878
WELL_FLUXES	0	-26001	0	-26001
AREAL_FLUXES	13312	0	13312	0
IMBALANCE	0	-354	0	-356
TOTAL	49527	-49881	49523	-49879
ERROR %	-0.7		-0.7	

Table F.32 Vertical fluid influx and outflux between slices including the basal sand and gravel layer with the randomly assigned windows in till layer, pumping 26000 m³/d for 365 days.

		FENCE																
		1	2	3	4	5	6	7	8	9	10	11	12	13	14	15	16	17
	SLICE	m³/d	m³/d	m³/d	m³/d	m³/d	m³/d	m³/d	m³/d	m³/d	m³/d	m³/d	m³/d	m³/d	m³/d	m³/d	m³/d	m³/d
sand/gravel	1	-73	309	166	-11	-2301	-207	-812	-75	290	-465	-5005	44	-9869	-353	7	286	-735
clay	2	-849	353	670	92	-6925	-215	-878	-151	-973	-534	-4652	96	-11162	-330	117	369	-508
clay	3	-782	199	163	-8	-5812	-104	-156	-127	-2053	-561	-7559	95	-8041	-384	-47	-111	-288
aquifer	4	-444	238	147	123	-5564	-583	-594	-201	-1472	-296	-3697	98	-5311	-250	-8	343	-493
till	5	-48	180	179	-40	-874	1212	633	106	-429	-489	-509	106	-1400	-121	508	869	534
sand/gravel	6	18	118	147	47	399	608	431	100	54	-67	54	91	60	4	191	193	269
bedrock	7	18	111	136	51	336	360	293	63	36	47	61	89	24	40	212	258	302
Fluid flux in negative/downward direction																		

Table F.33 Vertical fluid influx and outflux between slices including the basal sand and gravel layer with the borehole database assigned windows in the till layer. Pumping 26,000 m³/d for 365 days.

		FENCE																
		1	2	3	4	5	6	7	8	9	10	11	12	13	14	15	16	17
LAYER	SLICE	m³/d	m³/d	m³/d	m³/d	m³/d	m³/d	m³/d	m³/d	m³/d	m³/d	m³/d	m³/d	m³/d	m³/d	m³/d	m³/d	m³/d
sand/gravel	1	-73	309	165	-11	-2299	-208	-813	-75	290	-465	-5001	25	-9853	-354	9	286	-730
clay	2	-848	353	669	91	-6922	-216	-880	-151	-973	-535	-4649	76	-11145	-331	118	369	-508
clay	3	-782	199	163	-8	-5810	-104	-162	-128	-2053	-562	-7556	76	-8025	-385	-46	-111	-289
aquifer	4	-444	239	147	123	-5561	-597	-589	-201	-1472	-291	-3694	75	-5296	-249	-6	344	-488
till	5	-48	180	179	-40	-868	1177	627	104	-430	-479	-507	79	-1381	-118	515	869	547
sand+gravel	6	18	118	147	48	404	568	436	104	54	-59	58	73	77	8	203	189	293
sandstone	7	18	111	136	51	317	357	323	67	36	47	62	76	24	40	212	258	303
		Fluid flux in negative/downward direction																

Table F.34 Vertical fluid influx and outflux between slices for model using borehole database assigned windows in till layer, pumping 26,000 m³/d for 365 d. Basal sand and gravel layer excluded.

		FENCE																
		1	2	3	4	5	6	7	8	9	10	11	12	13	14	15	16	17
	SLICE	m³/d	m³/d	m³/d	m³/d	m³/d	m³/d	m³/d	m³/d	m³/d	m³/d	m³/d	m³/d	m³/d	m³/d	m³/d	m³/d	m³/d
sand/gravel	1	-75	303	147	-20	-2296	-220	-850	-78	288	-461	-5014	38	-9848	-352	37	308	-706
clay	2	-855	345	647	81	-6936	-227	-919	-162	-984	-528	-4656	93	-11143	-329	133	387	-499
clay	3	-787	195	145	-17	-5830	-107	-171	-136	-2070	-555	-7574	91	-8019	-384	-45	-108	-289
aquifer	4	-446	237	133	132	-5524	-715	-734	-227	-1480	-271	-3692	87	-5296	-231	8	401	-492
till	5	-48	178	173	-49	-824	1031	595	82	-445	-419	-498	94	-1387	-92	599	1010	667
sandstone	6	18	111	136	55	344	248	322	60	36	50	59	78	35	38	230	300	371
		Fluid flux in negative/downward direction.																